

N O T I C E

THIS DOCUMENT HAS BEEN REPRODUCED FROM
MICROFICHE. ALTHOUGH IT IS RECOGNIZED THAT
CERTAIN PORTIONS ARE ILLEGIBLE, IT IS BEING RELEASED
IN THE INTEREST OF MAKING AVAILABLE AS MUCH
INFORMATION AS POSSIBLE

Report No. 33574-F

10 December 1980

ORBIT TRANSFER VEHICLE (OTV)
ADVANCED EXPANDER CYCLE ENGINE
POINT DESIGN STUDY

FINAL REPORT


Contract NAS 8-33574

VOLUME II: STUDY RESULTS

PREPARED FOR

NATIONAL AERONAUTICS AND SPACE ADMINISTRATION
GEORGE C. MARSHALL SPACE FLIGHT CENTER
MARSHALL SPACE FLIGHT CENTER, ALABAMA 35812

Prepared by:


J. A. Mellish
Study Manager

Approved by:


L. B. Bassham
Program Manager

Aerojet Liquid Rocket Company
P.O. Box 13222
Sacramento, California 95813

ACKNOWLEDGEMENT

The following ALRC personnel have contributed significantly to the data and information contained in this report.

S. P. Abbott, Turbomachinery Design Analysis
G. D. Aldrich, Structural Analysis
P. E. Brown, Structural Analysis
P. S. Buckmann, Turbomachinery Mechanical Design
K. L. Christensen, Engine System Steady-State Analysis
R. L. Ewen, Thermal Analysis
J. E. Dever, Controls System Design
J. I. Ito, Thrust Chamber Assembly Design Analysis
H. V. Kiser, Thrust Chamber Assembly Mechanical Design
B. R. Lawver, Engine Simulation Computer Model
B. K. Lindley, Turbomachinery Mechanical Design
S. A. Lorenc, Turbomachinery Design Analysis
A. V. Lundback, Controls System Design
E. Lueders, Structural Analysis
H. H. Mueggenburg, Thrust Chamber Assembly Mechanical Design
M. Murphy, Materials Analysis
J. L. Pieper, Performance Analysis
D. H. Saltzman, Engine Simulation Computer Model
R. H. Schultz, Design Layouts

PRECEDING PAGE BLANK NOT REPRODUCED

FOREWORD

This final report is submitted for the Orbit Transfer Vehicle (OTV) Advanced Expander Cycle Engine Point Design Study per the requirements of Contract NAS 8-33574, Data Procurement Document No. 578, Data Requirement No. MA-05. This work was performed by the Aerojet Liquid Rocket Company (ALRC) for the NASA/Marshall Space Flight Center.

The study consisted of the generation of a performance-optimized engine system design for an Advanced LOX/Hydrogen Expander Cycle Engine. The designs of the components and engine were prepared in sufficient depth to calculate engine and component weights and envelopes, turbopump efficiencies and recirculation leakage rates, and engine performance. Engine control techniques were established, and new technology requirements were identified.

The NASA/MSFC COR was Mr. D. H. Blount. The ALRC Program Manager was Mr. L. B. Bassham, and the Study Manager was Mr. J. A. Mellish.

The final report is submitted in two volumes:

Volume I: Executive Summary

Volume II: Study Results

TABLE OF CONTENTS

	<u>Page</u>
I. Summary	1
A. Study Objectives and Scope	1
B. Study Results and Conclusions	3
II. Introduction	15
A. Background	15
B. Orbit Transfer Vehicle Characteristics	15
C. Engine Requirements	16
D. Principal Assumptions and Guidelines	21
E. Structural Design Criteria	22
III. Task Discussions	24
A. Task I - Steady-State Computer Model	24
B. Task II - Heat Transfer, Stress, and Fluid Flow Analysis	30
1. Heat Transfer Analysis	30
2. Thrust Chamber Assembly Design Analysis	34
3. Structural Analysis	43
4. Pump Hydraulic Design Analysis	70
5. Materials Analysis	86
C. Task III - Component Mechanical Design and Assembly Drawings	91
1. Igniter/Injector Assembly	91
2. Combustion Chamber Design	96
3. Regeneratively Cooled Nozzle Design	101
4. Radiation-Cooled Nozzle and Deployment Mechanism	104
5. Gimbal Assembly	110
6. Oxygen Turbopumps Design	112
7. Hydrogen Turbopumps Design	127
8. Propellant Valves	156

TABLE OF CONTENTS (cont.)

	<u>Page</u>
D. Task IV - Engine Transient Simulation Computer Model	167
E. Task V - Engine Control	169
1. Propellant Flow Control Valve Operation	172
2. Modulating Valve Operation	173
3. Actuation Systems	175
4. Auxiliary Valve Requirements	182
5. Engine Controller Requirements	187
6. Areas Requiring Further Study	195
F. Task VI - Engine Configuration Layout	197
1. Engine Assembly	197
2. Engine System Structural Analysis	202
3. System Effectiveness and Safety	206
G. Task VII - Engine Data Summary	222
1. Engine Operating Characteristics	222
2. Engine Performance	231
3. Engine Life	240
4. Engine System and Component Weights	240
5. Envelope Data	242
H. Task VII - Technology Requirements	244
1. Engine Turbopump Drive Power Technologies	248
2. Development and Operational Risk Reduction Technologies	252
3. Engine Performance Technologies	266
I. Task IX - Computer Software/Documentation	268
IV. Conclusions and Recommendations	269
A. Conclusions	269
B. Recommendations	270
References	272

LIST OF TABLES

<u>Table No.</u>		<u>Page</u>
I	Current vs Initial Baseline Engine Characteristics	7
II	Advanced Expander Cycle Engine Performance at Design and Off-Design O/F	9
III	Technology Recommendation Summary	14
IV	OTV Engine Point Design Requirements	17
V	Man-Rating, Safety, and Reliability Imposed Requirements	20
VI	OTV Expander Cycle Engine Steady-State Model Sample Output	26
VII	AEC Thermal Analyses Design and Off-Design O/F Summary at Rated Thrust	33
VIII	OTV Injector Design Parameters	38
IX	OTV Chamber Geometry	39
X	Rao Nozzle Contour Data	41
XI	Chamber Low-Cycle Thermal Fatigue Results	48
XII	Main LOX TPA Margins Summary	55
XIII	Main LH ₂ TPA Margins Summary	67
XIV	LO ₂ Boost Pump Design Parameters	77
XV	LO ₂ Main Pump Design Parameters	78
XVI	LH ₂ Boost Pump Design Parameters	83
XVII	LH ₂ Main Pump Design Parameters	85
XVIII	LO ₂ TPA Gas Turbine Design Point Performance	123
XIX	LH ₂ Main Pump Labyrinth Seal Geometry and Flowrates	142
XX	LH ₂ Main TPA, Summary of Flowrate Analysis	146
XXI	LH ₂ TPA Gas Turbine Design Point Performance	152
XXII	Actuation System Study Summary	176
XXIII	OTV Auxiliary Valve Summary	188
XXIV	OTV Digital Controller Power Density Determination	192
XXV	Engine System Stress Summary, Thermal and Mechanical Loading	204
XXVI	Engine System Stress Summary, Combined Inertia Loading	205

LIST OF TABLES (cont.)

<u>Table No.</u>		<u>Page</u>
XXVII	Engine Reliability Requirements	209
XXVIII	Failure Rate Distribution of Twin-Engine System	214
XXIX	Advanced Expander Cycle Engine Operating Specification	223
XXX	Advanced Expander Cycle Engine Pressure Schedule	230
XXXI	Advanced Expander Cycle Engine Baseline Performance	232
XXXII	Advanced Expander Cycle Engine Performance at Design and Off-Design O/F	233
XXXIII	Comparison of the Standard and "Shortcut" Procedure for Calculating the Performance of the Regeneratively Cooled ASE	238
XXXIV	Comparison of Simplified Model Predictions to Experimental Specific Impulse for H ₂ /O ₂ Engine Systems	239
XXXV	Advanced Expander Cycle Engine Weight Data	241
XXXVI	Advanced Expander Cycle Engine Envelope Data	243
XXXVII	Component Technology Program Priorities	247

LIST OF FIGURES

<u>Figure No.</u>		<u>Page</u>
1	Baseline Advanced Expander Cycle Engine Flow Schematic	4
2	Engine Layout	10
3	Simplified JANNAF Performance Methodology Predicts Engine Cycle Performance	29
4	AEC Engine Coolant Flow Schematic	32
5	Coolant Jacket Pressure Drop vs Thrust	35
6	Effect of Low-Thrust Operation Upon Coolant Exit Temperature	36
7	Combustion Chamber and Throat Geometry	40
8	Predicted Chug Stability Threshold	42
9	Mechanical Properties of Zirconium Copper	44
10	Mechanical Properties of Electroformed Nickel	45
11	Low-Cycle Fatigue, Lower-Bound Design Curve for Zirconium Copper	47
12	LOX TPA Impeller Computer Model Geometry	50
13	LOX TPA Turbine Rotor Computer Model Geometry	51
14	Fuel TPA 3rd Stage Impeller Computer Model Geometry	59
15	Fuel TPA 3rd Stage Impeller Tangential Stress	60
16	Fuel Turbine Rotors Computer Model Geometry	62
17	Fuel Turbine Rotors Tangential Stress	63
18	LO ₂ Pumps-Fluid Dynamic Interface	71
19	LH ₂ Pumps-Fluid Dynamic Interface	74
20	Igniter/Injector Assembly (ALRC Drawing No. 1191990)	92
21	Combustion Chamber Layout (ALRC Drawing No. 1191995)	98
22	Chamber and Tube Bundle Nozzle Design (ALRC Drawing No. 1191991)	99
23	Regeneratively Cooled Nozzle Design (ALRC Drawing No. 1191995)	103
24	Engine and Nozzle Extension Layout (ALRC Drawing No. 1193100)	115

LIST OF FIGURES (cont.)

<u>Figure No.</u>		<u>Page</u>
25	Gimbal Assembly (ALRC Drawing No. 1191993)	111
26	LO ₂ Boost Pump Cross Section (ALRC Drawing No. 1191996)	113
27	LO ₂ Main Pump Cross Section (ALRC Drawing No. 1191999)	115
28	LO ₂ TPA Turbine Meridional Flow Passage	124
29	LH ₂ Boost Pump Cross Section (ALRC Drawing No. 1191994)	128
30	LH ₂ Main TPA Cross Section (Baseline), Separate Pump-Turbine Housings (ALRC Drawing No. 1191997)	130
31	LH ₂ Main TPA End View (Baseline) Design (ALRC Drawing No. 1191997)	131
32	LH ₂ Main TPA Cross Section (Alternate Design): Common Pump and Turbine Housing (ALRC Drawing No. 1191998)	132
33	LH ₂ Main Pump Axial Thrust Balance	136
34	LH ₂ Main TPA Series Flow Thrust Balancer - Labyrinth/Land	137
35	LH ₂ Main TPA Series Flow Thrust Balancer, OD/ID Land	138
36	LH ₂ Main TPA Hydrostatic Thrust Balancer/Face Seal	139
37	LH ₂ TPA Seal Types	141
38	Eccentric Wear Ring Seal Whirl Forces	144
39	Labyrinth Seal Extreme Operating Positions	145
40	LH ₂ Boost and Main Pump Flow Schematic	147
41	LH ₂ Main TPA Critical Speed Analysis	149
42	LH ₂ Main TPA Critical Speed as a Function of Bearing Radial Stiffness, 3-Stage Pump	150

LIST OF FIGURES (cont.)

<u>Figure No.</u>		<u>Page</u>
43	LH ₂ TPA Turbine Meridional Flow Passage	156
44	LH ₂ Boost Pump-Planetary Drive Concept	157
45	Propellant Flow Control Valve (ALRC Drawing No. 1193175)	159
46	Modulating Valve (ALRC Drawing No. 1193180)	165
47	Baseline Advanced Expander Cycle Engine Flow Schematic	170
48	Modulating Valve Cross Section	174
49	Engine Purge and Relief System Schematic	185
50	OTV Engine Conceptual Control Schematic	190
51	OTV Engine Controller Size Estimate	191
52	OTV Engine Control Logic	193
53	Engine Layout (ALRC Drawing No. 1193100)	198
54	Meeting Crew Risk Requirements	210
55	ALRC Engine Reliability History	213
56	Baseline Advanced Expander Cycle Engine Flow Schematic	228
57	Critical Component Technology Program Logic	246

I. SUMMARY

A. STUDY OBJECTIVES AND SCOPE

The major objectives of the OTV Advanced Expander Cycle Engine Point Design Study were to (1) generate a performance-optimized engine system design for an Advanced LOX/Hydrogen Expander Cycle Engine; (2) provide sufficient design and analysis of the engine and components to produce accurate engine and component weights and envelopes, turbopump efficiencies and recirculation leakage rates, and engine performance; (3) establish engine control techniques; and (4) identify new technology requirements.

Specific study objectives were as follows:

- ° Prepare detailed computer models of the engine to predict both the steady-state and transient operation of the engine system
- ° Prepare mechanical design layout drawings of the following components:
 - Thrust chamber and nozzle
 - Extendible nozzle actuating mechanism and seal
 - LOX turbopump
 - LOX boost pump
 - Hydrogen turbopump
 - Hydrogen boost pump
 - Propellant control valves
- ° Perform the necessary heat transfer, stress, fluid flow, dynamic, and performance analyses to support the mechanical design.

I, A, Study Objectives and Scope (cont.)

- ° Determine effective control points and methods to control the engine operation through start and shutdown transients as well as steady-state operation. These include thrust and mixture ratio control.
- ° Determine optimum actuation drive methods for engine control elements.
- ° Define controller requirements.
- ° Prepare an engine configuration layout drawing to show the spatial arrangement of the various engine components with consideration of system effectiveness, safety, and the impact upon maintainability as well as engine performance.
- ° Prepare an engine data summary to include the engine and component layout drawings, the performance and life predictions, and the engine and component weights and physical envelopes.
- ° Identify any new technology required to perform detailed design, construction, and testing of the engine.
- ° Prepare and deliver computer software/documentation for the steady-state and transient engine models.
- ° Prepare a final report at the completion of the study which documents the technical details and programmatic assessments resulting from the study. The final report is submitted in two volumes:

Volume I: Executive Summary

Volume II: Study Results

I, A, Study Objectives and Scope (cont.)

To accomplish the program objectives, a program consisting of nine major technical tasks and a reporting task was conducted. These tasks were as follows:

- ° Task I: Steady-State Computer Model
- ° Task II: Heat Transfer, Stress, and Fluid Flow Analysis
- ° Task III: Component Mechanical Design and Assembly Drawings
- ° Task IV: Engine Transient Simulation Computer Model
- ° Task V: Engine Control
- ° Task VI: Engine Configuration Layout
- ° Task VII: Engine Data Summary
- ° Task VIII: Technology Requirements
- ° Task IX: Computer Software/Documentation
- ° Task X: Reporting and Performance Reviews

This report presents the study results, supporting data, assumptions, rationale, conclusions, and recommendations. The main body of the report, Section III: Task Discussions, is separated into the technical task packages listed above to facilitate reporting.

B. STUDY RESULTS AND CONCLUSIONS

The designs and data presented in this report are based upon the results of work performed in this Point Design Study as well as the OTV Phase A Engine Study evaluations and optimizations conducted for Contract NAS 8-32999 (Ref. 1 and 2).

The O₂/H₂ Advanced Expander Cycle Engine is powered by a series turbine drive cycle which is shown in Figure 1. The engine uses hydraulically driven boost pumps, with the flow tapped off the main pump stages. Fuel flows from the pump discharge to the thrust chamber where 85%

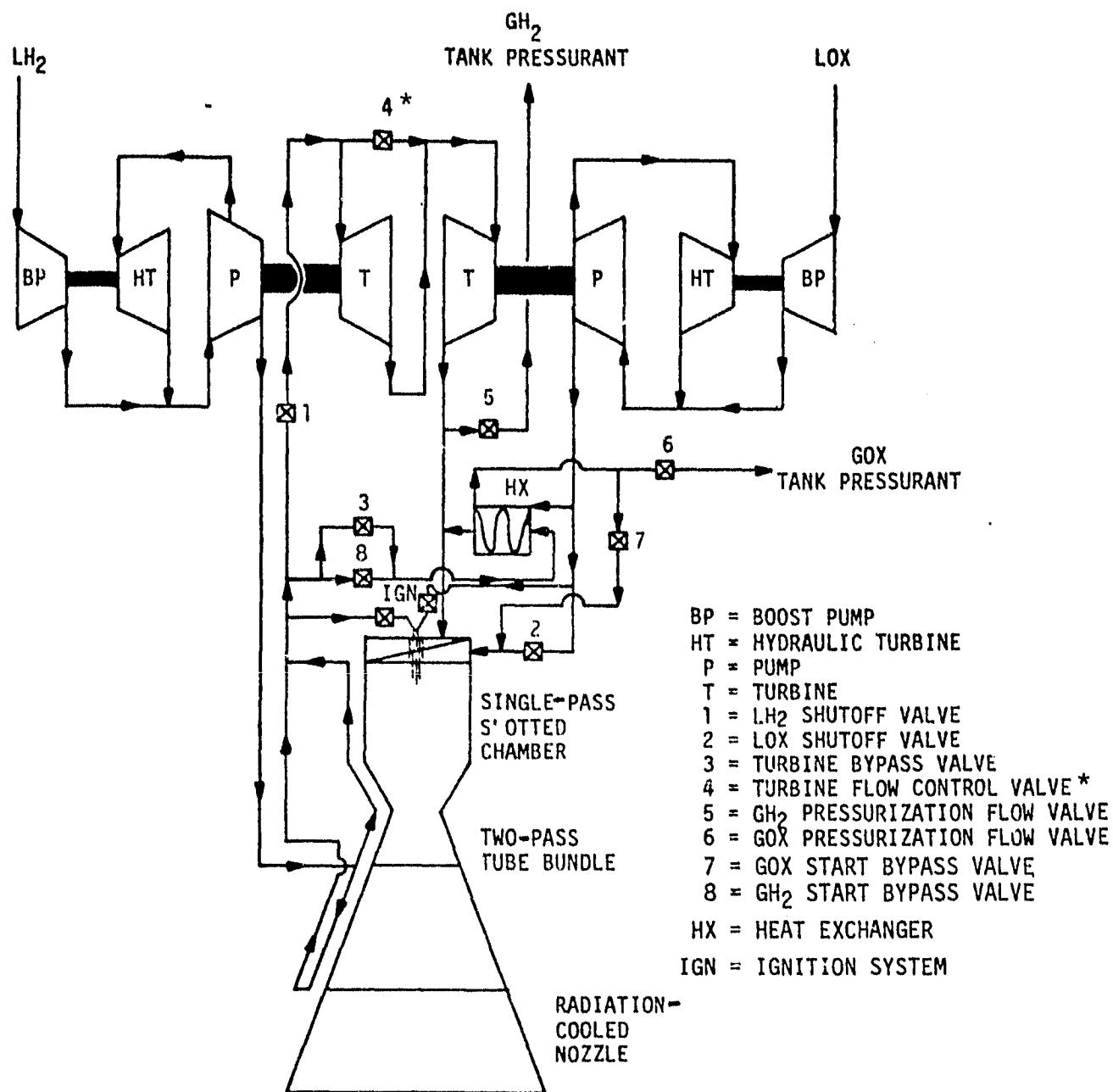


Figure 1. Baseline Advanced Expander Cycle Engine Flow Schematic

I, B, Study Results and Conclusions (cont.)

of the hydrogen flow is used to cool the slotted copper chamber in a single pass from an area ratio of 10.6:1 to the injector head end. Fifteen (15) percent of the hydrogen is used to cool the tube bundle nozzle in two passes from an area ratio of 10.6:1 to the end of the fixed nozzle ($\epsilon = 172:1$) and return. The coolant flows are merged, and 6% of the total engine hydrogen flow is used to bypass both turbines to provide cycle power balance margin and thrust control. The remaining hydrogen flow first drives the fuel pump turbine and then drives the oxidizer pump turbine. After driving the oxidizer pump turbine, a small amount of heated hydrogen is tapped off for hydrogen tank pressurization. The remaining hydrogen flow is then injected into the combustion chamber.

At rated thrust operation, oxidizer flows from the main pump discharge directly to the thrust chamber and is injected in a liquid state. A small amount of oxidizer is tapped off and heated by the hydrogen turbine bypass flowrate in a heat exchanger to provide LOX tank pressurization.

The extendible nozzle is radiation-cooled. A lightweight, state-of-the-art columbium nozzle extension was selected on the basis of experience gained on the Transtage, Apollo, SPS, and OMS engine programs.

The engine is also capable of operating in a tank head idle mode and is adaptable to extended low-thrust operation at a thrust level of 1.5K lb.

The purpose of the tank head idle mode is to thermally condition the engine without non-propulsive dumping of propellants. This is a pressure-fed mode of operation at a thrust level of approximately 50 lb and a vacuum specific impulse estimated at 400 sec. During this mode of operation, the main fuel and oxygen valves (numbers 1 and 2 on the schematic) are closed.

I, B, Study Results and Conclusions (cont.)

All of the fuel bypasses the turbines through valve number 3 so that the pumps are not rotating. The heat exchanger in the turbine bypass line gasifies the oxygen which then flows through valve number 7 to the chamber. Tank pressurization is not supplied during this operating mode, and valves 5 and 6 remain closed. The pressurization valves are opened as the engine is brought up to steady-state, full-thrust operation.

The OTV Point Design Engine is adaptable to operation at 10% of rated thrust (i.e., 1.5K lbf) with minor modifications. This low-thrust operating point is a dedicated condition and the engine is not required to operate at both the 15K and 1.5K thrust levels on the same mission. To operate at low thrust, the oxidizer injection elements must be changed to smaller size ones, and an orifice must be installed in the line downstream of the chamber coolant jacket. The alternate low-thrust capability is discussed in Reference 3.

On the basis of the Phase A OTV Engine Study results, an engine with the characteristics shown on Table I was baselined to initiate this point design study. The current baseline characteristics resulting from this study are also shown in Table I for reasons of comparison. The primary change is a lower area ratio which results from accommodating the extendible nozzle translation mechanism. This causes a reduction in the total engine length with the nozzle deployed in order to stay within the minimum 60-in. stowed length requirement. Another difference is in the engine weight. The Phase A weight number was estimated by scaling historical designs and data, whereas approximately 75% of the current weight has been estimated from the preliminary component designs. Further changes in the data can be anticipated as more design iterations are performed and as the Advanced Expander Cycle Engine design matures.

TABLE I
CURRENT VS INITIAL BASELINE ENGINE CHARACTERISTICS

	<u>Initial Design Baseline</u> (1)	<u>Current Baseline</u> (2)
Vacuum Thrust, lb	15,000	15,000
Vacuum Specific Impulse, sec	477.2	475.4
Total Flowrate, lb/sec	31.43	31.56
Mixture Ratio (Nominal)	6.0	6.0
Oxygen Flowrate, lb/sec	26.94	27.05
Hydrogen Flowrate, lb/sec	4.49	4.51
Chamber Pressure, psia	1200	1200
Nozzle Area Ratio	473	435
Nozzle Exit Diameter, in.	60.7	58.2
Engine Length, in.		
Extendible Nozzle Stowed	60.0	60.0
Extendible Nozzle Deployed	120.0	109.6
Engine Dry Weight, lb	502	574

(1) Based upon Phase A Study results

(2) Based upon Point Design Study results

I, B, Study Results and Conclusions (cont.)

The current baseline engine delivered performance at design and off-design mixture ratio operation is shown in Table II. The table also presents the vacuum specific impulse at both the rated and low-thrust operating points. The chamber pressure of 1200 psia at the nominal operating point was selected on the basis of results obtained in the Phase A cycle and thrust chamber geometry optimization studies (Ref. 2). The series turbine drive cycle, a chamber length of 18 in., and a contraction ratio of 3.66 were selected and fixed as baselines in this study. This engine is considered to be representative of a 1980 technology baseline. Technology verification and advancements plus further optimization studies and tradeoffs are planned in future work. Some changes in the operating chamber pressure and performance are anticipated as a result of these forthcoming efforts.

The engine has been designed for 1200 thermal cycles and 10 hours of accumulated run time. Therefore, the component designs illustrated in Section III.D of this report are based on the minimum service life requirement (300 cycles or 10 hours) with a safety factor of 4 applied to lower-bound data. This service life is not predicted to be reduced when the engine is operated at mixture ratios between 6.0 and 7.0. Similarly, low-thrust operation (i.e., 1500 lbf) at mixture ratios between 6.0 and 7.0 is not predicted to reduce this service life.

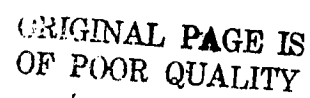
The engine performance, weight, envelope, and service life data, as well as the engine and component layout drawings, were summarized and presented in the Task VII, Engine Data Summary, report submitted for this contract (Ref. 4). This information is also presented in Sections III.C, Component Mechanical Design and Assembly Drawings, and III.G, Engine Data Summary, of this report.

The engine configuration layout drawing showing the packaging relationship of the engine components is shown in Figure 2. With the

TABLE II
ADVANCED EXPANDER CYCLE ENGINE PERFORMANCE AT DESIGN AND OFF-DESIGN O/F
(Rated and Low-Thrust Operation)

Thrust, lb	Engine Mixture Ratio	Thrust Chamber Pressure, psia	Engine Delivered Vacuum Specific Impulse, sec.	Flowrates, lb/sec	
				Fuel	OX
15000	6.0	1200	475.4	4.51	27.05
15000	6.5	1180	474.9	4.21	27.37
15000	7.0	1162	471.0	3.98	27.87
1500	6.0	125	459.7	.466	2.80
1500	7.0	121	451.7	.415	2.91

Notes: (1) Injector elements are modified for the low-thrust condition.
(2) Engine length with extendible nozzle retracted = 60".



10

1. B, Study Results and Conclusions (cont.)

extendible nozzle in the stowed position, the engine is 60 in. long. This length is measured from the top of the gimbal block to the end of the tube bundle nozzle. The engine is 109.6 in. long and has an area ratio of 435:1 with the extendible nozzle deployed. Approximately 10.4 in. of potentially available deployed length is lost in the area of the extendible nozzle deployment mechanism and attachment plane. Further design refinements could increase the deployed length up to a maximum of 120 in., with a resulting area ratio of 473:1 and a performance increase of 1.8 sec (see Table I).

As part of this program, two engine computer models were delivered to NASA/MSFC. One of the programs is the Task I, Steady-State Computer Model (Ref. 5), and the second is the Task IV, Engine Transient Simulation Computer Model (Ref. 6).

Documentation submitted in these computer models included:

- ° User's Manual
- ° FORTRAN Program Listing
- ° Program Flow Charts
- ° Sample Inputs and Outputs

At the request of the NASA/COR, a FORTRAN card deck was submitted for the steady-state model. The transient model was submitted on tape. Both programs are compatible with a Univac 1108 system.

Section III.H of this report presents supporting research and technology programs which are recommended for the purpose of filling basic data gaps and/or providing critical information prior to initiating experimental engine and engine development programs. These technology programs, submitted to NASA/MSFC in a critical component and experimental plan (Ref. 7),

I, B, Study Results and Conclusions (cont.)

are required to verify or improve the engine cycle power balance, reduce the engine development and operational risk, or increase the engine performance. The overall recommendations are summarized in Table III.

It should be recognized that all of the designs and data presented in this report represent the first iteration in the design analysis process. Schedule and funding limitations did not permit design iterations or incorporation of improvements that were suggested by this initial effort. The number of "loose ends" which remain as the result of these limitations are being documented in this report to facilitate their being addressed in future efforts.

TABLE III
TECHNOLOGY RECOMMENDATION SUMMARY

- ° Expander Cycle Engine Component Critical Technology Programs
Should Be Initiated To:
 - Reduce Risk
 - Verify Power Balance
 - Verify Performance
- ° Component Technology Should Address High-and Low-Thrust Operation
- ° Continue Point Design Studies to Optimize the Advanced Expander
Cycle Engine
- ° Conduct Detailed Design Analysis of a Breadboard Advanced Expander
Cycle Engine
- ° Fabricate and Test a Breadboard Expander Cycle Engine and its Components

II. INTRODUCTION

A. BACKGROUND

The Space Transportation System (STS) includes an Orbit Transfer Vehicle (OTV) that is carried into low-Earth orbit by the Space Shuttle. The primary function of this OTV is to extend the STS operating regime beyond the Shuttle to include orbit plane changes, higher orbits, geosynchronous orbits and beyond. The NASA and the DoD have been studying various types of OTV's in recent years. Data have been accumulated from the analyses of the various concepts, operating modes, and projected missions. With the inclusion of man in these transportation scenarios, it becomes necessary to reach for the safest and most fully optimized propulsion stage.

The purpose of this study was to generate a performance-optimized engine system design for a man-rated Advanced LOX/Hydrogen Expander Cycle Engine. This engine concept was originally conceived by ALRC on the OTV Phase A Engine Study, Contract NAS 8-32999, and recommended to NASA in October 1978. The recommendation was based upon a thorough evaluation of the engine's performance, envelope, reusability, and man-rating requirements, along with a desire to reduce the development risk of the OTV engine. Once approved by NASA, our engine cycle recommendation led to further evaluations of the advanced expander cycle engine concept, finally culminating in this Point Design Study effort.

B. ORBIT TRANSFER VEHICLE CHARACTERISTICS

The Manned Orbit Transfer Vehicle (MOTV) has, as its goal, the same basic characteristics as the Space Shuttle, i.e., reusability, operational flexibility, and payload retrieval, along with high reliability and low operating cost. This vehicle is planned to be a cryogenic stage, with the baseline design mission being a four-man, 30-day sortie to geosynchronous orbit (GEO). The required round trip payload to GEO and return to low-Earth

II, B, Orbit Transfer Vehicle Characteristics (cont.)

orbit (LEO) is 13,000 lbm. The weight of the OTV, including propellants and payload, cannot exceed 97,300 lbm. While an Orbiter of 100,000 lbm payload capability is assumed, the OTV must be capable of interim operation with the present 65,000 lbm Orbiter. The cargo bay dimensions of the 100,000 lbm Orbiter are assumed to be the same as those of the 65,000 lbm Orbiter, i.e., a cylinder 15 ft in diameter and 60 ft in length. The OTV cannot exceed 34 ft in length. The OTV is to be Earth-based and designed to return from geosynchronous orbit for rendezvous with the Orbiter in LEO. Both Aeromaneuvering Orbit Transfer Vehicles (AMOTV) and All-Propulsive Orbit Transfer Vehicles (APOTV) are considered for this mission. These vehicles are described in NASA Technical Memorandum TMX-73394, "Orbit Transfer Systems with Emphasis on Shuttle Applications - 1986-1991" (see Ref. 8).

C. ENGINE REQUIREMENTS

The requirements for the Manned Orbit Transfer Vehicle (MOTV) engine were derived from numerous NASA in-house and contracted studies. These requirements, specified by the Contract Statement of Work (SOW), are listed below and summarized in Table IV.

1. The engine shall operate as an expander cycle with liquid hydrogen and liquid oxygen propellants.
2. Engine vacuum thrust shall be 15K lb at an engine O₂/H₂ weight flowrate mixture ratio of 6.0.
3. Engine length with the two-position extendible nozzle retracted will be no greater than 60 in.

TABLE IV
OTV ENGINE POINT DESIGN REQUIREMENTS

- RATED VACUUM THRUST: 15,000 LB
- PROPELLANTS: HYDROGEN AND OXYGEN
- POWER CYCLE: EXPANDER
- TECHNOLOGY BASE: 1980 STATE-OF-THE-ART
- ENGINE MIXTURE RATIO: NOMINAL = 6.0 RANGE = 6.0 TO 7.0
- PROPELLANT INLET CONDITIONS:

		<u>H₂</u>	<u>O₂</u>
BOOST PUMP	NPSH, FT	15	2
	TEMP., °R	37.8	162.7
- SERVICE LIFE BETWEEN OVERHAULS: 300 CYCLES OR 10 HRS
- SERVICE FREE LIFE: 60 CYCLES OR 2 HRS
- ENGINE NOZZLE: CONTOURED BELL WITH EXTENDIBLE/RETRACTABLE SECTION
- MAXIMUM ENGINE LENGTH WITH NOZZLE RETRACTED: 60 IN.
- GIMBAL ANGLE: +15°, -6° PITCH
 ±6° YAW
- PROVIDE GASEOUS HYDROGEN & OXYGEN TANK PRESSURIZATION
- MAN-RATED WITH ABORT RETURN CAPABILITY
- MEET ORBITER SAFETY AND ENVIRONMENTAL CRITERIA
- MAX P_c DEVIATIONS: ±5% OF STEADY-STATE PRESSURE
- ADAPTABLE TO EXTENDED LOW-THRUST OPERATION (1.5kLBF)

II, C, Engine Requirements (cont.)

4. Engine design and materials technology are to be based on 1980 state-of-the-art criteria.
5. The engine must be capable of accommodating programmed and/or command variations in mixture ratio over an operating range of 6:1 to 7:1 during a given mission. The effects on engine operation and lifetime must be predictable over the operating mixture ratio range.
6. The propellant inlet temperatures shall be 162.7°R for the oxygen boost pump and 37.8°R for the hydrogen boost pump. The boost pump inlet NPSH at full thrust shall be 2 ft for the oxygen pump and 15 ft for the hydrogen pump.
7. The service-free life of the engine cannot be less than 60 start/shutdown cycles or two hours of accumulated run time, and the service life between overhauls cannot be less than 300 start/shutdown cycles or 10 hours of accumulated run time. The engine shall have provisions for ease of access, minimum maintenance, and economical overhaul.
8. When operating within the nominal prescribed range of thrust, mixture ratio, and propellant inlet conditions, the engine shall not incur chamber pressure oscillations, disturbances, or random spikes greater than ± 5 percent of the mean steady-state chamber pressure during its service life. Deviations to be expected in emergency modes shall be predictable.

II, C, Engine Requirements (cont.)

9. The engine nozzle is to be a contoured bell with an extendible/retractable section.
10. Engine gimbal requirements are to be $+ 15^\circ$ and -6° in the pitch plane and $\pm 6^\circ$ in the yaw plane.
11. The engine is to provide gaseous hydrogen and oxygen autogenous pressurization for the propellant tanks.
12. The engine is to be man-rated and capable of providing abort return of the vehicle to the Orbiter orbit.
13. The engine design shall meet all of the necessary safety and environmental criteria of being carried in the Orbiter payload bay and operating in the vicinity of the manned Orbiter.
14. The engine must be adaptable to extended low-thrust operation of approximately 1.5K lb vacuum thrust. Kitting of the engine's injectors, turbine flow area, and other constraining components may be considered, as may the inclusion of a heat exchanger to gasify the LOX for low-thrust operation. The engine mixture ratio shall be maintained as high as allowed for by cooling and power constraints, but no greater than 7:1.

In addition to the specified requirements, the Phase A OTV Engine Study (Ref. 2) identified design impacts resulting from the man-rating, safety, and reliability requirements. These are summarized in Table V. A multiple-engine installation is necessary to meet the crew safety requirements.

TABLE V
MAN-RATING, SAFETY, AND RELIABILITY IMPOSED REQUIREMENTS

- ° Engine should be Designed for a Multi-Engine Installation
(Preferably Twin Engines)
- ° Series-Redundant Main Propellant Valves Required
- ° Redundant Spark Igniter Required
- ° Dual Coils will be used on all Valves Identified by FMEA
as Single-Point Failures

II, C, Engine Requirements (cont.)

Series-redundant main propellant valves are required to assure that the engine will shut down and that leakage of propellant through the engine into the Orbiter's payload bay is inhibited. Redundant spark ignition is required to assure that the engine will start on all burns. Dual-coils are required to assure that the actuator will function and provide sufficient force to open critical valves.

All of the specified and derived requirements are presented in an OTV Design Requirements Handbook (Ref. 9) which should be considered a first cut at an engine specification of this type.

All of the specified and identified requirements were incorporated in our point design as part of this study.

D. PRINCIPAL ASSUMPTIONS AND GUIDELINES

The following principal assumptions and guidelines were provided by NASA/MSFC and were used to conduct this engine design study.

1. All engine designs and characteristics will be compatible with the OTV requirements and will be based on 1980 technology.
2. All dimensional allowances will be within Shuttle payload bay specifications, including dynamic envelope limits. (This does not preclude extendible nozzles.)
3. Since the engine and OTV will be designed to be returned to Earth in the Shuttle for subsequent reuse, reusability with minimum maintenance/cost for both unmanned and manned missions is a design objective.

II, D, Principal Assumptions and Guidelines (cont.)

4. The OTV engine shall be designed to meet all of the necessary safety and environmental criteria of being carried in the Shuttle payload bay and operating in the vicinity of the manned Shuttle.

E. STRUCTURAL DESIGN CRITERIA

The following minimum safety and fatigue-life factors were utilized. It is important to note that these factors are only applicable to designs whose structural integrity and adherence to required parameters has been verified by comprehensive structural testing in accordance with the factors specified below. Where structural testing is not feasible, more conservative design factors will be supplied by the procuring agency.

1. The structures shall not experience gross yielding (total net section) at 1.1 times the limit load, nor shall failure be experienced at 1.4 times the limit load. For pressure-containing components, failure shall not occur at 1.5 times the limit pressure.
2. Limit load is the maximum predicted external load, pressure, or combination thereof expected during the design life.
3. Limit life is the maximum expected usefulness of the structure expressed in time and/or cycles of loading.
4. The structure shall be capable of withstanding at least four times the limit life based on lower-bound fatigue property data.

II, E, Structural Design Criteria (cont.)

5. Pressure-containing components shall be pressure-tested at 1.2 times the limit pressure at the design environment, or appropriately adjusted to simulate the design environment, as a quality acceptance criterion for each production component prior to service use.

III. TASK DISCUSSIONS

This section presents the results, data, designs, and supporting analyses of each technical task performed in the conduct of this program. The work effort is separated by task and reported by task. It should be noted that many of the tasks and subtasks were conducted in parallel due to schedule and funding limitations. Therefore, it was not possible to conduct design iterations, with the result that the results of all tasks and subtasks have not been entirely incorporated into the engine design and data presented in this report. However, design and analysis recommendations have been made and documented so that future efforts can pick up where this initial design effort has left off. We highly recommend that further design definition be continued in order to optimize and fully characterize the Advanced Expander Cycle Engine.

A. TASK I - STEADY-STATE COMPUTER MODEL

The objective of this task was to provide a computer model of the engine system steady-state operation.

An existing ALRC computer model was modified to simulate the ALRC Advanced Expander Cycle Engine. This modified computer model, designated OTV MOD7, is a FORTRAN computer program which performs the engine cycle power balance and performance predictions for design and off-design operation of the engine. The off-design operation encompasses a mixture ratio range from 5 to 10 and thrust levels from the nominal 15,000 lbf to low-thrust operation at 1.5K lbf. This model was delivered to NASA/MSFC as part of Task IX, and the User's Manual was issued as a separate report (Ref. 5). This document describes the program, provides instructions for implementing and executing the program, describes the inputs and outputs, explains the program subroutines and their operation, and discusses the program error generated messages. In addition, a complete FORTRAN program listing, detailed computer generated flow charts, a sample output, and a card deck were submitted to the NASA/COR.

III, A, Task I - Steady-State Computer Model (cont.)

The computer model is compatible with the Univac 1108 computer and takes approximately 10 sec to run each case.

A sample program output for the OTV Expander Cycle Engine steady-state model is presented in Table VI. Engine performance, envelope, and weight data are displayed on one page, and the engine pressure schedule and power balance parameters are shown on the second page. This output represents the baseline parameters that have been updated to reflect the modifications that resulted from the study. The weight and envelope data shown are fixed values for the baseline engine and are not calculated in this version of the computer model. They are displayed for engine data summary purposes and can be changed to reflect design revisions by changing the program's inputs or constants.

The current baseline cycle modelled in the program is a fully regeneratively cooled (with LH₂) series turbines expander cycle. The power balance calculation is done by iterative determination of the fuel circuit turbine pressure ratio. The iteration is repeated until the resulting chamber pressure is equal to the specified chamber pressure. The power balance and the performance can be evaluated at rated and low-thrust operation at design and off-design mixture ratios. Baseline turbomachinery values are inputs to the program.

Procedures for calculating the performance of liquid propellant rocket engines have been formulated and recommended by the JANNAF Performance Standardization Working Group and are documented in CPIA No. 246 (Ref. 10). Two basic approaches, based on both "rigorous" and "simplified" procedures, have been recommended.

TABLE VI
 OTV EXPANDER CYCLE ENGINE STEADY-STATE MODEL SAMPLE OUTPUT (Sheet 1 of 2)

ENGINE PERFORMANCE		ENGINE WEIGHTS (LSM)	
1. THRUST (LBS)	15000.00	1. CHAMBER	7.80
2. CHAMBER PRESSURE (PSIA)	1230.02	2. INJECTOR	30.00
3. MIXTURE RATIO	8.00	3. CHAMBER	47.30
4. TOTAL FLOW RATE (LBM/SEC)	31.55	4. COPPER NOZZLE	27.00
5. LOX FLOW RATE (LBM/SEC)	27.04	5. TURE PICLE NOZZL	29.40
6. FUEL FLOW RATE (LBM/SEC)	4.51	6. RAD NOZZLE	82.00
7. ISP (SEC/SEC)	486.11	7. NOZZLE DEPLOY SYS	72.00
8. NOZZLE EFFICIENCY	.9929	8. FUEL RICH PREBURNERS	.00
9. ENERGY RELEASE EFFICIENCY	1.0000	9. VALVES AND ACTUATORS	72.70
10. KINETIC EFFICIENCY	.9957	10. LOX BOOST PUMP	5.60
11. BOUNDARY LAYER LOSS (LBS)	163.32	11. LH2 BOOST	8.50
12. ISP EFFICIENCY (SEC/SEC)	475.40	12. LOX IPA (HI SPD)	26.00
13. THRUST TO WEIGHT RATIO	26.11	13. LH2 IPA (HI SPEED)	26.00
		14. MISC. VALVES	12.60
		15. LINES	37.00
		16. IGNITION SYSTEM	9.20
		17. ENGINE CONTROLLER	35.00
		18. MISCELLANEOUS	37.00
		19. HEAT EXCHANGER	5.00
		20. TOTAL ENGINE WEIGHT	514.00

ENGINE SIZE (IN AND IN**2)

1. CHAMBER LENGTH	7.000
2. CHAMBER DIAMETER	4.000
3. CHAMBER LENGTH	18.000
4. NOZZLE LENGTH	84.000
5. TURE PICLE NOZZLE	60.000
6. RAD NOZZLE	100.000
7. NOZZLE DEPLOY SYS	50.000
8. FUEL RICH PREBURNERS	1.000
9. VALVES AND ACTUATORS	40.000
10. LOX BOOST PUMP	11.000
11. LH2 BOOST	172.000
12. LOX IPA (HI SPD)	81.000
13. LH2 IPA (HI SPEED)	63.000
14. MISC. VALVES	100.000

ORIGINAL PAGE IS
 OF POOR QUALITY

TABLE VI (cont.)

POWER BALANCE
EXPANDER CYCLE:
SERIES TURBINES
NO REHEAT
BOOST PUMPS

PRESSURE SCHEDULE (PSIA)

	FUEL CIRCUIT	LOX CIRCUIT
1. PUMP INLET	48.59	48.58
2. PUMP DISCHARGE	2515.92	1439.26
3. PUMP DISCHARGE	2567.00	1487.74
4. CIRC PRESSURE DROP	11.08	25.19
5. VALVE INLET	2549.13	1462.55
6. VALVE PRESSURE DROP	24.12	14.73
7. VALVE OUTLET	2525.11	1447.82
8. LINE PRESSURE DROP	31.23	15.11
9. COOLANT JACKET INLET	2492.88	--
10. COOLANT JACKET PRESSURE DROP	90.53	--
11. COOLANT JACKET OUTLET	2402.34	--
12. LINE PRESSURE DROP	31.23	--
13. FUEL CIRCUIT TURBINE INLET	2372.69	--
14. FUEL CIRCUIT TURBINE PRESSURE RAT.	1551.50	--
15. FUEL CIRCUIT TURBINE EXIT	1219.19	--
16. REHEAT TURBINE PRESSURE DROP	13.14	--
17. CIRC PRESSURE INLET	1206.05	--
18. CIRC PRESSURE TURBINE INLET	1192.91	--
19. CIRC PRESSURE TURBINE PRESSURE RAT.	1182.40	--
20. CIRC PRESSURE TURBINE EXIT	1062.40	--
21. REHEAT PRESSURE DROP	34.09	--
22. REHEAT INLET	1028.31	1432.70
23. REHEAT PRESSURE DROP	110.41	214.80
24. REHEAT INJECTION FACE	1217.90	1217.90
25. REHEAT PRESSURE DROP	17.53	17.88
26. CHAMBER PRESSURE	1200.32	1200.02

FLOW RATES (LBM/SEC)
TEMP DROP (DEGREES R)
CIRCUIT (LBM-R)

(FC=FUEL CIRCUIT)
(CC=OX CIRCUIT)

(T-S=TOTAL TO STATIC TEMP)
(T=TOTAL TEMP)

HORSEPOWERS
AND EFFICIENCIES

(FC=FUEL CIRCUIT)
(CC=OX CIRCUIT)

(T-S=TOTAL TO STATIC TEMP)
(T=TOTAL TEMP)

1. FC TURBINE FLOW	4.24
2. CC TURBINE FLOW	4.24
3. FC TURB T DROP (T-S)	64.01
4. CC TURB T DROP (T-S)	16.74
5. FC TURB INLET T (T)	535.60
6. FC TURB EXIT T (T)	485.84
7. CC TURB IN T (T)	485.84
8. CC TURB EXIT T (T)	474.67
9. DRIVE GAS CP	3.652
10. DRIVE GAS GAMMA	1.395
11. BYPASS FLOW	.27

1. FC TURB HORSEPOW	1576.25
2. CC TURB HORSEPOW	244.84
3. FC PUMP SHP	1276.05
4. CC PUMP SHP	244.24
5. FC TURB EFF	.758
6. CC TURBINE EFF	.567
7. FUEL PUMP EFF	.633
8. OX PUMP EFF	.625
9. OX FLOW	27.54
10. TOTAL FUEL FLO	4.51

III, A, Task I - Steady-State Computer Model (cont.)

The rigorous approach is intended to provide the best currently available analytical calculation procedure for absolute performance prediction. It consists of 17 detailed steps, using reference computer programs to model fundamental fluid and combustion processes. While these reference computer programs utilize the best available mathematical formulations of the mechanistic combustion processes, the procedure is costly in terms of both engineering man-hours and computer run time.

The simplified approach provides a very cost-effective procedure, with almost comparable accuracy when properly utilized. This procedure is described in Section 3 of Reference 10. As depicted schematically in Figure 3, it consists of starting with one-dimensional equilibrium specific impulse (I_{sp0DE}) and correcting the performance downward for contributing component performance losses. Subtracting the kinetic, divergence, and boundary layer losses from I_{sp0DE} in Figure 3 provides a hypothetical "perfect injector performance" that is degraded for the real nozzle losses. This performance is further degraded by the energy release loss which accounts for the injector-related performance inefficiencies due to incomplete propellant vaporization and/or non-uniform gas-phase mixing. When chamber pressure becomes too high, it may become necessary to provide auxiliary cooling from the combustion gas-side through such means as barrier or zone mixture ratio cooling, film cooling, or transpiration cooling. This loss is not applicable to the OTV Expander Cycle Engine.

The simplified JANNAF performance prediction methodology relationships have been incorporated into the computer program. This program and other versions were developed by ALRC in-house efforts during the last two years. The simplified JANNAF performance methodology predictions have been calibrated for O_2/H_2 propellants with high exit area ratio nozzles by using the expander cycle RL-10 and high-pressure, staged combustion Advanced

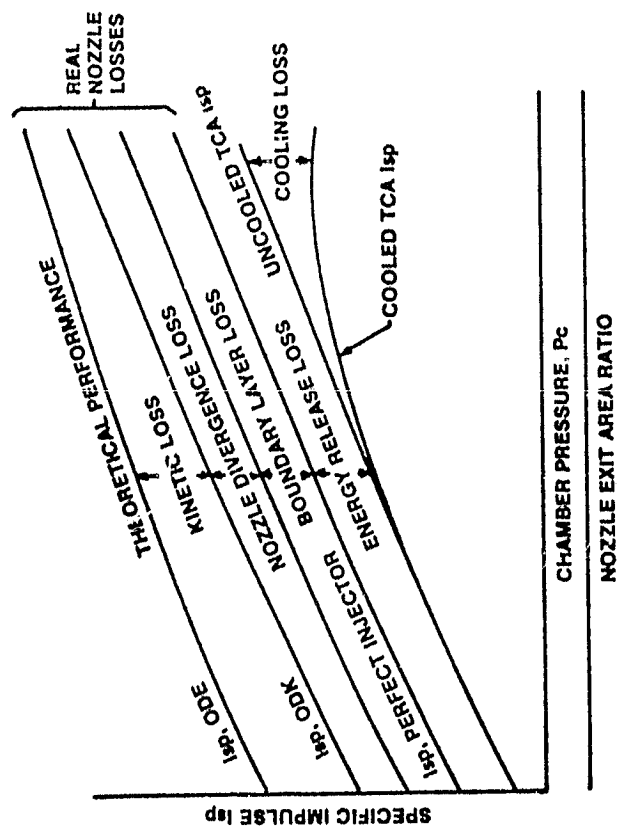


Figure 3. Simplified JANNAF Performance Methodology Predicts Engine Cycle Performance

III, A, Task I - Steady-State Computer Model (cont.)

Space Engine (ASE) experimental test data. The analysis correlated both the experimental ASE and RL-10 delivered performance well within $\pm 1\%$ Isp. Thus, this model is invaluable in accurately determining the delivered performance.

Transient behavior is not included in this model but is evaluated by the Task IV computer model. In addition, more detailed steady-state evaluations can be conducted with the transient computer model described in Section III.D. The transient model has more complete analytical descriptions and simulations of all engine components than the simplified steady-state model. The steady-state condition is a special case in the transient model.

The steady-state power balance model (OTV MOD7) is recommended for preliminary design studies, while the steady-state case should be evaluated on the transient model during detailed engine design studies.

B. TASK II - HEAT TRANSFER, STRESS, AND FLUID FLOW ANALYSIS

The objective of this task was to provide the analyses required to define the engine and engine component mechanical design parameters and support the engine model simulations. This included the heat transfer, materials, stress, and fluid flow analyses of the thrust chamber and nozzle, oxygen turbopump, and the hydrogen turbopump. The analyses conducted and the results obtained are discussed in this section.

1. Heat Transfer Analysis

The Phase A and Phase A Extension Studies provided the foundation for the thrust chamber assembly thermal design. The results are summarized herein.

III, B, Task II - Heat Transfer, Stress, and Fluid Flow Analysis (cont.)

The Advanced Expander Cycle Engine (AEC) coolant flow schematic is shown in Figure 4. This coolant scheme was selected as a result of optimization studies conducted for the Phase A and Phase A Extension OTV Engine Study work (Ref. 1 and 2). Eighty-five (85) percent of the hydrogen flow is used to cool the chamber in a single pass from an area ratio of 10.6:1 to the injector end. Fifteen (15) percent of the hydrogen is used to cool the fixed nozzle in parallel with the chamber in a two-pass tube bundle. The temperature data on the figure is shown for the design point thrust and mixture ratio of 15,000 lb and O/F = 6.0. The thermal analysis results are summarized in Table VII for the design and off-design mixture ratio conditions. Pressure drop data shown pertains to the losses in the channels or tubes only and does not include the manifold losses.

Expander cycle engines depend upon high heat input to the combustion chamber walls to achieve the system power balance. Thus, the selection of thrust chamber geometry (contraction ratio and combustor length) is influenced by engine cycle considerations. Studies show that the total heat load (coolant temperature rise) is increased as L' increases and contraction ratio decreases. This increases the turbine inlet temperature but increases system pressure drops. Optimization studies (Ref. 2) resulted in the selection of a contraction ratio of 3.66 and a combustor length (L') of 18 inches.

A columbium radiation-cooled nozzle extension was selected during the Phase A studies and baselined for this study. Analyses, facilitated by the most recent experience with the OMS Engine (OMS-E), show that columbium with an oxidation-resistant coating will meet the engine's service life requirements. The minimum attachment area ratio for the design point thrust and chamber pressure for the columbium nozzle extension at an attachment point wall temperature of 2450°F is approximately 100:1. These wall temperature criteria were for the OMS-E nozzle extension which was designed to meet a

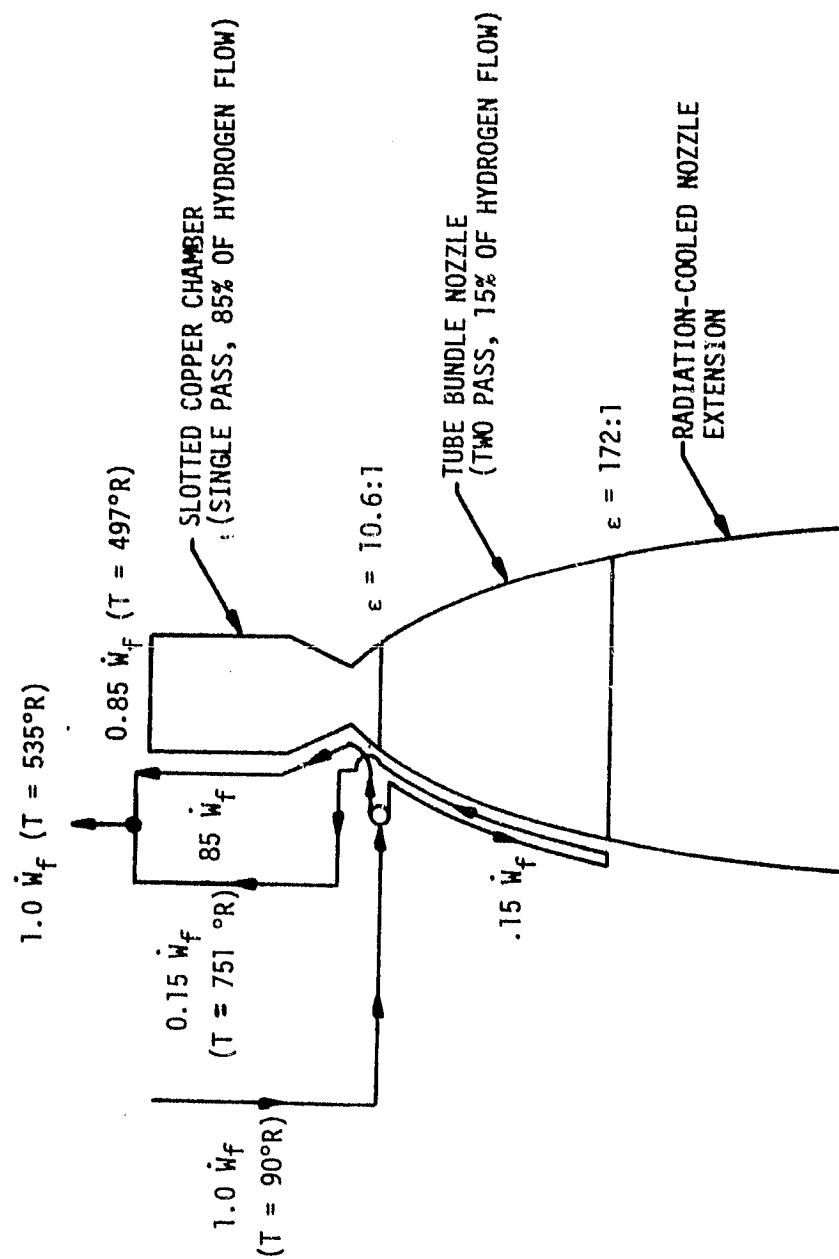


Figure 4. AEC Engine Coolant Flow Schematic

TABLE VII
AFC THERMAL ANALYSIS DESIGN AND OFF-DESIGN O/F SUMMARY AT RATED THRUST

	<u>Mixture Ratio</u>	
	<u>6.0</u>	<u>7.0</u>
Combustion Chamber Coolant Flowrate, lb/sec	3.816	3.358
Slotted Copper Chamber Area Ratio	10.6	10.6
Chamber Pressure Drop, psia	92	76
Coolant Inlet Temperature, °R	90	90
Chamber Coolant Temperature Rise, °R	407	431
Fixed Tube Bundle Nozzle Flowrate, lb/sec	0.674	0.592
Tube Bundle Nozzle Area Ratio	172	172
Tube Bundle Coolant Pressure Drop, psia	11	8
Tube Bundle Coolant Temperature Rise, °R	661	672
Turbine Inlet Temperature, °R	535	557
Chamber Length * 18 in.		
Contraction Ratio * 3.66		

III, B, Task II - Heat Transfer, Stress, and Fluid Flow Analysis (cont.)

4000 cycle life (i.e., 1000 cycles x a safety factor of 4). The Point Design Engine's nozzle extension attachment point is 172:1. The selection of this point provides a natural interface between the nozzle tube bundle and extendible nozzle, allows for slightly more coolant heat input, and provides service life design conservatism.

Thermal analyses were also performed for the low-thrust condition. They show that the chamber life at low-thrust operation is not penalized and is, in fact, better. The tube bundle must be designed for the low-thrust operating point in order to meet the life requirement. This results in smaller, higher pressure drop tubes than would have been necessary if the tube bundle had been designed for the rated thrust condition. However, the higher pressure drop tubes do not present a problem and do not penalize the engine at rated thrust because the tube bundle pressure drop, which is in parallel with the chamber, is on the order of 10 psi compared to a chamber coolant pressure drop in excess of 90 psi. The coolant jacket pressure drop and exit temperature data are plotted as a function of thrust on Figures 5 and 6.

Low-thrust operation at 10% of rated thrust was considered feasible from a cooling standpoint. An orifice downstream of the coolant jacket is recommended to maintain the coolant jacket exit pressure above the critical pressure of hydrogen (188 psia). This orifice is required at low thrust to avoid the problems associated with two-phase coolant flow.

2. Thrust Chamber Assembly Design Analysis

Thermodynamic, hydraulic, and stability analyses were also undertaken to support the mechanical design of the TCA (Thrust Chamber Assembly) components. These analyses were refinements to the Phase A work.

RATED VACUUM THRUST = 15,000 LB
MIXTURE RATIO = 6.0

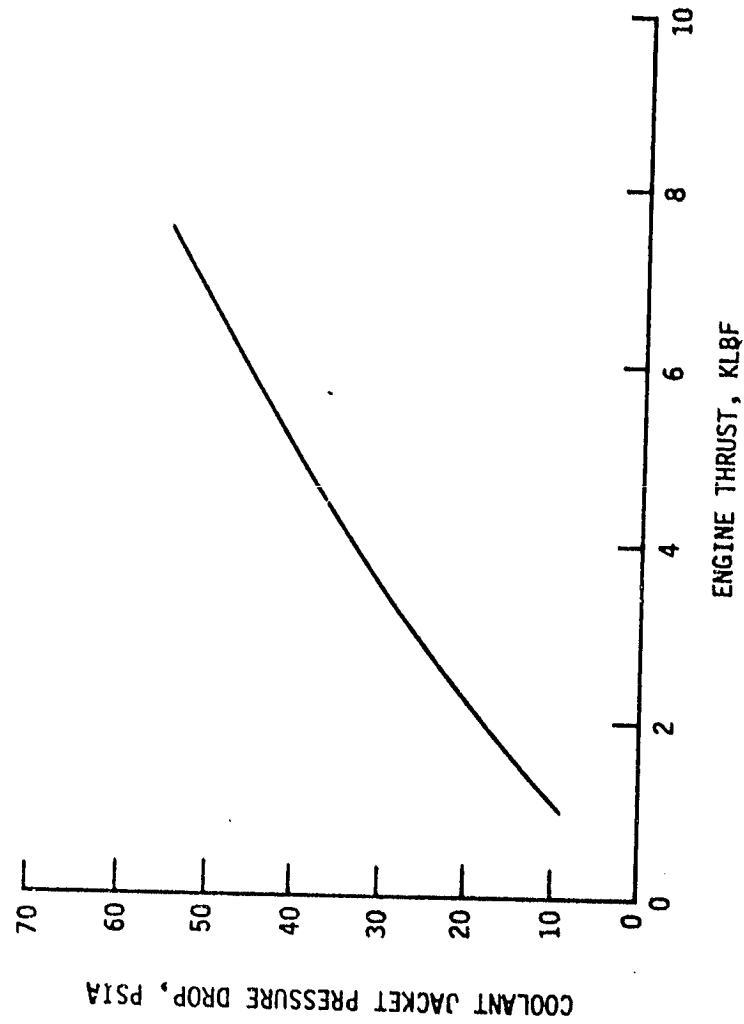


Figure 5. Coolant Jacket Pressure Drop vs Thrust

RATED THRUST = 15,000 LB

ENGINE MR = 6.0

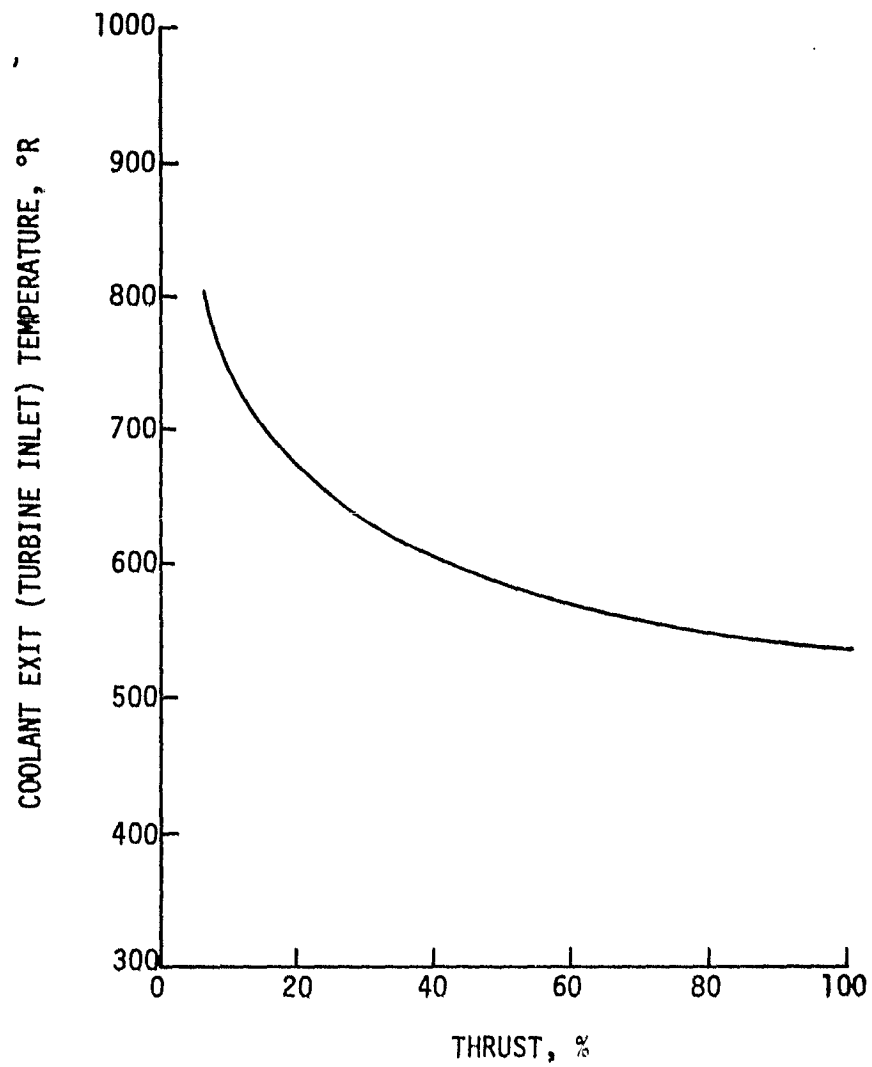


Figure 6. Effect of Low-Thrust Operation Upon Coolant Exit Temperature

III, B, Task II - Heat Transfer, Stress, and Fluid Flow Analysis (cont.)

The recommended configuration is a swirl coaxial injector with characteristics as shown in Table VIII. Recommended are eighty-four elements that are arranged in four rows (circles). The oxidizer flows through the center element which has a diameter of 0.1 inch. The hydrogen flows through the annulus surrounding the oxidizer element. The resonator cavity design recommendations are based upon design experience obtained on the ALRC OMS and ITIP programs. The cavity is designed so that dynamic chamber pressure oscillations do not exceed $\pm 5\%$.

The recommended chamber geometric parameters are shown in Table IX and described schematically in Figure 7. The nozzle contour data are summarized in Table X.

A chug stability margin analysis of the OTV engine point design was also conducted at $O/F = 6.0$. This analysis was a more rigorous refinement, using a standard chug analysis program to confirm the preliminary estimates of Reference 3. The predicted stability margin is shown in Figure 8. The marginal chug stability threshold is predicted to occur around $P_c = 570$ psia or at approximately 47% thrust. Since this value is in good agreement with the preliminary estimate made in Reference 3, the previous conclusions and recommendations arrived therein are valid. These conclusions are that an injector "kit" is required to operate the engine at a thrust level lower than 50% of its rated value and that 10% of rated thrust operation is feasible. The recommended injector "kits" are smaller diameter oxidizer coaxial injection elements. These smaller elements are required to increase the oxidizer pressure drop and to avoid chugging instability.

TABLE VIII
OTV INJECTOR DESIGN PARAMETERS

Injection Element Type:	Swirl Coaxial Element
Coaxial Element Quantity:	84
No. Rows:	4 (30 + 24 + 18 + 12 = 84)
Oxidizer Metering Orifice Dia. =	.100 (in.)
Oxidizer Swirl Cone Angle =	30° half angle
Oxidizer Element Tip OD/Fuel Annulus ID =	.150 (in.)
Fuel Annulus OD =	.200 (in.)
Oxidizer Element Tip Recess =	.100 (in.)
Resonator	
No. of Cavities =	12
Cavity Depth =	1.0 (in.)
Width =	0.4 (in.)
Overlap =	0.125 (in.)

TABLE IX
OTV CHAMBER GEOMETRY

Chamber Length, L'	=	18.0 (in.)
Chamber Diameter	=	5.34 (in.)
Throat Diameter	=	2.79 (in.)
Upstream Radius = 1.0 RT	=	1.395 (in.)
Convergent Inlet Radius = 3.0 RT	=	4.185 (in.)
Alpha-Inlet Angle, α_i	=	20°
Downstream Radius = 1.0 RT	=	1.395
Downstream Throat Tangency Angle, θ_t	=	41°

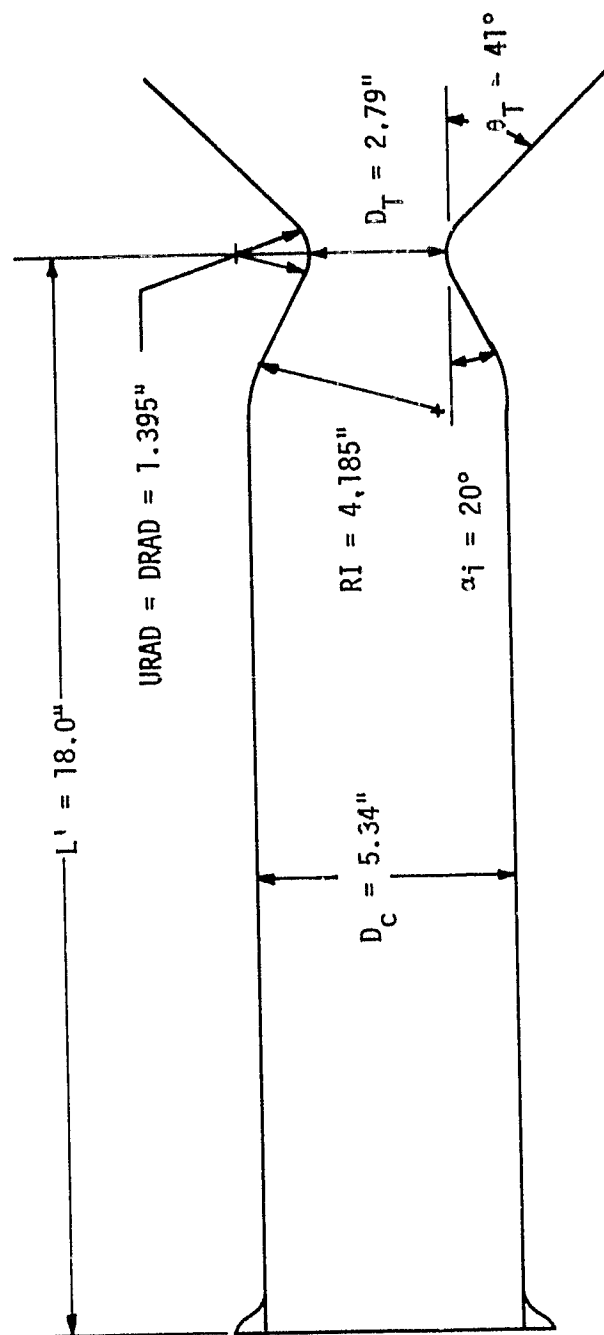


Figure 7. Combustion Chamber and Throat Geometry

TABLE X
RAO NOZZLE CONTOUR DATA

<u>Radius In.</u>	<u>Length In.</u>	<u>Area Ratio</u>
1.395	0	1.0
2.280	1.54	2.67
3.501	3.00	6.29
4.444	4.21	10.2
6.444	7.08	21.3
10.379	14.05	55.4
14.798	24.19	112.5
18.430	34.75	174.5
22.228	48.54	253.9
26.254	67.47	354.2
29.166	85.39	437.1
30.343	94.17	473.1

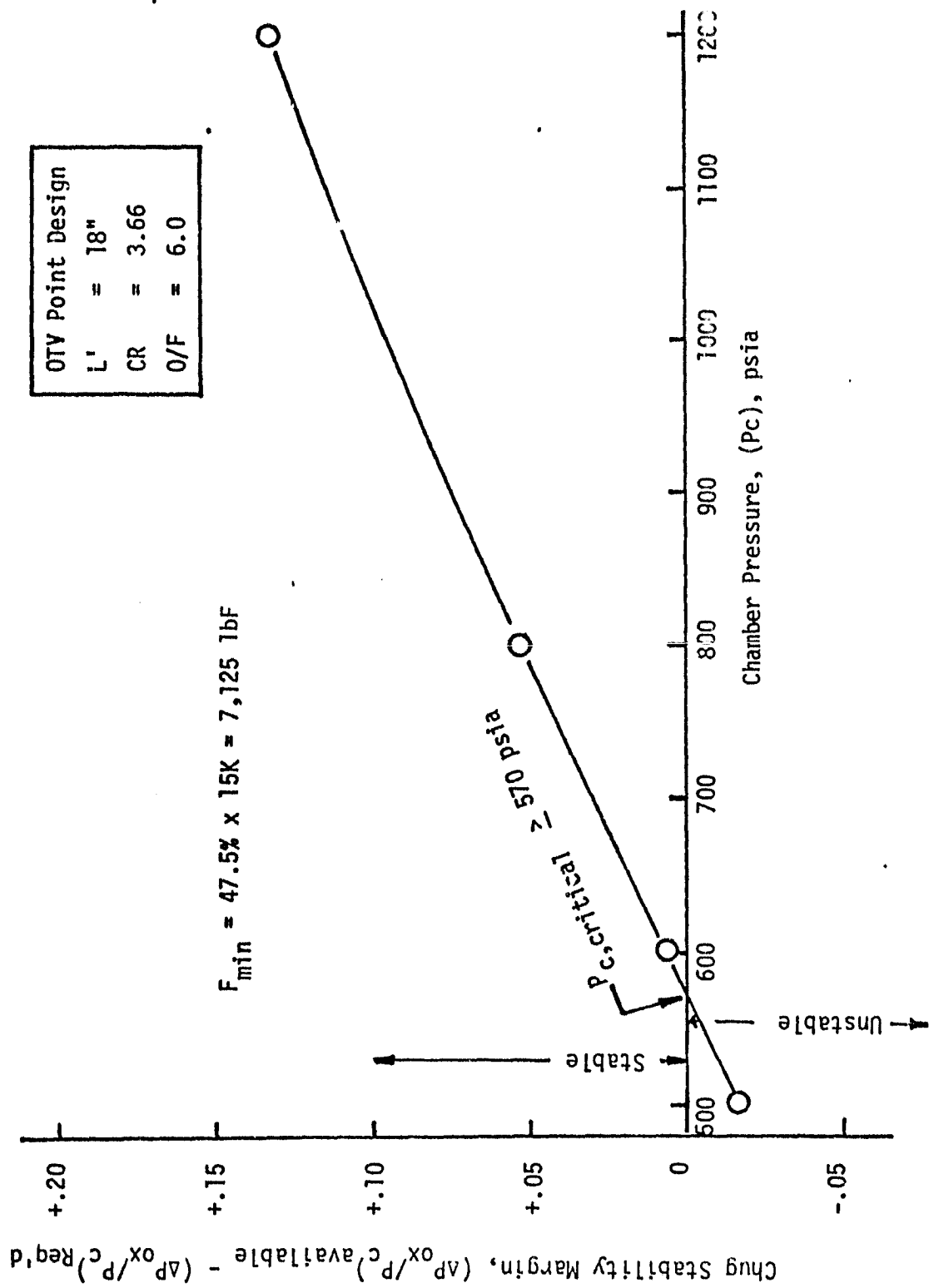


Figure 8. Predicted Chug Stability Threshold

III, B, Task II - Heat Transfer, Stress, and Fluid Flow Analysis (cont.)

3. Structural Analysis

This section summarizes the results of stress and low-cycle fatigue evaluations of the engine and its components.

a. Thrust Chamber Structural Analysis

Stress and low-cycle fatigue analyses were performed to substantiate the structural adequacy of the baseline chamber design. The chamber is a slotted configuration. The channel geometries at various locations throughout the chamber were obtained from thermal analysis and are summarized below.

° Throat

Slot Width = 0.04 in.

Slot Depth = 0.121 in.

Web (land) Thickness = 0.04 in.

Wall Thickness = 0.030 in.

° Cylindrical Section

Slot Width = 0.070 in.

Slot Depth = 0.256 in.

Web (land) Thickness = 0.081 in.

Wall Thickness = 0.030 in.

The chamber material is zirconium copper, with properties conforming to Figure 9. The chamber outer shell (closeout) material is electroformed nickel, with properties as shown in Figure 10.

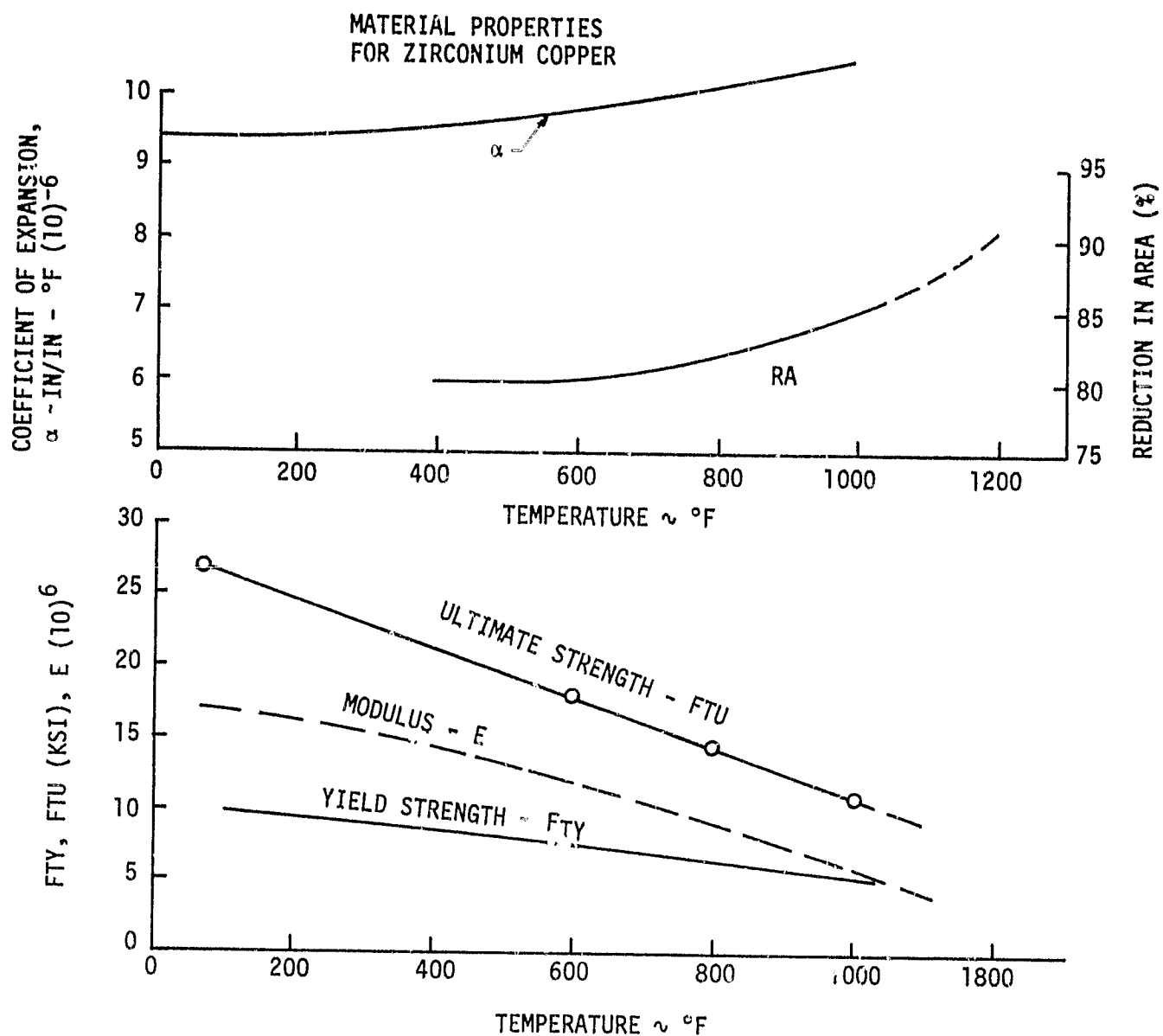


Figure 9. Mechanical Properties of Zirconium Copper

ORIGINAL PAGE IS
OF POOR QUALITY

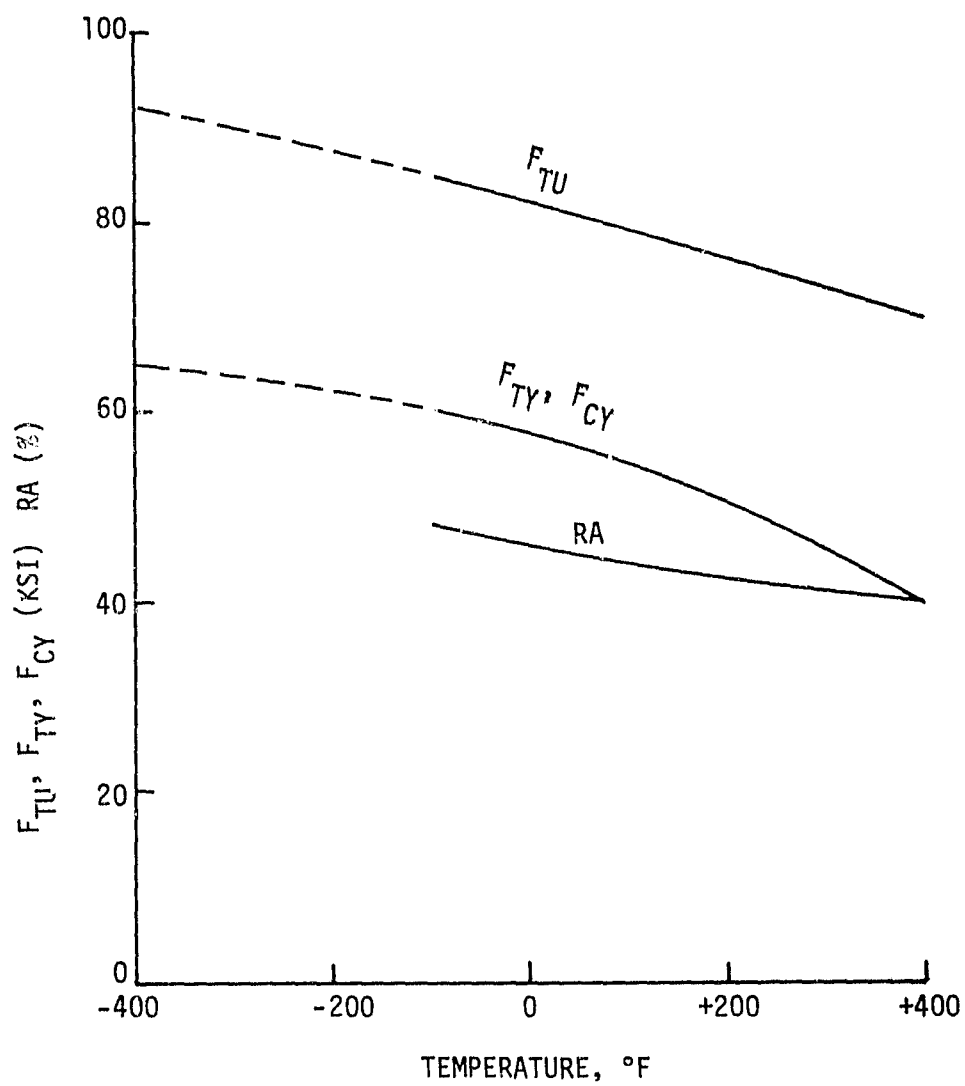
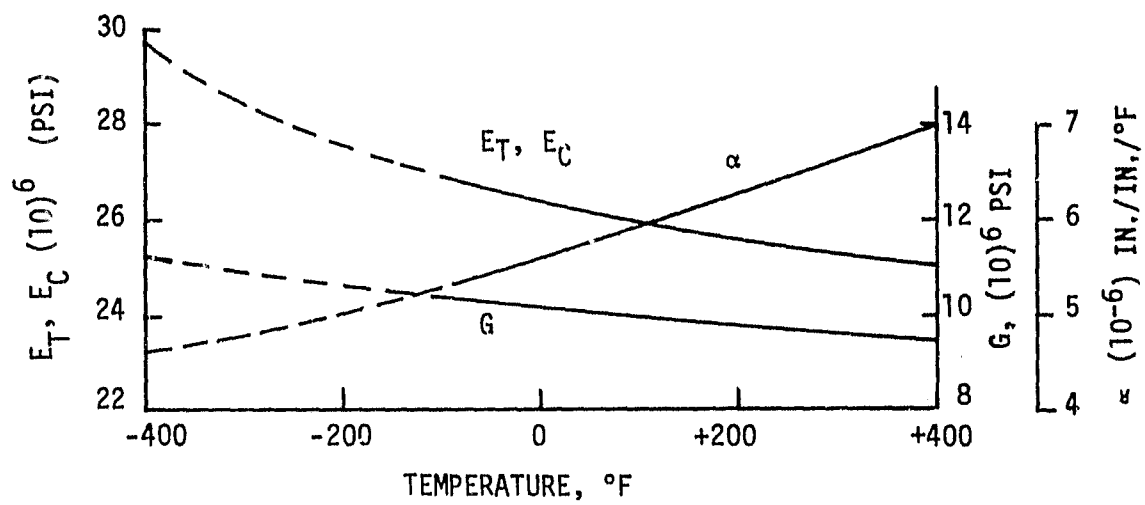


Figure 10. Mechanical Properties of Electroformed Nickel

III, B, Task II - Heat Transfer, Stress, and Fluid Flow Analysis (cont.)

The results indicate that the zirconium copper liner is structurally adequate to sustain the predicted differential pressures. The electroformed nickel closeout is assumed to carry all pressure hoop membrane loads, and the required thickness was determined on that basis. Minimum closeout thickness is 0.035 in. for the throat region, and 0.070 in. for the cylindrical section.

The low-cycle fatigue prediction is based on an elastic/plastic iterative plane strain solution of wall sections taken from the throat and cylindrical regions. The predicted service life (N_f) for the chamber is based on the maximum effective strain, determined for either section by using a factor of 4 on the lower-bound design curve for zirconium copper shown in Figure 11. Results determined from this investigation are presented in Table XI. The design was limited to a gas-side wall temperature of 800°F.

It is recommended that an axisymmetric finite element model of the chamber, throat, and nozzle be used to conduct this analysis in support of the next design iteration.

b. Main LOX Turbopump Assembly (TPA) Structural Analysis

(1) LOX TPA Impeller and Turbine Rotor Stress Analysis

The main LOX TPA impeller and rotor were analyzed to determine their respective structural adequacy at the steady-state operating speed of 34,720 RPM and in their thermal environments. The impeller steady-state environment is liquid oxygen at -290°F, while the turbine rotor operates at steady state with gaseous hydrogen at 60°F. Nitronic-50 was selected as the material for the impeller and rotor for this first analysis because it is compatible with both the hydrogen and oxygen environments and is sufficiently strong to withstand the design loads.

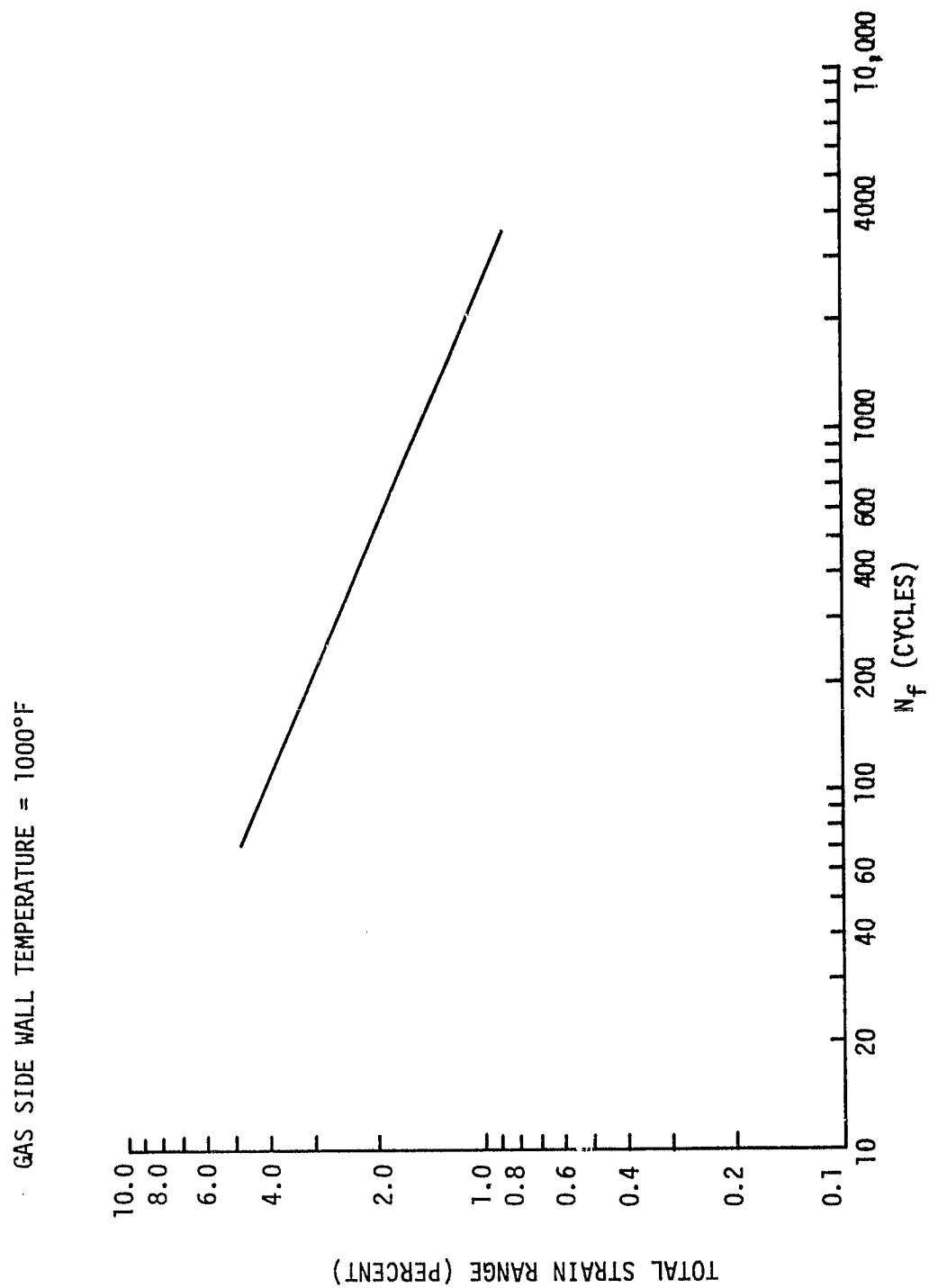


Figure 11. Low-Cycle Fatigue, Lower-Bound Design Curve for Zirconium Copper

TABLE XI
CHAMBER LOW-CYCLE THERMAL FATIGUE RESULTS

<u>Location</u>	<u>T_{GS}</u> (°F)	<u>T_{BS}</u> (°F)	<u>EFNI</u> <u>t(IN)</u>	<u>ε_T</u> (%)	<u>N_f</u> <u>Cycles</u>	<u>N_{REQ}</u> <u>Cycles</u>	<u>K_E</u>
Throat	615	-219	.035	1.11	460	300	1.4
Cylinder	757	33	.070	1.265	350	300	1.87

T_{GS} = Gas-Side Temperature

T_{BS} = Backside Temperature

EFNI t = Electroformed Nickel Closeout Thickness

ε_T = Total Strain

N_f = Number of Cycles (Includes factor of 4)

K_E = Strain Concentration Factor

III, B, Task II - Heat Transfer, Stress, and Fluid Flow Analysis (cont.)

A finite element computer program was used to analyze these components. The two-dimensional models for the impeller and rotor are shown in Figures 12 and 13, respectively.

The results of this analysis show that the Nitronic-50 impeller and rotor have positive margins of safety under the operating conditions. The minimum margins of safety were calculated to be 2.53 for the impeller and 0.48 for the turbine rotor. Hence, the designs are structurally adequate.

A-286 bolts are used to tie down the impeller and rotor disks. A 260 ± 5 in.-lb preload is considered adequate to hold both the impeller and turbine rotor with positive bolt margins.

(2) LOX TPA Shaft Stress Analysis

The LOX TPA shaft was analyzed in two parts: (1) the turbine end shaft and (2) the pump impeller shaft. The shaft was assumed to be made of Nitronic-50 with an A-286 through bolt. (See Figure 27 of Section III,C, ALRC Drawing number 1191999.)

The maximum effective stress found in the turbine end shaft is 9,650 psi which allows for an ample 7.4 margin of safety. Predicted fatigue life, using this stress level with appropriate stress concentration factors applied, is greater than the required $8.3 (10)^7$ cycles. Determination of the number of cycles required was based upon the 10-hour service life as follows:

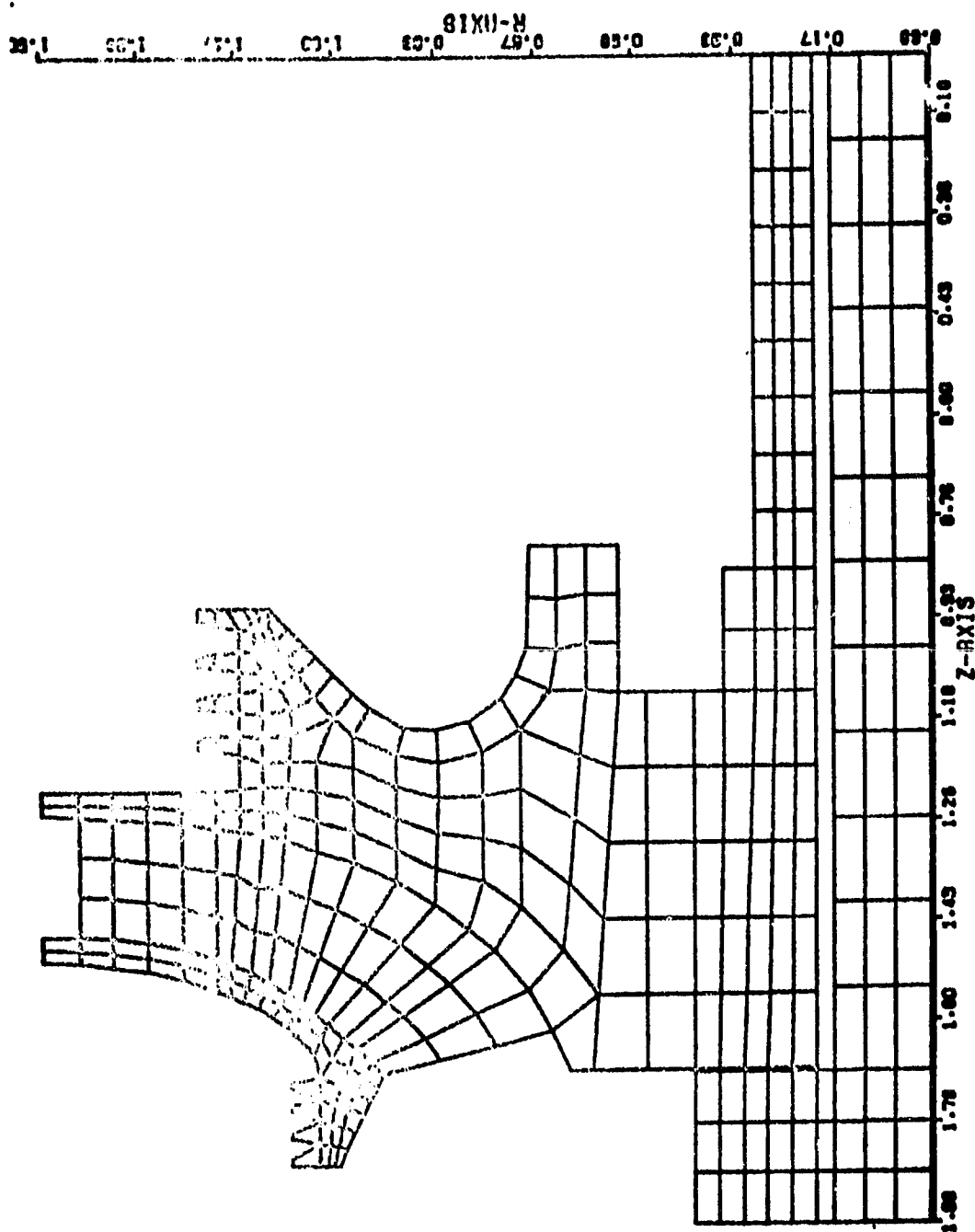


Figure 12. LOX TPA Impeller Computer Model Geometry

ORIGINAL PAGE IS
OF POOR QUALITY

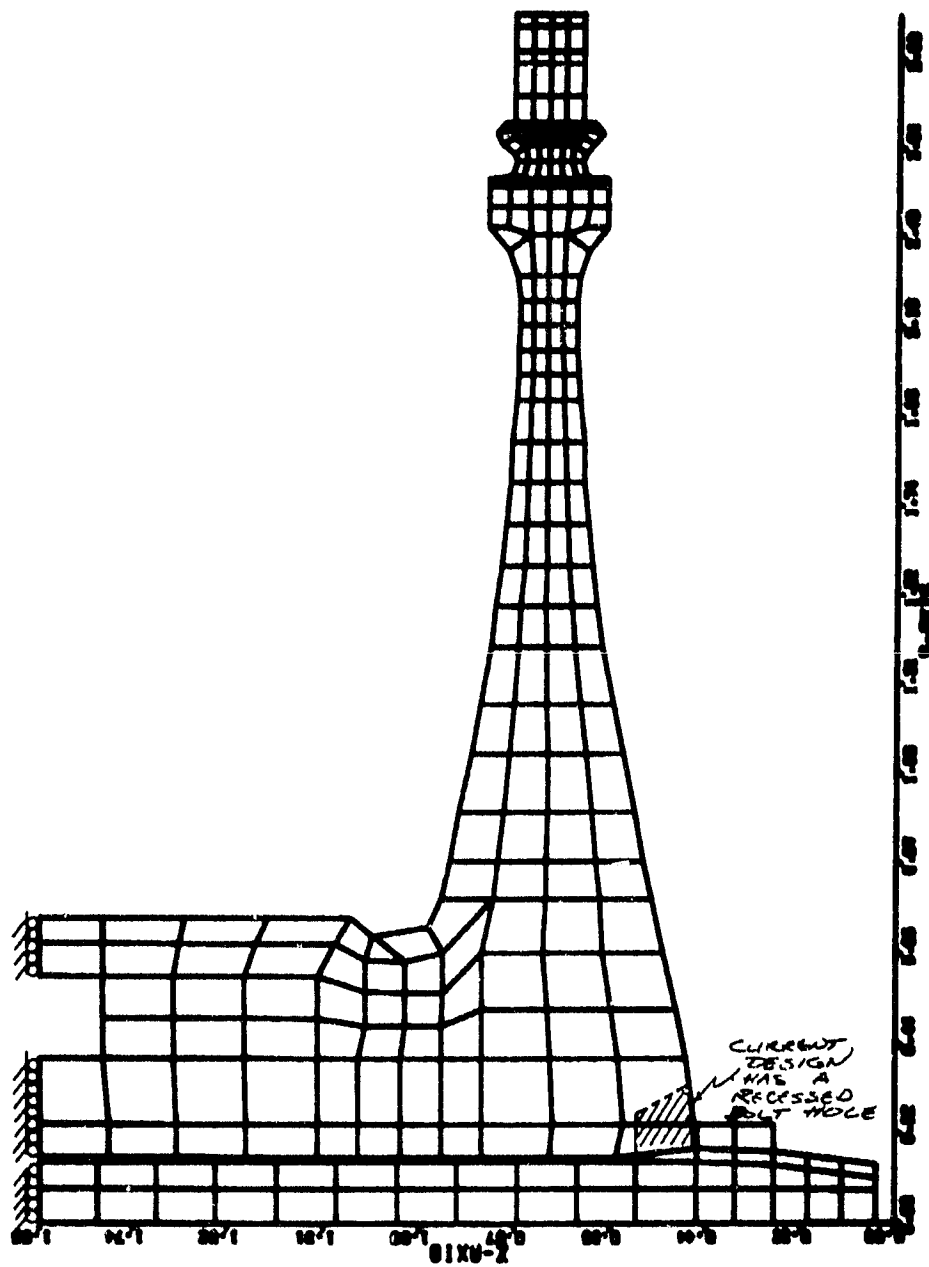


Figure 13. LOX TPA Turbine Rotor Computer Model Geometry

III, B, Task II - Heat Transfer, Stress, and Fluid Flow Analysis (cont.)

$$N = 34720 \text{ RPM} \times 10 \text{ HRS} \times \frac{60 \text{ MIN.}}{\text{HR}} \times \frac{1 \text{ CYCLE}}{\text{REV}}$$

$$N = 2.08 (10^7) \text{ Cycles W/O Factor of 4}$$

$$N_{REQ} = 4 (2.08 [10]^7) = 8.33 (10)^7 \text{ Cycles}$$

A maximum effective stress in the impeller shaft equal to 44,786 psi was found in the spline runout region. The minimum margin of safety, based on the yield strength at an operating temperature of -320°F, is 1.52.

It was concluded that the OTV LOX turbopump shaft is capable of meeting the structural and fatigue-life requirements established for the component.

(3) LOX TPA Housing Stress Analysis

The LOX TPA housing was analyzed in four major parts: (1) the turbine inlet manifold torus, (2) the turbine exit manifold torus, (3) the turbine end spherical dome, and (4) the pump inlet housing flange. (See Figure 27 of Section III,C.) Nitronic-50 was assumed to be the housing material. The following results were obtained:

(a) Turbine Inlet Manifold Torus

Maximum hoop membrane stress is 9,268 psi. The margin of safety for this stress level, based on ultimate strength for Nitronic-50, is 7.3.

III, B, Task II - Heat Transfer, Stress, and Fluid Flow Analysis (cont.)

(b) Turbine Exit Manifold Torus

Maximum hoop membrane stress is 12,185 psi.

The margin of safety is 5.4.

(c) Turbine Exit Manifold Spherical Dome

Maximum hoop membrane stress is 12,000 psi.

The margin of safety is 5.4.

A flaw growth analysis indicates that a 0.07-in. flaw depth, equivalent to 70% of dome wall thickness, will not propagate to a through-flaw condition during a predicted service of 300 cycles including a factor of 4.

On the basis of this preliminary evaluation, the LOX TPA housing was found to be structurally capable of sustaining the predicted pressure loading.

The following recommendations are made on the basis of this preliminary stress analysis:

° Exit Manifold Flange Bolts

A minimum of 28 1/4 in. - 28 ϕ bolts are required. This requirement is based on the flange dimensional constraints and on a yield strength allowable bolt load.

III, B, Task II - Heat Transfer, Stress, and Fluid Flow Analysis (cont.)

- ° Pump Inlet Housing Flange

A minimum of 15 1/4 in. - 28 ϕ bolts is considered adequate.

- ° In the follow-on design phase, a detailed two-dimensional finite element analysis of the housings, flanges, and bolts is essential.

- ° The high-pressure torus must be evaluated with three-dimensional finite element analyses.

(4) LOX TPA Structural Analysis Summary

A summary of the major components analyzed, along with their respective minimum calculated margins of safety, is presented in Table XII. Nitronic-50 was assumed as the principal material for all components.

It should be recognized that this analysis was intended to provide preliminary stress information for ascertaining the feasibility of the design. In view of this intent, the minor design and load changes that were made as the design effort progressed were not necessarily included in these analyses. Nonetheless, the analyses have been conducted in sufficient depth to allow the LOX TPA to be rated as a good first iteration design. For the next design phase, in addition to refining geometry and loads, the following items should be added to the structural analysis effort:

TABLE XII
MAIN LOX TPA MARGINS SUMMARY

<u>Component</u>	<u>Material</u>	<u>Margin of Safety</u>
1. Impeller	Nitronic 50	2.53
2. Turbine Disk	Nitronic 50	.48
3. Shaft		
a. Turbine End Shaft	Nitronic 50	7.4
b. Impeller Shaft	Nitronic 50	1.52
c. Tie Bolt	A-286	0.0
4. Housings		
a. Inlet Torus	Nitronic 50	7.3
b. Exit Torus	Nitronic 50	5.4
c. Exit Closure	Nitronic 50	5.4
d. Bolts	A-286	0.0

III, B, Task II - Heat Transfer, Stress, and Fluid Flow Analysis (cont.)

(a) Impellers

1. Determine the vane stresses for speed and pressure loading by using three-dimensional finite elements.
2. Perform fracture mechanics evaluations.

(b) Turbine Disks

1. Determine the blade stresses.
2. Calculate the disk-bending vibration modes.
3. Perform fracture mechanics evaluations.

(c) Shafts

1. Evaluate the splines for stress and life.
2. Determine seal deflections.

(d) Housings

1. Calculate detailed two-dimensional stresses in the bolted flange joints.
2. Perform three-dimensional analyses of the high-pressure torus housings.

III, B, Task II - Heat Transfer, Stress, and Fluid Flow Analysis (cont.)

3. Perform fracture mechanics evaluations.

(e) Critical Speed

1. Determine the TPA critical speeds to include the shafts, the TPA housing, and the method of external support.
2. Consider the effects of gyroscopic stiffening.
3. Perform rotor dynamic stability analyses by considering unbalance, fluid damping, internal friction, and the characteristics of the fluid film within the running shaft seals.
4. Establish criteria for shaft vibration limits.
5. Provide detailed bearing stiffness evaluations.

After completion of the above additional items, the LOX turbopump assembly would be considered certified by analysis and ready for production drawings.

III, B, Task II - Heat Transfer, Stress, and Fluid Flow Analysis (cont.)

c. Main Fuel Turbopump Assembly (TPA) Structural Analysis

(1) LH₂ TPA Impeller Stress Analysis

The main LH₂ TPA third-stage impeller was analyzed for rotational stresses to determine its structural adequacy at the steady-state operating speed of 90,000 RPM and in a hydrogen environment at -400°F. In view of its flight weight, titanium 5Al 2.5Sn ELI was selected as the construction material. While titanium will embrittle in hydrogen at room temperature, it can be used in the cryogenic environment.

A finite element computer program was used to analyze the impeller. The two-dimensional model is shown in Figure 14.

The results of this analysis showed that the maximum stress equal to 50 ksi occurred at the impeller bore for the operating speed of 90,000 RPM. The minimum margin of safety was found to be .43. A plot of hoop stress distribution is shown in Figure 15.

The third-stage fuel impeller is adequate at the design speed of 90,000 RPM. The margin of safety is sufficiently high to predict that when the design of the vanes and the pressure distribution is completed during the next design phase, the impeller hub should still be adequate.

Based on the third-stage impeller analysis data, it can be inferred that the first- and second-stage impellers are also adequate inasmuch as the outer radius portions of the hub are not as heavy as those of the third-stage impeller.

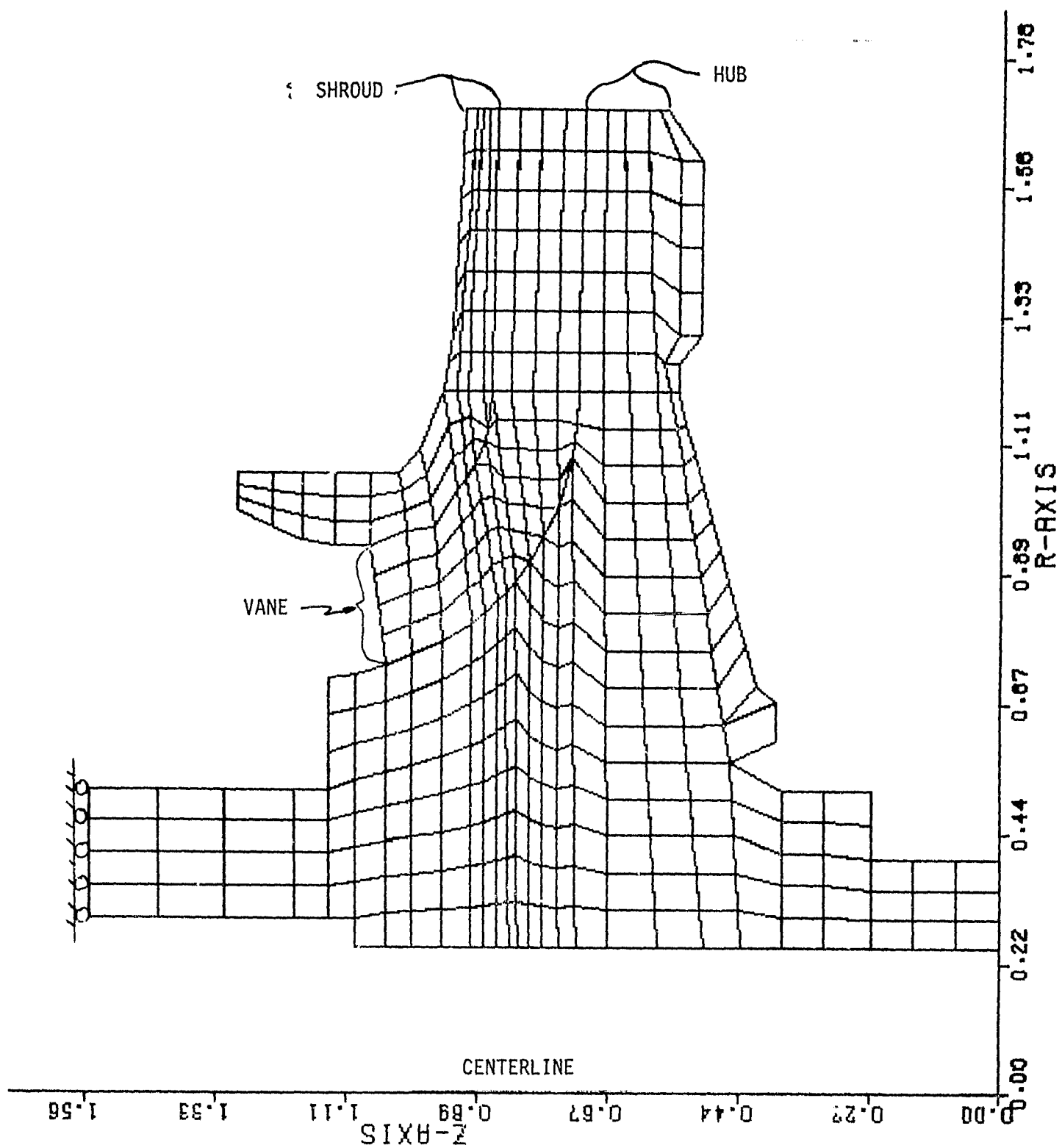


Figure 14. Fuel TPA 3rd Stage Impeller Computer Model Geometry

STRESS IN KSI
SPEED = 90,000 RPM

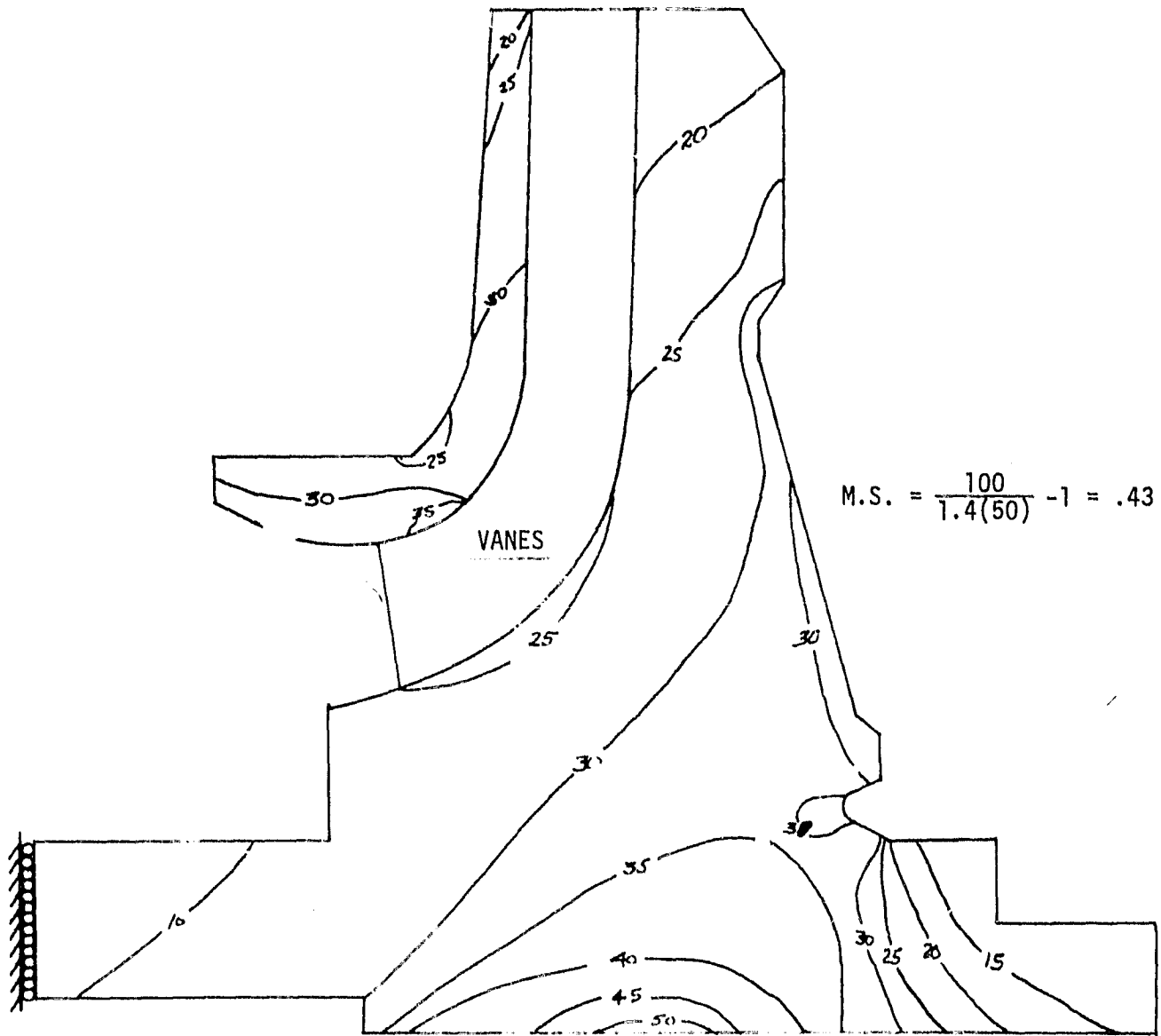


Figure 15. Fuel TPA 3rd Stage Impeller Tangential Stress

III, B, Task II - Heat Transfer, Stress, and Fluid Flow Analysis (cont.)

(2) LH₂ TPA Turbine Stress Analysis

The fuel turbine rotors were also analyzed to establish the structural capability at a 90,000 RPM steady-state operating speed. The hydrogen environment is -350°F at the disk and +75°F at the blades. The material selected for the analysis was Nitronic-50 which can be used in this hydrogen environment.

As before, a two-dimensional finite element computer model was used to determine the tangential stresses. This model is shown in Figure 16.

The results show that the maximum tangential stress (106,800 psi) occurs at the disk inner radius (Figure 17). This gives a margin of safety of +0.17 on yield and 0.30 on ultimate strength.

On the basis of this analysis, the turbine rotors are deemed structurally adequate as designed.

(3) LH₂ TPA Shaft Stress Analysis

The LH₂ TPA shaft was analyzed in three parts: (1) first-stage, (2) second-stage, and (3) third-stage impeller shafts. The third-stage impeller shaft was found to be the most critical and is discussed herein. (The design is shown in Figure 30, ALRC Drawing No. 1191997, of Section III.C.)

A maximum effective stress equal to 51,370 psi occurs in the spline runout region. A corresponding fatigue-life greater than the required $2.2 (10)^8$ is predicted in using this stress level with the appropriate stress concentration factors applied. The static margin of safety

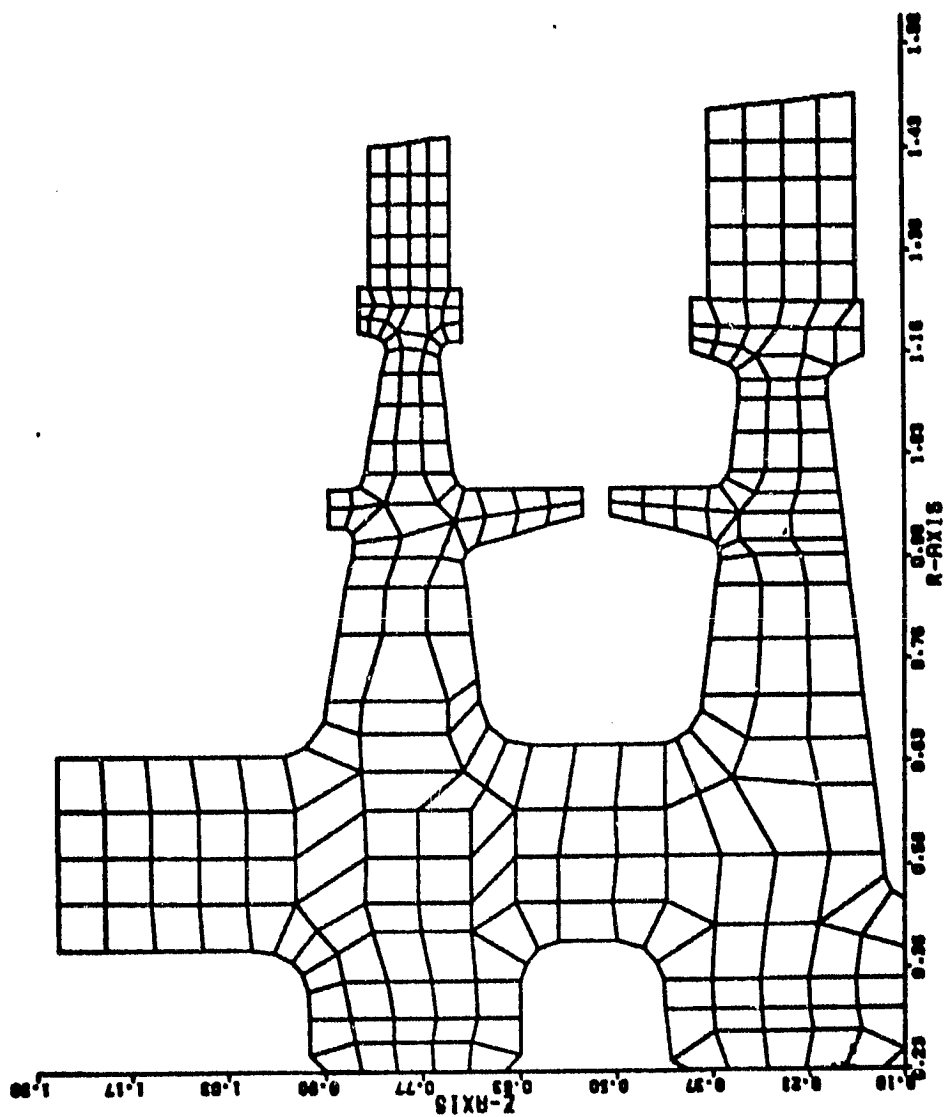


Figure 16. Fuel Turbine Rotor Computer Model Geometry

N = 90,000 RPM

STRESS IN KSI

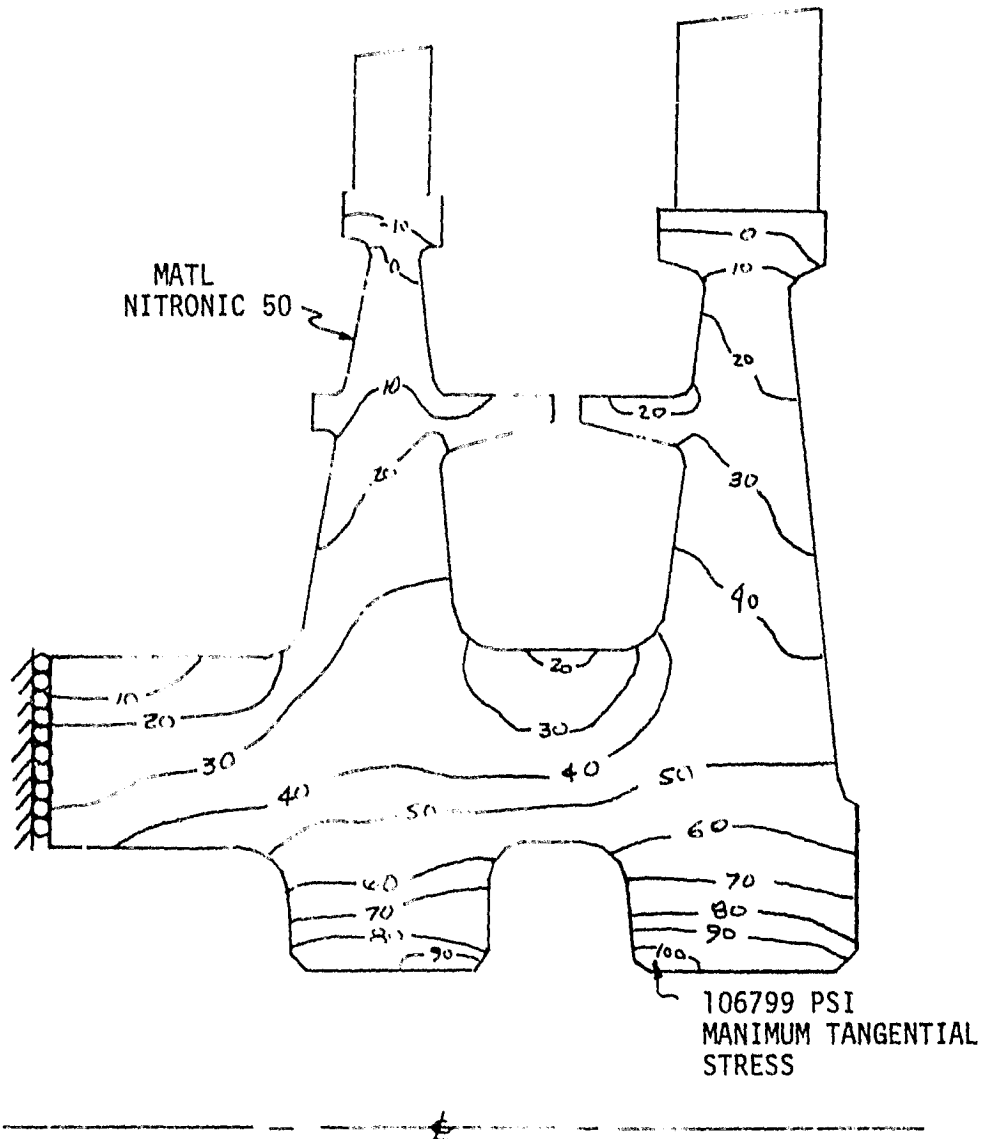


Figure 17. Fuel Turbine Rotors Tangential Stress

III, B, Task II - Heat Transfer, Stress, and Fluid Flow Analysis (cont.)

is 1.11 based on ultimate strength. The number of cycles required was based upon the 10-hour service life as follows:

$$N = 90000 \text{ RPM} \times 10 \text{ HRS} \times \frac{60 \text{ MIN}}{\text{HR}} \times \frac{1 \text{ CYCLE}}{\text{REV}}$$

$$N = 5.4 (10)^7 \text{ Cycles W/O Factor of 4}$$

$$N_{REQ} = 4 (5.4 [10]^7) = 2.16 (10)^8 \text{ Cycles}$$

Based upon the analysis, the shaft design was found to be structurally capable of meeting the design requirements with the following recommendations:

° Tie Bolts

The use of 3/8 in. - 24 threads with a minimum 0.3 in. effective thread engagement is required.

° Impeller Retaining Nut

The use of 5/16 in. - 20 threads with a minimum 0.3 in. effective thread engagement is required.

~ Shaft

Minimum fillet radii greater than 0.05 in. are recommended.

III, B, Task II - Heat Transfer, Stress, and Fluid Flow Analysis (cont.)

(4) LH₂ TPA Housing Analysis

On the basis of a preliminary evaluation, the LH₂ TPA housing appears to be structurally adequate. Nitronic-50 was assumed as the turbine housing material. Titanium 5Al 2.5Sn ELI was assumed for the pump housing which is separate from the turbine housing in this design (see Figure 30 of Section III.C). The following results were obtained:

(a) Turbine Inlet Manifold Torus

Maximum hoop membrane stress is 50,267 psi.
For this stress level, the margin of safety is 0.54 based on ultimate strength for Nitronic-50.

(b) Turbine Outlet Manifold Torus

Maximum hoop membrane stress is 27,991 psi.
The margin of safety is 1.76 based on ultimate strength for Nitronic-50.

(c) Turbine Outlet Manifold Spherical Dome

Maximum hoop membrane stress is 14,130 psi.
The margin of safety is 4.5.

The following recommendations are made on the basis of this preliminary stress analysis:

III, B, Task II - Heat Transfer, Stress, and Fluid Flow Analysis (cont.)

- ° Turbine Outlet Manifold Flange Bolts

A minimum of 10 1/4 in. - 28 ϕ bolts are required. This requirement is based on the flange drawing dimensional constraints and on bolt tensile yield allowable load.

- ° Bearing Housing Flange

A minimum of 6 1/4 in. = 28 ϕ bolts are recommended.

- ° Turbine Inlet Housing Flange

A minimum of 15 1/4 in. = 28 ϕ bolts are recommended.

- ° In the follow-on design phases, a detailed finite element analysis of the inlet/outlet manifold interface structure is highly recommended.

(5) LH₂ TPA Structural Analysis Summary

The major components analyzed, along with their respective minimum calculated margins of safety, are summarized in Table XIII.

It should be recognized that this analysis was intended to provide preliminary stress information for ascertaining the feasibility of the design. In view of this intent, minor design and load changes that were made as the design progressed were not necessarily included in these analyses. Nonetheless, the analyses were conducted in sufficient depth to

TABLE XIII
MAIN LH₂ TPA MARGINS SUMMARY

<u>Component</u>	<u>Material</u>	<u>Margin of Safety</u>
1. 3rd Stage Impeller	Titanium	.43
2. Turbine Disks	Nitronic 50	0.17
3. Shafts		
a. Main Shaft	Titanium	4.4
b. Tie Bolt	A-286	0.0
c. Impeller Shafts	Titanium	1.11
4. Housings		
a. Turbine Inlet Manifold	Nitronic 50	0.54
b. Turbine Outlet Manifold Torus	"	1.76
c. Turbine Outlet Manifold Dome	Nitronic 50	4.5

III, B, Task II - Heat Transfer, Stress, and Fluid Flow Analysis (cont.)

allow the fuel TPA to be rated as a good first iteration design. For the next design phase, in addition to refining geometry and loads, the following items should be added to the structural analysis effort.

(a) Impellers

1. Determine the hub stresses for the first- and second-stage impellers.
2. Determine the vane stresses for speed and pressure loading by using three-dimensional finite elements.
3. Perform fracture mechanics evaluations.

(b) Turbine Disks

1. Determine the blade stresses.
2. Calculate the disk-bending vibration modes.
3. Calculate the curvic coupling stresses.
4. Perform fracture mechanics evaluations.

(c) Shafts

1. Evaluate the splines for stress and life.

III, B, Task II - Heat Transfer, Stress, and Fluid Flow Analysis (cont.)

(d) Housings

1. Calculate detailed two-dimensional stresses in the bolted flange joints.
2. Perform three-dimensional analyses of the high-pressure torus housings.
3. Perform fracture mechanics evaluations.

(e) Critical Speed

1. Determine the TPA critical speeds to include the shafts, the TPA housing, and the method of external support.
2. Consider the effects of gyroscopic stiffening.
3. Perform rotor dynamic stability analyses by considering unbalance, fluid damping, internal friction, and the characteristics of the fluid film within the running shaft seals.
4. Establish criteria for shaft vibration limits.
5. Undertake a detailed bearing stiffness evaluation.

III, B, Task II - Heat Transfer, Stress, and Fluid Flow Analysis (cont.)

4. Pump Hydraulic Design Analysis

a. Requirements

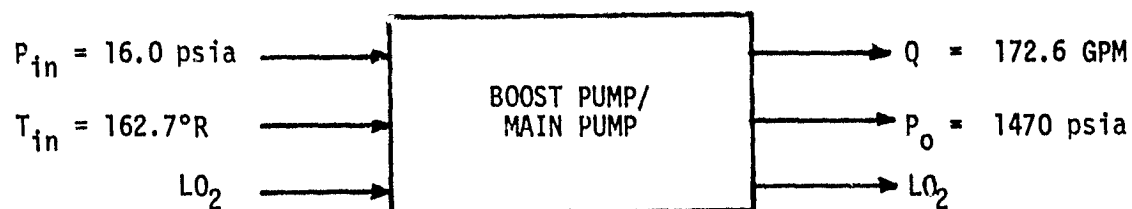
(1) LO₂ Boost Pump Requirements

The boost pump component operates between the suction line flange and the main pump inlet flange. Its fluid-dynamic interface is presented in Figure 18. The data of Figure 18 is based on related information given in Reference 9. The specified values represent the arithmetic average between data given for the mixture ratios of 6 and 7. It should be noted that the boost pump discharge conditions and the boost pump drive system are not specified. It is the designer's choice to select these discharge conditions (which also become the main pump inlet conditions) such that the overall pump performance exhibits high efficiency at a low weight.

The low head-rise oxygen boost pump is required to supply sufficient head to the main oxidizer pump to preclude it from cavitating. In general, the more head that is supplied as NPSH to the main pump, the higher the speed at which it can operate and, consequently, the smaller it becomes. However, the more head the boost pump must supply, the more shaft horsepower is demanded by the overall system since the boost pump is driven by fluid tapped off the main pump. This fluid recirculates through the boost pump drive turbine and then must be "repumped" by the main pump. This relationship can be seen in the following formula:

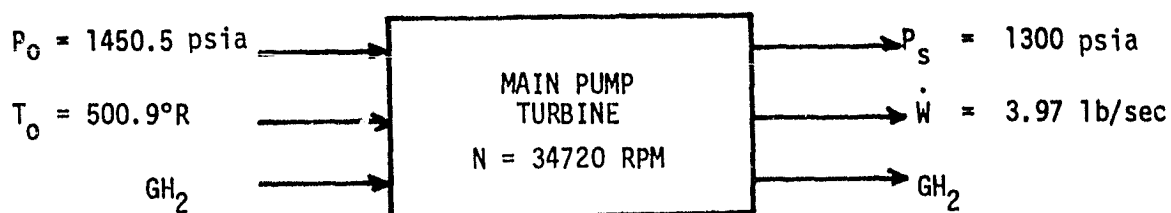
$$SHP_{MP} = W_D \frac{[\Delta H_S + \Delta H_{BP} (\frac{1}{\eta_{BP} \eta_T} - 1)]}{550 \eta_{MP}}$$

NOTE: Data from Reference (9). OTV Design Handbook
data represents arithmetic average of data given
for the mixture ratios 6.0 and 7.0.



Efficiency Goal: 60.7%

NOTE: OTV Design Handbook specifies 63.6%
including 5% power for boost pump drive



Efficiency Goal: 76.0%

PUMP: Inlet - Axial
Exit - Tangential

TURBINE: Inlet - Tangential
Exit - Tangential

OBJECTIVE: Maximize Efficiencies
Minimize Weight

Figure 18. LO₂ Pumps-Fluid Dynamic Interface

III, B, Task II - Heat Transfer, Stress, and Fluid Flow Analysis (cont.)

SHP = Shaft Horse Power
W = Weight Flow
H = Head Rise
 η = Efficiency

SUBSCRIPTS

MP = Main Pump
BP = Boost Pump
T = Boost Pump Hydraulic Turbine
D = Delivered Weight Flow
S = System

The main pump speed is established to provide a reasonably efficient single-stage pump. This results in an inlet NPSH requirement of 64 feet for the main pump. With a 10 psi allowance for line drop, the required boost pump head rise is 82 ft.

Since two engine operating points are required (Ref. 9 lists the requirements for both $MR = 6$ and $MR = 7$), a calculated average of the two was used to size the rotating machinery. This means a slight off-design operation (less than 2%) at each of the engine design points.

(2) LO_2 Main Pump Requirements

The main oxygen pump component operates between the boost pump discharge flange and the main pump discharge flange. Its fluid-dynamic interface is also shown in Figure 18.

III, B, Task II - Heat Transfer, Stress, and Fluid Flow Analysis (cont.)

The main oxidizer pump delivers the required engine flowrate against the system pressure drop. The main pump also supplies the "hydraulic power" to drive the oxidizer boost pump. This power (flow) is taken off at the pump discharge. The main pump turbine is driven by heated hydrogen (at approximately 60°F) at a very low pressure ratio.

(3) LH₂ Boost Pump Requirements

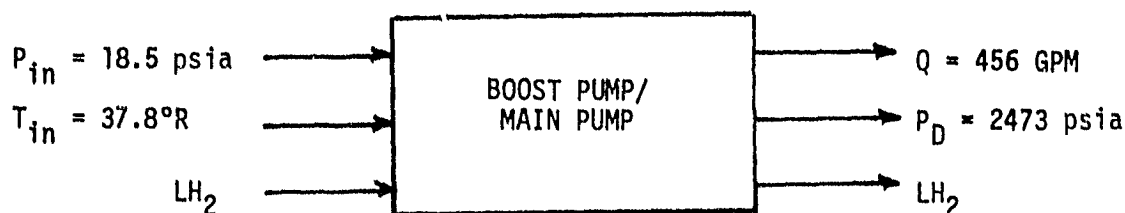
The purpose of the fuel boost pump is to raise the relatively low NPSH of the tank to a significantly higher pressure. This higher pressure is applied to the main stage and allows it to operate at a higher shaft speed and, accordingly, perform its function more efficiently with an associated decrease in size and weight.

The Design Requirements Handbook (Ref. 9) for the OTV Advanced Expander Cycle Engine (AEC) identified the engine mixture ratio between 6.0 and 7.0. The more stringent design condition is associated with the mixture ratio of 6.0. The boost pump component operates between the suction line flange and the main pump inlet flange. Its fluid-dynamic interface is shown in Figure 19. Again, it is the designer's choice to select adequate boost pump discharge conditions (which also become the main pump inlet conditions) such that the overall pump performance exhibits high efficiency at a low weight.

(4) LH₂ Main Pump Requirements

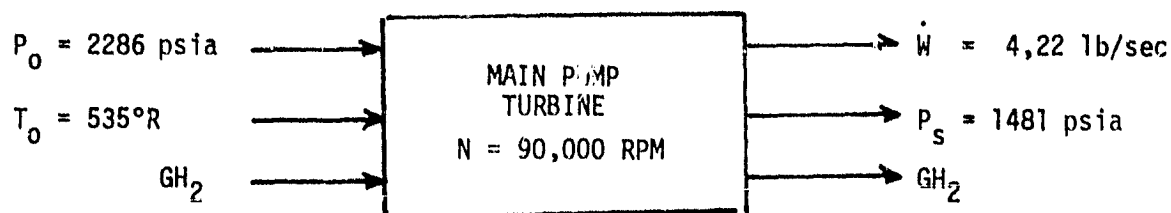
The main hydrogen pump operates between the boost pump discharge flange and the main pump discharge flange. Its fluid-dynamic interface is shown in Figure 19. The data given in Figure 19 is based on related information given in Reference 9. It should be noted that the specific values given represent the data for the mixture ratio of 6.

NOTE: Data from Reference (9). OTV Design Handbook
data is for mixture ratio of 6.0



Efficiency Goal: 63.6%

NOTE: OTV Design Handbook specifies 65.5%
including 3% power for boost pump drive



Efficiency Goal: 75.0%

PUMP: Inlet - Axial
Exit - Tangential

TURBINE: Inlet - Tangential
Exit - Tangential

OBJECTIVE: Maximize Efficiencies
Minimize Weight

Figure 19. LH₂ Pumps-Fluid Dynamic Interface

III, B, Task II - Heat Transfer, Stress, and Fluid Flow Analysis (cont.)

The main hydrogen pump delivers the required engine flowrate against the system pressure drop. The main pump also supplies the "hydraulic power" to drive the hydrogen boost pump and to supply the oxygen main pump with bearing cooling flow. This power (flow) is taken off at the pump first-stage discharge.

The main pump turbine is driven by heated hydrogen (at approximately 75°F) at a relatively low pressure ratio.

b. Oxygen Pumps Hydraulic Analysis

(1) Oxygen Boost Pump Hydraulic Analysis

The addition of the thermodynamic suppression head (TSH) supplements the given net positive suction head (NPSH) to a total of

$$\text{NPSH} + \text{TSH} = 2 \text{ ft} + 3.9 \text{ (at } 162.7^\circ\text{R)} = 5.9 \text{ ft}$$

The inlet flow velocity, cm_1 , is set by the cavitation parameter $\text{NPSH} + \text{TSH}/cm_1^2/2g = K$. The value of $K = 5.4$ is taken from cavitation data on similar type pumps. The inlet flow coefficient is selected at .091 to be consistent with the inlet blade angle and the incidence-to-blade-angle ratio. From the cavitation parameters, the inlet eye of 3.06 in. and the speed of 7398 RPM are calculated.

The discharge head coefficient is taken from data of existing similar designs covering the range of specific speed. A head coefficient value of .37 at the mean and a discharge flow coefficient of .19 at the tip are state-of-the-art values.

III, B, Task II - Heat Transfer, Stress, and Fluid Flow Analysis (cont.)

Three type of drives are considered: 1) partial admission tip turbine, 2) full admission hub turbine, and 3) a fluid coupling or torque converter. The latter has not been demonstrated as a boost pump drive and, therefore, is not deemed feasible although it has the potential of giving the highest overall efficiency.

Since more design and test experience has been developed for the tip turbine, the full admission hub turbine is not selected. In order to obtain high efficiency, the hub turbine requires the drive flow to be tapped off at a lower pressure level. Low energy flow can be taken from the high-speed inducer discharge; however, one problem is that the flowrate is high (50 GPM) and that the line and manifold size required will result in a bulky unit.

Since more experience and design development data are available for it, the partial admission tip turbine drive is chosen even though its efficiency is low.

Table XIV presents a summary of the boost pump hydraulic performance.

(2) Oxygen Main Pump Hydraulic Analysis

The hydraulic design summary is shown in Table XV. The inducer receives the flow directly from the boost pump. The boost pump is "sized" for 40.6 psi head rise, which is equivalent to a discharge pressure of 56 psia. The main pump inducer is sized for an inlet pressure of 48 psia, which leaves approximately 8 psi for the line loss. This appears to be adequate since the boost pump is directly attached; however, this 8 psi "pad" should be preserved in case the boost pump is removely mounted.

TABLE XIV
LO₂ BOOST PUMP DESIGN PARAMETERS

	<u>Rotor</u>	<u>Stator</u>
Shaft Speed, RPM	7410	
Head, Ft	82.3	
Flow, GPM	173.5	
Specific Speed, $\text{RPM} * \text{GPM}^{1/2} * \text{Ft}^{-3/4}$	3566	
Efficiency, %	66	
Inlet Dia, Inches	3.06	2.96
Inlet Vane Angle (Tip), Degree	8	40
Inlet Flow Coefficient	.091	.19
Discharge Flow Coefficient	.19	.19
Discharge Vane Angle (Tip), Degree	39	90
Head Coefficient	.29	.26
No. Vanes	3/15	17

TURBINE

Tip Dia, Inches	3.8
Hub Dia, Inches	3.4
Flow, GPM	17
Admission, %	3
Nozzle Angle, Degree	15
Specific Diameter, $\text{Ft}^{5/4} * \text{CFS}^{-1/2}$	11.8
Specific Speed, $\text{RPM} * \text{CFS}^{1/2} * \text{Ft}^{-3/4}$	4.0
Efficiency, %	52

TABLE XV
LO₂ MAIN PUMP DESIGN PARAMETERS

(Sheet 1 of 2)

	<u>Inducer</u>	<u>Impeller</u>
Speed, RPM	34,720	34,720
Inlet Pressure, PSIA	48.0	270
Inlet Temperature, °R	164.3	-
NPSH, Ft	66	380
Flow, GPM	196.2	226
Specific Speed, $\text{RPM} \cdot \text{GPM}^{1/2} \cdot \text{Ft}^{-3/4}$	5,000	1,500
Suction Specific Speed, $\text{RPM} \cdot \text{GPM}^{1/2} \cdot \text{Ft}^{-3/4}$	21,000	6,000
Inlet Diameter, Inches	1.77	1.77
Exit Diameter, Inches	1.77	2.85
Inlet Blade Angle, Degree	10	-
Exit Blade Angle, Degree	10	25
Head Coefficient	.2	.49
Flow Coefficient Inlet	.114	.20
Flow Coefficient Exit	.17	.12
No. Vares	4	9
Head Rise, Ft	450	2,390
Efficiency, %	75	71
Delivered Weight Flow, Lb/sec		30.1
Delivered Head, Ft		2,840
Combined Efficiency, %		61.5
Required Horsepower, SHP		252.5
	<u>Diffuser</u>	
Flow, GPM	196.2	
Inlet & Discharge Width, Inches	.165	
Throat Height, Inches	.224	
Exit Height, Inches	.358	
Inlet Angle (Zero Incidence), Degree	10.2	
Base Circle Diameter, Inches	3.175	

	<u>Diffuser</u>
Throat Velocity, Ft/sec	170
Exit Velocity, Ft/sec	106
No. Vanes	10
<u>LEAKAGE AND PARASITIC FLOWS</u>	
LH ₂ Flow for Cooling of Turbine End Bearing	5 GPM (supply from hydrogen TPA) 2 GPM (return to hydrogen TPA)
LH ₂ Flow Through Seal (Mixed with Helium)	3 GPM
LO ₂ Flow Through Seal (Mixed with Helium)	.5 GPM
Helium Purge Flow at 500 PSIA	.1 lb/sec

III, B, Task II - Heat Transfer, Stress, and Fluid Flow Analysis (cont.)

The inducer has a 10° inlet angle which results from the inlet flow coefficient and the incidence-to-blade-angle ratio. Even with the boost pump, the main pump inducer must operate at a suction specific speed of 21,000. At this value, the head loss is small. The tip radius is held constant through the inducer while the hub radius is increased to raise the flow coefficient from .114 to .17. With a head coefficient of .2, the inducer will have a constant blade angle from the inlet to the discharge.

Since the bearing and labyrinth flows are returned between the inducer discharge and the impeller inlet, the impeller flow coefficient increases to .2 even though the flow channel remains approximately the same as the inducer discharge.

With a return flow of approximately 30 GPM, the impeller specific speed is 1500. At this specific speed, a flow coefficient of .12 and a head coefficient of .49 are selected. The blade angle at discharge of the impeller is set at 25° with 9 vanes.

c. Hydrogen Pumps Hydraulic Analyses

(1) Design Approach

The function of the fuel pumping system is to accept the fuel (liquid hydrogen) from the tank and raise the pressure to a magnitude consistent with the engine operating cycle. This is accomplished by a boost pump and a gas-turbine-driven multistage centrifugal pump. The AEC engine design requirements handbook (Ref. 9) identifies the total inlet pressure to the boost pump as 18.5 psia and the total discharge pressure of the turbopump as 2473 psia. For this study, it is assumed that a pumping system operating between these two pressures and supplying the required flow of 456 GPM is consistent with the engine cycle requirements.

III, B, Task II - Heat Transfer, Stress, and Fluid Flow Analysis (cont.)

Impellers for the pumping system are separated into three elements: a boost impeller, an inducer, and multistage centrifugal impellers. The boost pump impeller's purpose is to increase the inlet pressure for the following main stage. Its design is based on the available NPSH from the tank. The inducer's purpose is to provide a sufficiently high pressure at the inlet to the following centrifugal stages. Without this increased pressure, flow recirculating back to the inlet of the first centrifugal stage will flash to a vapor and choke the inlet. Choking seriously degrades pump performance. The centrifugal stages perform the bulk of the effort in terms of generating the required pressure for the engine cycle. However, the efficiency of the centrifugal stages is lower than those of the axial flow boost pump and inducer. Accordingly, the pressure generation schedule (i.e., the pressure rise of each element of the system) directly affects the overall efficiency of the pumping system. Also, since the two axial elements exhibit greater efficiency than the centrifugal stages, the pressure generation requirements imposed on the axial elements in an optimized system will be as high as practical.

(2) Hydrogen Boost Pump Hydraulic Analysis

Two hydraulic designs are prepared for the fuel boost pump. The first is the baseline design which reflects the data and information contained in the Design Requirements Handbook. This baseline hydraulic design is the one used in completing the mechanical design. The subsequent design departs from the handbook requirements in terms of the pressure generated by each element of the pumping system, except for the inlet NPSH and main stage discharge pressure. This improved design represents a more optimized and efficient configuration.

III, B, Task II - Heat Transfer, Stress, and Fluid Flow Analysis (cont.)

Hydraulic performance for the baseline and improved design fuel boost pump is depicted in Table XVI. The baseline design parameters shown in the table reflect a boost pump employing a hydraulic tip turbine to drive the impeller. Hydrogen flow to drive this turbine is extracted from the discharge of the first centrifugal stage of the main pump. The hydrogen leaving the tip turbine is mixed with the boost pump through-flow and then enters the main hydrogen pump.

With a flow of 94 GPM, the head differential between tip turbine inlet and outlet is 22809 ft and yields an efficiency of 51%.

The improved design is a hub-mounted hydraulic turbine yielding an efficiency of 66% with a head change of 7136 ft at a flow of 129 GPM. The flow for driving this hub turbine is extracted from the main stage inducer.

The suction specific speed of the boost pump impeller for both designs is approximately 40,000. This value is conservative and does not fully utilize the thermodynamic suppression head (TSH) available from liquid hydrogen. Utilization of the available TSH can be accomplished by increasing the speed of the impeller. However, as boost pump shaft speed approaches main turbopump shaft speed, the need for a boost pump diminishes. Accordingly, a turbopump design which does not include a boost pump seems feasible and is recommended for analysis in a future study addressing this subject.

TABLE XVI
LH₂ BOOST PUMP DESIGN PARAMETERS

<u>Impeller</u>	<u>Baseline</u>	<u>Improved</u>
Flow, GPM	456	456
Inlet Pressure, PSIA	18.5	18.5
Discharge Pressure, PSIA	60.0	49.9
Inlet NPSH, Ft.	15	15
Shaft Speed, RPM	26647	29647
Specific Speed, $\text{RPM} * \text{GPM}^{1/2} * \text{Ft.}^{-3/4}$	2552	3500
Suction Specific Speed, $\text{RPM} * \text{GPM}^{1/2} * \text{Ft.}^{-3/4}$	40326	43076
Horsepower, HP	15.1	10.7
Efficiency, %	73	78
Head Coefficient	.287	.246
Inlet Flow Coefficient	.08	.075
Discharge Tip Diameter, Inches	3.350	2.83
<u>Hydraulic Turbine</u>		
Configuration	Tip	Hub
Head Change, FT.	22809	7136
Flow, GPM	94	129
Efficiency, %	51	66
Power, HP	29.6	16.2
Admission, %	6	29
Tip Diameter, Inches	4.35	1.50

III, B, Task II - Heat Transfer, Stress, and Fluid Flow Analysis (cont.)

(3) Hydrogen Main Pump Hydraulic Analysis

The main fuel pump raises the LH₂ pressure from 51 psia to 2473 psia and delivers a flowrate of 4.49 lb/sec (456 GPM). The pump consists of three centrifugal pump stages and an axial flow inducer driven by a two-stage, warm-gas hydrogen turbine. The design point speed is 90,000 RPM. The three main stages provide an N_s value near 1,000 which results in high efficiency without excess complexity. The high-speed inducer provides a high static inlet pressure to avoid vapor generation at the centrifugal stage inlet caused by the high enthalpy fluid returning to the inlet.

Similar to the boost pump hydraulic design, a baseline and improved version of the main fuel turbopump hydraulic design are analyzed. Table XVII summarizes the relevant values associated with each design.

In both the baseline and improved design, the overall head rise (including the boost pump) is identical. However, the head rise of corresponding components of the two designs varies. The baseline design is characterized by equal head rise for each of the three centrifugal impellers. The improved design reflects constant specific speed, N_s , for the centrifugal components. The efficiency of the hydrogen main pump may be further increased through a modification of the pressure-generating schedule. It seems feasible to obtain higher efficiency by increasing the head rise associated with the inducer stage and lowering the head rise per stage of the three centrifugal stages.

A comparison of the overall turbopump performance is shown at the bottom of Table XVII. The important difference between the

TABLE XVII
LH₂ MAIN PUMP DESIGN PARAMETERS

<u>Inducer</u>	<u>Baseline</u>	<u>Improved</u>
Head Rise, FT	3,000	5,076
Flow, GPM	547	582
Efficiency, %	80	82
Specific Speed, $\text{RPM} * \text{GPM}^{1/2} * \text{FT}^{-3/4}$	5,202	3,500
Suction Specific Speed, $\text{RPM} * \text{GPM}^{1/2} * \text{FT}^{-3/4}$	11,238	11,861
Tip Diameter, Inches	1.90	1.88
Power, HP	36.5	64.2
Head Coefficient	.17	.30
Blades	4	4
<u>Stage I</u>		
Head Rise, FT	25,302	26,873
Flow, GPM	572	572
Efficiency, %	66.5	71.0
Specific Speed, $\text{RPM} * \text{GPM}^{1/2} * \text{FT}^{-3/4}$	1,072	1,025
Tip Diameter, Inches	3.37	3.19
Power, HP	374	386
Head Coefficient	.464	.550
Blades	10	10
<u>Stage II/III</u>		
Head Rise, FT	25,302	23,842
Flow, GPM	478	478
Efficiency, %	65.0	71.0
Specific Speed, $\text{RPM} * \text{GPM}^{1/2} * \text{FT}^{-3/4}$	981	1,025
Tip Diameter, Inches	3.37	3.01
Power, HP	331	286
Head Coefficient	.464	.550
Blades	10	10
<u>Overall</u>		
Head Rise, FT	78,910	79,633
Flow, GPM	456	456
Efficiency, %	59.6	63.3
Power, HP	1,072	1,022

III, B, Task II - Heat Transfer, Stress, and Fluid Flow Analysis (cont.)

two designs lies in the required shaft horsepower and the efficiency. The improved design exhibits an efficiency gain of more than 3% over the baseline design. It should be noted that the boost pump is hydraulically driven by LH₂ from the first-stage centrifugal impeller. Accordingly, the horsepower values reported include the effects of driving the boost pump. The efficiency values are based on the assumption that 15% of engine flow (i.e., 68.4 GPM) is associated with recirculating flow for lubricating, cooling, and thrust-balancing. In addition, the inducer and first centrifugal stage are supplying the boost pump turbine with a flow of 94 GPM.

5. Materials Analysis

The purpose of this subtask was to provide the structural analysts with tensile and thermal material property data for use in the stress analyses.

The selection of materials for the OTV engine requires consideration of their reactivity with the hydrogen and oxygen propellants, their cryogenic properties, fabricability, mechanical properties, and density.

The material candidates discussed herein are to be compatible with temperatures and propellants to which they will be exposed in each component application. Selection of a preferred material for each component is based on fabricability, weight considerations, and the structural requirements.

Thermal and tensile property data for zirconium copper, A-286, Nitronic-50, CRES 304L, electroformed nickel, and titanium 5Al 2.5Sn ELI was prepared and submitted to NASA along with the OTV Engine Design Requirements Handbook (Ref. 9). Some of the factors which must be considered in selecting materials for this engine application are discussed herein.

III, B, Task II - Heat Transfer, Stress, and Fluid Flow Analysis (cont.)

Aluminum, titanium, stainless steel, and nickel base alloys are the primary candidates. The aluminum and titanium alloys are generally preferred due to their relatively low density; however, the aluminum alloys are also relatively low in strength and the titanium alloys are incompatible with hot and warm hydrogen in the hot-gas system. The stainless steels are strong and generally compatible with the oxygen and hydrogen environments, but they do have a lower strength-to-weight ratio. The nickel base alloys are stronger yet, but they are more difficult to fabricate and are embrittled by room temperature hydrogen. A more detailed description of the advantages, disadvantages, and limitations of the main candidate alloys is presented in the paragraphs which follow.

a. Aluminum Alloys

Aluminum alloys offer the obvious advantage of low density, which is of vital importance to the OTV engine design. Complex configurations such as impellers, stators, and housings can be readily cast using A-356 aluminum. Simpler configurations can be machined from wrought 6061 aluminum stock. Both of these alloys are weldable for ease of fabrication. Aluminum alloys have demonstrated good service in cryogenic applications and have frequently been used in LOX environments. Hydrogen embrittlement data is less complete. However, there are no reported embrittlement effects in 1100, 6061, and 7075 wrought aluminum alloys, and none are anticipated for A-356. One area of caution in using wrought aluminum alloys is the thermal contraction of aluminum when cooled from room temperature to -420°F. The thermal expansion coefficient for aluminum is significantly greater than that of stainless steels, titanium, and nickel base alloys. Any design using aluminum should take this into account when establishing clearances and interference fits.

III, B, Task II - Heat Transfer, Stress, and Fluid Flow Analysis (cont.)

The major drawback of aluminum alloys is their relatively low strength. Aluminum is only applicable to low stressed components not exposed to temperatures significantly above room temperature since heat-treatable aluminum alloys rapidly weaken above 200°F.

The aluminum alloys should find greatest application in the pump housings and, possibly, the pump impellers and turbine housings, depending on the stresses and temperatures experienced by these components.

b. Titanium Alloys

Titanium alloys have tensile properties comparable to high-strength stainless steels but with half the density. Titanium alloys can be cast in complex configurations, such as impellers, and are machinable and weldable in either the cast or wrought form. Titanium performs well in cryogenic environments and has a thermal expansion coefficient similar to 440 C stainless steel (a common bearing alloy). The mismatch in expansion coefficients of titanium and austenitic stainless steels is less severe than with aluminum, but it still should be taken into account in the design.

All titanium alloys are completely incompatible with LOX in that titanium can be explosively detonated by impact in a LOX environment. Titanium is compatible with cryogenic hydrogen but will begin to form titanium hydrides slightly above room temperature which will seriously degrade the titanium alloy mechanical properties.

The major applications for considering titanium alloys (primarily Ti5Al 2.5Sn ELI, which has been extensively used in cryogenic applications) are LH₂ pump impellers, housings, shafts, valves, and lines. Areas to avoid in using titanium alloys are all LOX components and the H₂ turbines.

III, B, Task 11 - Heat Transfer, Stress, and Fluid Flow Analysis (cont.)

c. Austenitic Stainless Steels

Austenitic stainless steels offer a range of tensile strength (30 ksi to 90 ksi yield strength) and are completely compatible with the oxygen and hydrogen environments at all temperatures. A-286 is the highest-strength alloy, but it is only available in the wrought form and is difficult to weld and braze. 22-13-5 (Armco Nitronic-50) is a moderate-strength stainless steel which is readily brazed or GTA-welded, but which is also only available in the wrought form. The 300 series stainlesses (347, 321, 316, 304, etc.) are the lowest-strength steels, but they are readily castable, weldable, and brazable. All of the austenitic stainless steels have very good cryogenic properties and could safely be used exclusively in the OTV engine if the weight penalty of these relatively dense alloys were acceptable.

Austenitic stainless steels can be considered for any OTV component where the stresses are too high for aluminum or where the environment is incompatible with titanium.

d. Martensitic Stainless Steels

Martensitic stainless steels in general have poor cryogenic fracture toughness and resistance to hydrogen embrittlement; however, there are two specific applications where they can be used. 400 C stainless is the standard bearing alloy commonly used in cryogenic applications and has been demonstrated to perform well in both LOX and LH₂ pumps. The other application for consideration of a martensitic alloy is the LOX pump shaft. 15-5 PH H1150-M is a precipitation hardenable martensitic alloy which has shown good cryogenic toughness and is compatible with thermal expansion coefficients with 440 C, which simplifies the interference fits between the

III, B, Task II - Heat Transfer, Stress, and Fluid Flow Analysis (cont.)

440 C bearings and the LOX pump shaft. Since the embrittling effects of hydrogen on this alloy have not been established, they should not be considered for use in the H₂ system.

e. Nickel Base Alloys

All nickel base alloys are embrittled to some extent by hydrogen and consequently are not normally considered for hydrogen. However, the hydrogen embrittlement effect is reduced at cryogenic temperatures, and INCO 718 has the highest usable tensile strength of all the candidate alloys within these environmental limits. INCO 718 has good cryogenic properties and is compatible with LOX. It is castable, but difficult to braze.

INCO 718 can be considered for any of the highly stressed components, with the exception of the H₂ turbine housing or disk, both of which operate at too high a temperature in hydrogen.

f. Copper Base Alloys

The copper base alloys are compatible with oxygen and hydrogen and have good cryogenic properties, but they do not offer any significant mechanical advantage over the austenitic stainless steels. However, the copper alloys generally have excellent thermal conductivity, which is important in regeneratively cooled components.

Zirconium-strengthened copper (Zr-Cu or Zirc-copper) offers excellent thermal conductivity, good strength up to 1000°F, and is compatible with the hydrogen used as the coolant. Consequently, it is the preferred choice for the combustion chamber.

III, Task Discussions (cont.)

C. TASK III - COMPONENT MECHANICAL DESIGN AND ASSEMBLY DRAWINGS

The primary objective of this task was to provide mechanical design and assembly drawings of the major engine components. The component designs were prepared in only sufficient depth to reveal manufacturing difficulties, allow leakage and cooling flows to be assessed, calculate weights, and determine technology requirements. Therefore, the resulting designs are not firm, and further iterations in the designs and data can be expected as the advanced expander cycle engine design matures.

1. Igniter/Injector Assembly

The OTV ignition system employs redundant igniters (shown mounted on the OTV injector in Figure 20) to meet the man-rating requirement. Each igniter is a small thruster which can accept either liquidous, two-phase, or gaseous propellants. These are ignited by using a very low energy spark. The igniter produces a hot-gas torch of sufficient energy to provide reliable, rapid main-stage ignition.

The igniter design concept was developed on the Ignition System for Space Shuttle Auxiliary Propulsion System (Contract NAS 3-14338). The igniter has been used successfully on a number of rocket engines, including the Extended Temperature Range ACPS Thruster Investigation (Contract NAS 3-16775), the Hydrogen-Oxygen Auxiliary Propulsion for the Space Shuttle Program (Contract NAS 3-14354), and the Integrated Thruster Assembly Investigation Program (Contract NAS 3-15850).

The ignition system consists of 5 major components: (1) a GLA spark plug; (2) Model 427200-4871 Valcor coaxial type poppet valves; (3) a stainless steel/nickel body which forms or contains all manifolding and seals,

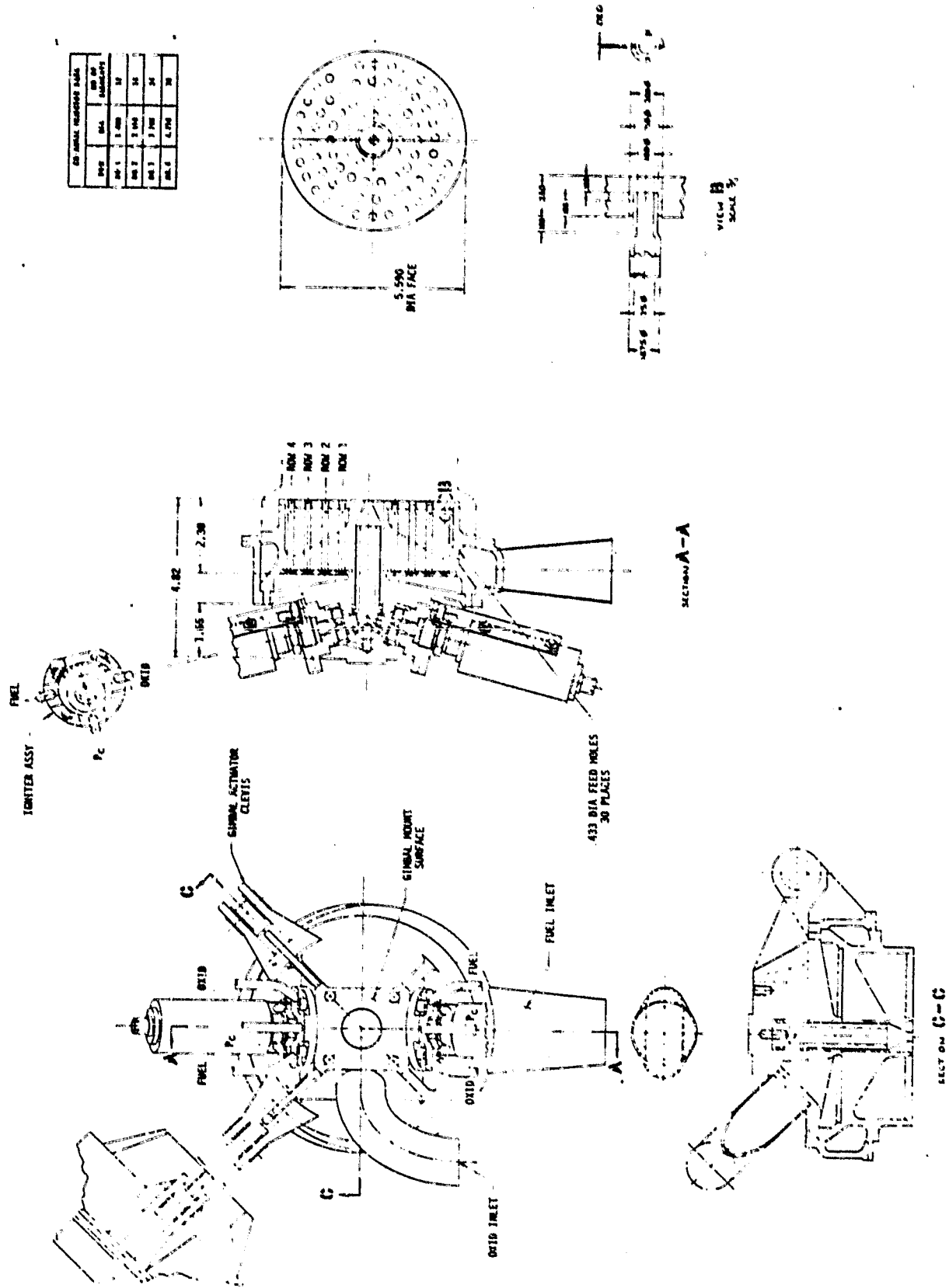


Figure 20. Igniter/Injector Assembly (ALRC Drawing No. 1191990)

III, C, Task III - Component Mechanical Design and Assembly Drawings (cont.)

propellant metering and injection orifices, a platform for mounting the spark plug and valves, plus all necessary instrumentation ports and a flange for attachment to the injector; (4) a hydrogen-cooled chamber; and (5) a high-voltage GLA capacitance discharge power supply.

The capacitance discharge power supply is integral with the spark plug. The igniter assembly is located in the injector oxidizer manifold cover plate directly below the gimbal mount surface. The igniter propellant valves are located in close proximity to the igniter/injector adjacent to the ignition power supply.

A 10% core fuel flow is injected via 24 radial inflow rectangular orifices which are formed by a bonded photoetched nickel-plate. The bulk of the fuel (90% bypassing the core) flows through a stainless steel metering platelet into an annulus surrounding the igniter injector from which it flows towards the forward end of the igniter chamber to distribute into 12 slotted coolant passages surrounding the barrel section of the igniter chamber. The passage dimensions and flow are selected to provide the necessary cooling of the chamber which contains the oxidizer-rich hot gas.

The oxygen flows from the valve through a balancing orifice into a low-volume manifold and is injected via 6 like-on-like (LOL) doublet elements which produce 6 axial fans flowing radially inward to the center electrode. The 12 oxidizer orifices are formed by a single photoetched nickel platelet bonded to the lower face of the igniter body. All of the oxygen flows through the annular spark gap formed between the central electrode and the igniter chamber wall and provides the required electrode cooling.

The igniter flows during steady-state operation to keep the plenum cool.

III, C, Task III - Component Mechanical Design and Assembly Drawings (cont.)

Spark rates at selected energy levels for the igniter were measured on the Extended Temperature Range Thruster Program. The power supply employed was a GLA Model 48136 variable energy system. The unit was calibrated at a 0.127-cm (0.050-in.) spark gap to give the following energy levels and spark rates:

10	mJ	500 sparks/sec
25	mJ	500 sparks/sec
50	mJ	300 sparks/sec
100	mJ	150 sparks/sec

A layout of the injector configuration is also shown on Figure 20. The injector uses coaxial elements because this element type has an extensive history of operation with GH_2/LO_2 propellants over a broad range of thrust and chamber pressure conditions. The injection pattern is a four-row array of 84 elements uniformly distributed over the injector face.

Because the hydrogen is injected as a gas (at 90°F) and because the cryogenic LOX immediately flashes into a gas upon injection into the hot combustion chamber, combustion is expected to occur very close to the injector face. This results in the need for injector face cooling to ensure that the low temperatures required for high-cycle life are maintained. Regenerative cooling of the injector face, coupled with discrete face fuel film cooling, provides the most reliable method of ensuring face integrity over a range of operating conditions. Thus, the injector faceplate material is a laminate of photoetched copper-faced platelets brazed to a structural steel backup plate. The extremely accurate photoetched flow control passages assure uniform flow across the entire injector face. The photoetched face platelet concept also permits the incorporation of a filter screen into the platelet stack. This faceplate concept precludes problems associated with flow

III, C, Task III - Component Mechanical Design and Assembly Drawings (cont.)

control and flow distribution encountered with Rigimesh, a commercially available porous sintered stainless steel wire material used on a variety of rocket engines with varied success.

The injector faceplate is designed to be electron-beam-welded at its outer periphery and near the center of the injector body. A preliminary injector stress analysis indicates that the injector face will not have to be physically attached to each injector element oxidizer post. In the event of a subsequent, more detailed stress analysis revealing that the injector face requires additional support, it may be brazed to the injector element oxidizer posts.

The fuel inlet torus surrounding the injector body is designed for constant flow velocity to assure uniform fuel distribution into the injector fuel manifold through 30 equally spaced holes. These 30 holes are spaced (circumferentially) midway between the 30 coaxial elements in the outer row of the injector pattern. The fuel manifold, which is located directly behind the injector faceplate, is designed of sufficient size to assure uniform fuel distribution to all 84 injection elements. The oxidizer manifold is located forward of the fuel manifold directly below the redundant torch igniters.

The oxidizer tubes are recessed approximately one tube diameter into the faceplate. They are held concentrically within the fuel discharge orifice by four small tabs integral with the faceplate. The oxidizer tubes are designed to be integral to the injector body or to be brazed into the injector body. Both design features have been used in the past and will be studied in depth before a final selection is made for detailed design. The LOX enters the oxidizer tubes tangentially so as to form a hollow cone spray as it ejects from the tube into the surrounding GH_2 . The tangential

III, C, Task III - Component Mechanical Design and Assembly Drawings (cont.)

oxidizer flow is established by means of flow passages located in a stack of photoetched and bonded platelets which are located immediately upstream of the tube inlet. To preclude the possibility of contamination reaching one of these tangential flow control passages, the platelet stack incorporates a filter platelet similar to that designed for the fuel circuit. The injector oxidizer manifold is created by electron-beam-welding the outside diameter of the closure plate to the injector body and by brazing the central portion of the closure plate which contains, in its center, the cooled igniter chamber.

The fuel manifold is created by machining the manifold cavity from the injector face side if the oxidizer tubes are to be brazed into the injector body. If the oxidizer tubes are integral with the injector body, the fuel manifold will be machined by the electrical-discharge method. The fuel enters the fuel manifold through 30 radially drilled feed holes. The number of holes corresponds to the number of injection elements in the outermost row to provide uniform fuel distribution across the back of the injector face. The fuel inlet manifold which surrounds the 30 feed holes also serves as a main structural component of the injector.

Although combustion instability problems are not expected, a resonator cavity is provided around the injector periphery. The cavity is designed so that dynamic pressure oscillations do not exceed $\pm 5\%$. The resonator cavity is created when the forward end of the combustion chamber is electron-beam-welded to the injector body.

2. Combustion Chamber Design

The design of the combustion chamber required consideration of man-rating requirements as well as its usage in an advanced expander cycle engine. These requirements resulted in the selection of a milled slot design concept. The reasons for its selection are listed below.

III, C, Task III - Component Mechanical Design and Assembly Drawings (cont.)

- ° The high-conductivity liner with its integral fins provides heat transfer enhancement which minimizes liquid side flux. This results in less required coolant velocity, in turn resulting in reduced jacket pressure drop, which is important to the expander cycle efficiency.
- ° The utilization of high conductivity material (zirconium copper) with the slot type thrust chamber reduces wall temperature gradients to enhance cycle-life and facilitates conformance with structural criteria.
- ° The use of tube-walled construction involves numerous fabrication variables, excessive component quantity and complexity, and the requirement for large quantities of high-pressure brazed interfaces.
- ° The selection of thrust chamber geometry (contraction ratio and combustor length) is influenced by engine cycle considerations. Studies show that the total heat load (coolant temperature rise) is increased as L' increases and contraction ratio decreases. While this increases the turbine inlet temperature, it increases system pressure drops. Optimization studies performed during the Phase A work effort resulted in the selection of a contraction ratio of 3.66 and a combustor length L' of 18 inches.

The combustion chamber design is illustrated in Figures 21 and 22. The chamber ID, which is 5.34 in., is cylindrical for 13.54 in. and then converges at a 30° half-angle to a throat diameter of 2.79 inches.

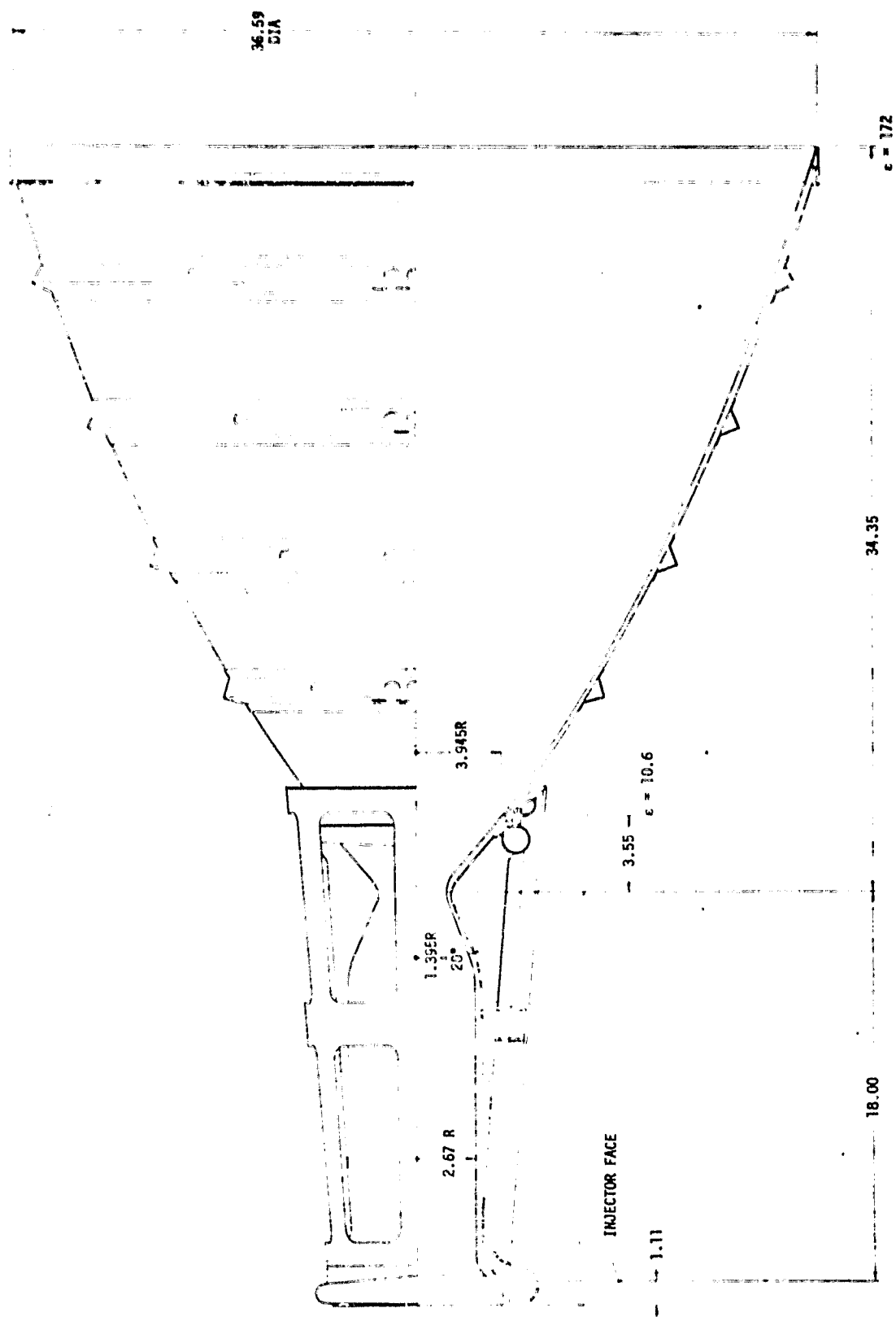


Figure 22. Chamber and Tube Bundle Nozzle Design (ALRC Drawing No. 1191991)

III, C, Task III - Component Mechanical Design and Assembly Drawings (cont.)

The thrust chamber gas-side wall contains 113 coolant slots which are equally spaced in a zirconium copper liner. The coolant slots are closed out with electroformed nickel. The coolant enters the chamber at an area ratio of 10.6. The inlet manifold is located 4.20 in. below the throat. The coolant flows axially for a distance of 22.20 in. toward the forward end of the chamber. The coolant is collected in a manifold outboard of the resonator cavities and exits radially into the chamber's coolant outlet manifold.

Twelve resonator cavities are located at the forward end of the thrust chamber and are bounded by the injector body OD and chamber ID. The resonator entrance width is 0.300 and remains constant for a depth of one inch. The cavities are tuned to match the first tangential (1T) acoustic mode. The injector face outside-radius-to-chamber-inside-radius overlap is 0.125 inch. The coolant passages that are in line with the 12 partitions between the resonator cavities will extend partially through the partition to regeneratively cool it.

Zirconium copper has been selected as the gas-side wall material. The inlet manifold and the exit manifold flange are made of CRES 304L and are designed to be brazed to the zirconium copper chamber prior to closing the chambers coolant slots with electroformed nickel. A conical support structure surrounds the entire chamber to provide a load path for gimbal-induced loads from the nozzle extension in addition to providing a means of attachment for engine components. The support structure is designed to be secured by electron-beam-welding it to the forward and aft end CRES 304L flanges of the chamber. The conical support structure has a circumferential channel located at its inside diameter approximately midway along its length to provide additional structural rigidity. Openings in the cone will provide access for mounting components and routing propellant and service lines.

III, C, Task III - Component Mechanical Design and Assembly Drawings (cont.)

Both the chamber inlet and outlet manifolds are designed for constant flow velocity to assure proper coolant distribution within the chamber. The chamber inlet manifold is integral with the inlet manifold of the regeneratively cooled nozzle. This feature permits the regeneratively cooled nozzle tubes to be brazed directly into the zirconium copper chamber wall. This eliminates 1) the need for a separate manifold feeding the nozzle, 2) a bolted flanged interface, including a hot-gas seal, and 3) the adverse reliability inherent in a flanged interface. This design feature requires that the brazing of the tube bundle be performed prior to electroforming the closeout of the chamber coolant slots in order to avoid potential blistering of the electroformed nickel. The design of the cooled nozzle is discussed in the following section.

3. Regeneratively Cooled Nozzle Design

The regeneratively cooled nozzle design is physically attached to the chamber as shown in Figures 22 and 23. Rather than extending the slotted chamber configuration to minimize weight, a two-pass tube bundle configuration was selected for the nozzle. Because the nozzle gas-side pressure is extremely low (i.e., 17.55 psi at the forward end to 0.52 psi at the aft end) whereas the chamber must operate at 1200 psi, gas-side braze joints are acceptable for the man-rated OTV system.

The forward end of the nozzle is located at an area ratio of 10.6:1, 4.35 in. below the chamber throat at a contour ID of 9.100 in., and ends at an area ratio of 172:1, 34.35 in. below the throat at a contour ID of 35.46 inches.

A total of 326 coolant tubes are spaced equally around the nozzle contour. The tubes taper from an 0.089-in. OD with a wall thickness of

III, C, Task III - Component Mechanical Design and Assembly Drawings (cont.)

0.007 in. at the forward end to an 0.361-in. OD with a wall thickness of 0.010 in. at the aft end. The tube wall materials under consideration for the nozzle include 347 CRES, Armco Nitronic 40, and A-286. The first structural analysis iteration indicates that 347 CRES is a satisfactory material for the man-rated system. All three materials have been brazed successfully at ALRC, although the A-286 material would require special processing and preparation to assure reliable braze joints. The greatest amount of experience has been with 347 CRES. The forward ends of the tubes are brazed into the aft end of the zirconium copper chamber. The aft ends of the tubes are brazed into a 347 CRES turnaround manifold.

To provide tube bundle rigidity, four circumferential ring stiffeners are brazed to the exterior of the tube bundle. To assure that the deployable radiation-cooled nozzle will properly align, center itself, and seal with the regeneratively cooled nozzle, a stainless steel flange has been designed to be brazed to the tube bundle approximately 8 in. from the aft end. This flange accommodates the bushings for the extension/retraction mechanism screw, a gasket seal gland, and one of two spring-loaded alignment rings. The second alignment ring is located in the outer periphery of the copper turnaround manifold.

4. Radiation-Cooled Nozzle Extension and Deployment Mechanism

The radiation-cooled nozzle extension assembly is shown as part of the engine assembly layout in Figure 24. It consists of a contoured radiation-cooled nozzle, an extension/retraction mechanism, and a mechanical drive system.

In the extended position, the radiation-cooled nozzle is located 34.35 in. below the throat at a contour ID of 35.46 in. and extends

III, C, Task III - Component Mechanical Design and Assembly Drawings (cont.)

an additional 50.3 in. to an exit area ratio of 435:1. The retracted position of the nozzle is such that its exit plane is at the same axial station as that of the regeneratively cooled nozzle (172:1) which is 34.35 in. below the throat.

The 50.3-in. length of the radiation-cooled nozzle is based upon the following design criteria:

- ° Component penetration above the gimbal plane is limited to 6.5 inches. This distance is required to redirect the axially oriented propellant inlet lines to the horizontal and into the gimbal plane.
- ° An integral part of the nozzle is a thin-wall cylindrical ring assembly, approximately 9.3 in. long, which contains the nozzle attachment flange. The ring assembly is not exposed to the hot products of combustion as it extends axially up the outside of the regeneratively cooled nozzle. Its function is to permit extension of the nozzle flange up to the deployment ring where it is bolted to the extension/retraction mechanism. Its cylindrical length is controlled by the maximum distance down the external contoured surface of the regeneratively cooled nozzle so that the deployment ring can be located without exceeding the 35.46 ID of the radiation-cooled nozzle. This axial distance is approximately 9.3 inches.

Design of the radiation-cooled nozzle is based upon the highly successful nozzle used on the OMS engine. The primary candidate

III, C, Task III, - Component Mechanical Design and Assembly Drawings (cont.)

material is C-103 columbium alloy. An oxidation-resistant coating such as aluminide or silicide slurry is required on all surfaces of the nozzle. The thickness of the nozzle is increased at the exit end where a U-shaped stiffening ring approximately .080 in. thick is located. Vibration tests with the OMS nozzle defined the need for a stiffening ring of this type.

The radiation-cooled nozzle incorporates a bolt-on flange and is designed to be removed and replaced from the aft end. If required, it can be manually removed from the engine while in orbit.

Redundant seals are employed between the extendible nozzle and the regeneratively cooled nozzle to prevent hot-gas leakage. Preliminary studies indicate that the low temperatures on the backside tip of the regeneratively cooled nozzle will permit the use of an elastomeric-type diametric seal. The nozzle joint is also sealed by an elastomeric gasket-type face seal made of silicone rubber. The gasket seals between the nozzle mounting ring and the support ring which is brazed to the tube bundle "V" band and also between the extendible nozzle flange and the nozzle mounting ring. A positive seal is assured by serrations machined in the surfaces of all parts that contact the seal. The amount of gasket "crush" between the mating parts is controlled by interlocking lips. The seal is located in a cool area well removed from the heat input to the extendible nozzle, but more complete thermal analysis must be performed to verify that this region does not reach a steady-state temperature in excess of the capabilities of elastomers. The sealing concept described is both positive and insensitive to machining tolerances. It does require that the seal be held in compression during the engine firing mode. Leakage rates of specific seals and seal interface designs must be evaluated by testing.

Nozzle alignment is concerned primarily with the angular difference between a theoretical centerline through the nozzle throat and

III, C, Task III - Component Mechanical Design and Assembly Drawings (cont.)

injector end of the thrust chamber and a theoretical centerline through the throat and the exit plane of the nozzle. Misalignment tolerances are usually quite small, on the order of 0.25° or less, because the engine is usually mounted to the vehicle using the thrust chamber centerline as the mounting guide and generally placing it parallel with the vehicle centerline. For single engine/nozzle vehicles, these centerlines are also coincident.

Because the OTV engine is not fixed but, rather, gimbaled, a slight movement of the gimbal actuators can compensate for small amounts of misalignment. This action reduces total gimbal movement in that direction by a like amount.

For an engine with an extendible nozzle, it can be assumed that misalignment in the fixed portion of the engine is small and can be held to conventional tolerances by conventional methods. This is not true of the extendible radiation-cooled nozzle extension. The nozzle is supported by the extension/retraction mechanism and moved into its extended position by the mechanical drive system. It must be carefully designed to reduce the misalignment between it and the fixed portion of the nozzle. Misalignment of the extendible nozzle would occur within the divergent portion of the nozzle, at the joint attachment, and at a high area ratio of 172:1. Consequently, a severe misalignment at this point could result in the following:

- ° Loss of performance.
- ° One side of the nozzle may protrude into the hot-gas exhaust stream and become overheated.
- ° Seal surfaces may not mate properly, resulting in an inability to effect an adequate seal.
- ° All or any part of the above may simultaneously occur.

III, C, Task III - Component Mechanical Design and Assembly Drawings (cont.)

In view of these potential problems, it is important to keep misalignment between fixed and moving portions of the extendible nozzle assembly to a minimum. This probably would require meeting a tolerance comparable to that allowed for conventional nozzles.

The radiation-cooled nozzle can be aligned with the fixed portion of the nozzle in two ways: (1) through the screw shafts and support system or (2) directly to the fixed nozzle. The use of the screw shafts and support system to accomplish alignment is a poor choice because the screw shafts and supports must first be aligned with the fixed part of the nozzle before the extendible nozzle can be aligned with the screw shafts. Alignment of the screw shafts to the fixed portion of the nozzle is very difficult, no matter how many screw shafts are employed. Alignment would most likely be accomplished by line-boring the bearing holders in relation to the extendible nozzle centerline.

A much better way is the selected method of aligning the extendible nozzle directly to the fixed nozzle. Because both parts are concentric and turned on a lathe or spun, it is more natural to interface the two parts and accomplish alignment with the interface.

A spring-loaded nozzle centering device, consisting of a one-piece spring positioned in a groove on the lower support ring for the extension/retraction mechanism, is used. The spring is fabricated from a single piece of sheet stock, formed to the desired cross-sectional shape and diameter, and slotted at approximately 0.4 in. intervals to create discrete, radially oriented springs. A second centering spring is positioned just upstream of the diametric seal located on the tip of the regeneratively cooled nozzle. This spring assures final centering of the nozzle and a more uniform loading on the seal. This type of centering spring holds the nozzle in as

III, C, Task III - Component Mechanical Design and Assembly Drawings (cont.)

perfect an alignment as possible within the machining tolerances of the two parts; moreover, it establishes a moment arm to resist lateral forces imposed on the extendible nozzle due to gimbaling and other vehicle-imposed loads.

The function of the guide and support system is delineated by its definition: i.e., to guide and support the nozzle extension as it travels between its stowed and extended position. The concept consists of three tubular steel screw shafts located 120° apart around the fixed portion of the nozzle. Each screw shaft is an axially oriented threaded tubular shaft approximately 1 in. in diameter by 53 in. long. Each shaft is mounted in an elastomeric supported sleeve bearing located in the brazed flange fixed to the lower tube bundle "V" band support. This permits the final alignment to be accomplished by engagement of mating parts at the end of travel. Thus, the need for close tolerances in the placement of the screw shafts is greatly reduced. The other end of the threaded shaft is mounted in a bearing in the gearbox which is rigidly attached to the upper support ring. The gearbox houses a set of bevel gears which translate the rotational power from the horizontally oriented flexible drive shaft to the axially oriented screw shaft. A threaded lug or nut on each screw shaft is rigidly attached to the nozzle attachment ring which, in turn, is bolted to the nozzle. Screw shaft rotation within each lug results in an axial displacement of the extendible nozzle. Consequently, the nozzle extension is guided, supported, and translated by the threaded shaft.

A small reversible 28-volt DC drive motor, suitable for vacuum operation and having integral spur reduction gear sets and provisions for three separate power takeoffs, is mounted on the engine structure just below the gimbal plane. A flexible drive shaft transmits power to each screw shaft. Since nozzle deployment or retraction time is not an important factor, the electric drive motor does not require a high power output. The motor

III, C, Task III - Component Mechanical Design and Assembly Drawings (cont.)

contains a mechanical lock that is automatically activated to prevent movement of the drive train components whenever the nozzle is in the extended or retracted position. When in the extended and locked position, a constant predetermined compression load exists on the extended nozzle face seal (between the extended nozzle and regeneratively cooled fixed nozzle), thereby assuring an effective seal. The motor also contains a tool attachment for manually extending or retracting the nozzle, if necessary. The fitting is designed to accept a standard or board-type tool available to the crew.

Three flexible drive shafts that have been designed for reversible rotation are used between the drive motor and screw shafts. They are of equal length to maintain screw shaft synchronization during operation. The upper support ring is a thin-wall, hollow ring assembly having a rectangular cross section. It supports the upper end of the screw shafts and, in turn, is supported by the primary structural supports for the extension/retraction mechanism. These supports are configured to be 1-in. diameter thin-wall tubes. There are 3 sets, 120° apart, each containing 3 struts. One strut is radially oriented and attached to the forward end of the chamber structural support, while the other two struts are attached to the chamber structural support in the throat region in a tangential manner, with one on each side.

5. Gimbal Assembly

The gimbal assembly shown in Figure 25 consists of two sub-assemblies: (1) thrust mount and (2) monoball, thrust lug and bolt assembly, and antirotation tie rod assembly. The structure provides the monoball gimbaling capability and the attach points for the hydraulic actuators and TCA. Thrust is transmitted from the back of the injector flange through the struts of the thrust mount and monoball assembly to the propellant tank bottom flange.

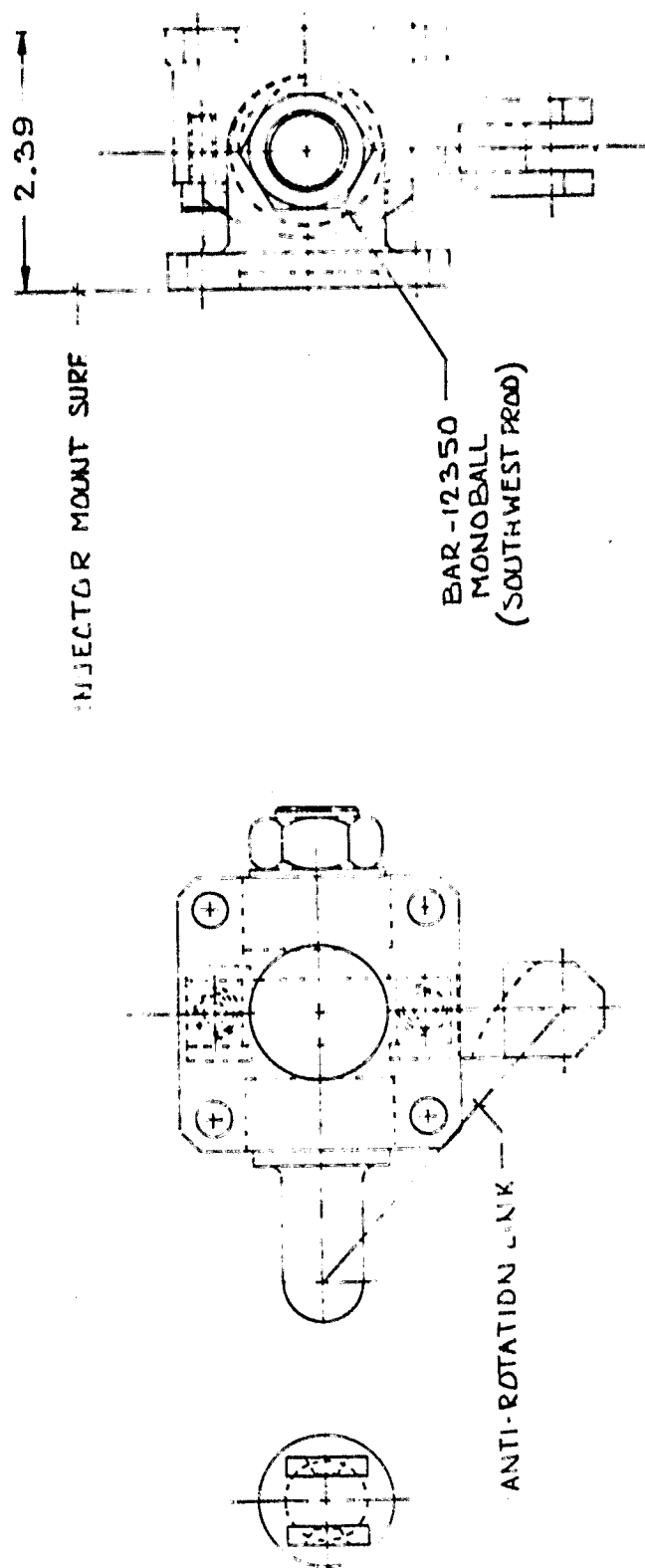


Figure 25. Gimbal Assembly (ALRC Drawing No. 1191993)

III, C, Task III - Component Mechanical Design and Assembly Drawings (cont.)

6. Oxygen Turbopump Design

a. Oxygen Boost Pump Mechanical Design

A cross section showing the details of the mechanical design and the function of the LOX boost pump is presented in Figure 26.

Because of their small size, the impellers for both the inducer and the transition stage can be machined integral with the shaft. The shaft is carried on a roller bearing and a ball thrust bearing or two ball bearings, with one restrained axially. The axial thrust is controlled by placing a labyrinth at the impeller discharge at the largest possible radius. The leakage flow through the labyrinth feeds the bearings and returns to suction through the spinner. If it is determined that the hard particle content in the oxygen exceeds the bearing allowable, the flow must be filtered.

Because the hydraulic turbine is velocity-compounded, there is very little differential pressure from side to side. The axial thrust from this type of turbine is small. Another advantage with a velocity-compounded turbine is the small leakage through the turbine labyrinth. The turbine is attached to the tandem stage of the inducer by brazing a ring to the vane tips. Since the vanes have a small angle, they have the ability to carry torque without high bending stress.

The flow from the turbine is mixed with the delivered flow at the guide vanes. The velocity of the two streams is matched so that mixing losses are minimized.

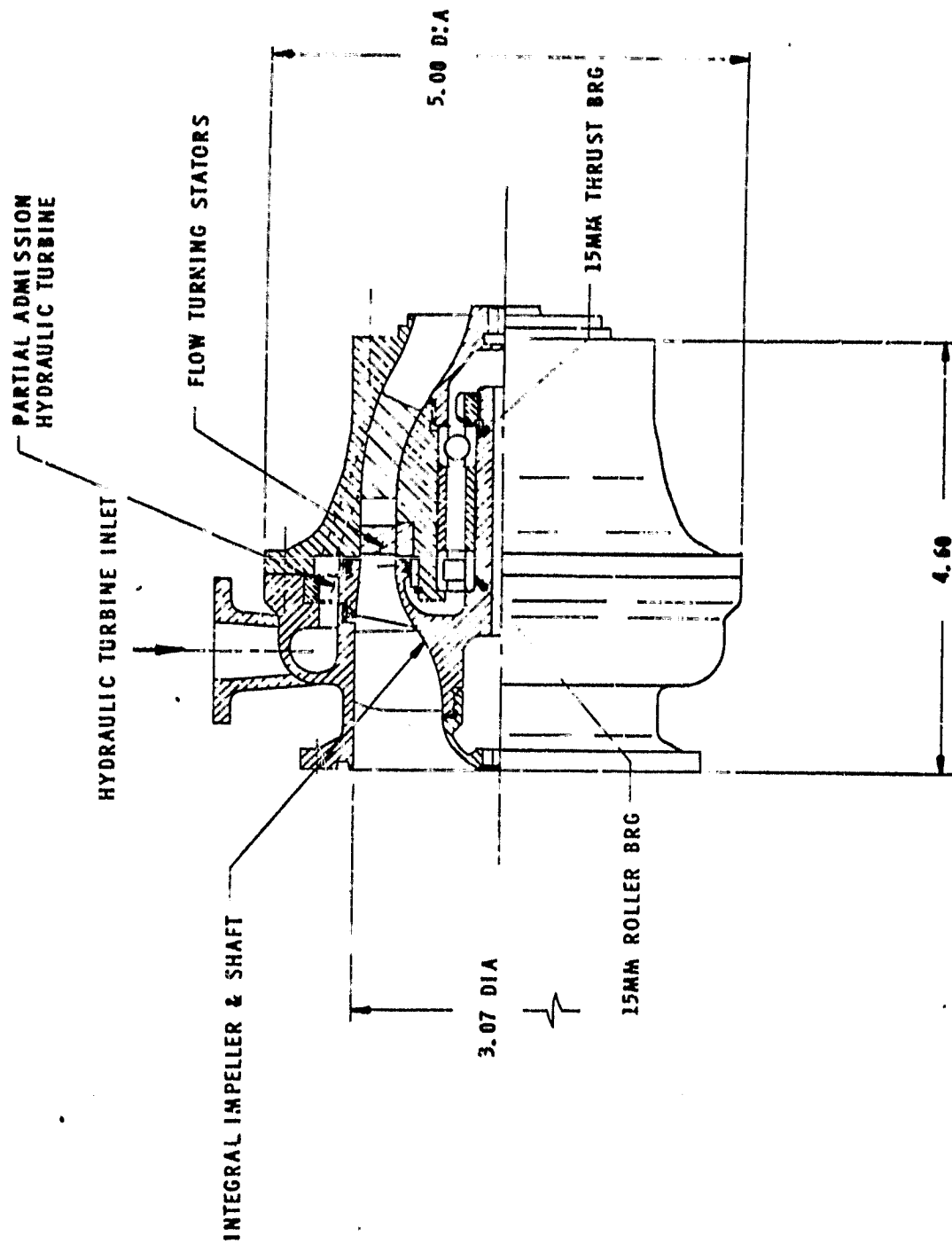


Figure 26. L0₂ Boost Pump Cross Section (ALRC Drawing No. 1191996)

III, C, Task III - Component Mechanical Design and Assembly Drawings (cont.)

The bearing housing loads are carried to the external housing through the guide vanes. These vanes are approximately 1/4 in. thick at the maximum point for about 25% flow blockage. These vanes are only used to support the bearings, not to turn the flow.

The stator vanes which turn the flow are in an inserted section. This allows them to be machined from the OD for better control of shape and thickness. A cast blade will most likely be thicker than desired without the required surface finish.

b. Oxygen Main Pump Mechanical Design

As shown in Figure 27, the main pump is made up of two pumping elements, an inducer and an impeller, which are directly connected together. The inducer, which can run at a relatively high speed without cavitating, provides sufficient head to the impeller to keep it from cavitating. The head split is approximately 15% to 85%.

The inducer has a cylindrical tip to make it less sensitive to axial displacement. The impeller has front and back shrouds with cylindrical labyrinths. Flow from the bearing package is returned between the inducer and the impeller where the pressure is high enough to prevent flashing of the liquid oxygen due to the heat removed from the bearings.

A major mechanical design consideration is interpropellant sealing. With the turbine driven by warm H_2 gas (41°F), a positive separation must take place between the turbine and pump. There are two basic options. First, the turbine end bearing(s) can be lubricated with liquid oxygen. This method requires that the interpropellant seal package be located between the turbine bearing and the turbine which results in a relatively short bearing-to-bearing span and a long span between turbine bearing

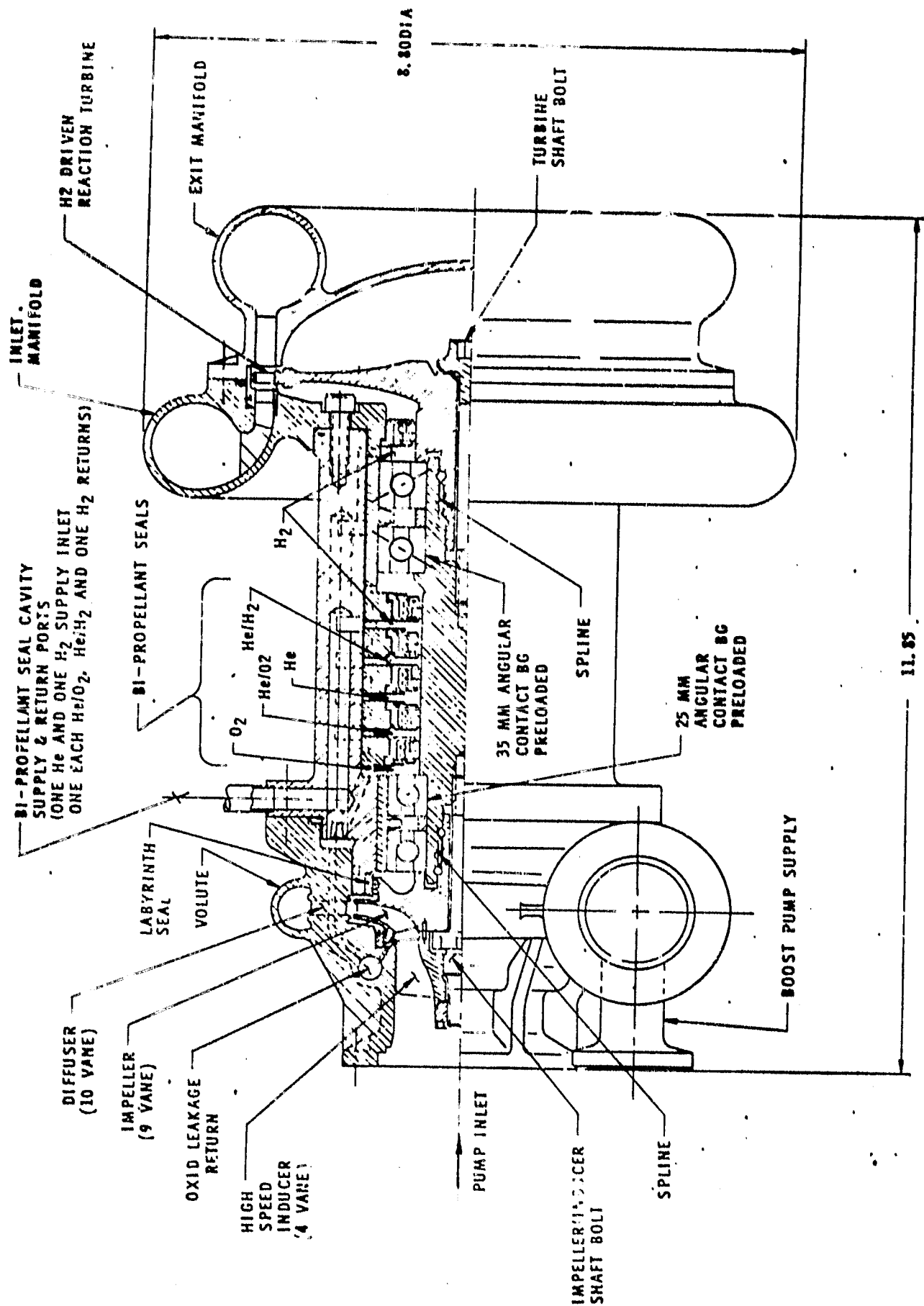


Figure 27. L₂ Main Pump Cross Section (ALRC Drawing No. 1191999)

III, C, Task III - Component Mechanical Design and Assembly Drawings (cont.)

and turbine. Because the turbine is the largest (heaviest) component on the shaft, the shaft diameter must be increased to avoid operation above the first critical speed. The second method is to lubricate the turbine end bearing(s) with liquid hydrogen. This is the selected concept and has the advantage of placing the turbine in close proximity to the bearing and also giving a reasonable bearing-to-bearing span. The liquid hydrogen is tapped off the second stage of the main hydrogen pump, flowed through the bearings, and returned to the inlet of the main hydrogen pump second stage. Although some of this liquid hydrogen leaks into the warm H_2 -gas driven turbine, this should not cause any problems. The leakage rate is small since the differential pressure across the seal is very small.

The pump end bearings take their flow from the impeller backside labyrinth leakage flow through the bearings and are returned to a manifold which feeds the flow between the pump inducer and pump impeller.

The interpropellant seal package shown in the design consists of five circumferential-type shaft seals. Helium is introduced between the second and third seal (counting from the pump end bearings) at a pressure sufficiently high for helium to leak under both seals and mix with oxygen on the pump-side seal and hydrogen on the turbine-side seal. These mixtures can either be returned to their respective tanks where the propellant is condensed and the helium gas is used to pressurize the tank or they can be dumped overboard at a location where mixing can be avoided.

An alternative to this interpropellant seal concept is to use a burn-off seal. This seal has the potential for reducing system complexity by eliminating the need for both the helium supply and the hydrogen supply from the main hydrogen pump. However, until such time as this alternative approach has been fully developed, the more conventional sealing method is recommended.

III, C, Task III - Component Mechanical Design and Assembly Drawings (cont.)

The selected bearings are a pair of back-to-back sets of deep-groove angular contact bearings which are located at each end. These could possibly be replaced with single four-point contact bearings which have a split inner race. The back-to-back bearing sets are preloaded axially with springs so that there is no radial looseness. The turbine end pair are 35mm bearings which are locked in the housing so that one will carry axial thrust in one direction and the other in the opposite direction. The pump end pair are 25mm bearings which are allowed to move axially in the housing and carry only radial load.

Initially, it was thought that the turbine could be velocity-compounded with very small wheel differential pressure and that the axial thrust would be unaffected by the flow direction through the turbine. However, due to increased power requirements, it became necessary to design the turbine for some reaction. The pressure difference across the wheel is significant inasmuch as the flow direction in the turbine must be away from the pump to reduce the axial thrust to an acceptable level. With this concept, the labyrinth on the backside of the impeller can be set so the calculated value of axial thrust is zero. In reality there are variations in the pressure schedules. This results in some axial thrust. If it is assumed that these variations do not exceed $\pm 10\%$ of the design thrust forces, then the worst-case axial thrust value is ± 600 lb and the RMS value is ± 300 lb. At the RMS value, the bearing B_{10} life is slightly greater than 1000 hours.

It should be noted that the bearing flow is not filtered. If the propellants exhibit hard contamination exceeding the bearing capability, then a filtering scheme must be incorporated.

A lumped mass model of the rotating components was analyzed for critical speed. With a bearing radial stiffness greater than

III, C, Task III - Component Mechanical Design and Assembly Drawings (cont.)

2.5×10^5 lb/in., the first critical speed exceeds the operating speed by 25%. At normal bearing stiffnesses, the first critical speed is 2.5 times the operating speed.

Essentially, the entire main oxidizer pump, turbine, manifolds, inducer, impeller, shaft, and housing are made of Nitronic 50. Only the bearings and possibly the bearing housings are fabricated from steel. The seal housings are made of titanium, while the springs are stainless steel and the segmented rings are made of carbon.

With the materials as described above, little, if any, problem with differential thermal growths is anticipated. However, if the shaft is made of steel, the splines have to be designed for a female in the shaft so that both the expansion and the centrifugal loading tend to increase the interference fits of the pilots. The splines are sized for a maximum of 30,000 psi shear and 10,000 psi bearing stress.

All static seals except the three exterior seals are of the piston ring type. A very small leakage through the overlapped piston ring seal is tolerated. The piston ring seals, which seal axial leakage flow, are used because they require only a small envelope. The three outside seals, which seal against internal pressure, are of the conno-seal type (AS 4061).

c. Oxygen Main TPA Gas Turbine Design

(1) Requirements and General Considerations

The Advanced Expander Cycle Engine turbopump assemblies require low-pressure-ratio turbines driven by a warm hydrogen gas. The turbines are coupled fluid-dynamically, i.e., the LOX turbine is in series (downstream) with the LH₂ turbine.

III, C, Task III - Component Mechanical Design and Assembly Drawings (cont.)

Previous studies (OTV Phase A, Contract NAS 8-32999) indicate that in order to meet the engine performance prediction, the hydrogen TPA requires a two-stage axial flow turbine and the oxygen TPA requires a single-stage axial flow turbine. These studies indicate further that the reaction blading must be applied, requiring tight leakage control. Also, because of the low pressure ratios, the turbine performance is sensitive to the manifold losses. This requires well-designed large inlet and exhaust systems.

(2) Selected Concepts

The OTV engine cycle operates the turbines with low temperature hydrogen gas (75°F) at low pressure ratios. These conditions permit the utilization of the same materials for the rotor blades and the disks; consequently, the blades and the disks can be machined from the same forging. Shrouds are necessary to permit reduction of tip leakage which can have considerable effect on the efficiency of the low aspect ratio reaction blading. Due to the low aspect ratio and the hub-to-tip ratio, untwisted blading can be used without an appreciable loss in efficiency.

The objective in manifold design is to minimize the pressure loss and provide a uniform radial and circumferential velocity distribution at the inlet to the nozzles. Similarly, the exhaust collector is designed for as low a pressure drop as possible. Ultimately, manifolds and exhaust collectors are designed with emphasis not only on turbine performance, but also on the minimization of the duct losses and the overall system packaging.

For the LOX and LH₂ turbine inlet manifolds, a rollover scroll having tangential inlet is selected as best suited to system

III, C, Task III - Component Mechanical Design and Assembly Drawings (cont.)

packaging. A set of vanes is used to channel the flow into the nozzles and also serves as a structural support for the manifold.

The gas exit for both oxygen and hydrogen TPA turbines is accomplished with a scroll having a tangential outlet.

(3) Fluid-Dynamic Design Method

In order to realistically predict the turbine efficiency and flow passage geometry, it is necessary to conduct a loss analysis which takes into consideration the effect of significant fluid-dynamic parameters. In this analysis, the losses are divided into the following three groups:

- a. Inlet Manifold Loss
- b. Blading Loss
- c. Exhaust Collector Loss

The scroll-type manifold with tangential inlet is expected to have a pressure loss coefficient no higher than 1.0 (Ref. 11). The pressure loss coefficient, γ_1 , is defined as follows:

$$\gamma_1 = \frac{P_{oi} - P_{oe}}{P_{oi} - P_i}$$

where:

- P_{oi} = Total pressure at the scroll inlet
- P_{oe} = Total pressure at the scroll exit
- P_i = Static pressure at the scroll inlet

Blade loss analysis is based upon the method of Ainley and Mathieson (Ref. 12 and 13). The losses are divided into the following:

III, C, Task III - Component Mechanical Design and Assembly Drawings (cont.)

- a. Primary Loss
- b. Secondary Loss
- c. Tip Clearance Loss

In addition to these losses, disk friction is also taken into account.

The estimated exhaust collector loss coefficient based on exit dynamic head is 1.5.

Using the loss analysis iteratively, turbine flow passage is calculated and turbine performance is predicted via the computer program reported in Reference 13.

The following design point specifications are based on the conditions which are predicted downstream from the hydrogen TPA gas turbine. They represent a refinement of the information given in Figure 18 and were taken from a later cycle power balance.

- a. Total Inlet Pressure, $P_0 = 1494$ psia
- b. Total Inlet Temperature, $T_0 = 487^\circ\text{R}$
- c. Static Exit Pressure, $P_2 = 1323$ psia
- d. Rotational Speed, $N = 34720$ RPM
- e. Flowrate, $\dot{W} = 4.22$ lb/sec

The final total pressure loss coefficients used in the analysis are as follows:

III, C, Task III - Component Mechanical Design and Assembly Drawings (cont.)

<u>Stage</u>	<u>Blade Row</u>	<u>Total Loss Coefficient</u>
1	Manifold	0.79
	Stator	0.115
	Rotor	0.186
	Collector	1.5

The results of the analysis are summarized in Table XVIII. Figure 28 shows the meridional flow passage of the turbine.

(4) Oxygen TPA Turbine Conclusions

Design point analysis is conducted to determine the flow passage geometry and performance of the oxygen TPA turbine. The results are as follows:

- Single-stage reaction turbine
- Pitch diameter = 5.545 inches
- Overall velocity ratio = 0.483
- Estimated static efficiency = 66.7%

These results are based on a detailed blade loss analysis which can be used for blade profile design. However, only an approximate study was made of the manifold losses. In the design of inlet and exhaust manifolds, considerations are given not only to the turbine performance but also to the engine system requirements. Cold-flow testing will be necessary to develop the most effective turbine inlet and exhaust configurations.

TABLE XVIII
LO₂ TPA GAS TURBINE DESIGN POINT PERFORMANCE

<u>Parameter</u>	<u>Stage</u>	<u>Overall Turbine, Including Manifolds</u>
Work, BTU/lb	40.8	40.8
Flowrate, lb/sec	4.15	4.15
Static Pressure Ratio	1.105	1.130
Stage Loading Factor	0.60	-
Stage Flow Coefficient	0.328	-
Velocity Ratio	0.533	0.483
Static Efficiency, %	82.3	67.7

The estimated disk friction loss is 3.86 HP. When this loss is included, the overall turbine efficiency is 66.7%.

DESIGN POINT
 $P_o = 1494$ psia
 $T_o = 487$ °R
 $P_c = 1323$ psia
 $\dot{W} = 4.22$ lb/sec
 $N = 34,720$ RPM
 FLUID: GH_2

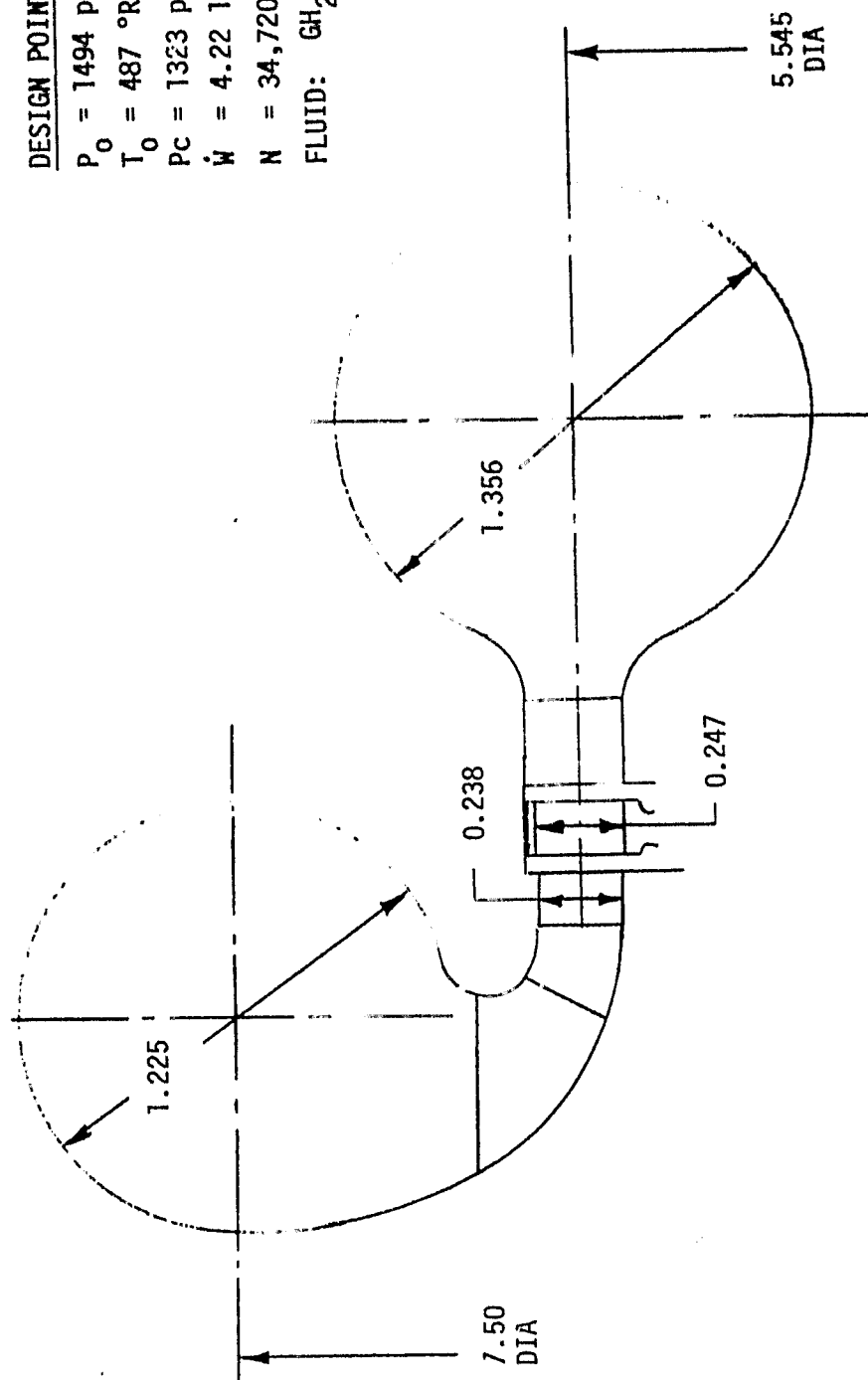


Figure 28. L0₂ TPA Turbine Meridional Flow Passage

III, C, Task III - Component Mechanical Design and Assembly Drawings (cont.)

d. Recommendations for Future Study, Oxygen TPA's

As a result of limited time and resources available to conduct this TPA design, certain items could only be addressed superficially and remaining problems could only be identified but not totally resolved. As a minimum, further design iterations are required in the following areas:

- (1) Reevaluate material selections for boost and main pumps.
- (2) Confirm that the pressure schedules of the purge system, the oxygen and the hydrogen pumps are compatible at all modes of anticipated engine operation (startup, shutdown, idle, transient, full power) to ensure successful and safe performance of the interpropellant seal.
- (3) Determine if the bearing coolants require filtering.
- (4) Establish solutions to problems which could arise at engine shutdown as propellant backflows into the bearings.
- (5) Conduct a turbine design iteration incorporating recommended study modifications.
- (6) Reevaluate the boost pump configuration to determine the possibility of standardizing the hydrogen and oxygen boost pumps and the feasibility of a two-stage hub turbine boost pump with high-speed inducer tap-off as a more effective design approach.

III, C, Task III - Component Mechanical Design and Assembly Drawings (cont.)

(7) Finalize turbine inlet and exit manifold geometry in more detail, emphasizing the performance of the two turbines in a series system.

(8) Conduct a literature search for small-size turbines, emphasizing small blade size and tip clearance leakage control.

e. Oxygen TPA's Technology Areas

The oxygen TPA preliminary design, as baselined in this report, consciously utilizes only design features which are within the present state of the art. Certain performance improvements and design simplifications could result if some of the following design features were to pass their technology status and could then be implemented in the final design. The most significant technology areas to be considered are as follows:

(1) Development of a burn-off seal to replace the spacious and heavy purge seal.

This concept allows leakages from pump and turbine to mix. It is particularly attractive for the LOX pump of the OTV engine because the temperature of the hydrogen in the turbine is relatively low and because no spontaneous reaction of the resulting potentially explosive O_2-H_2 mixture in the seal area of the turbopump is to be expected. The mixture will not burn or explode without being ignited.

It seems feasible to transport the mixture collected in the seal cavity by means of a jet pump (eductor) to a catalyst bed where oxygen and hydrogen recombine to water (steam).

III, C, Task III - Component Mechanical Design and Assembly Drawings (cont.)

By keeping the pressure in the interseal cavity low, the quantity and, therefore, the energy content of the mixture present in the turbopump that could be liberated in case of an accidental ignition (e.g., by metallic rub) is greatly reduced.

The driving jet flow could conceivably be supplied by the vent flow tapped off downstream of the first seal element (pressure breakdown seal) of the high-pressure turbine seal package.

Added safety features could be provided through the utilization of flame arrestors in order to avoid backfiring and ignition of the mixture in the lines or in the bearing cavity.

(2) Development of a drive system for the boost pump which would have a higher efficiency than the present concept. Fluid coupling, torque converter, or friction drive systems may be considered.

(3) Structure a development program which is geared towards the minimization of gas turbine inlet and outlet manifold pressure losses. An optimal manifold design will increase overall turbine efficiency without excessive increase in envelope size and weight.

7. Hydrogen Turbopumps Design

a. Hydrogen Boost Pump Mechanical Design

The LH₂ boost pump is illustrated in Figure 29. It is driven by a partial admission hydraulic tip turbine. The turbine, in turn, is driven by hydrogen flow obtained from the first stage of the main hydrogen turbopump. The hydrogen that leaves the tip turbine is mixed with the boost

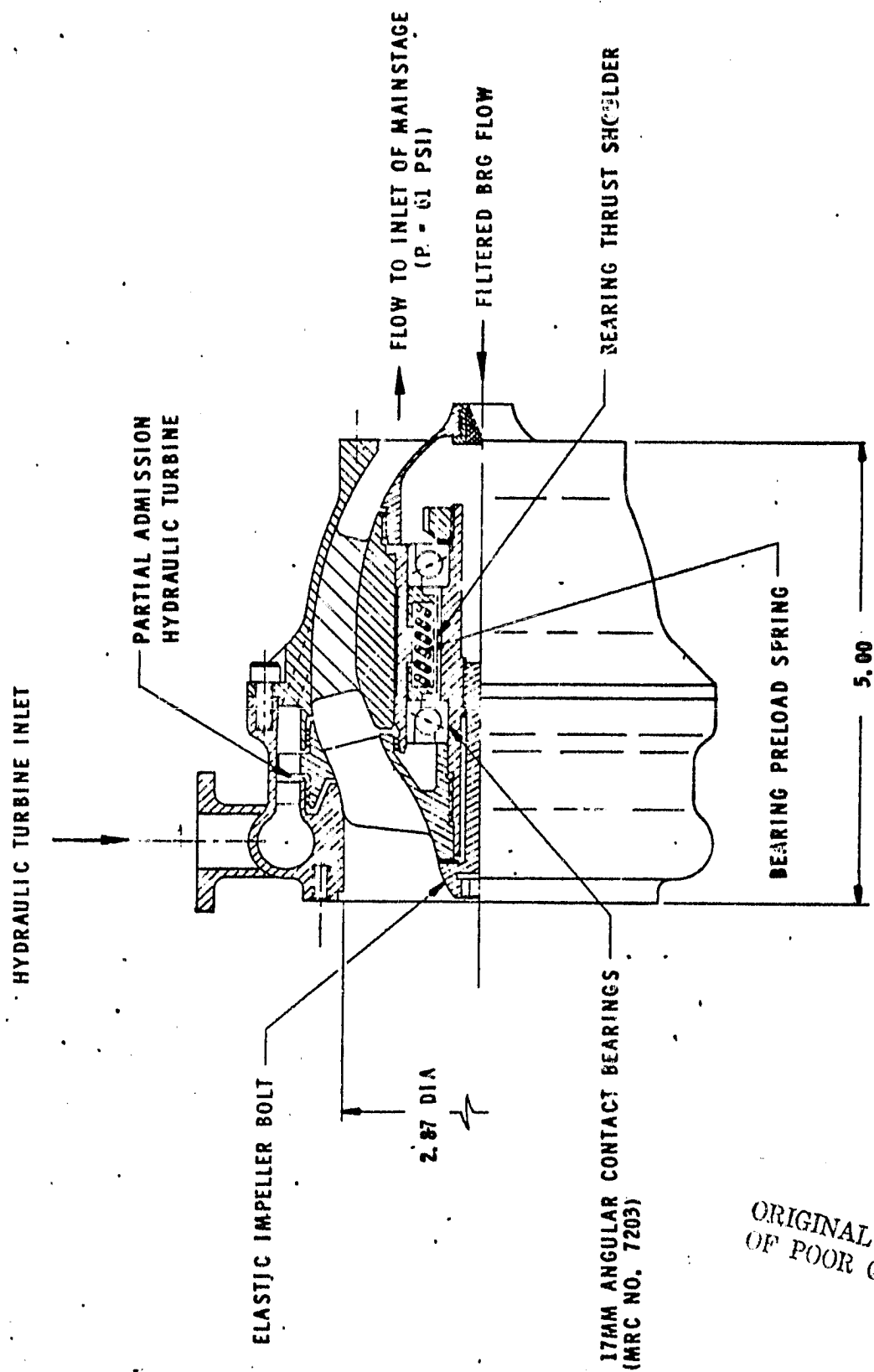


Figure 29. LH₂ Boost Pump Cross Section (ALRC Drawing No. 1191994)

III, C, Task III - Component Mechanical Design and Assembly Drawings (cont.)

pump through-flow after which it reenters the main hydrogen pump. The boost pump discharge flow is axial to facilitate close coupling of the boost and main turbopump assemblies in the engine package.

The hydraulic turbine is hub-mounted. With a flow of 129 GPM, it yields an efficiency of 66% with a head change of 7136 ft.

The boost pump operates at an NPSH of 15 ft, delivers a discharge pressure of 50 psia, and is 78% efficient.

b. Main LH₂ Pump Mechanical Design

The main high-speed hydrogen turbopump baseline design is shown on Figures 30 and 31. The pump is a three-stage machine that is driven by a two-stage turbine. The pump operates at a speed of 90,000 RPM, with a pressure of 2531 psia. The turbine inlet temperature of 535°R provides a benign operating environment considered desirable for this man-rated application.

Layouts were prepared for two design options. The baseline design shown in Figures 30 and 31 incorporates a separate pump and turbine housing. This permits the use of lightweight titanium for the pump housing and a material that is compatible with room temperature hydrogen for the turbine housing. The preliminarily selected material is Nitronic-50. The alternate design incorporates a one-piece housing which is shown in Figure 32. For this design, the housing must be compatible with room temperature hydrogen throughout to avoid embrittlement. Consequently, this one-piece housing is made of Nitronic-50 with flange joints at both the pump inlet and turbine exhaust ends. The discussion which follows is generally applicable to both design concepts.

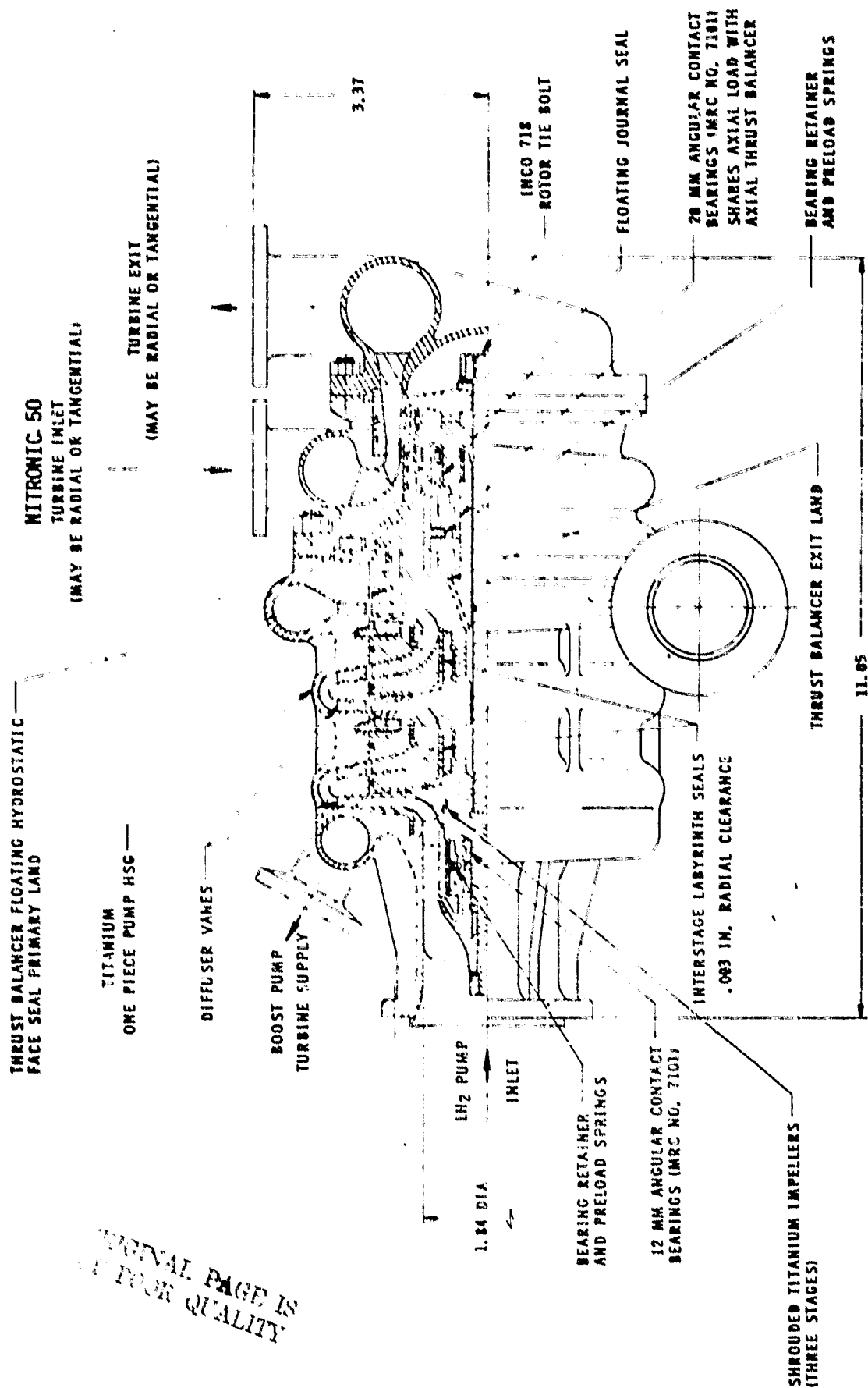


Figure 30. LH₂ Main TPA Cross Section (Baseline), Separate Pump-Turbine Housings (ALRC Drawing No. 1191997)

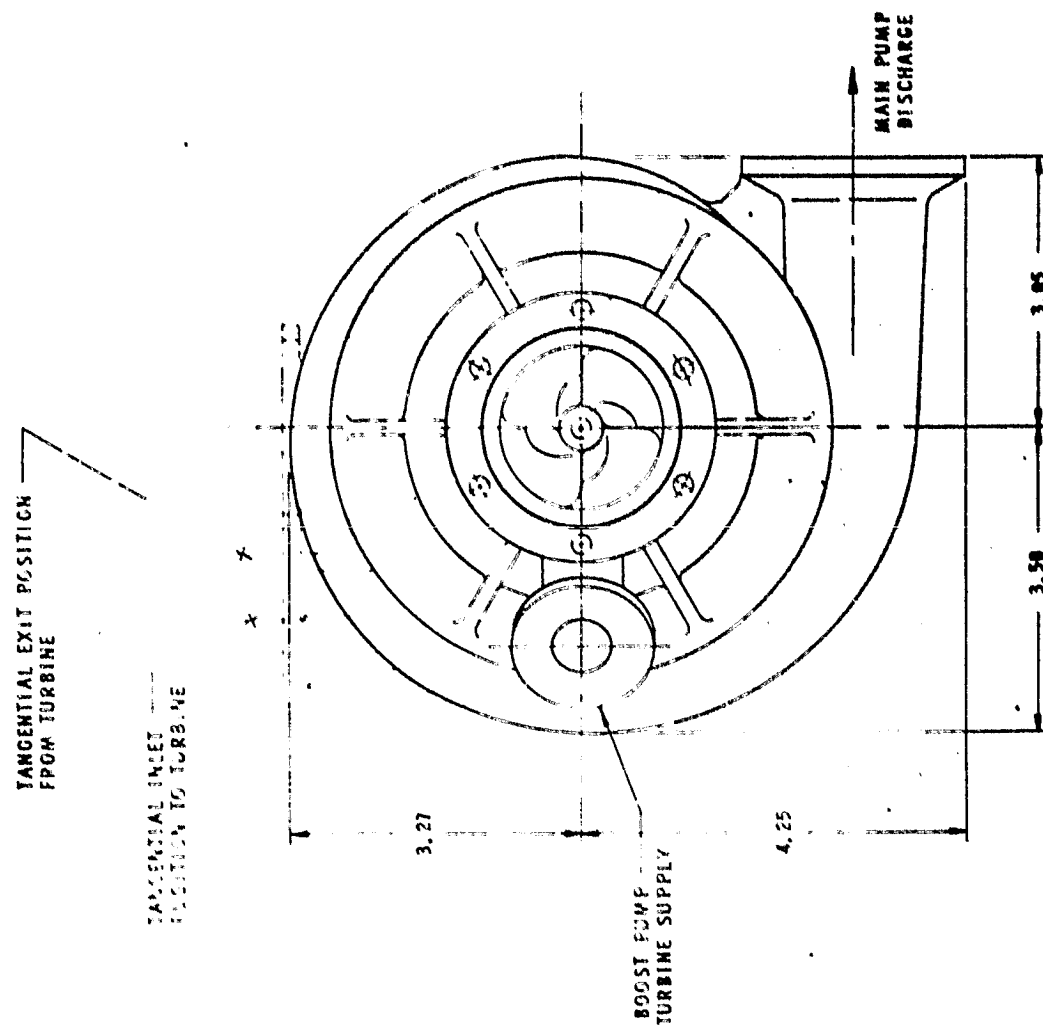


Figure 31. LH₂ Main TPA End View (Baseline Design) (ALRC Drawing No. 1191997)

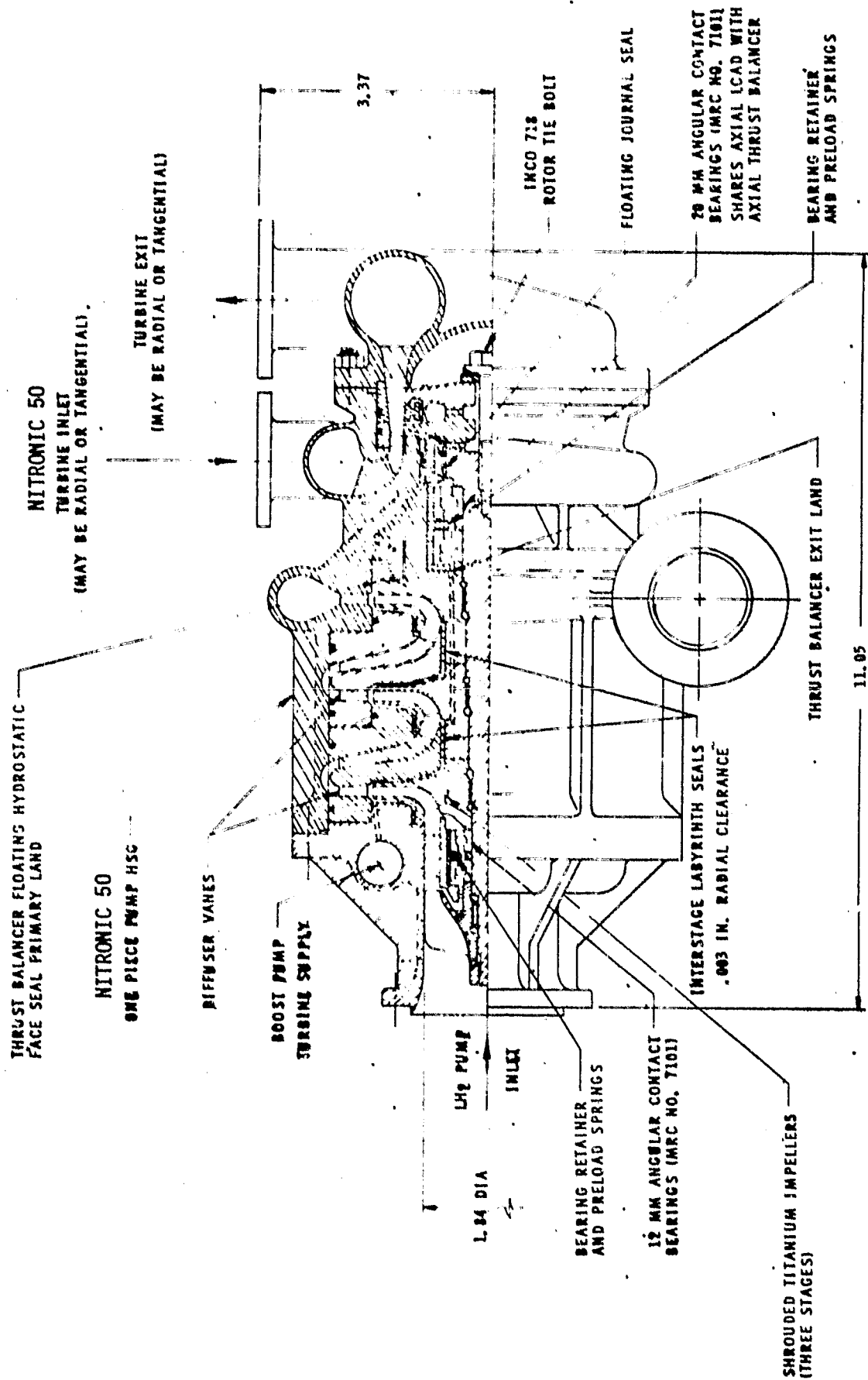


Figure 32. LH₂ Main TPA Cross Section (Alternate Design): Common Pump
 and Turbine Housing (ALRC Drawing No. 1191998)

III, C, Task III - Component Mechanical Design and Assembly Drawings (cont.)

The basic design philosophy and design practices used in this effort are in agreement with the guidelines provided in References, 14, 15, 16, 17, 18, 19, and 20.

The main fuel turbopump consists of an axial flow inducer followed by three shrouded centrifugal pump stages driven by a two-stage axial-flow warm hydrogen gas turbine. The fuel pump impellers are shrouded to aid tolerance and axial thrust control. Each front shroud has a wear ring seal just over the impeller inlet to control return leakage from the impeller exit to the impeller inlet. The present configuration shows a straight labyrinth, which is the simplest and most reliable application. A stepped labyrinth can reduce flow but has less predictable thrust, while a hydrostatic seal has about one third the flow and predictable thrust but is more sophisticated.

There is an interstage shaft seal between each centrifugal impeller. This seal controls flowrate from the impeller inlet to the previous impeller exit. Diffuser vanes and crossover passages are encased in removable disks. The rotating assembly is a built-up construction with an elastic tie bolt to maintain structural integrity. The rotating assembly is supported on a set of angular contact bearings between the inducer and first impeller and between the third impeller and the first turbine disk. The pump end bearing set supports radial loads but permits axial motion. The turbine bearing set provides radial support and axial restraint. Since the potential thrust variations are much higher than the rolling elements' bearing capacity, a hydraulic thrust balancer is located on the backside of the third impeller. Pressure from the third-stage impeller operates the balancer, returning the exit flow to the second impeller inlet. To prevent turbine gas from entering the bearing cavity, a high-pressure turbine seal controls leakage to the turbine and an adjacent seal controls flow to the bearings.

III, C, Task III - Component Mechanical Design and Assembly Drawings (cont.)

Rolling element bearings are restricted in DN values in high-speed machines. When operating near the upper limit of about two million, the load capacity is reduced in order to maintain an acceptable fatigue-life. The ball centrifugal loading caused by high angular shaft speed uses a large percentage of the available load capacity. The high speed also imposes high loads on the bearing cages. The cage must present a low profile to allow the proper amount of lubricant through the bearing. Accordingly, the life of rolling contact bearings is limited at high speed. Radial loads are minimized by having symmetrical impeller discharges and very accurate mechanical balance. Critical speeds are located at least $\pm 25\%$ away from the operating speed to avoid dynamic amplification. The selected bearing design is a pair of angular contact bearings, preloaded back-to-back to maintain a minimum stiffness and to avoid skidding of the rolling elements. The pump end bearings are 10mm inside diameter, selected for hydraulic passage clearance. The turbine end bearings are 20mm inside diameter and are not restricted at the outside diameter but are maximized at the base to transmit the torque and provide for a high stiffness shaft. The pump end bearings provide radial support but are free to move axially in the retainer. The turbine end bearings provide radial support and share the axial load with the hydraulic thrust balancer.

High pressures on the impeller and turbine disk faces generate axial shaft loads several orders of magnitude higher than the bearing capacity. Consequently, an axial thrust balancer is required. The design and location of this balancer are largely influenced by the configuration of the pumps. Ideally, the axial thrust should be balanced at each rotating element: i.e., impeller, turbine, running rings, etc., as close as possible with the residual carried by a thrust balancer or thrust bearing. The thrust balancer should have a capacity on the order of $\pm 5\%$ of the shaft axial force. In this pump design, the impellers are shrouded with straight labyrinths at the front shroud impeller inlet and on the shaft between each impeller. With this design, each impeller has a net thrust of approximately 850 lb towards the inlet. The front of all three impellers is identical. The back of the third-stage impeller differs from the back of the first and second-stage ones

III, C, Task III - Component Mechanical Design and Assembly Drawings (cont.)

by the axial thrust balancer. The turbine pressure forces result in a net force towards the pump inlet due to the large exposed area on the downstream side of the second-stage turbine disk. The net force on all disk faces is 2600 lb at the design point, excluding the thrust balancer face. The normal operating force for the thrust balancer compensates the 2600 lb force and provides a variable force of ± 3600 lb. A diagram of the axial thrust balance is shown in Figure 33.

The axial thrust balancer is located on the backside of the third-stage impeller and uses its discharge pressure for axial balancing purposes. The working differential pressure is created by returning the thrust balancer exit flow to the inlet of the second-stage impeller. In order to compensate for variable axial loads, it is necessary to have the thrust balancing system sensitive to axial motion. The method selected for this concept is a series flow system, with a fixed geometry flow restrictor in series with a variable flow restrictor. This is referred to as a single-acting balancer since the variable pressure acts on only one disk face. Three series flow thrust balancers were evaluated: (1) the straight labyrinth in series with the exit land; (2) the impeller tip land in series with the exit land; and (3) the hydrostatic face seal in series with the exit land. The performance of these balancers is shown in Figures 34, 35, and 36. The tip seal has a flowrate similar to the labyrinth seal type but has a higher axial stiffness. The hydrostatic seal type has stiffness similar to the tip seal type but has a much lower flow. Since performance optimization is a design goal, the hydrostatic seal design (as shown on the preliminary design drawing) was selected.

Wear ring seals are required at the impeller front shrouds, and shaft interstage seals and turbine seals are required between high and low pressure zones to minimize leakages and provide axial thrust balance control. At the turbine, a double seal is used to control liquid

AXIAL FORCES (LB)

2601 ← 2601 ± 3600.18

2601 ± 3600

714

714

2601

898

850

139

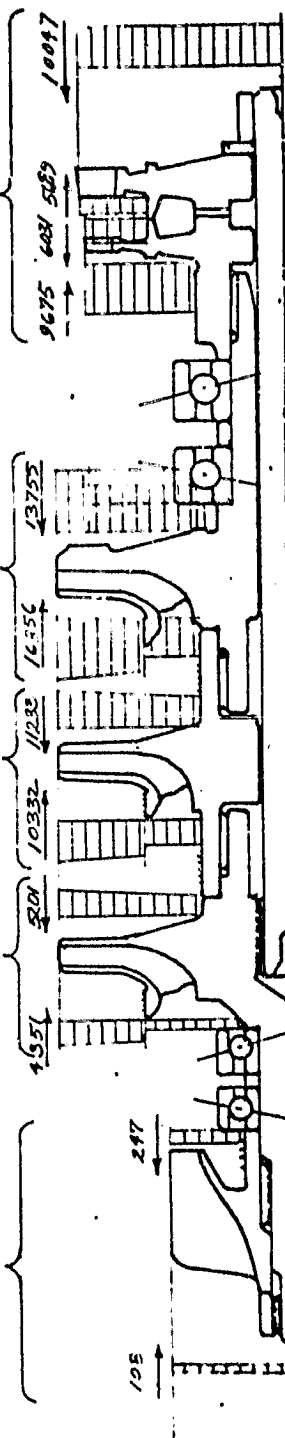


Figure 33. LH₂ Main Pump Axial Thrust Balance

$R_o = 1.685$
 $R_i = .6$
 $C_o = .003 \text{ IN.}$
 $P_s = 2317. \text{ LB/IN.}^2$
 $P_e = 950. \text{ LB/IN.}^2$
 $h = .025$

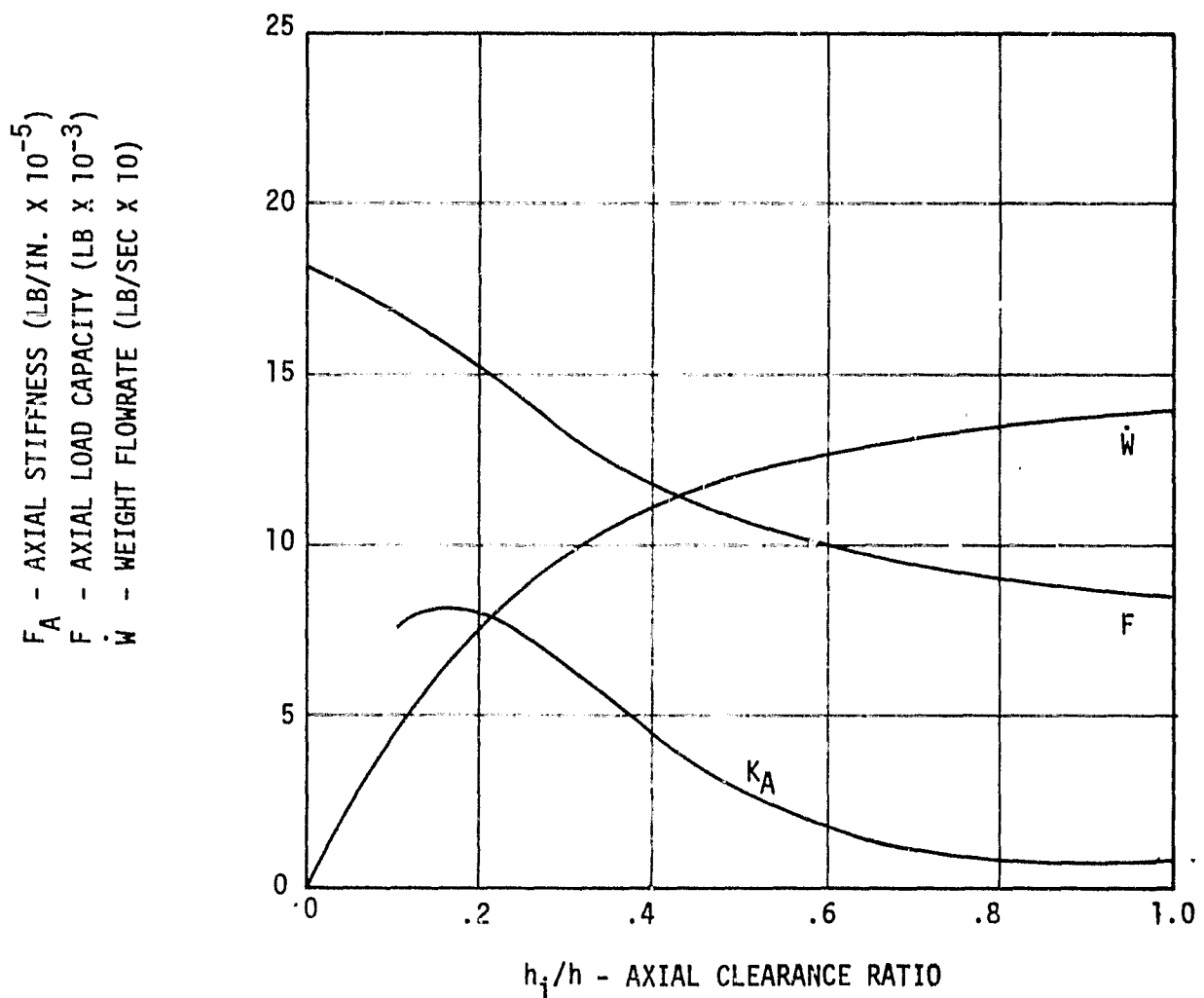


Figure 34. LH_2 Main TPA Series Flow Thrust Balancer-Labyrinth/Land

$R_o = 1.685 \text{ IN.}$

$R_i = .6 \text{ IN.}$

$h = .010 \text{ IN.}$

$P_s = 2317. \text{ LB/IN.}^2$

$P_e = 950. \text{ LB/IN.}^2$

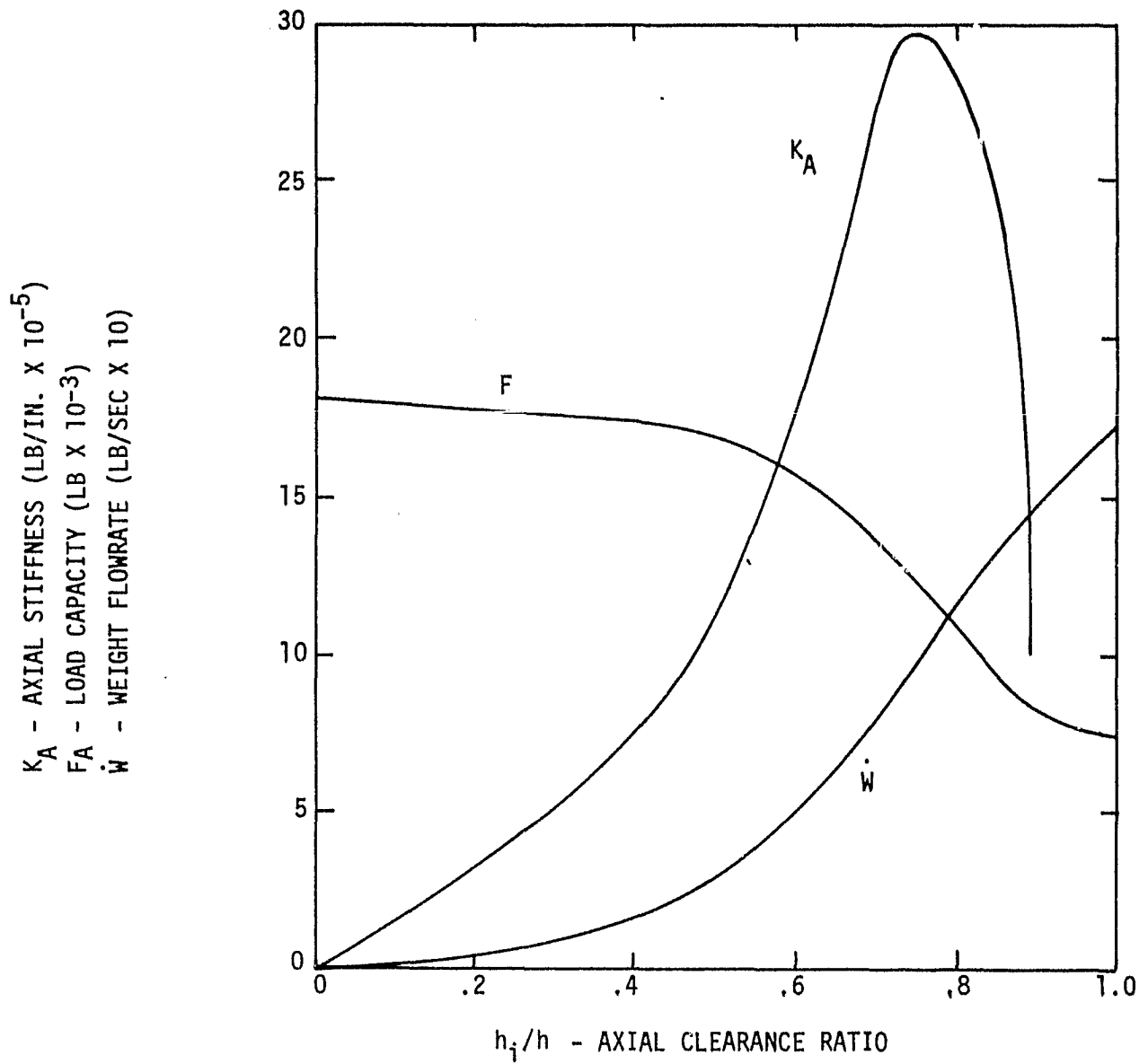


Figure 35. LH_2 Main TPA Series Flow Thrust Balancer, OD/ID Land

SPEED $N = 90,000$ RPM

$R_\phi = 1.324$ IN.

$R_D = 1.6$ IN.

NUMBER OF RECESSES 8

DIA. OF ORIFICE .015 IN.

FLUID LH_2

SUPPLY PRESSURE 2317. (LB/IN.²)

EXIT PRESSURE 1633 (LB/IN.²)

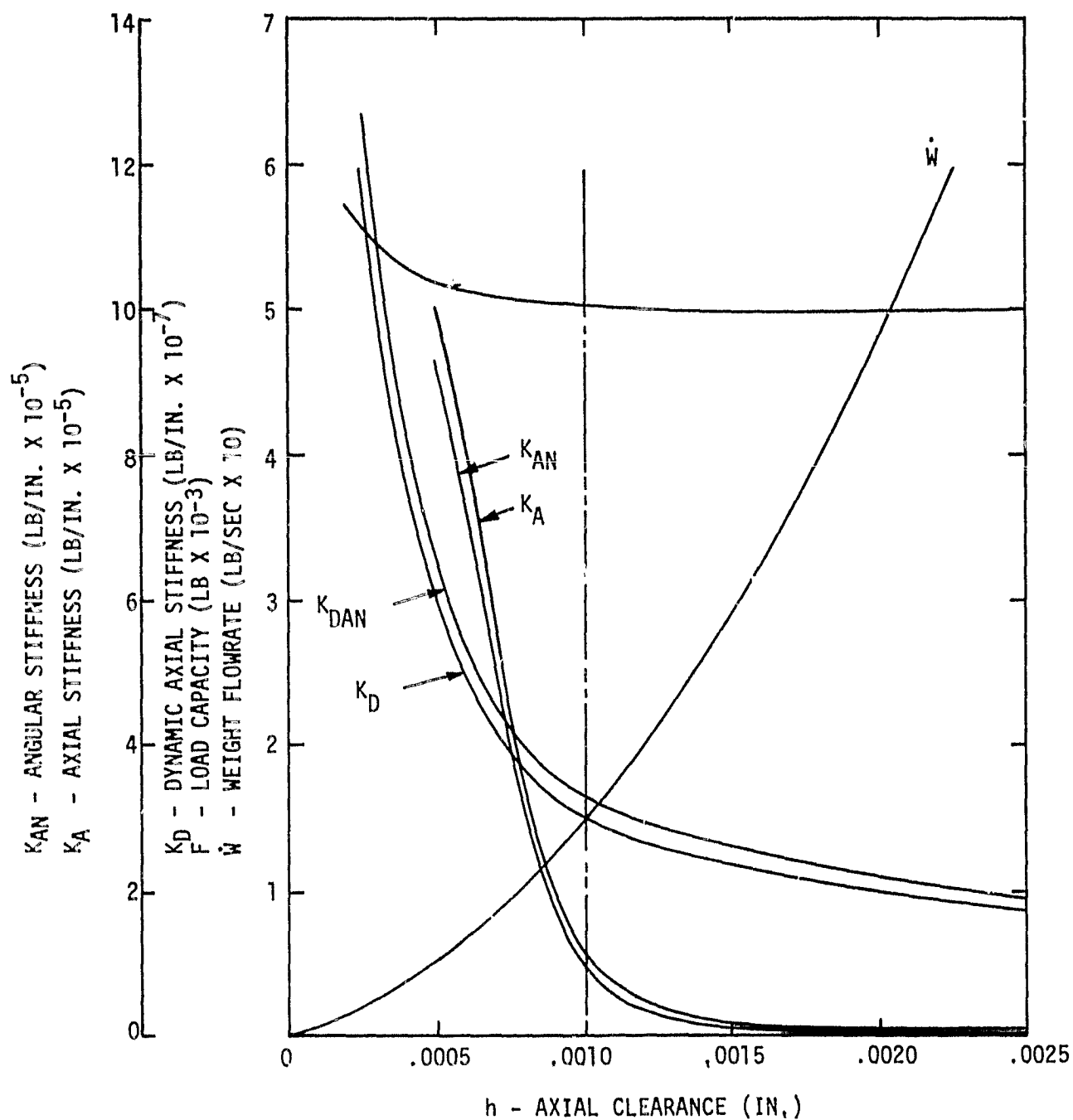


Figure 36. LH_2 Main TPA Hydrostatic Thrust Balancer/Face Seal

III, C, Task III - Component Mechanical Design and Assembly Drawings (cont.)

hydrogen leakage into the gaseous hydrogen of the turbine and liquid hydrogen leakage to the bearing. To keep a positive flow to the turbine and prevent backflow of turbine gases, the seals are pressurized from the third-stage impeller. Figure 37 shows three seal types considered for utilization as a double-seal application. The floating ring seal is reflected in the baseline design. It is characterized by low leakage and low start torque. Alternate seal concepts are hydrostatic face seals and regenerated shaft riding seals. Both of these have higher starting torques. The turbine-side seal has a pressure drop of 500 psi and seals a liquid and gas zone. Flow to the bearings is controlled by this seal and must function with a pressure drop of 1500 psi. This is a liquid-to-liquid seal. Supply pressure to the seal ring is directly from the third-stage impeller discharge and provides a high-pressure liquid barrier between the warm gas turbine and the LH₂ bearings. Flow goes to both the turbine and the bearings. The sealing element is a floating ring seal design that follows shaft motions by the hydrostatic forces supplied by the seal pressure drop. The axial pressure-balanced design allows radial tracking of the rotor with minimal force. These journal seals exhibit lower starting torques than face seals which have a spring load to overcome. The surface velocity of these seals is about 430 ft/sec. Since this is above rubbing contact seal speed, controlled gap seals are required. The flowrate to the turbine is approximately 0.1 lb/sec and about 0.2 lb/sec to the bearing.

Pump impeller wear ring seals are used on the shrouded impeller designs to minimize the return flow and balance axial thrust by controlling pressure area forces. The advantage of the wear ring seals is the freedom of axial motion without rubs. The return leakage represents an efficiency penalty which must be minimized by controlling the leakage. Labyrinths are normally used for this application due to their simple construction; however, hydrostatic seals may be used to operate at a minimum controlled gap (Ref. 2). Table XIX shows the performance and geometry for

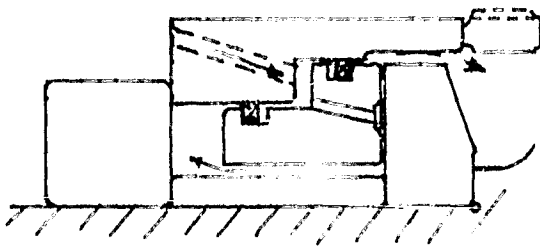
TURBINE SEALS

FLOATING RING SEALS



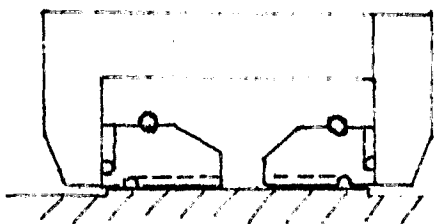
- LOW LEAKAGE CONTROLLED GAP
- LOW START TORQUE

HYDROSTATIC FACE SEAL



- VERY LOW LEAKAGE
- HIGH-SPEED TRACKING CAPABILITY
- RUBBING START

SEGMENTED SHAFT RIDING SEALS



- CLOSE CLEARANCE
- RUBBING START LIKE FACE SEALS
- VERY LOW LEAKAGE

Figure 37. LH₂ TPA Seal Types

TABLE XIX
LH₂ MAIN PUMP LABYRINTH SEAL GEOMETRY AND FLOWRATES

LOCATION	R(IN)	L(IN)	C(IN)	N _{TEETH}	T(IN)	$\Delta P(LB/IN^2)$	Q(GPM)	\dot{W} LB/SEC
First-Stage Shaft	.4	.2	.003	4.	.008	20.	2.29	.023
First-Stage Impeller	1.	.2	.003	4.	.008	622.	35.7	.374
Second-Stage Shaft	.6	.4	.003	5.	.008	155.	8.6	.091
Second-Stage Impeller	1.	.2	.003	4.	.008	622.	35.2	.38
Third-Stage Shaft	.6	.4	.003	5.	.008	155.	8.6	.091
Third-Stage Impeller	1.	.2	.003	4.	.008	622.	34.6	.386

III, C, Task III - Component Mechanical Design and Assembly Drawings (cont.)

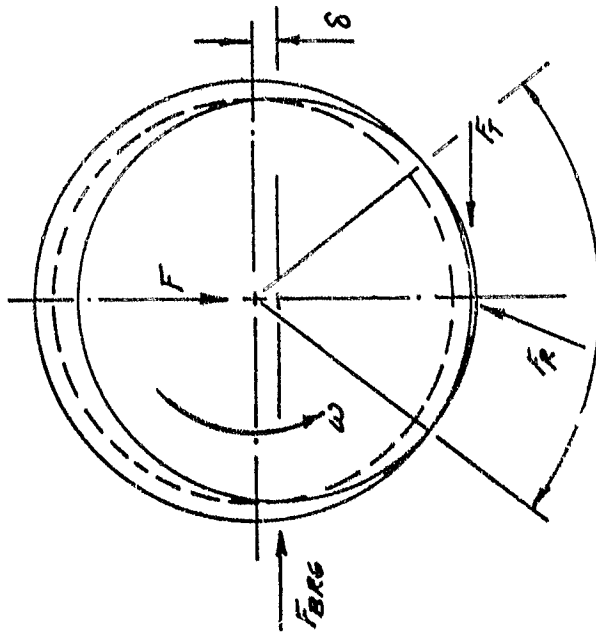
labyrinth seals used on the impellers and shafts. Another advantage of the hydrostatic seal is the predictability of the seal load. Straight and stepped labyrinth designs are subject to tolerances which may cause axial and radial rotor loads. Typical sources of radial load on the rotor from the labyrinth seal are schematically shown in Figures 38 and 39.

The overall system flow schematic, including boost and main pump, is shown in Figure 40. Through-flows, impeller wear ring flows, thrust balancer flows, bearing flows, turbine seal leakage flow, and hydraulic turbine flow are identified by flow range. Table XX defines flow magnitude at selected stations as indicated in Figure 40. It should be noted that for some of the flows called out in Table XX, two values are given. The higher value corresponds to the flows resulting from the utilization of conventional labyrinth seals, a series-flow double-band thrust balancer, and a hydraulically driven boost pump. The lower values correspond to a more advanced hydrostatic seal design, an articulated hydrostatic thrust balancer, and a traction-drive-powered boost pump.

c. Main LH₂ TPA Critical Speed

It is an advantage to have all rotor bearing assembly critical speeds above the operating speed, especially if any engine throttling is required. Operation near a critical speed amplifies bearing loads, absorbs energy, and results in large relative deflections between the rotating and stationary members unless special designs are used. Critical speeds can generally be raised above operating speeds by using bearings with high stiffness. Another reason for having stiff bearings is to resist the steady unsymmetrical pressure loads that may result from the high pump pressure. A critical speed analysis was performed for the baseline three-stage hydrogen turbopump as a function of bearing stiffness. The results of this analysis, which represents

MECHANICAL WHIRL FORCES
 PROPORTIONAL TO MAGNITUDE OF
 RADIAL FORCE AND COEFFICIENT
 OF FRICTION, NORMAL TO DIRECTION
 OF RADIAL FORCE (BACKWARD
 PRECESSION)



HYDRODYNAMIC WHIRL FORCE
 DEPENDENT ON FLUID PROPERTIES,
 ROTOR SPEED AND CLEARANCE AND
 ECCENTRICITY RATIO FOR MAGNITUDE
 AND DIRECTION (FORWARD PRECESSION)

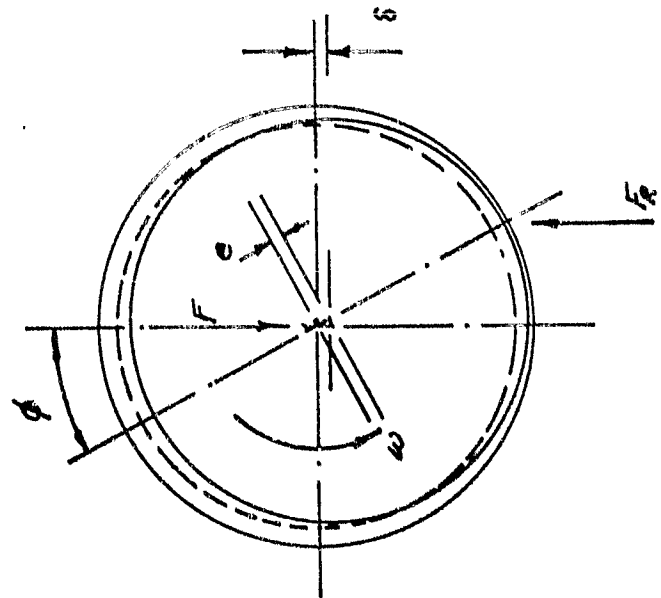
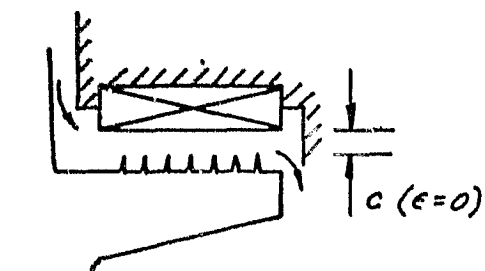
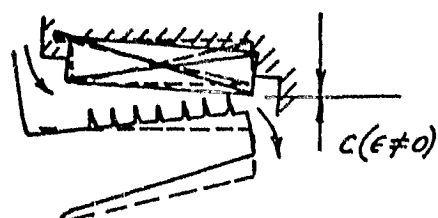


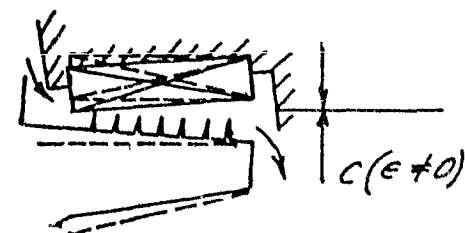
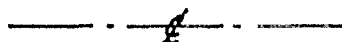
Figure 38. Eccentric Wear Ring Seal Whirl Forces



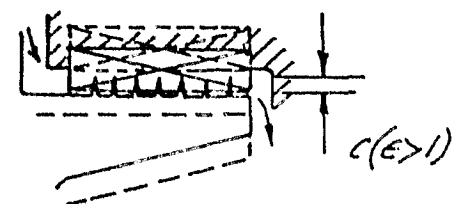
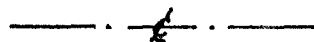
THEORETICAL DESIGN CONDITIONS,
NO DEFLECTIONS, MISALIGNMENTS,
OR TOLERANCES, RADIAL FORCES ZERO.



OUTER TOOTH LESS CLEARANCE,
HYDROSTATIC RESTORING FORCE.



INNER TOOTH LESS CLEARANCE,
HYDROSTATIC FORCE TENDING TO
CAUSE GREATER ECCENTRICITY



RUBBING ECCENTRIC LABYRINTH,
HYDROSTATIC FORCE TENDING TO
CAUSE GREATER ECCENTRICITY AND
A TANGENTIAL FRICTION FORCE CAUSING
A BEARING FORCE NORMAL TO RUB
RESULTING IN TENDENCY FOR BACKWARD
PRECESSION.



Figure 39. Labyrinth Seal Extreme Operating Positions

TABLE XX
LH2 MAIN TPA, SUMMARY OF FLOWRATE ANALYSIS

STA	P LB/IN ²	T *R	P LB/IN ²	Q GPM	W LB/SEC	%
2	61.	37.8	-	470.	4.62	103%
3	61.		-	558.6	5.5	123%
4	51.		-	558.6	5.5	123%
5	143.		-	596.	5.87	130%
6	764.6		-	605.	5.96	133%
7	764.6		622.	35.7	.374	7.9%
8	764.6		35.	101.	1.0	23%
9	730.		-	91.	.9	20%
10	81.		-	91.	.9	20%
11	920.		-	5.	.05	1%
12	920.		-	532.-678.	5.27-6.72	1.17-150%*
13	920.		155.	8.6	.091	2%
14	1541.6.		-	524.-666.	5.36-6.81	1.19-152%
15	1541.6		622.	35.2	.38	7.8%
16	1636.		-	5+	.05+	1%
17	1636.		-	520.-671.	5.32-6.86	1.18-153%*
18	1636.		155.	8.6	.091	2%
19	2317.		-	505.-651.	5.32-6.86	1.18-153%*
20	2317.		622.	34.6	.386	7.7%
21	2473.		-	456.	4.49	100%
22	2317.		1367.	14.2-152.	.15-1.6	3.3-35.6%*
23	950.		-	33.-170.	.35-1.8	7.7-40.%
24	2250.		-	29.	.3	6.6%
25	2250.		350.	75.	.1	2.2%
26	2286	535.	-	3156.	4.22	94%
27	1900.		-	3231.	4.32	96%
28	1840.		-	3231.	4.32	96%
29	1840.		278.	42.	.056	1.2%
30	1562.		-	3231.	4.32	96%
31	1481.		-	3231.	4.32	96%
32	2250.		1300.	18.	.2	4.4%
33	950.		30.	31.-161.	.35-1.8	7.7-40%

* This value depends on type of thrust balancer used

High Value: labyrinth seal/series flow double land thrust balancer/hydraulic turbine boost pump

Low Value: hydrostatic seal/traction drive boost pump/articulated hydrostatic thrust balancer

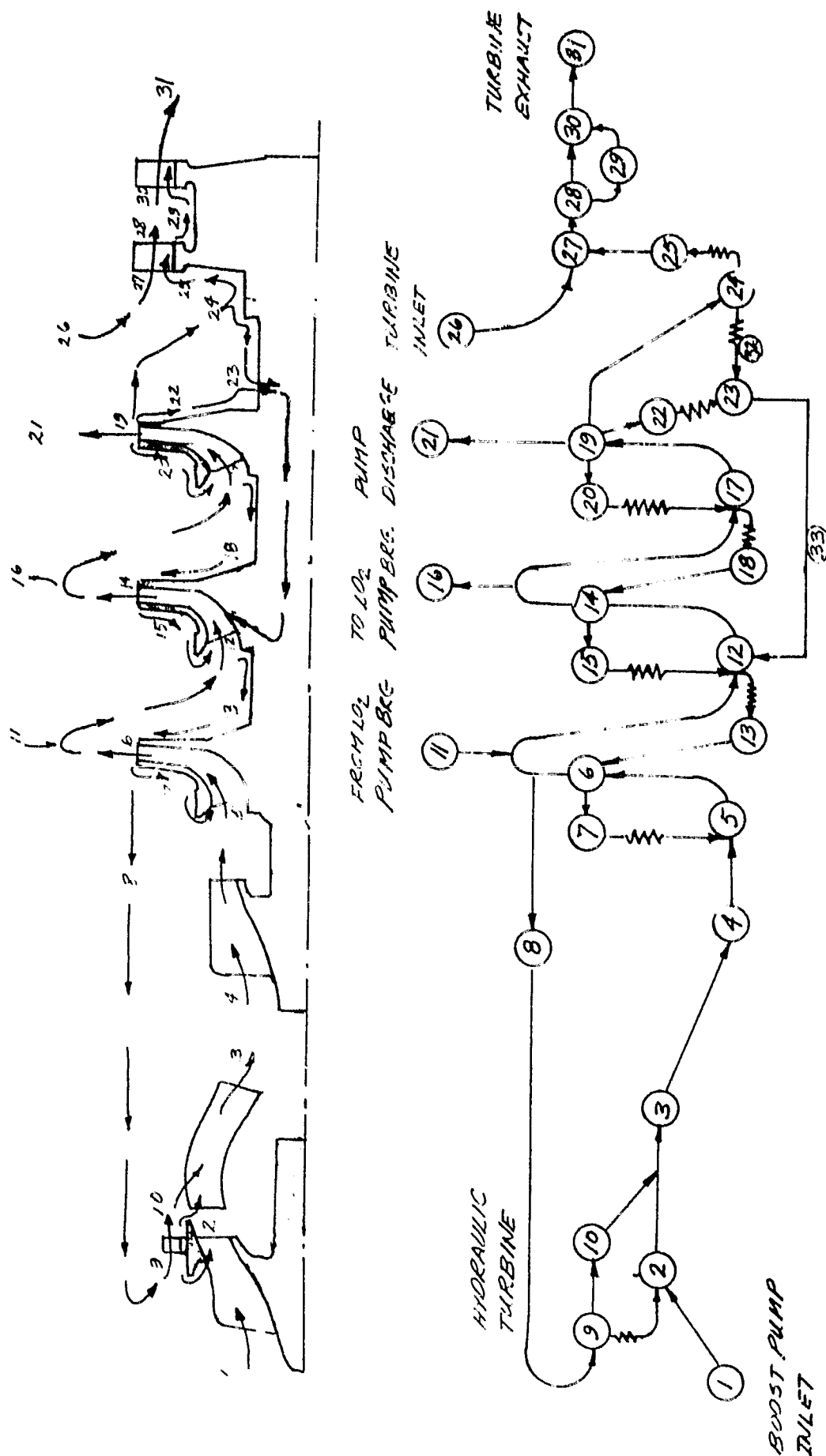


Figure 40. LH₂ Boost and Main Pump Flow Schematic

III, C, Task III - Component Mechanical Design and Assembly Drawings (cont.)

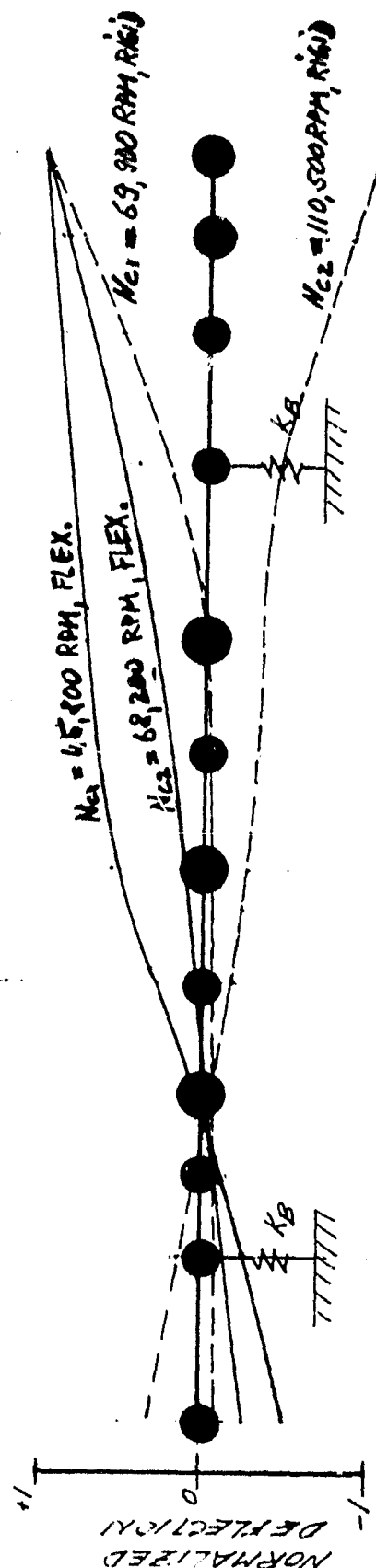
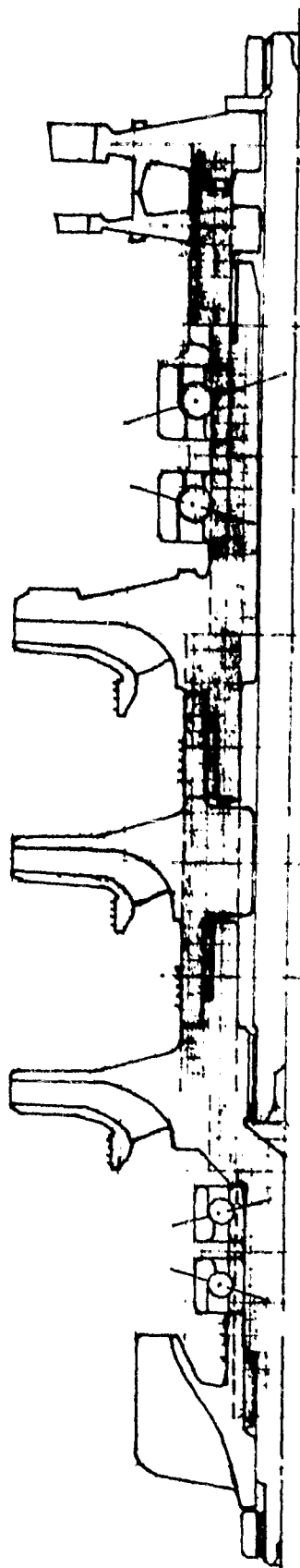
the first three critical speeds as a function of bearing stiffness, are shown in Figures 41 and 42. The third critical speed at low bearing stiffness is the free-free beam mode and is above the design operating speed. A single 20mm bearing stiffness is approximately $.25 \times 10^6$ lb/in., depending on loads and internal geometry, and since there is a set of bearings at each end of the rotor, the stiffness is on the order of $.5 \times 10^6$ lb/in. (see Ref. 21 and 22). At this stiffness, the first and second critical speeds are very close to the operating speed. Generally, a margin of 25% is selected to avoid damaging amplifications of load at the operating speed. To achieve this margin, a support stiffness of $.15 \times 10^6$ at the bearings is required with the mass-elastic properties of the shaft, turbine, and impeller. This represents a solution for a single-speed (90,000 RPM) design but does not accommodate engine throttling. Operating on or through a critical speed is possible with the proper balancing and damping, but due to the low viscosity of LH₂, available damping is extremely small. It would be desirable to adjust the mass-elastic system to avoid critical speeds within the operating range.

d. Hydrogen Main TPA Gas Turbine Design

The design process for the LOX TPA turbine was described in Section III,C,6,c.

The following design point conditions were established for cycle power balance data:

1. Total Inlet Pressure, $P_0 = 2286$ psia
2. Total Inlet Temperature, $T_0 = 535^\circ\text{R}$
3. Static Exit Pressure, $P_2 = 1481$ psia
4. Rotational Speed, $N = 90,000$ RPM
5. Flowrate, $W = 4.22$ lb/sec



n	1	2	3	4	5	6	7	8	9	10	11	12
L (IN)	1.											
R_0 (IN)	.3	.5	.5	.7	.7	.7	.7	.7	.8	.6	.5	
R_i (IN)		.3	.45	.65	.65	.65	.65	.5	.5	.65	.65	
n' (LB)	.099			.3	.029	.31	.029	.45	.036	.086	.301	.136

Figure 41. LH₂ Main TPA Critical Speed Analysis

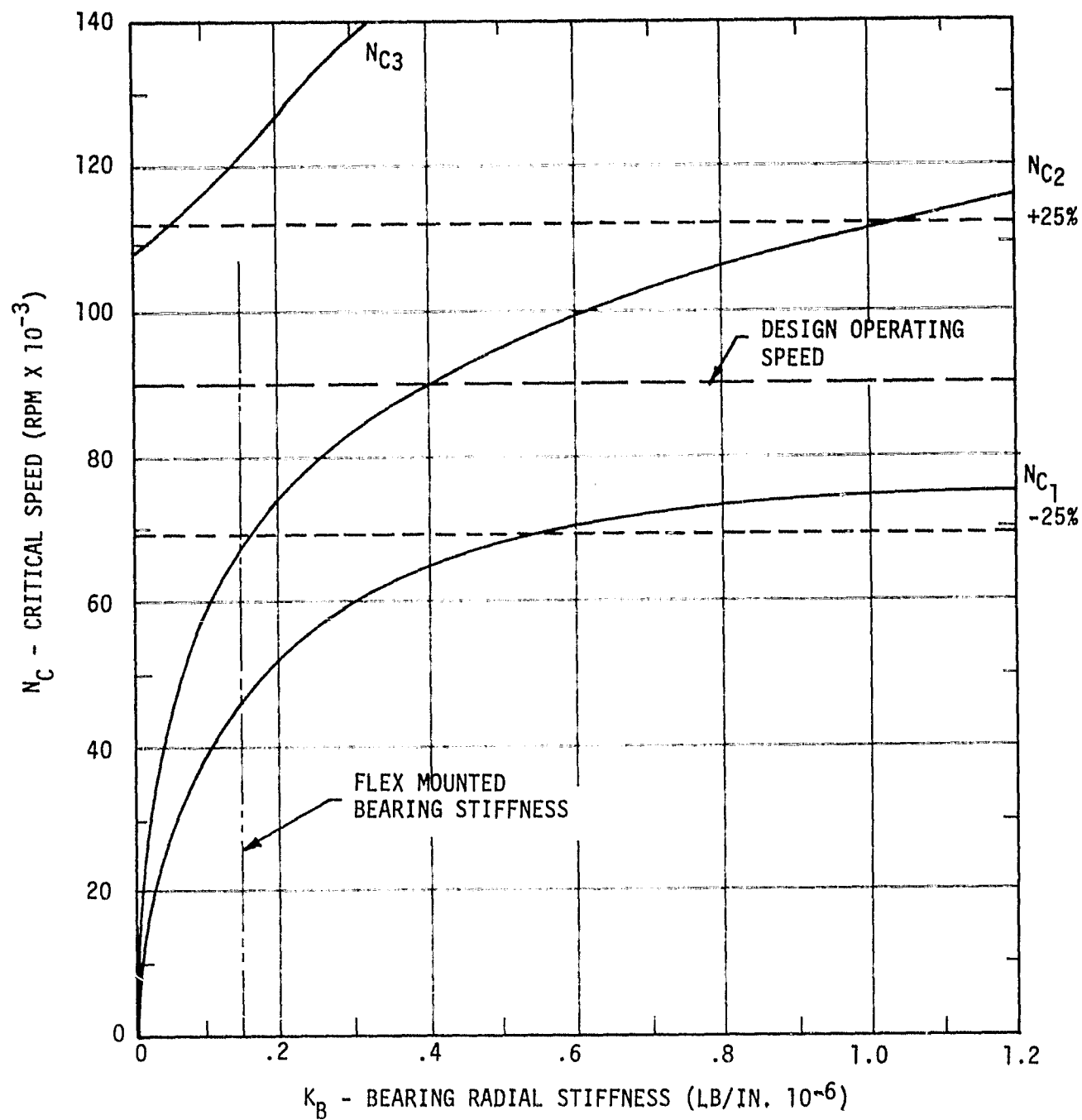


Figure 42. LH_2 Main TPA Critical Speed as a Function of Bearing Radial Stiffness, 3-Stage Pump

III, C, Task III - Component Mechanical Design and Assembly Drawings (cont.)

The hydrogen gas properties are as follows:

1. Specific Heat at Constant Pressure = 3.652 BTU/lb/°R
2. Specific Heat Ratio = 1.395
3. Gas Constant = 804.91 ft/°R
4. Absolute Viscosity = 0.6×10^{-5} lb/ft-sec

The final total pressure loss coefficients resulting from the iteration procedure at the design point are as follows:

<u>Stage</u>	<u>Blade Row</u>	<u>Total Loss Coefficient</u>
1	Manifold	0.79
	Stator	0.168
	Rotor	0.241
2	Stator	0.175
	Rotor	0.213
	Collector	1.5

The results of the design point analysis are summarized in Table XXI.

A design point analysis was conducted to determine the flow passage geometry and performance of the hydrogen TPA turbine. The results are as follows:

- ° Two-stage Reaction Turbine
- ° Pitch Diameter = 3.31 in.
- ° Overall Velocity Ratio = 0.387
- ° Estimated Static Efficiency = 76.8%

TABLE XXI
LH₂ TPA GAS TURBINE DESIGN POINT PERFORMANCE

<u>Parameter</u>	<u>First Stage</u>	<u>Second Stage</u>	<u>Both Stages</u>	<u>Overall, Including Manifolds</u>
Work, BTU/lb	87.7	87.7	175.4	175.4
Flowrate, lb/sec	4.08	4.08	4.08	4.08
Static Pressure Ratio	1.241	1.236	1.505	1.543
Stage Loading Factor	0.7	0.7	-	-
Stage Flow Coefficient	0.308	0.308	-	-
Velocity Ratio	0.555	0.557	0.398	0.387
Static Efficiency, %	80.	80.7	82.2	77.7

The estimated disc friction loss is 11.3 HP. When this loss is included, the overall turbine efficiency is 76.8%

III, C, Task III - Component Mechanical Design and Assembly Drawings (cont.)

The meridional flow passage for the turbine is shown conceptually in Figure 43. These results are based on a detailed blade loss analysis which can be used for blade profile design. However, only an approximate study was made of the manifold losses. In the design of the inlet and exhaust manifolds, consideration must be given not only to the turbine performance, but also to the engine system requirements. Cold-flow testing will be necessary to develop the most effective turbine inlet and exhaust configurations.

e. Recommendations for Future Study, Hydrogen TPA's

As a result of limited time and resources available to conduct this TPA design, certain issues could only be addressed preliminarily, and remaining problems could only be identified but not totally resolved. As a minimum, further design iterations are required in the following areas:

- (1) Reevaluate material selection for boost and main pumps.
- (2) Determine if the hydrogen propellants which are used for bearing cooling require filtering.
- (3) Evaluate the pros and cons of the following:
 - (a) Two-stage main pump, with high-head inducer
 - (b) Three-stage main pump, increased head rise in inducer stage
 - (c) Four-stage main pump, no boost pump

DESIGN POINT

$P_o = 2286$ psia
 $T_o = 535$ °R
 $P_c = 1481.5$ psia
 $\dot{W} = 4.22$ lb/sec
 $N = 90,000$ RPM
FLUID: GH_2

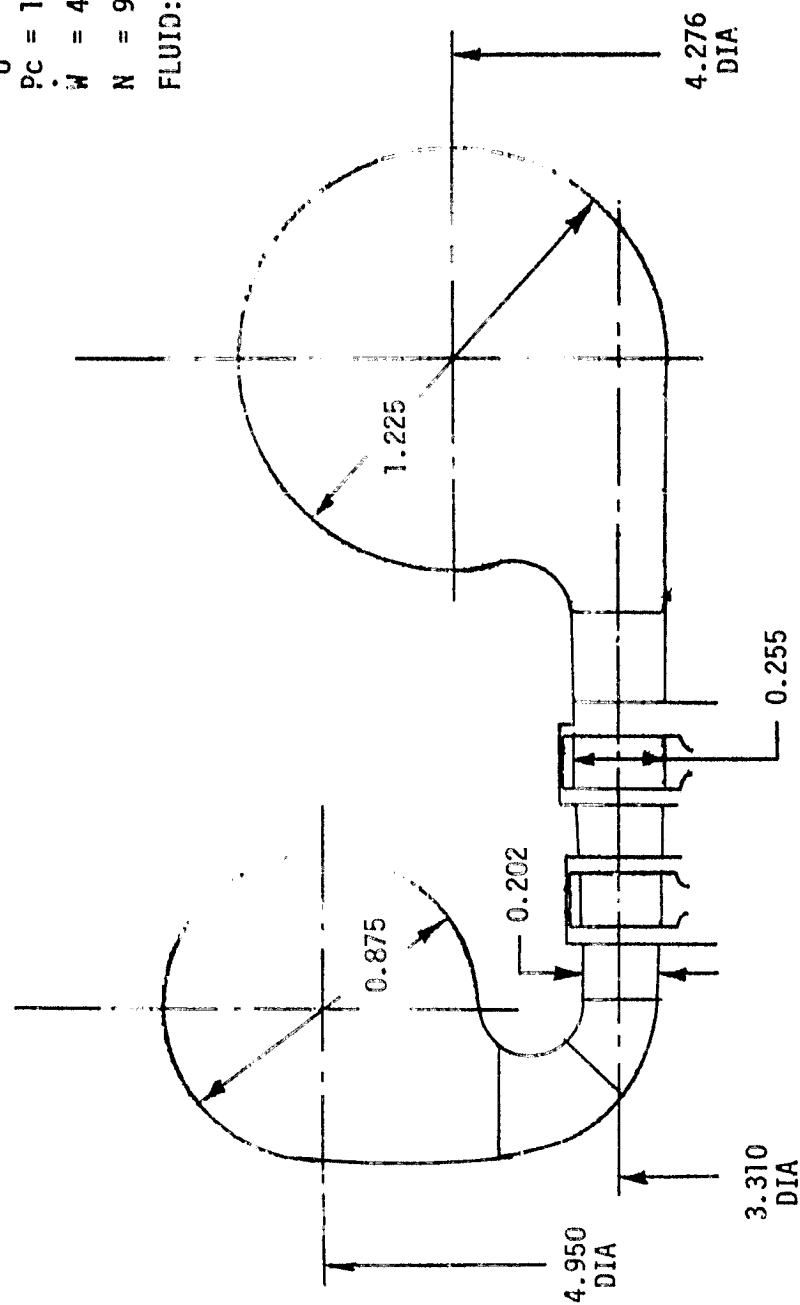


Figure 43. LH₂ TPA Turbine Meridional Flow Passage

III, C, Task III - Component Mechanical Design and Assembly Drawings (cont.)

- (4) Evaluate a main pump design with fluid film bearings.
- (5) Evaluate the structural loads of a TPA design with a solid steel shaft driving the impellers through splines.
- (6) Reevaluate the pilot and drive arrangement for the turbine to avoid loosening up under speed.
- (7) Adjust the mass-elastic system to avoid critical speeds within the operating range.
- (8) Analyze the turbine inlet and exit manifold geometry in more detail, emphasizing the performance of the two-turbine-in-series system.
- (9) Conduct a literature search for small-size turbines, emphasizing small blade size and tip clearance leakage control.

f. Hydrogen TPA's, Technology Areas

The hydrogen boost and main pump preliminary designs as baselined in this report consciously utilize only design features which are within the present state of the art. The one exception is the thrust balancer. The analysis addresses two state-of-the-art concepts: (1) the straight labyrinth in series with the exit land and (2) the impeller tip land in series with the exit land. Furthermore, it addresses one advanced concept: the hydrostatic face seal in series with the exit land. It is this latter advanced design which is shown in the baseline design drawing.

III, C, Task III - Component Mechanical Design and Assembly Drawings (cont.)

Certain performance improvements and design simplifications could result if some of the following design features were to pass their technology status and could then be implemented in the design. The most significant technology areas to be considered are as follows:

(1) Development of a hydrostatic thrust balancer and journal bearings with satisfactory performance during startup, steady-state, and shutdown phases.

(2) The development of floating hydrostatic ring journal seals for application as interstage shaft seals and impeller wear ring seals. These seals can provide a considerable reduction in leakage flowrate and, due to their floating design, have a low radial load on the rotating assembly.

(3) Development of a planetary traction boost pump drive which is mechanically coupled with the main pump shaft (see Figure 44). Such a drive system would have an efficiency of about 95% and would reduce boost pump outside dimensions and eliminate external high-pressure hydrogen lines. Since planetary drives are compact, the loads in this application are low. Bearing coolant supplied from the main pump may be provided at sufficient pressure to balance impeller thrust and reduce bearing loads while cooling the bearings and planetary set. Another advantage of this design over the hydraulic turbine drive concept is its inherent avoidance of mixing higher-temperature turbine shroud seal leakage flow with lower-temperature, low-pressure flow at the boost pump inlet.

8. Propellant Valves

The basic approach used in selecting the valve and actuator designs for this application was maximum utilization of past experience,

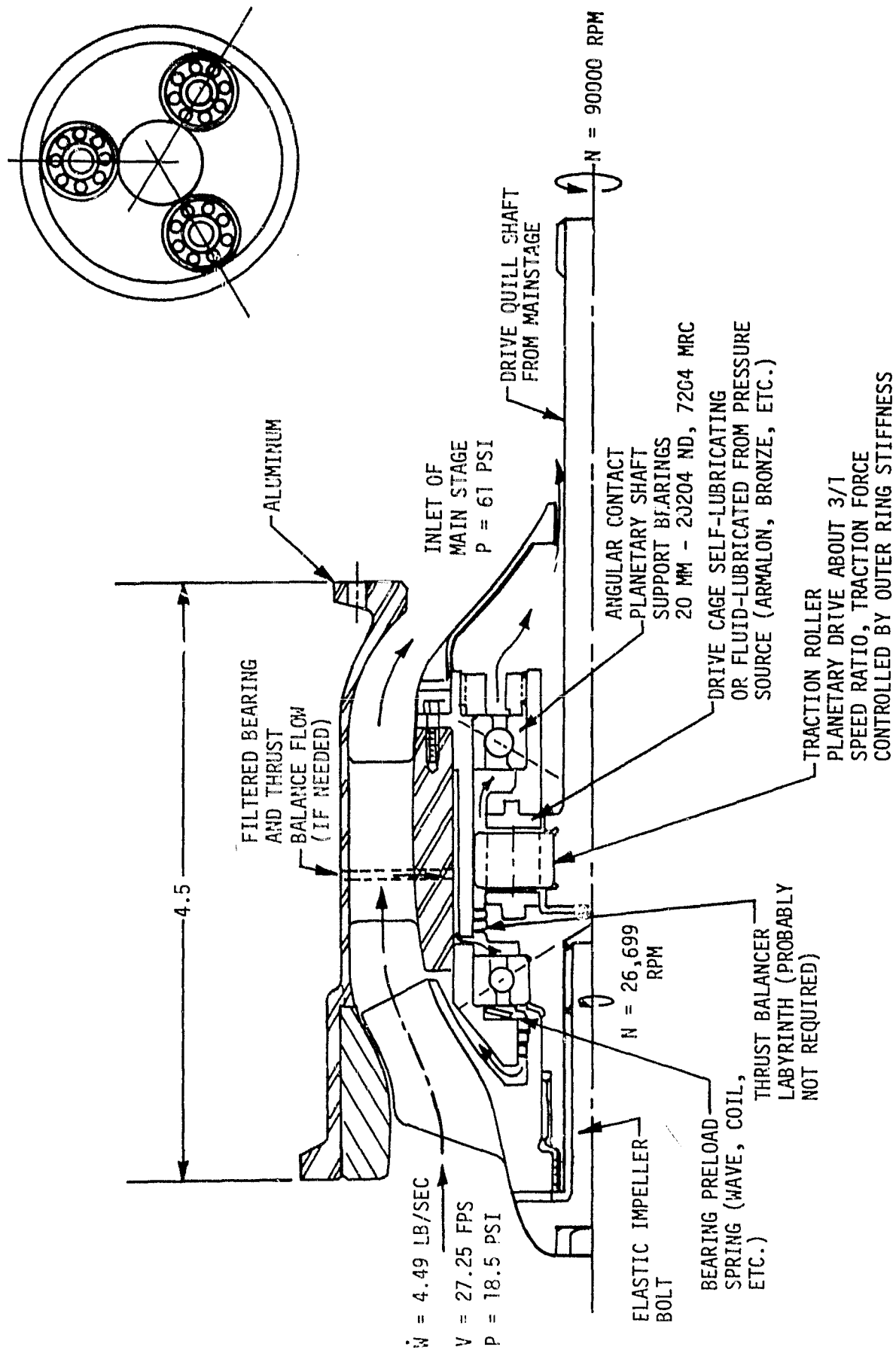


Figure 44. LH₂ Boost Pump-Planetary Drive Concept

III, C, Task III - Component Mechanical Design and Assembly Drawings (cont.)

coupled with use of a minimum number of valve types. As a result, two basic valve types are considered as adequate for all of the main control elements (excluding the auxiliary systems and the actuator control valves). The two basic designs are: (1) a pneumatically operated on-off ball valve for propellant flow control and (2) an electric-motor-driven modulating poppet valve for turbine speed control.

The valve locations analyzed were shown on the engine cycle schematic (Figure 1). The turbine flow control valve should be relocated to bypass the oxygen pump turbine. This study result was obtained too late to be incorporated into the design.

Two versions of the ball valve are used in the engine. Single valves are used for the fuel and oxidizer start bypass valves, and series-redundant versions are used for the main fuel and oxidizer propellant shutoff valves. Both versions use common parts wherever practical. Series-redundant main shutoff valves were recommended as a result of safety and reliability analyses conducted for the Phase A studies. They are redundant to assure that the engine will shut down.

The modulating valve has only one configuration and will be used for the turbine bypass valve and for the turbine flow control valve.

a. Propellant Flow Control Valve

A ball valve was selected for this application because of its high flow capacity at low pressure differentials and for its tight sealing capabilities. The former is especially critical during tank head startup; the latter for cargo bay storage and orbital coast. The valve design shown in Figure 45 evolved directly from, and includes many features of, the series-redundant bipropellant valve used on the Space Shuttle's OMS engine.

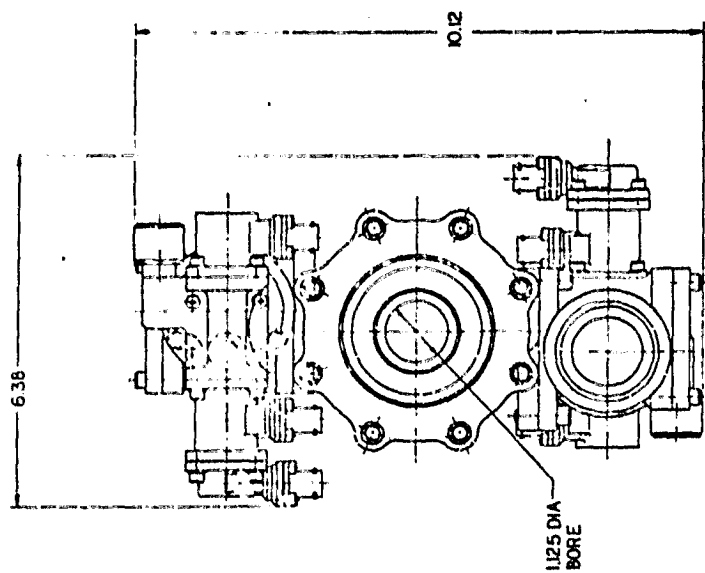
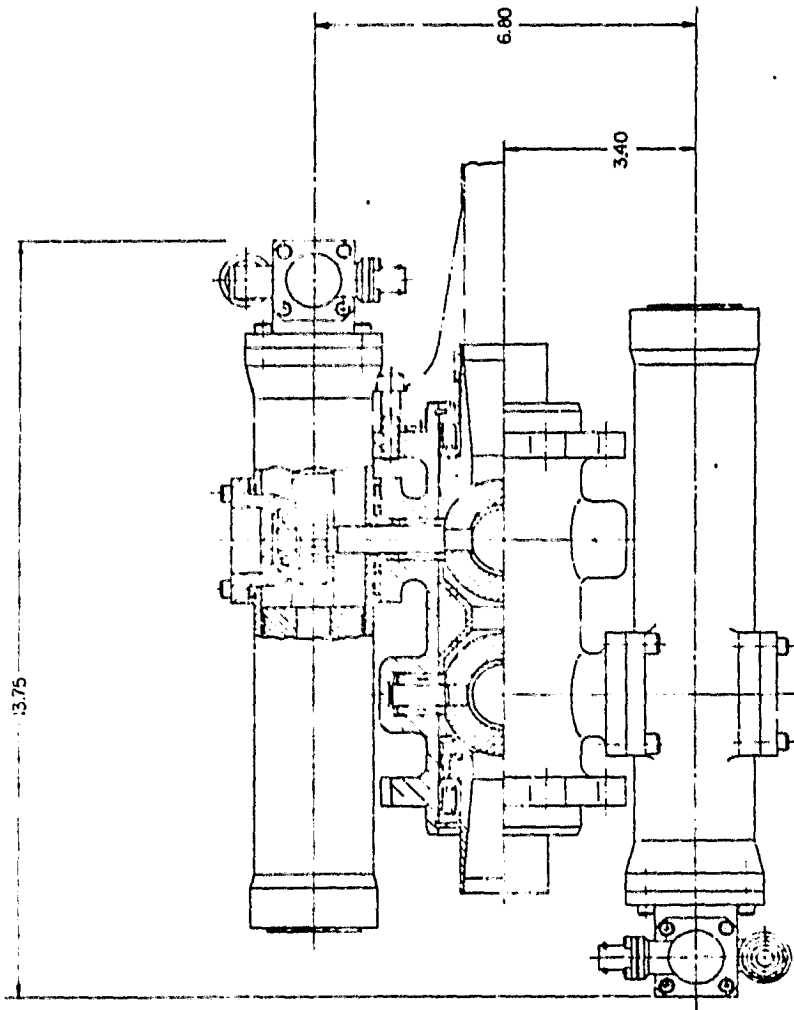
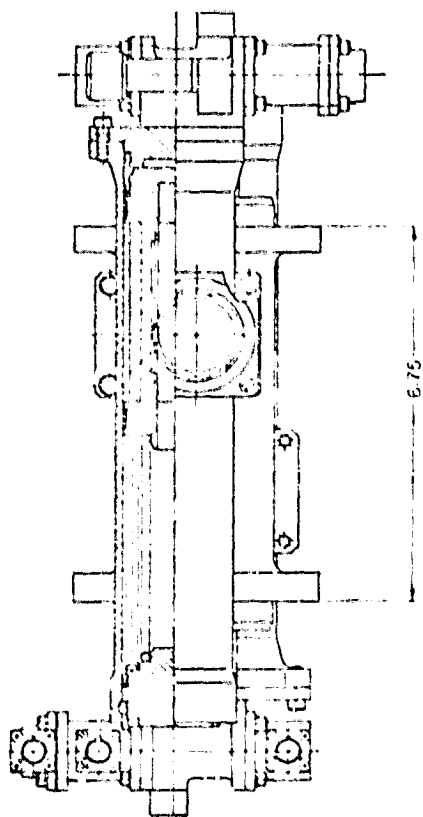


Figure 45. Propellant Flow Control Valve (ALRC Drawing No. 1193175)

III, C, Task III - Component Mechanical Design and Assembly Drawings (cont.)

The basic propellant flow control valve is a normally closed, two-way, two-position ball valve operated by a single-acting, spring-closed, pneumatic piston-type actuator by means of a rack and pinion drive. Operation of the actuator is controlled by a normally closed, spring-loaded, three-way, two-position, dual-coil solenoid valve.

The solenoid signal is supplied by the engine controller, and the actuation fluid (GN₂) is supplied (and regulated) by the engine's self-contained pneumatic pack. Ball valve response time is controlled by orifices installed in the GN₂ supply and vent lines.

Design features of the basic propellant flow control ball valve (which constitutes one-half of the series-redundant valve shown in Figure 45) are described in the following paragraphs.

(1) Shutoff Seal Assembly

The keystone of any shutoff valve design is the main shutoff seal. The spring-loaded seal cartridge design has proved to be a very reliable leak-tight seal in past programs. The cartridge concept incorporates several features consistent with good sealing: i.e., self-centering capability (ball in a cone), freedom to follow ball support deflections, predictable seal loading, good seal support and containment (for cold-flow control), plus ease of maintenance and installation. These features, combined with proper ball and seal surface preparation and quality control, result in a shutoff seal that will meet an assumed leakage requirement of 1×10^{-4} scc/sec, which is based upon past experience.

When the propellant flow control valves are closed, pump discharge pressure drops off rapidly and a pressure relief valve vents any pressure buildup (due to warming of the fluid trapped between the balls)

III, C, Task III - Component Mechanical Design and Assembly Drawings (cont.)

back to the propellant tanks. Consequently, the valves seal against tank head pressure only when stored in the cargo bay or when coasting in orbit. As a result, a relatively low seal loading force (force pushing the seal against the ball) is needed. If, for example, twenty pounds per circumferential inch of seal loading is used, the resultant estimated leakage is 10 scc/hr helium at room temperature and less than 10 scc/sec helium at liquid hydrogen temperature.

Due to the low seal loading required, the seal cartridge can be designed to minimize pressure loading effects on the shutoff seal. This is accomplished by selecting a cartridge balance seal with a seal-groove inner diameter that is the same as the mean contact diameter of the shutoff seal. By sizing the balance seals in this manner, any differential area between the main shutoff seal and the balance seal will be small, and the pressure force component of the shutoff sealing force will be minimized, resulting in a relatively constant seal force. The cartridge balance seals are shown conceptually as two pressure-loaded radial seals; however, a bellows type or any other type of seal could be substituted as well. The final balance seal configuration will be selected during the detail design phase after more extended analyses.

The low sealing force results in another feature that simplifies the valve; i.e., the seal can be designed to be in contact throughout the full 90° of ball travel. This is in contrast to the OMS ball valve which is lifted off the seal during the first 10° of motion by means of an eccentric built into the ball. Elimination of the eccentric on the present design permits the use of smaller actuator springs since the springs do not have to overcome the torque produced by the inlet pressure acting on the shutoff seal area (force) times the eccentric (lever arm).

III, C, Task III - Component Mechanical Design and Assembly Drawings (cont.)

Several cartridge seal/ball design concepts were identified as possible backups should further analyses uncover unforeseen problems. These designs are slightly more complex and have not been investigated in any depth. Possible backup designs include: (1) a cam-actuated seal lift off, allowing for higher seal loads; (2) an eccentric ball valve with downstream seal (the eccentric tends to help the springs close the valve and would also allow for higher seal loads); and (3) an eccentric ball valve similar to the OMS valve, which would result in a larger actuator.

(2) Flow Control Element

Flow through any ball valve is controlled by the relative position of the bore through the ball and the shutoff seal. Flow control as applied here refers to on-off control.

The ball is fabricated from hardened stainless steel for wear and scratch resistance. A cylindrical flow bore and two square shaft bores are machined through the ball. This ball configuration is shown for its simplicity. During the detail design phase, an effort would be made to reduce the weight of the ball either by contouring the outer surface of the ball or by using a hollow sphere.

(3) Valve Shaft Assembly

The valve shaft arrangement has been used in the OMS bipropellant valve. While this arrangement may allow larger ball-shaft displacements than some other arrangements, the split shaft provides significant size, weight, and assembly advantages. The increased ball movement can be compensated for by proper design, i.e., bearing placement as near the ball as possible, use of a cartridge shutoff seal design to allow the seal to follow the ball, and a sufficient shaft-bearing length-to-diameter ratio to provide adequate support.

III, C, Task III - Component Mechanical Design and Assembly Drawings (cont.)

Use of the separate cylindrical sleeve in the valve flow bore permits assembly of the short stub shaft through the ball, thereby eliminating the need for a seal on the stub shaft. The sleeve holds the stub shaft in position and is, in turn, held in position by the pinion shaft.

The longer pinion shaft, in addition to helping support the ball, also transmits torque from the actuator to the ball. It is supported by a standard roller bearing near the ball at one end and a duplex ball bearing at the other end. An integral stub gear and a dynamic shaft seal are located between the two bearings. This arrangement results in the least amount of deflection for the gear and seal.

A single-shaft seal between the valve and actuator is considered adequate since any leakage into the actuator spring cavity can be vented back to the tank, and the shaft seal, combined with the static actuator seals, provides dual seals between the propellant and the exterior. The shaft seal tentatively selected is a Delta Seal, manufactured by the Rudolph E. Kruger Co., Newport Beach, CA. It consists of a filled TFE seal ring that is squeezed between the bottom of the actuator housing, the valve shaft, and a spring-loaded seal retainer. Past experience has shown good results with this seal at extreme temperatures and high pressures.

b. Modulating Valve

The operating requirements for the modulating valve are somewhat unique in that downstream valve pressure is independent of the flow-rate through the valve. Since the modulating valve, in parallel with the turbine(s), can bypass a maximum of 10% of the total gas flow (for turbine speed control), the larger flow through the turbines rather than through the valve determines the relative pressure. This feature simplifies the design of the

III, C, Task III - Component Mechanical Design and Assembly Drawings (cont.)

valve in that the differential pressure is relatively high and is constant for a given turbine flow.

The modulating valve configuration selected for this application is shown in Figure 46. It is an in-line, pressure-balanced poppet valve with independent, redundant electric motor actuation. Each motor is powered through an electrical harness which is independent of the other motor's harness so that damage to one harness will not affect the functioning of the valve.

The modulating valve is part of a closed loop control system which includes the electronic controller. Valve position is set by the controller, and the output is verified by the various engine parameters monitored by the controller. By trimming the turbine speeds relative to each other and to the total flow requirements, the engine maintains the required mixture ratio.

The design features of the modulating valve are described in the following paragraphs.

(1) Flow Metering

Flow through the modulating valve is metered by the annular orifice formed between the valve seat's inner diameter and the flow plug's outer diameter. The flow plug can be shaped to give (within reason) whatever flow versus valve position characteristics are needed to obtain optimum turbine control.

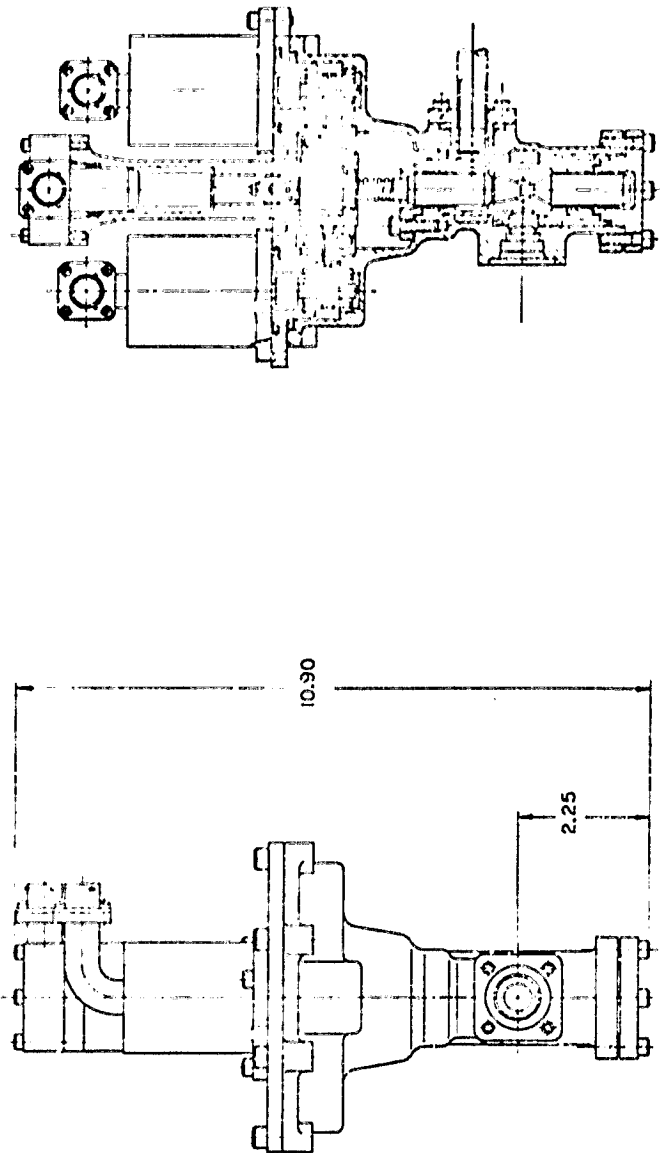
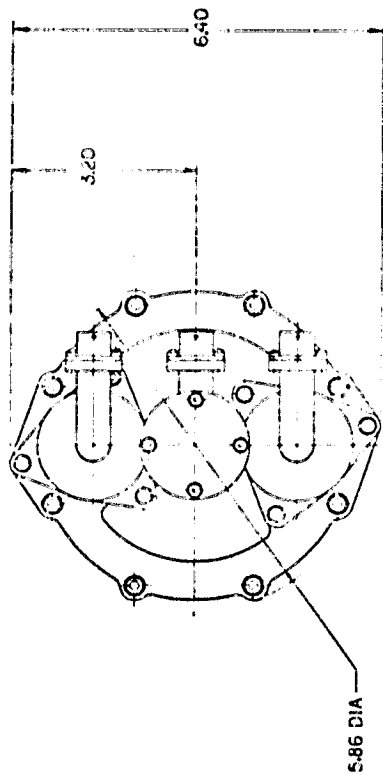


Figure 46. Modulating Valve (ALRC Drawing No. 1193180)

III, C, Task III - Component Mechanical Design and Assembly Drawings (cont.)

(2) Shaft Seals

The modulating valve has two sets of dual shaft seals. Both seal sets consist of a Delta Seal (manufactured by the Rudolph E. Kruger Co. of Newport Beach, CA.) nearest the high-pressure side and an ALRC-design lipseal on the low-pressure side. The cavity between the two seals is vented, either overboard or back to the propellant tank. This dual seal (with vent) arrangement has proven to be very reliable in past ALRC testing under high pressures and extreme temperatures.

Use of dual seals on the balance piston does add frictional loads; however, these loads are much lower than the pressure loads that would exist without the balance piston.

(3) Shutoff Seal

The turbine bypass valve must provide a propellant shutoff seal, whereas the turbine flow control valve does not. For the sake of simplicity, however, both valves will have the same configuration. Preliminary selection of a shutoff seal type consists of a ball in a cone. Seal loading is provided by the pressure-balancing piston combined with the motor stopping force.

Another shutoff seal concept for this application is a flat-on-flat type which would be insensitive to both wear and temperature. Additional analyses will be required during the subsequent design phase to select a final seal configuration.

III, Task Discussions (cont.)

D. TASK IV - ENGINE TRANSIENT SIMULATION COMPUTER MODEL

The primary objective of this task was to formulate a computer program to simulate the transient behavior of the cryogenic O₂/H₂ Expander Cycle Engine.

Existing models for this application were evaluated to determine the feasibility of tailoring an existing model to simulate the OTV Advanced Expander Cycle Engine. All existing models were found to have serious shortcomings. Based upon this evaluation, a new model was developed. A description of this model, along with a user's manual, are provided in a separate Task IV report for this contract (Ref. 6). Since the input and output examples described in Reference 6 are too lengthy to be included herein, the program is described briefly in subsequent paragraphs.

The user's manual transmitted to NASA/MSFC describes the program, provides instructions for implementing and executing the program, describes the inputs and outputs, explains the program subroutines and their operation, and discusses the program error generated messages. A complete FORTRAN program listing is also included in the user's manual.

A magnetic tape of the program was transmitted as part of the Task IX, Computer Software/Documentation, requirements.

The program has been designated as version number three of the Liquid Engine Transient Simulation program (LETS-3). The steady-state condition is also a special case of this transient model. The computer program is flexible but rather complex. It is intended for use in detailed design and development efforts.

III, D, Task IV - Engine Transient Simulation Computer Model (cont.)

The program solves the transient and steady-state equations describing the combustion, fluid flow, and heat transfer associated with cryogenic O_2/H_2 rocket engine systems, including the chill-down phase. This program can be used to simulate the effect of engine system component location and characteristics in addition to defining engine system start and steady-state requirements (i.e., valve location and sequencing for safe operation, steady-state operating point, power balance, and system pressure schedule).

The program has been designed with a maximum of flexibility to facilitate modeling of a variety of engine systems, including both pump- and pressure-fed types. The entire engine system, including tankage, can be modeled. The computer program is structured so that engine system descriptions and changes are made through input. No program changes are required to achieve modeling of any of a variety of engine systems. Engine system simulation flexibility is accomplished by linking together a library of component subroutines which include lines, pumps, valves, turbines, combustors, etc. Component linkage is accomplished entirely through input. The component subroutines contain equations and logic for simulating their transient and steady-state behavior. All program subroutines are written in FORTRAN IV language.

Each operation requires that start and shutdown transients occur in a safe and predictable manner. Operation in modes or regimes which could cause damage must be avoided. Typical rocket engine start problems are delayed ignition, which may result in extremely high-pressure spikes; manifold contamination caused by the backflow of a propellant; low frequency chugging, producing high thermal and mechanical loads; excessive pressure overshoot; unstable fuel flow in the regeneratively cooled thrust chamber circuit; flow variation due to injector thermal effects, pump cavitation, and pump stall. Typical shutdown problems are high thermal loads resulting from off-mixture

III, D, Task IV - Engine Transient Simulation Computer Model (cont.)

ratio operation, chugging, and manifold contamination. These transient problems are solved by the selection of appropriate valve locations, valve sequences, control methods, provision of an effective ignition system, and the use of adequate purges. This computer program will enable these selections to be made during the design phase of the engine development.

The LLTS-3 computer program has been developed to operate on the Univac 1108 computer. Core requirements for the program are as follows:

<u>I Bank</u>	<u>D Bank</u>	<u>Total</u>
18,200	42,000	60,200

Both printed and plotted outputs are available.

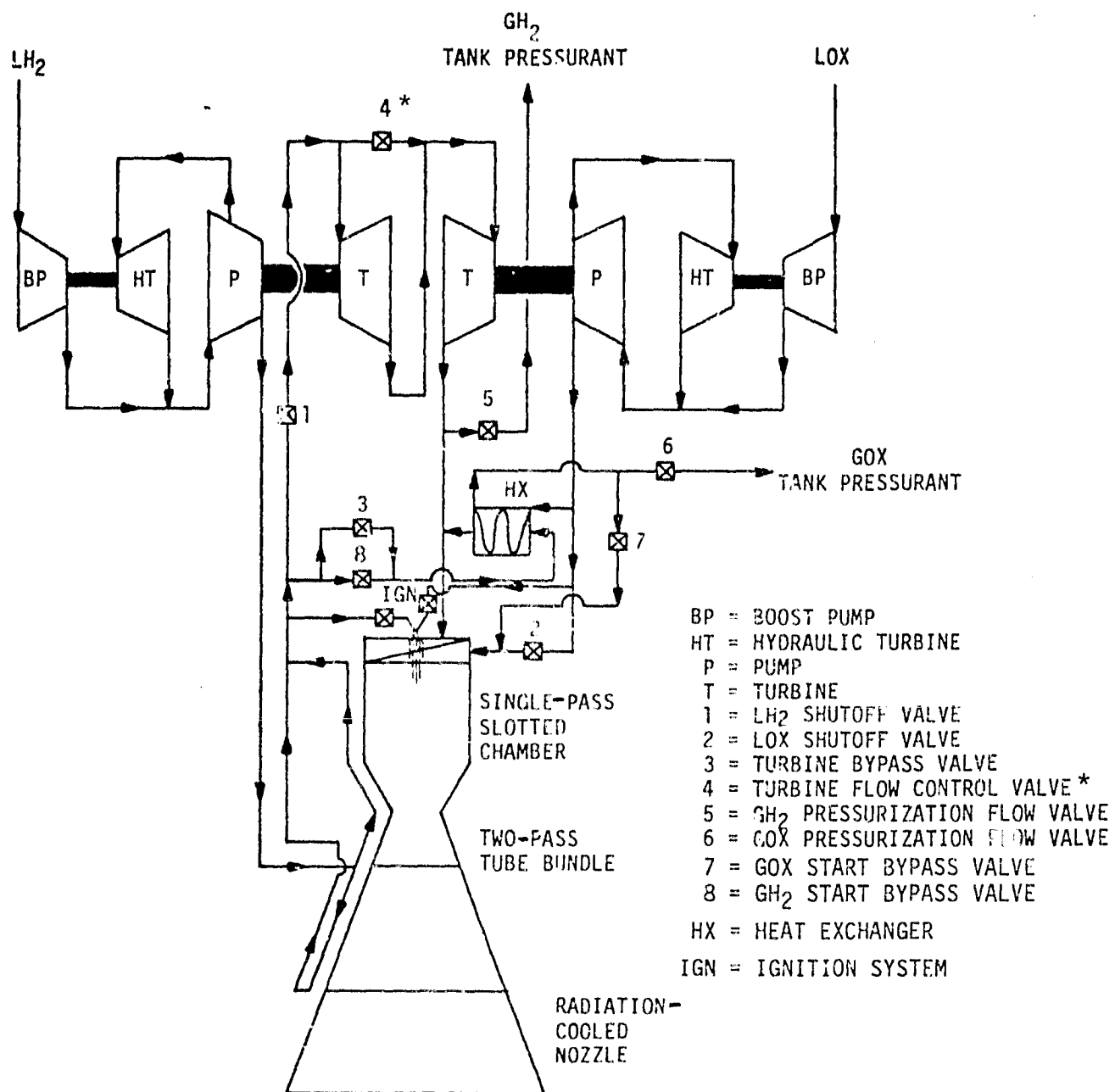
E. TASK V - ENGINE CONTROL

The major objectives of this task were to (1) determine effective control points and methods to achieve thrust and mixture ratio control; (2) determine suitable actuation systems; and (3) define controller requirements.

Engine operation is described in Section III,G of this report. The location of the valves is shown on the cycle schematic of Figure 47.

Two basic configurations were selected for the main propellant valves as described in Section III,C,3: (1) a pneumatically operated on-off ball valve for propellant flow control and (2) an electric motor-driven modulating poppet valve for turbine speed control.

The primary functions of the fuel shutoff valve are to terminate fuel flow at engine shutdown and to prevent flow through the turbines during



*TO BE RELOCATED TO BYPASS THE OXYGEN PUMP TURBINE

Figure 47. Baseline Advanced Expander Cycle Engine Flow Schematic

III, C, Task V - Engine Control (cont.)

the tank head idle mode. To provide these functions, the valve is a normally closed on-off valve. To provide high shutoff and leakage reliability, the valve is series-redundant and is fail-safe to the closed position in the event of electrical power loss. This valve is located downstream of the turbine bypass and GH_2 start bypass lines to provide the shutoff function during tank head idle.

The main purpose of the oxidizer shutoff valve is to terminate oxidizer flow at engine shutdown. The valve is located as close to the injector as possible to minimize the residual oxidizer in the system downstream of the valve at engine shutdown. This valve is a normally closed on-off valve and will be fail-safe to the closed position in the event of electrical power loss. To provide high reliability in the shutoff mode, the valve is series-redundant.

Two valves are required in the turbine bypass circuit. The GH_2 start bypass valve is an on-off valve that bypasses all the hydrogen flow during tank head idle mode operation. The turbine bypass valve is used to control the amount of flow bypassing the turbine during steady-state operation and to control the engine thrust. Nominally, 6% of the hydrogen flow bypasses the pump turbines.

The main function of the GO_2 start bypass valve is to control the flow of gaseous oxygen from the heat exchanger to the injector during the tank head idle mode. The valve is also required to remain closed at engine shutdown to prevent bypassing oxidizer flow around the LO_2 shutoff valve.

The turbine flow control valve is used to provide the engine mixture ratio control. Analysis conducted during the course of this study has shown that the turbine flow control valve should be placed in a line bypassing the oxygen pump turbine rather than the fuel pump turbine (see Figure 47).

III, E, Task V - Engine Control (cont.)

Schedule and funding limitations did not permit another design iteration to incorporate this feature. Approximately twice as much oxygen turbine bypass flow is required to obtain the same mixture ratio variation as when bypassing the fuel pump turbine. However, the effect upon the engine cycle power balance is only about one-half as much because the oxidizer pump horsepower requirement is approximately one-fourth.

The modulating valves are part of a closed loop control system which includes the electronic controller. Valve position is set by the controller, and the output is verified by the various engine parameters (flows, turbine speeds, chamber pressure, valve positions, etc.) monitored by the controller. By trimming the turbine speeds relative to each other and to the total flow requirements, the engine maintains the required mixture ratio and thrust level.

Valve operation is described in the following paragraphs. A valve design for the propellant flow control valve and for the modulating valve were shown in Figures 45 and 46, respectively.

1. Propellant Flow Control Valve Operation

Upon receipt of an electrical signal from the engine controller, a solenoid-operated valve opens and permits pressurized GN₂ to flow into the actuator. The resultant force created by the pressurized piston (which has been sized to provide twice the force needed to overcome the frictional forces and one and one-half times the force needed to overcome the mechanical, pressure, and flow-induced forces) moves the actuator piston away from the end cap and simultaneously compresses the springs and rotates the pinion. Torque and motion are transmitted by the pinion through the pinion shaft to the ball.

III, E, Task V - Engine Control (cont.)

As the ball rotates, the flow bore through the ball is uncovered and the propellant flow starts. Flow steadily increases with ball rotation until the fully open position (90° rotation) is reached. The ball valve remains in this position as long as sufficient pressure is applied to the piston.

For shutdown, the electrical signal to the solenoid valve is removed and the actuation control valve is returned to its closed position by means of a spring. In this position, the pressure on the piston is vented overboard. As the pressure in the actuator decays, the actuator springs move the piston back toward the end cap. The pinion, and thereby the ball, rotates because of the piston motion. As the ball rotates closed, propellant flow is choked off and is stopped completely when the valve reaches its fully closed position.

2. Modulating Valve Operation

A cross-sectional view of this valve is shown in Figure 48. Each modulating valve has dual rare-earth (Samarium Cobalt) motors similar to those used on the OMS gimbal actuator. Upon receipt of a signal from the engine controller, the motor(s) applies torque and angular motion to the large spur gear through small drive gears linked to each motor. Spur gear rotation turns the ball screw nut attached to it, and the ball screw - which is prevented from rotating - is moved in or out with respect to the valve seat. As the ball screw shaft position is changed, the flow area through the annular orifice is changed. This change continues until the desired output is reached; then valve shaft motion stops. The valve remains in this position until a new signal is received. Flow modulation continues throughout the engine run.

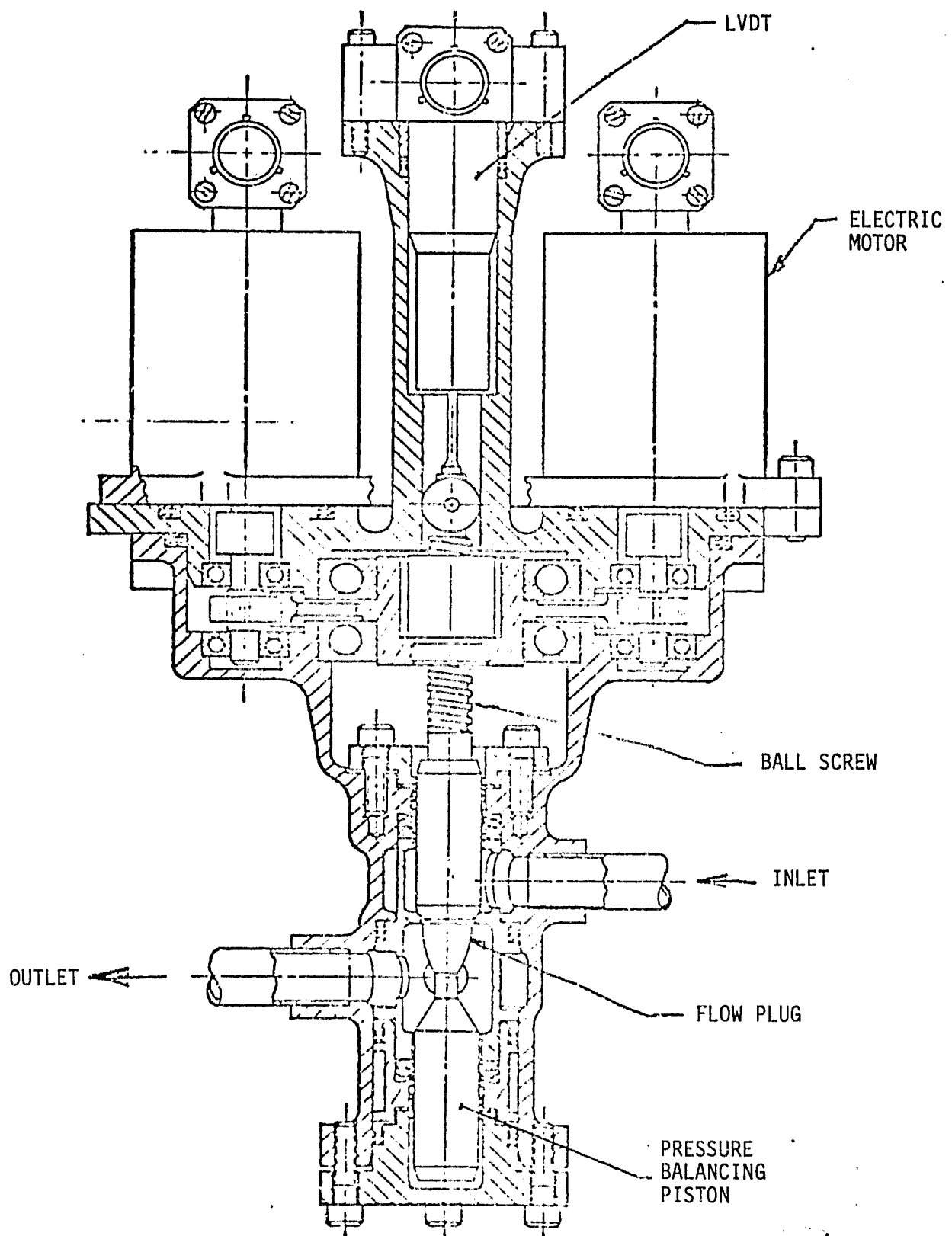


Figure 48. Modulating Valve Cross Section

III, E, Task V - Engine Control (cont.)

3. Actuation Systems

Four basic energy supply systems - pneumatic, propellant, hydraulic, and electric (and various combinations thereof) - were evaluated for application to the valves previously discussed.

The actuator trade study was conducted to determine reliability, complexity, weight, safety, control precision, and state-of-the-art parameters. Based upon the results, the pneumatically actuated shutoff valves and electric motor modulating valve actuation were selected. Table XXII summarizes the results of the systems study and gives a brief discussion of the pros and cons of each design.

The pneumatic actuation system selected for the shutoff valves consists of gaseous nitrogen pressurization to provide the opening force and of a spring for the closing force. This system was selected for the following reasons:

- ° The high-pressure system minimizes the actuator size.
- ° The valve will fail to the closed position.
- ° The system is state-of-the-art and is being used on the OMS engine.
- ° No materials compatibility problems emerged.
- ° No additional propellant leak paths are provided.

Electric motor actuation was selected for the modulating valves because the system is a straightforward, simple state-of-the-art design for a system requiring continuous actuation capability.

TABLE XXII
ACTUATION SYSTEM STUDY SUMMARY

Sheet 1 of 4

Actuation System Description	Energy Source	Pro	Con	Remarks
1. Single-acting, pressurized open, spring returned. Pressure supplied by an on-board helium bottle. Actuator position controlled by a 3-way, 2-position solenoid valve that applies pressure to the actuator piston to open and vents the actuator piston overboard to close.	Pneumatic	<ul style="list-style-type: none"> High pressure nitrogen minimizes the actuator piston size Actuator design is "State of the art" and has been used successfully on the Apollo and Space Shuttle's OMS engines No materials compatibility problems No propellant leak paths 	<ul style="list-style-type: none"> Actuator return spring greatly increases the force output required from the piston. Sealing of high pressure nitrogen. Excessive leak rate could deplete the nitrogen source and result in non-operation of the engine. Added cost, weight, complexity and packaging problems associated with the GN₂ supply system. 	
2. Same as above except use smaller gas bottle and recharge the bottle after each use with high pressure gaseous fuel (during engine burn). Original bottle charge could be isolated by a squib valve to facilitate storage.	Pneumatic	<ul style="list-style-type: none"> Recharge fluid readily available Explosive valve would give zero leakage during ground storage 	<ul style="list-style-type: none"> Gas bottle could leak to propellant tank during coast and prevent restart. Additional valves needed on gas bottle inlet and outlet to control pressure. 	
3. Same as Item 2 above except charge (or recharge) the gas bottle with liquid hydrogen which is then vaporized by an electrical heater to provide actuation pressure.	Propellant (& Electrical)	<ul style="list-style-type: none"> Actuation fluid readily available. Certain valves, e.g., the GO₂ start valve and the tank pressurization valves could be operated directly by rising pump discharge pressure. 	<ul style="list-style-type: none"> Electrical energy is required to vaporize propellant. Special accumulator (gas bottle) design required. Adds additional propellant leak paths. Bleed system required to assure that there would be sufficient liquid hydrogen in the accumulator. Valve response variable due to fluid density fluctuations 	Electric heater only needed for first start and for any restart after a long coast period
4. Double acting, pressurized open and closed, dual gas source for fail safe closed operation. Check valves in supply lines to prevent backflow.	Pneumatic (dual source)	<ul style="list-style-type: none"> Elimination of spring reduces actuation force requirements by approximately 80%. Positive position control 	<ul style="list-style-type: none"> A more complex pneumatic control valve required. Added system complexity, e.g. two independent pneumatic sources 	If one pneumatic source is deemed adequate could use two three-way pilot valves to pressurize actuator.

TABLE XXII (cont.)

Sheet 2 of 4

Actuation System Description	Energy Source	Pro	Con	Remarks
5. Same as item 4 above except gas source used only for start. During engine burn and shutdown actuation pressures supplied by the warmed fuel.	Pneumatic/ Propellant	<ul style="list-style-type: none"> • Smaller gas supply source needed • Could use servo valve since null leakage would only be back to propellant tank 	<ul style="list-style-type: none"> • Possible switching problems if shutdown signal occurs during the engine start transient. • Combining two pressure sources could be difficult. • Response may vary due to differences in gas densities at different times in the engine operating cycle. 	
6. Same as Item 4 except uses a single gas source. Auxillary "Energy Pac" (bottle with squib valve) available for emergency shutdown.	Pneumatic	<ul style="list-style-type: none"> • Secondary gas supply relatively small. • Squib valve would provide reliable gas seal insuring that gas would always be available for shutdown. 	<ul style="list-style-type: none"> • Use of explosive actuation. • Still requires two gas supplies even if one is smaller • Squib valve only good for one actuation. 	
7. Two completely separate systems (gas supply, actuators, electric harness, etc.) interconnected and synchronized by a common rack. Dual acting piston on each side.	Pneumatic	<ul style="list-style-type: none"> • System is truly redundant except for common rack. 	<ul style="list-style-type: none"> • Added weight, cost and complexity. • Although each side theoretically would need only 1/2 the total volume and be smaller in size the weight would not necessarily be 1/2. 	
8. Double acting, pressure operated piston type actuation. Gas pressure supplied by a GH_2 precharged, fuel recharged accumulator.	Pneumatic/ Propellant	<ul style="list-style-type: none"> • Recharge gas is plentiful. 	<ul style="list-style-type: none"> • Need to seal accumulator during storage, launch, and coast. 	
9. Single, double-acting, pressure operated piston with single source of gas supply. Valve to fail in place.	Pneumatic	<ul style="list-style-type: none"> • Simplest system studied. • Series redundant shut-off valves with independent actuators ensures propellant shutoff. 	<ul style="list-style-type: none"> • Prejudice against fail in-place actuation systems • Not used extensively in Aerospace applications. 	
10. Single-acting, pressurized open, spring closed. Pressure supplied by tap-off from gimbal actuator which is assumed to be hydraulic.	Hydraulic Oil	<ul style="list-style-type: none"> • High pressure system minimizes actuator piston size and thereby the hydraulic oil flow rate. • Existing on-board system (if assumption is valid). • Better lubricity (therefore longer life) than propellant and/or gas. • Good control, valve force is a small portion of the total actuator force. • With continuous pump flow could use servo valves for flow control, if required. 	<ul style="list-style-type: none"> • Main valves at low to cryogenic temperatures. Oil may freeze. • Leakage (high pressure), however should be less than gas. • Compatibility of leakage with LOX. • High spring load • If thermal barrier is needed to keep oil from freezing it will add weight and complexity to the design. • Interaction of gimbal actuator movement and valve movement on hydraulic oil availability. 	

TABLE XXII (cont.)

Sheet 3 of 4

Actuation System Description	Energy Source	Pro	Con	Remarks
11. Same as Item 10 above except that hydraulic supply system is part of the actuation system only and is not used anywhere else on the engine	Hydraulic Oil	<ul style="list-style-type: none"> * System pressure unaffected by other engine subsystems * Internal actuator leakage not a problem. * Can use servo valve for positioning 	<ul style="list-style-type: none"> * Requires motor, pump, reservoir valves and other components associated with a hydraulic system. 	
12. Single-acting, pressurized open and spring closed using fuel as the actuation fluid. Propellant tapped off of main engine line.	Propellant	<ul style="list-style-type: none"> * Actuation fluid readily available 	<ul style="list-style-type: none"> * Cryogenic temperature * Possibility of two-phase flow * Timing variations due to fluid density changes * No pressure available for engine start. 	
13. Same as Item 12 except actuator pressure is supplied by a pre-charged accumulator (with propellant) and the accumulator is recharged during use.	Propellant	<ul style="list-style-type: none"> * Actuation fluid readily available 	<ul style="list-style-type: none"> * Cryogenic temperature * Vaporization of fluid in accumulator during storage with subsequent pressure rise. * Requires bleeding system to obtain liquid in accumulator. 	<ul style="list-style-type: none"> * Could isolate accumulator prior to start-up with a squib valve to minimize leakage.
14. Same as Item 13 except has an auxilliary "Energy Pac" to insure adequate pressure in case of an emergency shutdown.	Propellant/ Pneumatic	<ul style="list-style-type: none"> * Energy pac ensures engine shutdown even if all of the accumulator fluid leaked out. * Satisfies redundancy requirements 	<ul style="list-style-type: none"> Same as Item 13 plus * Added weight (~ 1.3 lbs. per Pac) * Use of "Energy Pac" would probably be a one-shot shutdown with no subsequent start-up. 	
15. Motor drive open and closed with Electric auxillary spring for fail-safe closure in case of power failure.	Electric	<ul style="list-style-type: none"> * Straight forward, state of the art design 	<ul style="list-style-type: none"> * Actuator would be large and heavy. * Motor torque required to hold valve open would be high. * Multiple gear sets required, i.e., large gear reduction required. * High backlash, not ideal for precise valve control. * Temperature effects on gear box. 	
16. Motor driven spur gear to ball screw drive with auxillary spring to close valve in case of a power failure.	Electric	<ul style="list-style-type: none"> * State of the art design-similar to OMS gimbal actuator (sans spring) * Ball screw reduces gear train ratio required. 	<ul style="list-style-type: none"> * Spring drive of ball screw (closing) is very inefficient due to low linear to rotary torque conversion. * Fairly large envelope with attendant weight problem. 	

TABLE XXII (cont.)

Sheet 4 of 4

Actuation System Description	Energy Source	Pro	Con	Remarks
17. Redundant motor drive with single valve drive. Motor independently harnessed and controlled. Valve drive utilizes a worm gear to provide mechanical advantage. Motors sized so that one motor acting alone is sufficient to meet the response requirements of the valve.	Electric	<ul style="list-style-type: none"> • Simplicity of design. • Less temperature sensitive. • Able to provide right angled drive needed for valve rotation. • Second motor provides redundancy and replaces spring • Relatively small envelope and low weight. 	<ul style="list-style-type: none"> • High worm gear friction • High gear tooth loading • Trade off between smaller actuator and more harnessing and additional controller capacity. 	Two motors and speed reducers weigh approximately 7.5 lbs.
18. Same as Item 17 above except that the worm gear is replaced by a ball screw.	Electric	<ul style="list-style-type: none"> • Low friction, ball screw efficiency approximately 90% • Because of the multiple balls the thrust capacity of the ball screw is high. • Relatively small envelope and low weight. • Low backlash, large motor movement for small valve motion provide good valve position control. 	<ul style="list-style-type: none"> • Unknown temperature effects • Would need a crank mechanism for the ball valve. 	
19. Same as Item 18 except that the second motor is replaced by a gas driven turbine.	Electric/ Pneumatic	<ul style="list-style-type: none"> • Simpler controller required. • The harness to the second motor (turbine) would be simpler since it would only need to fire squib valve(s). • Would be slightly lighter than 2 electrical motors. 	<ul style="list-style-type: none"> • Gas distribution system needed (or "Eager Pac" at each valve.) • Eager Pac drive suitable for only one-shot therefore could only be used for emergency shutdown. 	

III, E, Task V - Engine Control (cont.)

The selected systems are discussed in more detail in the following paragraphs.

a. On-Off Ball Valve

The valve actuation systems study resulted in the selection of a single-acting, pneumatically opened/spring-closed actuator with a rack and pinion output drive for the on-off ball valve. This type of actuator provides fast response, a fail-closed capability upon loss of power or control signal, actuation pressure that is independent of propellant pressure (needed for engine start), and relative insensitivity to cryogenic temperature. This type of system needs a regulated pressure source with adequate capacity, flow, and pressure to meet the duty cycle of the engine. The integral pneumatic pack is designed to supply a pressure that is adequate to overcome twice the anticipated friction forces plus one and one-half times the combined mechanical, spring, flow, and pressure forces acting on the actuation system at any valve position. This philosophy assures that the actuators provide their function for this man-rated application.

The actuator shown in Figure 45 is essentially the same actuator as the one used on the OMS bipropellant valve, but with two major differences: (1) The OMS actuator had an actuator piston cavity and a spring cavity joined by a small shaft bore. During fabrication it was found that maintaining the needed tolerances and form controls with this arrangement was difficult; as a result, the OTV actuator has a straight-through bore. (2) The OMS actuator was for a bipropellant valve and was designed to open two parallel valves simultaneously. The OTV actuator has to open only one valve, so the actuator piston, rack, and spring guide have been combined into one part. This allows location of the actuator centerline nearer to the valve bore axis (the rack is offset with respect to the actuator centerline) and at the same time provides the rack with improved support from the two filled TFE bearings which have an excellent (2.0) length-to-diameter ratio.

III, L, Task V - Engine Control (cont.)

For drawing convenience, the valve and actuators in Figure 45 were shown in the same or in parallel planes. In actual use on the engine, this may or may not be the case. If required, the relative positions of the actuators with respect to the valve can be changed by rotating the actuators about the valve bore axis or about the pinion shaft axis. The solenoid-operated control valves can also be rotated (or moved) to accommodate the final engine configuration.

b. Modulating Valve

The actuator study resulted in selection of electric actuation for the modulating valve. Hydraulic actuation was eliminated in view of the absence of an existing hydraulic system on the engine and because of the problems associated with its use in, or near, components subjected to cryogenic temperatures. Although a pneumatic source (the pneumatic pack) is available, the capacity for continuous flow through a control valve needed for a dual-acting pneumatic piston, coupled with the compressibility of the gas, makes a pneumatic approach unacceptable. Electric actuation has the advantage of being readily available, easily routed, and relatively immune to temperature fluctuations.

Drive train friction has been reduced to a minimum by use of ball bearings. The drive screw nut support duplex bearings also counteract the thrust loads imposed on the valve shaft by friction, pressure, or flow.

The electric motor selected for the modulating valve is a rare-earth (Samarium Cobalt) motor similar to the motors used on the OMS gimbal actuator. Electronic commutation of the DC power supply (three-phase inverter) by the engine controller permits operation as a brushless DC motor, but in a smaller package.

III, L, Task V - Engine Control (cont.)

Disadvantages of the electric motor drive system, as compared to a hydraulic or pneumatic system, include the inability to package as much power within a given volume and the development of windage and electrical losses. Selection of a drive train that minimizes these disadvantages, wherever possible, is important to the overall size and weight of the modulating valve.

Several design features in the drive train (shown on Figure 48) tend to reduce the power requirements. These include (1) addition of a pressure-balancing piston (the bullet-shaped shaft section in Figure 48); (2) use of a ball screw to provide a mechanical advantage in moving the shaft, plus utilization of as large a gear ratio between the ball screw nut drive gear and the motor output gear as practical.

The pressure-balancing piston eliminates the downstream pressure force tending to open the valve and minimizes whatever flow forces there might be.

The ball screw provides a mechanical advantage of approximately seven to one due to the wedge action of the screw thread. One feature of the arrangement (shown in Figure 48) is that the seal friction is first reduced by the ball screw's mechanical advantage and then by the gear ratio, resulting in use of a smaller, faster motor.

4. Auxiliary Valve Requirements

A preliminary effort to define the basic OTV auxiliary valve requirements was also undertaken. Pneumatic supply system components, such as the regulator and relief valve, fill valve, and pneumatic supply tank, were not considered and will need to be included in subsequent studies.

III, L, Task V - Engine Control (cont.)

The functions to be performed by the OTV auxiliary valves which were considered include the following categories: (1) purge valves to provide a GHe purge for the H_2 flow passages and a GN_2 purge for the O_2 flow passages; (2) vent and/or relief valves to prevent excessive pressure buildup following engine shutdown; and (3) pilot valves to control the flow of GN_2 or GHe for the purpose of actuating the engine system valves.

a. Purge System

In defining the purge system, the following assumptions were made:

(1) The purge system will be required to remove moisture and condensable gases from the engine on the ground prior to engine test or prior to flight. This system will also be utilized to purge the engine system of propellants following engine ground test. It is assumed that an inflight purge will not be required prior to or following engine operation because of the aspirating effect of space vacuum on the system. If it is later determined that an inflight purge is necessary, the ground purge valves, combined with some additional volume in the pneumatic supply system, could be utilized to satisfy the requirement.

(2) On the ground, GHe will be used to purge the H_2 system and GN_2 will be used to purge the O_2 system. The tradeoff is the cost of GHe against the possibility of mixing the gases. The purge gas will be supplied by a GSE source. If an inflight purge is required, it is assumed that only the oxidizer system will need to be purged, using GN_2 to prevent the formation of a combustible mixture.

III, E, Task V - Engine Control (cont.)

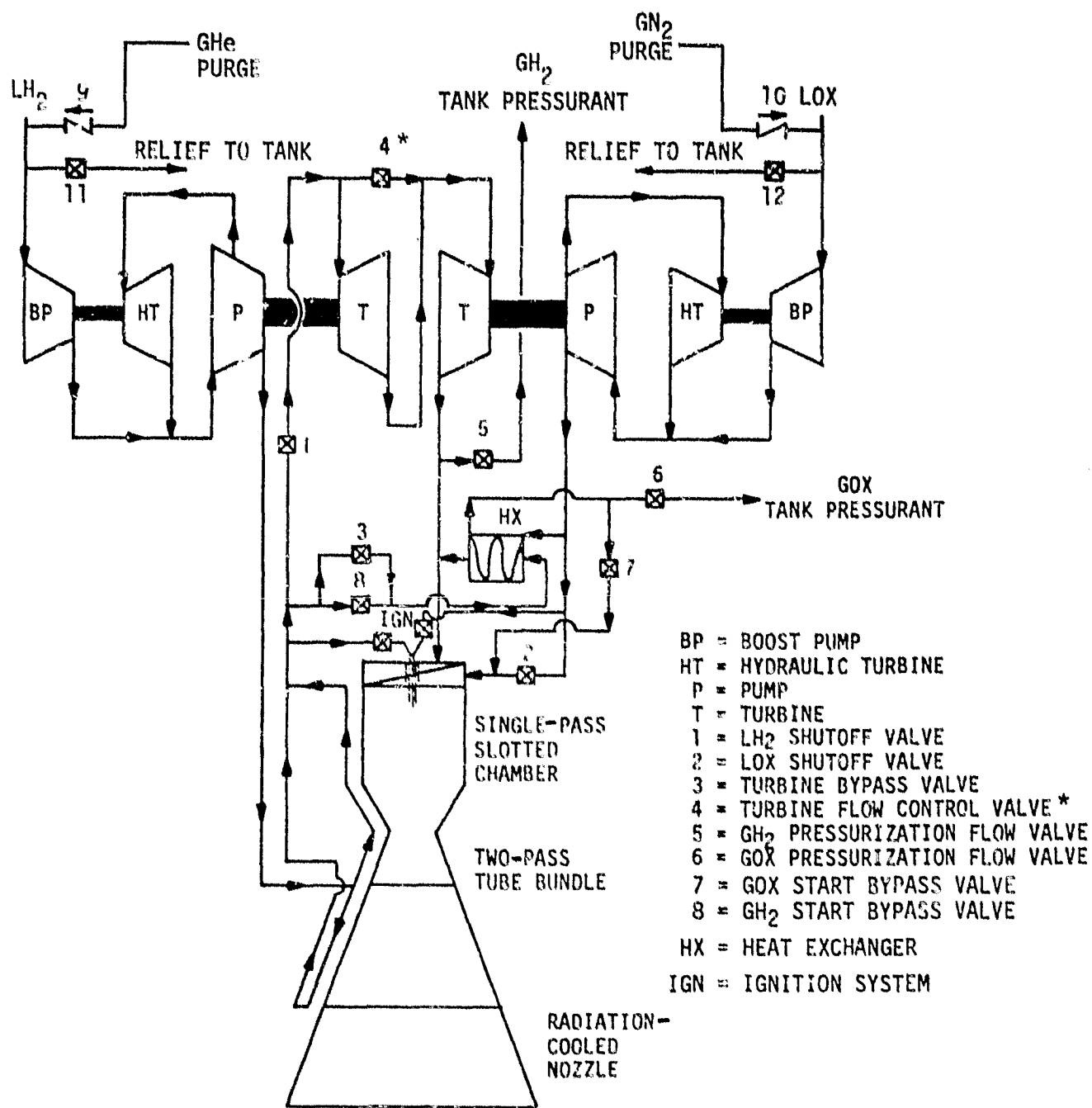
(3) Based on consultation with the pump designer, the purge flowrate should not exceed 0.01 lb/sec and the ΔP across the turbines should not exceed ~ 1 psid to prevent rotating the pumps and possibly damaging the dry shaft seals. Therefore, sufficient flow can be provided by using $1/4$ -in. direct-actuated solenoid valves. The purge lines are connected to the engine system just upstream of the boost pump inlets, as shown on the schematic of Figure 49. The other end of the fuel purge line is attached to a GHe disconnect at the engine interface panel. The oxidizer purge line is connected to a purge valve located on the pneumatic pack assembly. For redundancy, check valves (valves #9 and #10) are installed in the purge system and located at the interface between the purge system and the engine system.

(4) It is assumed that the purge method will be a continuous purge (duration TBD). On the fuel side, GHe is applied at the engine interface panel, and valves #8, 3, 1, and 4 will be alternately opened and closed for specified durations to ensure a complete purge. On the oxidizer side, the pneumatic pack GN₂ purge valve is opened, and valves #7 and 2 are alternately opened and closed to assure purging. The igniter valves are also cycled to ensure purging of the ignition system. Another possible method of purging is to alternately pressurize and depressurize the system. This method is effective in augmenting gas mixing.

(5) Additional purge distribution lines may be required for components (e.g., the control valve electric-motor actuators). These requirements will become evident as the engine design matures.

b. Relief System

The sections of the engine where pressure can build up following engine shutdown are between the vehicle pre-valves and downstream



*TO BE RELOCATED TO BYPASS THE OXYGEN PUMP TURBINE

Figure 49. Engine Purge and Relief System Schematic

III. E, Task V - Engine Control (cont.)

valves #1, 3, and 8 on the fuel side and 6, 7, and 2 on the oxidizer side (Figure 49).

At the present time, the GH₂ start bypass valve (valve #8) and the GOX start bypass valve (valve #7) are programmed to open when the vehicle pre-valves are closed to prevent pressure buildup. If passive relief is required, pressure-actuated relief valves would have to be added to the system. The best location for these valves (#11 and 12) is in the low-pressure side of the propellant feed system between the vehicle pre-valves and the boost pumps. Since the fuel system will contain liquid from the pre-valve to the thrust chamber, and GH₂ from the chamber jacket to the LH₂ shutoff valve, a relief valve may not be required on the fuel side because of the accumulator effect of the gas present in the system at engine shutdown. This will be a function of the relative gas and liquid volumes, initial and final pressures and temperatures, and the maximum allowable pressure in the low-pressure side of the system.

It is more likely that a relief will be required in the oxidizer system because that system will be primarily liquid, with a small amount of gas in the heat exchanger at engine shutdown.

Some of the tradeoffs between an active and passive relief system are as follows:

For an active system, control functions will need to be incorporated into the controller to hold the turbine and GOX start bypass valves in an open position until the liquid propellants have gassed off. A passive system will automatically vent an overpressure condition. Another advantage of using passive relief valves is that propellants can be vented back to the propellant tanks and are not lost overboard. This is the case when turbine and GOX start bypass valves are used to vent the system.

III, E, Task V - Engine Control (cont.)

However, a passive system will require the addition of two more valves with potential leak paths and possible failure-to-close modes.

In any event, additional definition of the engine system is required. For this initial design iteration, it is assumed that an active system will satisfy the relief requirements. If later studies show that a passive relief system is more advantageous, then the additional relief valve locations and envelopes will be as shown on the engine schematic (valves #11 and 12 on Figure 49) and on Table XXIII.

c. Pilot Valves

For this study, it was assumed that the LH₂ and LO₂ shutoff valves and the GH₂ and GOX start bypass valves are actuated by using GN₂ supplied from the engine pneumatic pack. Each shutoff valve has two actuators, whereas the bypass valves have one actuator each. Assuming one pilot valve for each actuator, a total of six pilot valves is required.

Because the engine valve response will be controlled by timing orifices, a 1/4-in. line size for the pilot valves and isolation valve should be adequate based on engine valve size and past experience. Valve envelope, operating pressure, and weight is listed on Table XXIII.

5. Engine Controller Requirements

A conceptual design for the OTV engine controller was identified on the basis of a digital processor and associated input/output electronics. A power-density study determined the controller size, weight, and power requirements, and a preliminary engine control logic flow chart was developed to support the engine transient simulation model to determine suitable control points/methods for thrust and mixture ratio control.

TABLE XXIII
OTV AUXILIARY VALVE SUMMARY

SYSTEM	COMPONENT TYPE	LINE SIZE (IN.)	ENVELOPE (L X W X H)	OPERATING FLUID	OPERATING PRESS (PSIG)	APPROXIMATE WEIGHT (LB.)
PURGE	DIRECT OPERATING SOLENOID (BAYONET MOUNT TO PNEUMATIC PACK)	.25	3.3x1.5x2.5	GN ₂	600 (ø INLET)	1.5
	CHECK VALVE	.25	2.5x1.0 DIA.	GN ₂	0-100	0.3
	CHECK VALVE	.25	2.5x1.0 DIA.	GHe	0-100	0.3
	DISCONNECT	.25	2.8x.75 DIA.	GHe	0-100	0.3
RELIEF (PASSIVE) (IF REQ'D)	INLINE PRESSURE RELIEF	.25	5.8x1.8 DIA.	LH ₂ /GH ₂	60	0.6
	INLINE PRESSURE RELIEF	.25	5.8x1.8 DIA.	LO ₂ /GO ₂	55	0.6
ACTUATION	ISOLATION - 2-WAY SOLENOID, N.C. (BAYONET MOUNT TO PNEUMATIC PACK)	.25	5.2x1.5x2.5	GN ₂	2500	1.25
	PILOT - 3-WAY SOLENOID (6 REQ'D.)	.25	5.6x2.5x2.5	GN ₂	100	1.5

III, E, Task V - Engine Control (cont.)

A microprocessor-based controller design including input/output signal conditioning, multiplexing, analog/digital conversion, interfacing, and output power drivers appears to be a feasible application for the engine controller function. The engine conceptual control schematic shown in Figure 50 depicts the controller elements and engine interface developed during the engine design definition phase.

The power, physical size, and weight requirements for the controller, as summarized in Figure 51 and Table XXIV, reflect valve, valve actuator, and igniter electrical loads estimated from the engine control components study. Note that the weight does not include the power supply. If the power supply weight were charged to the engine, it could double the values shown.

The controller power-density requirements are based upon both the SSME controller design as well as the more recent electronic controller designed for the OMS-E gimbal actuator. The power-density factors used were for the latter since the microprocessor-based system architecture is more closely represented.

The engine control logic flow chart of Figure 52 defines the preliminary engine start/shutdown sequence and thrust/mixture ratio control point selection for use with the engine transient simulation model. The desired objectives of this task included determination of engine conditioning at each of the operating modes (i.e., tank head idle, pumped idle, and full thrust), effectiveness of the pumped idle step control point, and the initiation point for thrust and mixture ratio closed loop control. Planned variations to the logic flow path included isolation of the thrust or mixture ratio control loop from the main program via hardware (separate microprocessor) to better evaluate control loop update time as well as the interactive effects

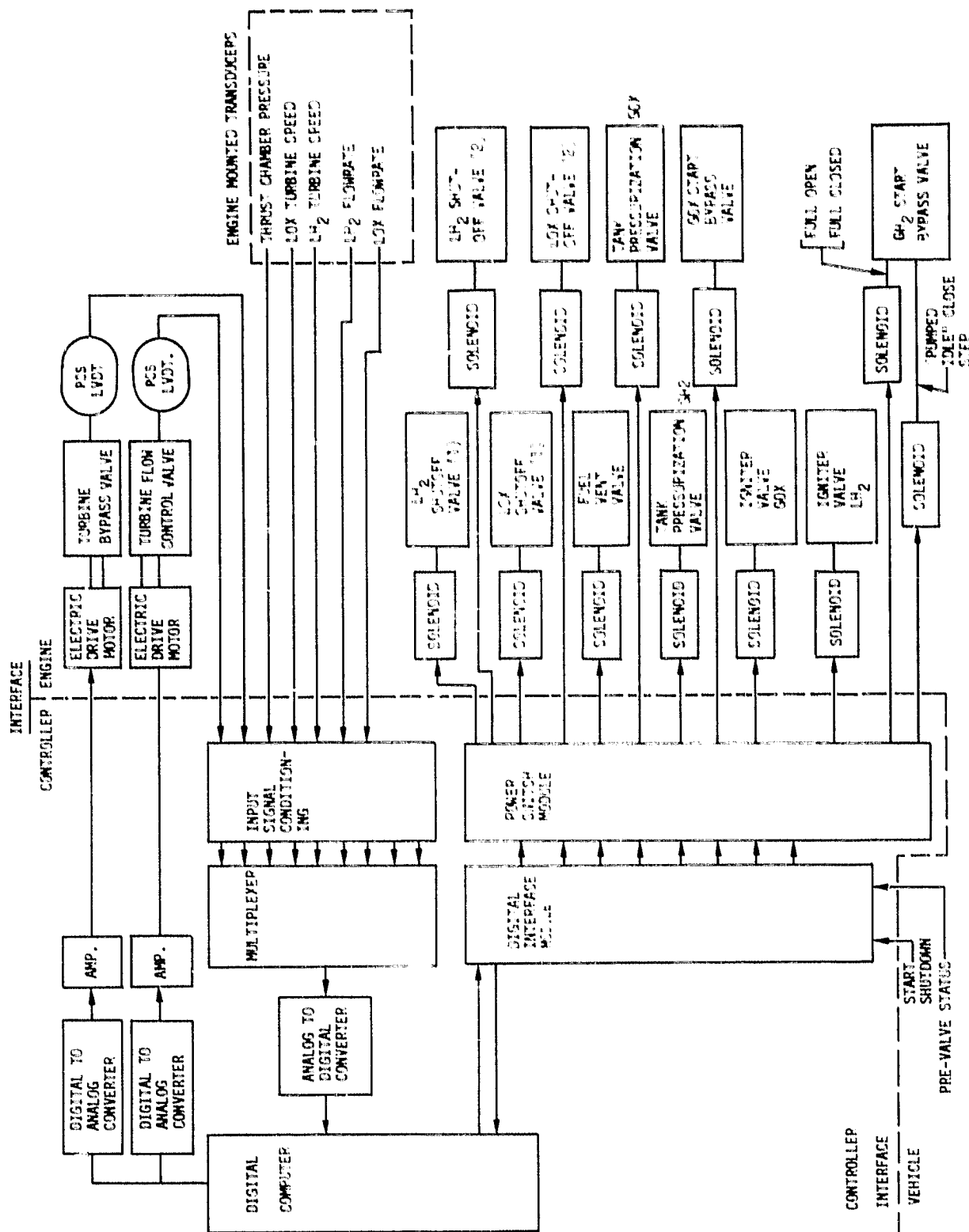
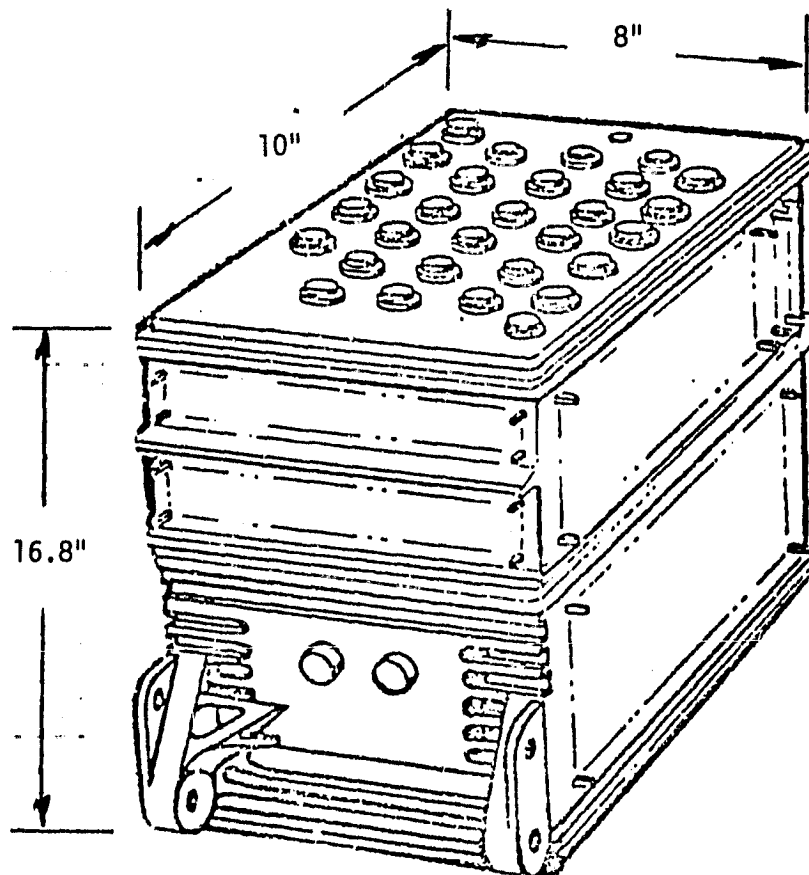


Figure 50. OTV Engine Conceptual Control Schematic



Weight: 34 lb
 Power 287 watts
 Output:
 Volume: 0.78 Ft³

- Notes: 1. The vehicle power supply weight/volume is not included as part of this assessment.
2. Controller is assumed to operate direct from vehicle power supply without need for power conversion equipment.

Figure 51. OTV Engine Controller Size Estimate

TABLE XXIV
OVT DIGITAL CONTROLLER POWER DENSITY DETERMINATION

	<u>Lbs.</u>	<u>Watts</u>	<u>Ft³</u>
Input Electronics	4.5	36.7	0.1
Digital Interface	4.3	36.8	0.1
Digital Computer	4.2	36.9	0.1
Output (Power) Electronics	<u>20.6</u>	<u>176.6</u>	<u>0.48</u>
Totals	33.6	287.0	0.78

Notes:

1. Basis is the OME Gimbal Actuator Controller in which both output (power) electronics and digital/analog MSI circuitry are utilized. In comparison, the LSI circuitry of the OTV controller would weigh less, whereas the output electronics would be almost identical.
2. Gimbal Actuator Controller power design, based upon continuous operation at altitude: 8.5 watts/lb and 43 lbs/ft³.
3. The above breakdown for the OTV controller is based upon the electronic elements shown in the OTV Control Schematic and presented with above power density factors applied.

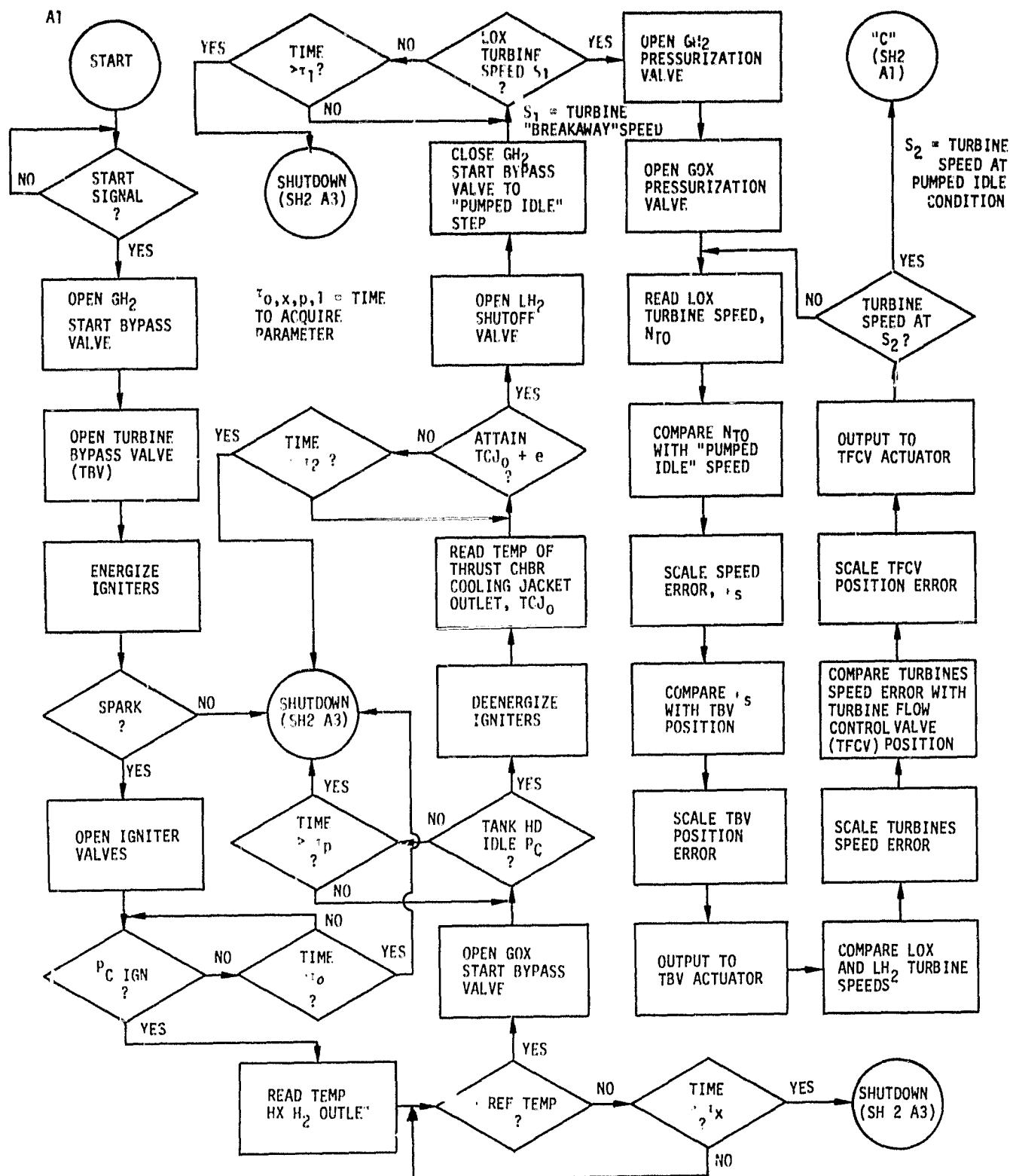


Figure 52. OTV Engine Control Logic (Sheet 1 of 2)

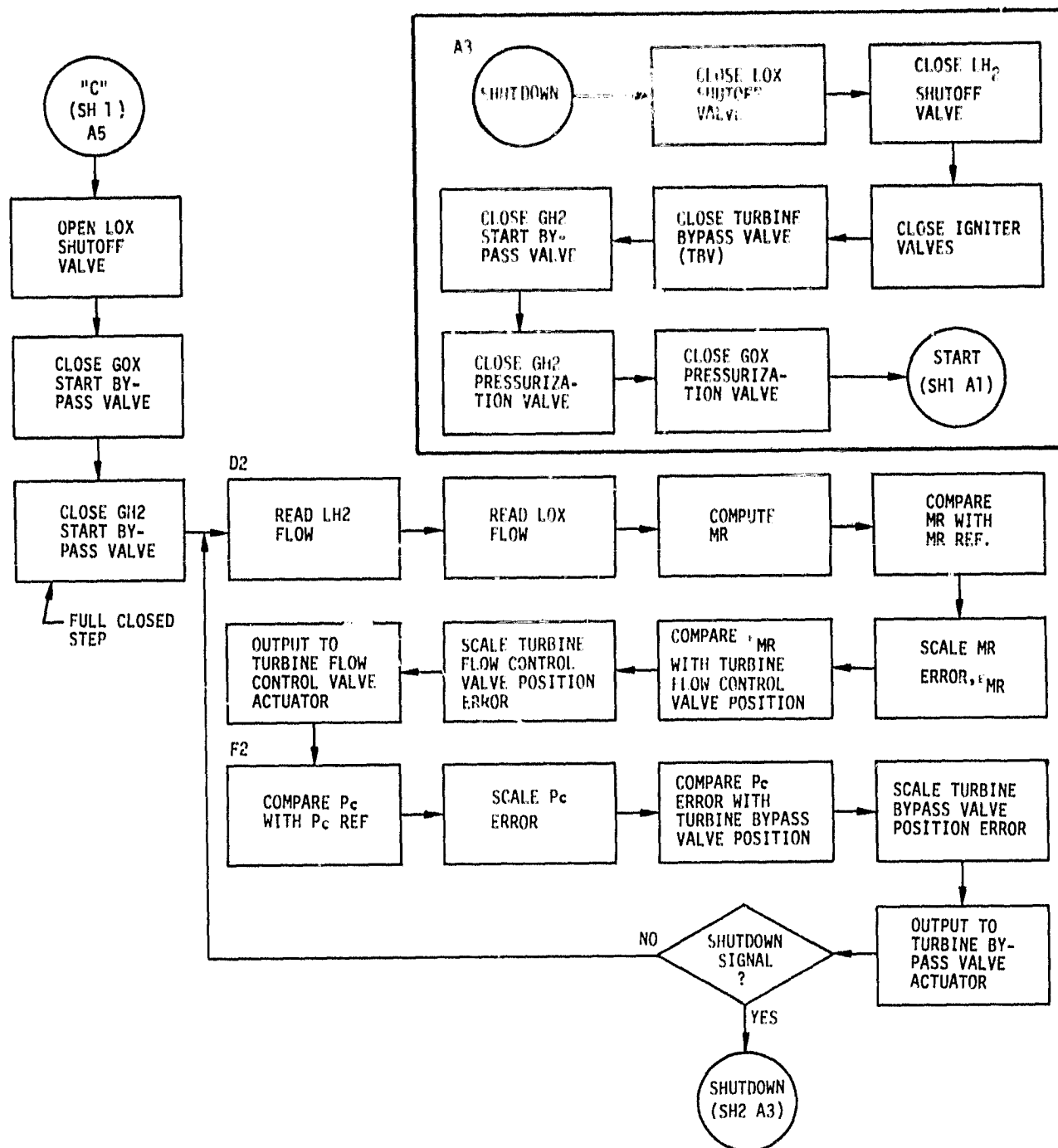


Figure 52. OTV Engine Control Logic (Sheet 2 of 2)

III, E, Task V - Engine Control (cont.)

between thrust and mixture ratio control upon engine performance. Difficulties were encountered with the engine transient simulation model and the planned iterations could not be conducted within this study program's schedule and funding constraints. This precluded verification of the logic flow path shown on Figure 52. Further flow chart definition is required in future design studies to baseline software design and computer memory requirements.

6. Areas Requiring Further Study

Wherever possible, the designs for the OTV Point Design engine controls have incorporated the best features of past ALRC designs. These proven design features, plus application of design analysis methods developed in the past use of these designs, have resulted in the valve configurations presented herein. Limitations imposed on this phase of the design has reduced overall analysis to the basics, i.e., flow, pressure loss, estimated leakage, predicted wear, rough weights, and preliminary motor sizes. During the detail design phase, these analyses must be refined and combined with additional analyses for heat transfer, stress and deflection magnitudes, and valve effects on engine performance.

The efficiency of the Advanced Expander Cycle Engine improves as the amount of heat used to warm the fuel is increased. Additional heat also results in a higher operating temperature for the components that are used in the fuel system. If the fuel temperature approaches 1000°R through use of advanced cooling concepts and schemes, consideration will have to be given to the effects of high temperature on the valve designs. While valves designed to withstand very low or very high temperatures are common, valves that can withstand both are not. While the design of valves for use at temperatures from 100°R to 1000°R is not beyond the state of the art, it would involve increased analyses and verification testing.

III, E, Task V - Engine Control (cont.)

If engine analysis determines that higher system temperatures are feasible and desirable, an effort should be made to verify the design integrity of specific valve elements (e.g., shutoff seals, shaft seals, bellows, if used, and ball screws) under the proposed operating conditions and in a configuration as close to actual use as possible.

In addition to the areas for expanded analyses discussed previously, the items listed below should be studied in greater detail to determine whether they should be incorporated into any future designs. Items for more study include, but may not be limited to, the following:

- ° Study the possibility of using a downstream shutoff seal cartridge with an eccentric ball for the propellant shutoff valve. This arrangement could result in smaller actuator springs and thus a smaller actuator.
- ° Investigate possible weight reductions resulting from material substitutions and/or improved analysis.
- ° Determine weight penalties (if any) imposed on designs for use at higher temperatures and/or those that require similar thermal expansion characteristics to accommodate large temperature ranges.
- ° Determine the optimum valve characteristics needed for maximum engine efficiency for each application and incorporate these features into the valve designs whenever practical.
- ° Determine thermal effects (both high, 1000°R, and low, 100°R) on seal designs, especially those fabricated from non-metallic materials.

III, Task Discussions (cont.)

F. TASK VI - ENGINE CONFIGURATION LAYOUT

The primary objective of this task was to provide an engine configuration layout drawing showing the packaging relationship of the primary engine components.

1. Engine Assembly

The engine assembly layout drawing showing the packaging of the components is presented in Figure 53. The engine is 60 in. long with the extendible nozzle in the stowed position. This length is measured from the top of the gimbal block to the end of the tube bundle nozzle. With the extendible nozzle deployed, the engine is 109.6 in. long and has an area ratio of 435:1. Approximately 10.4 in. of potentially available deployed length is lost in the area of the extendible nozzle deployment mechanism and attachment plane. Further design refinements could increase the deployed length to a maximum of 120 in., with a resulting area ratio of 473:1 and a performance increase of 1.8 sec over the baseline value of 475.4.

The seven-digit numbers next to the component callouts on the engine layout refer to ALRC drawing numbers for those components.

The main and boost pumps are in-line and close-coupled to reduce system pressure drops and to shorten the hydraulic turbine supply line to the boost pumps. The turbopumps are mounted on the same side of the engine to provide a short warm-gas line between the main pump turbines. This reduces the crossover duct pressure losses between turbines. A protective bulkhead is placed between the turbopumps to semi-isolate them from each other. This was done to prevent a failure and fire in one TPA causing a fire in the other. The engine controller is packaged on the other side of the engine from the TPA. The controller is wrapped around the engine rather than

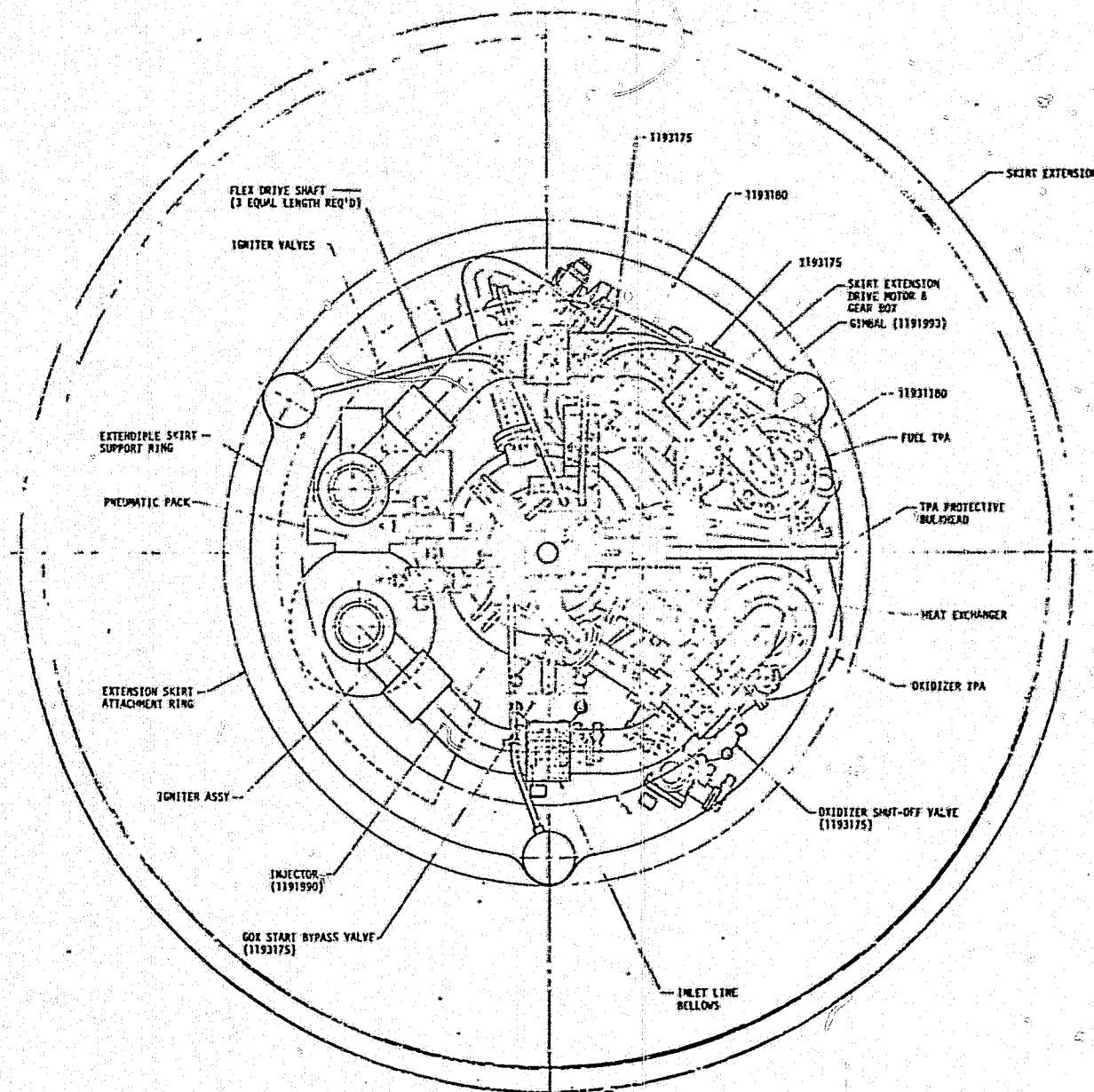


Figure 53. Engine Layout (ALRC Drawing No. 1193100) Sheet 1 of 3

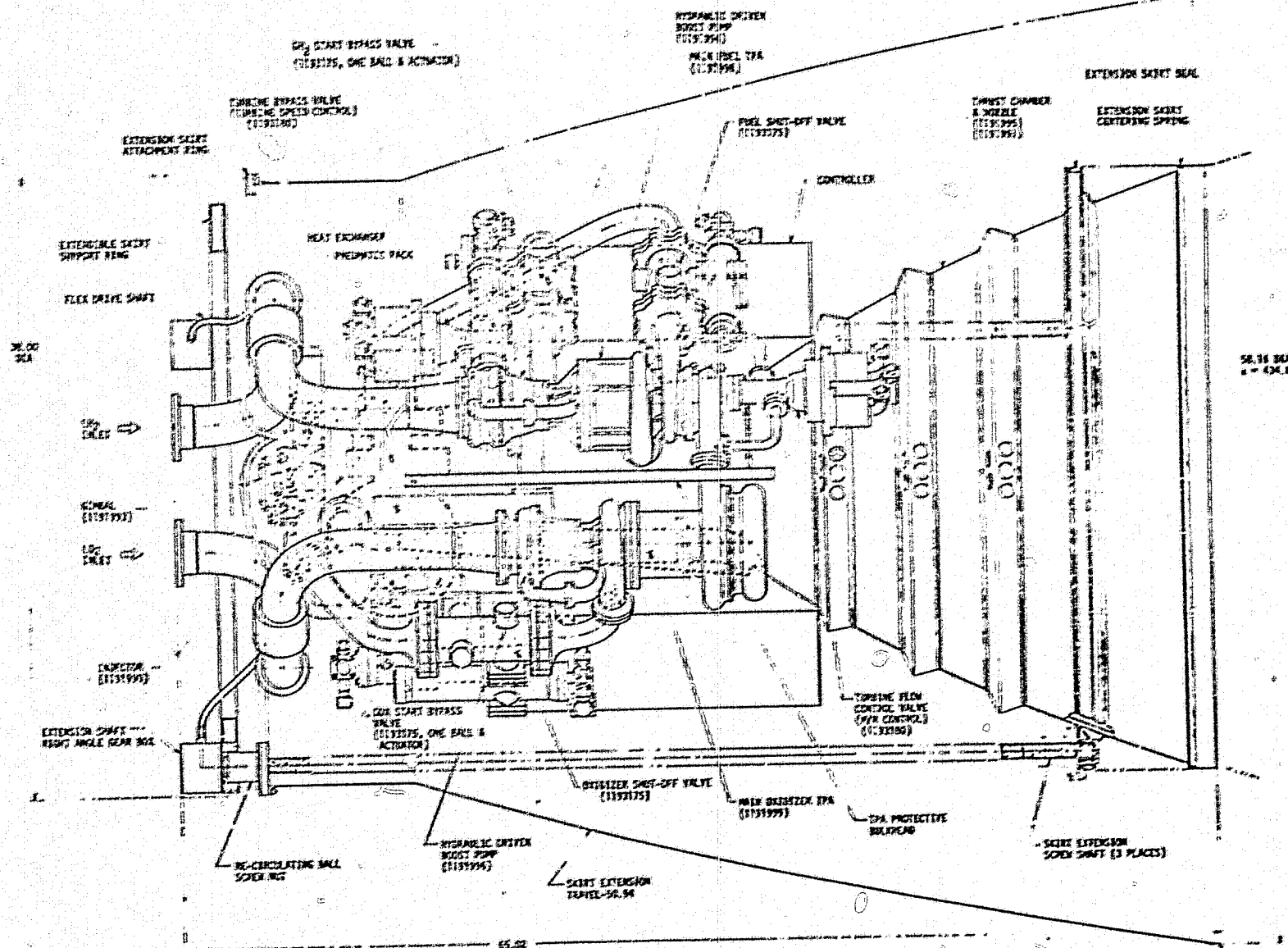
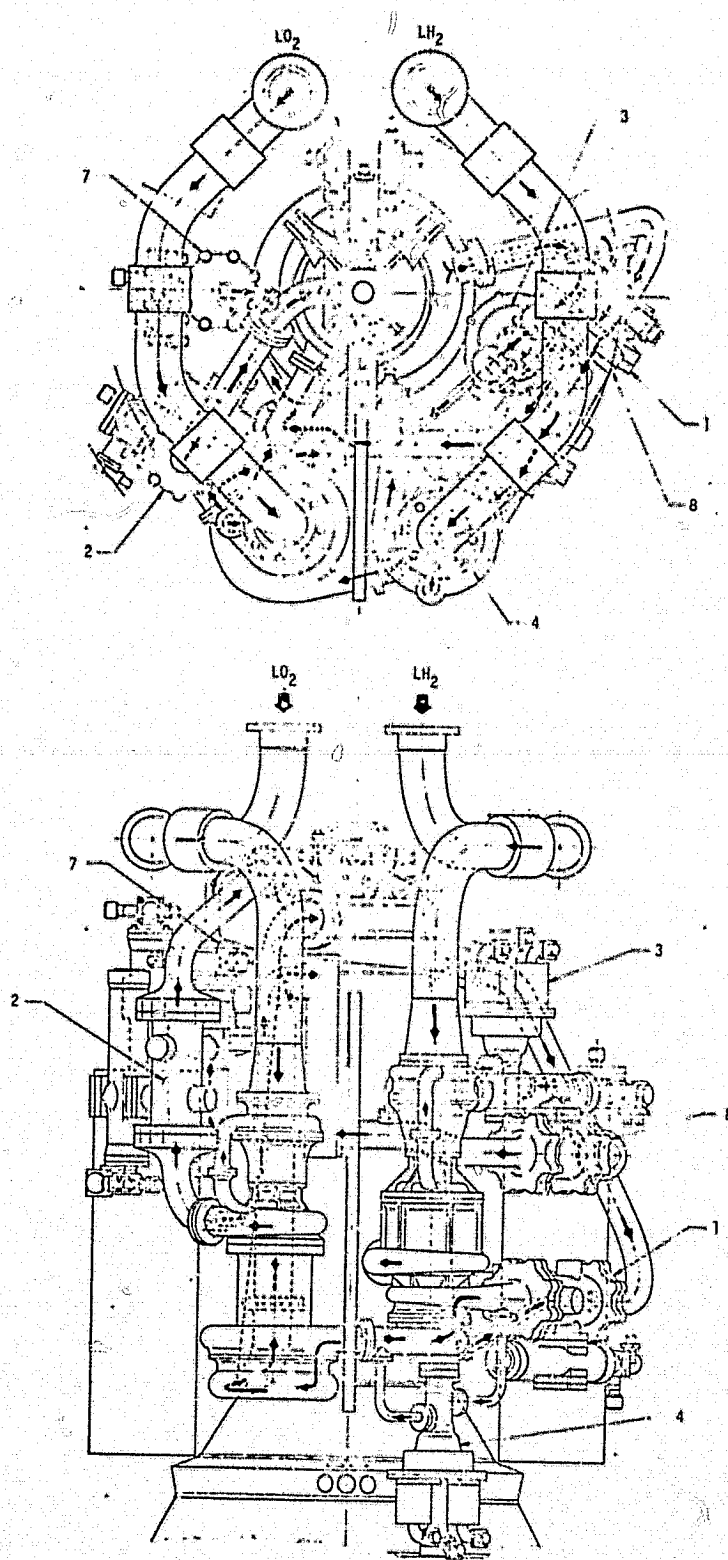


Figure 53. Engine Layout (ALRC Drawing No. 1193100) Sheet 2 of 3



ORIGINAL PAGE IS
OF POOR QUALITY

Figure 53. Engine Layout (ALRC Drawing No. 1193100) Sheet 3 of 3

III, F, Task VI - Engine Configuration Layout (cont.)

in the box shape shown in Section III,E,5. This wrap-around configuration is feasible.

The radiation-cooled nozzle, in the extended position is located 34.35 in. below the throat and extends an additional 50.3 in. to an exit area ratio of 435:1. The retracted position of the nozzle is such that its exit plane is at the same axial station as that of the regeneratively cooled nozzle (172:1) which is 34.35 in. below the throat.

The length of the radiation-cooled nozzle (50.3 in.) is based upon the following design criteria:

- ° Component penetration above the gimbal plane is limited to 6.5 inches. This distance is required to redirect the axially oriented propellant inlet lines to the horizontal and into the gimbal plane.
- ° A thin-wall cylindrical ring assembly, approximately 9.3 in. long, which contains the nozzle attachment flange is an integral part of the nozzle. The ring assembly is not exposed to the hot products of combustion since it extends axially up the outside of the regeneratively cooled nozzle as shown in the figure.

All major components are readily accessible for ease of maintenance or replacement on the line. The radiation-cooled nozzle incorporates a bolt-on flange and is designed to be removed and replaced. If necessary, removal could be accomplished in orbit if the nozzle could not be retracted prior to the OTV returning to the Orbiter's payload bay.

III, F, Task VI - Engine Configuration Layout (cont.)

The third sheet of Figure 53 also shows the propellant flow paths; the numbers listed refer to the valves shown on the engine schematic (Figure 47).

2. Engine System Structural Analysis

Preliminary stress and dynamic (modal survey) analyses were conducted for the purpose of establishing loads and stresses for the OTV engine assembly. The engine assembly and lines were modeled as a series of beam elements and lumped masses for analysis with the "SPAR" Finite Element Computer Program. Since the loading as well as component definitions are very preliminary in nature, this analysis should be updated as the engine design is improved.

The purpose of this analysis was to provide an initial survey of the loads and stresses in the chamber, the lines, and the nozzle deployment system. The loading cases include steady-state and startup thermal, flight "g" loading, actuation, and thrust.

This preliminary investigation shows that the maximum stress levels occur in the OTV thrust chamber system and are due to the start transient and steady-state thermal environments. A maximum steady-state thermal stress equal to -50,000 psi occurs in the thrust chamber region. This stress is caused by constraints imposed by the chamber throat bridge. The corresponding mechanical stress in the bridge is 16,300 psi. The actuating system rods are subjected to a 21,700 psi bending stress due to steady-state thermal expansion of the thrust chamber and nozzle.

The maximum thermal stress (-18,000 psi) in the propellant lines occurs in the LH₂/LOX turbine inlet line.

III, F, Task VI - Engine Configuration Layout (cont.)

Mechanical stress levels in the lines, struts, and actuating rods due to gimbaling (15° pitch, 6° yaw), inertia (1g) side loads, and thrust loads are well within the material allowable stress.

Table XXV lists the significant stresses for the various components that make up the OTV engine system.

Table XXVI lists the significant stress levels for the combined inertia loading $[2g(x) + 1.5g(y) + 4.2g(z)]$ when the nozzle extension is in the stowed position.

The following conclusions were drawn from an evaluation of the preliminary analysis results:

- ° The design is an acceptable first iteration.
- ° The propellant lines, chamber, chamber struts, stiffening cylinder, and actuating rods have loads and stresses of acceptable levels. When the loading combinations are made and the design is refined in the next design phase, the system can be made structurally adequate.
- ° Thermal stress levels are somewhat high in the chamber throat and barrel section, due, in part, to the axial constraint imposed by the stiffening cylinder. This can be alleviated by a refinement of the stiffening cylinder design.

TABLE XXV
ENGINE SYSTEM STRESS SUMMARY, THERMAL AND MECHANICAL LOADING

<u>COMPONENT</u>	<u>TYPE</u>	<u>STRESS</u>	<u>LOADING CONDITION</u>
		<u>MAGNITUDE (PSI)</u>	
Inlet Line LH ₂ & LOX	Thermal	320	Steady-State
	Mechanical	2878	Gimbal-15° Pitch
	Mechanical	1600	Gimbal-6° Yaw
LH ₂ /LOX Turbine Inlet	Thermal	7889	Steady-State
	Thermal	-18585	Start Transient
	Mechanical	-1600	Gimbal-15° Pitch
Fuel Turbine Inlet	Thermal	-5309	Steady-State
	Thermal	-23670	Start Transient
	Mechanical	890	Gimbal-15° Pitch
Chamber Coolant Jacket Inlet	Thermal	-2668	Steady-State
	Thermal	-11917	Start Transient
	Mechanical	-2320	Gimbal-15° Pitch
Pump Discharge	Thermal	6124	Steady-State
	Thermal	-12142	Start Transient
	Mechanical	1398	Gimbal-15° Pitch
Oxidizer Injector Inlet	Thermal	-23184	Steady-State
	Thermal	9451	Start Transient
	Mechanical	-1219	Gimbal-15° Pitch
Stiffening Cylinder	Thermal	16299	Steady-State
	Thermal	-5309	Start Transient
	Mechanical	-2340	Thrust
Thrust Chamber	Thermal	-50129	Steady-State
	Thermal	16731	Start Transient
	Mechanical	-5031	Thrust
Chamber Struts	Thermal	-16326	Steady-State
	Thermal	8057	Start Transient
	Mechanical	255	Thrust
Rods	Thermal	21763	Steady-State
	Bending		
	Thermal	-10421	Start Transient
	Mechanical	-177	Thrust

TABLE XXVI
ENGINE SYSTEM STRESS SUMMARY, COMBINED INERTIA LOADING
[2g (x) + 1.5g (y) + 4.2 (z)]
(NOZZLE EXTENSION STOWED)

<u>COMPONENT</u>	<u>JOINT NO.</u>	<u>DIRECT SZ (PSI)</u>	<u>BENDING</u>	
			<u>SZ1 (PSI)</u>	<u>SZ2 (PSI)</u>
Fuel Pump Inlet	13	-28	-274	2,187
LH ₂ /LOX Turbine Inlet	17	27	-2,207	926
Fuel Turbine Inlet Line	22	-39	-1,042	-189
Chamber Coolant Jacket Inlet	63	-254	-3,815	109
LOX Inlet	43	-29	668	-743
Fuel Injector Inlet	49	-27	1,620	87
Oxidizer Injector Inlet	60	122	2,134	2,046
Chamber Struts	70	-337	-468	-874
TCA Stiffening Cylinder	89	60	49	159

III, F, Task VI - Engine Configuration Layout (cont.)

The following recommendations are based on an evaluation of the analysis results:

- ° Further design refinement of the stiffening cylinder is required. To accomplish this, the transient thermal conditions and the thrust start transient loads must be defined and incorporated in the analysis. With this information, a system finite-element model can be used to evaluate the stresses parametrically with the vehicle stiffness. This analysis is a must for obtaining a good design.
- ° An axisymmetric finite-element model of the thrust chamber and nozzle should be accomplished in a future design refinement effort.

3. System Effectiveness and Safety

The purpose of this evaluation was to provide some insight into the inherent reliability and crew safety potential of the OTV point design engine. This section of the report discusses the following subjects:

- ° Quantitative Evaluation
- ° System Failure Modes, Failure Rate Distributions and Mission Effects
- ° Propellant Leakage
- ° Maintenance
- ° Conclusions and Recommendations

III, F, Task VI - Engine Configuration Layout (cont.)

a. Quantitative Evaluation

A rocket engine system, when used in conjunction with a man-rated vehicle, is considered to be "man-rated" if the probability of mission success is "satisfactory" and there is only a remote probability of crew "loss" due to engine-system-induced effects. It is a design philosophy which analyzes the influence of potential single-point failures which could jeopardize the safe return of the crew and/or mission success. Therefore, man-rating is quantified both in terms of engine reliability (R) and crew risk (CR).

Previous OTV man-rating evaluations established acceptable mission reliability and crew risk goals and determined the number of engines required to meet these goals (Ref. 1 and 23).

A "satisfactory" probability of mission success, as traditionally judged by aerospace experience, was established as .99 minimum. A crew risk goal of 2.5×10^{-4} was established by evaluating the "Shuttle Payload Safety Requirement" (NHB 1700.7) and the "Manned Spacecraft Criteria and Standards" (JSC M8080) documents and comparing the high-risk profession of astronauts to other hazardous career mortality rates. The acceptable crew risk value is comparable to that of an airline pilot.

Four engine system configurations were evaluated in these past studies: a single 20K engine, twin 10K engines, three 10K engines, and three 7K engines. A mission duty cycle of 5 burns per mission and quantifiable reliability parameters for catastrophic failure rate, fail-safe rate, and fail operational failure rate were used in the safety/reliability model.

III, F, Task VI - Engine Configuration Layout (cont.)

Table XXVII summarizes the single-engine reliabilities required to meet the mission reliability and safety requirements. As the engine-out capability of an engine system increases, the total system failure rate decreases and the system reliability increases. The inconsistency of the three 7K engine system is due to the disadvantage of having three times the chance of catastrophic failures overriding the partial engine-out capabilities. The three 10K engine system has complete engine-out capability (i.e., one redundant engine).

The Advanced Expander Cycle engine was also evaluated for its capability to meet the crew risk requirement with and without redundant components (internal redundancy) for the various engine systems. Adding redundant igniters, series-redundant shutoff valves, and dual-coil valve actuators decreases the single-engine failure rate by 33%. The results of the analysis are summarized in Figure 54. The figure shows the calculated total mission losses for each engine system as well as those resulting in the loss of the vehicle and crew.

The following conclusions were derived from the figure:

- ° A single-engine installation is impractical for meeting the crew risk requirement.
- ° Internal engine redundancy can significantly reduce crew risk.
- ° The three 7K engine system has no advantages in terms of mission reliability and crew risk because of the increased catastrophic failures.

ABLE XXVII
ENGINE RELIABILITY REQUIREMENTS

NUMBER ENGINES IN SYSTEM	NUMBER OF ENGINES REQUIRED DURING MISSION	SINGLE ENGINE RELIABILITY	SYSTEM RELIABILITY
1 20K	1 ALL BURNS	0.9996	0.9996
2 10K	2 FIRST BURN 1 SUBSEQUENT	0.9993	0.9997
3 10K	2 FIRST BURN 1 SUBSEQUENT	0.9983	0.99975
3 7K	3 FIRST BURN 2 SUBSEQUENT	0.9995	0.99965

ASSUMPTIONS: 5 BURNS PER MISSION
 5% OF THE SINGLE ENGINE λ DUE TO CATASTROPHIC FAILURE
 60% OF THE SINGLE ENGINE λ WILL STRAND CREW
 35% OF THE SINGLE ENGINE λ WILL NOT ENDANGER CREW LIFE

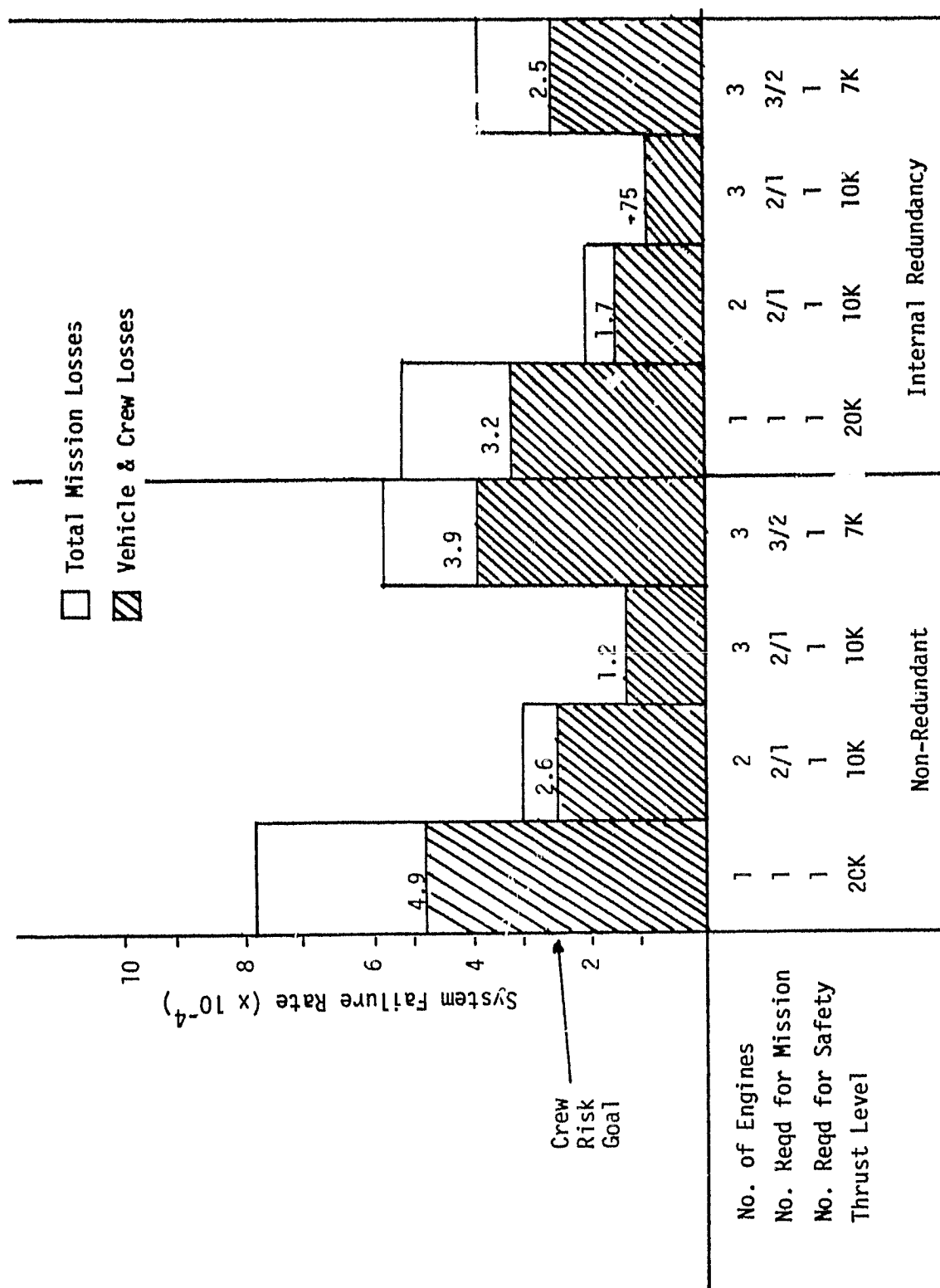


Figure 54. Meeting Crew Risk Requirements

III, F, Task VI - Engine Configuration Layout (cont.)

- ° The three 10K engine installation reduces crew risk because one engine is completely redundant. (The system weight and cost is also significantly increased.)
- ° The twin-engine installation, with component redundancy, meets the crew risk requirement. (This is the best choice when engine system cost and weight are factored into the trades.)

Other conclusions resulting from the studies (Ref. 23) were as follows:

- ° For all multi-engine systems, a single engine must have a proven reliability of at least .998 to meet crew risk requirements.
- ° The engine should carry instrumentation that could detect impending failures and shut down the engine before catastrophic failures can occur.
- ° A crew override should be provided to correct a failure in the hazard control system. If a good engine is shut down, the crew should have the final decision on whether to restart it. The crew should be provided with an option in situations where the risk is judged to be acceptable.

Combining all factors, i.e., internal redundancy, simplicity, hazard control system, crew override, and external redundancy, the high reliability and crew risk goals can be met.

III, F, Task VI - Engine Configuration Layout (cont.)

If these concepts are used in conjunction with effective testing during DDT&E, potential mistakes can be designed out inexpensively on paper rather than during production. An example of reaching higher reliabilities faster is shown in Figure 55. The ALRC philosophy on the OMS-E program concentrated on "making the engine right the first time." A single-engine reliability of .9992 was reached after only 476 tests. In comparison with the Apollo program, OMS-E achieved an order of magnitude advancement in the reliability with the same amount of testing. It is believed that we can do at least this well with the expander cycle OTV engine.

b. System Failure Modes and Effects Analysis

Through evaluation and comparison of the ALRC Point Design OTV Engine concept with historical engine failure data, a "top down" Failure Modes and Effects Analysis was conducted. This analysis shows the overall effect of an engine failure during a typical AMOTV fire-burn LEO-to-GEO-and-return mission. The crew safety and mission reliability analyses that were summarized in the preceding section show that a twin-engine concept is the best choice for meeting the man-rating, mission reliability, and payload requirements. Therefore, this study assumes that "failure" refers to the failure of one engine in this twin-engine installation.

Table XXVIII shows the percent failure rate distribution, the resulting failure rate contributed by a single engine, and the mission phase effects. Low performance accounts for the largest percentage of engine failures, although it is very unlikely to cause mission failure. Failure to start, failure to shut down, catastrophic failures, and failure to extend the nozzle are modes that would most likely jeopardize completion of the mission and could place the crew in danger. Further analysis is required to reveal the single-point failures within these particular failure modes.

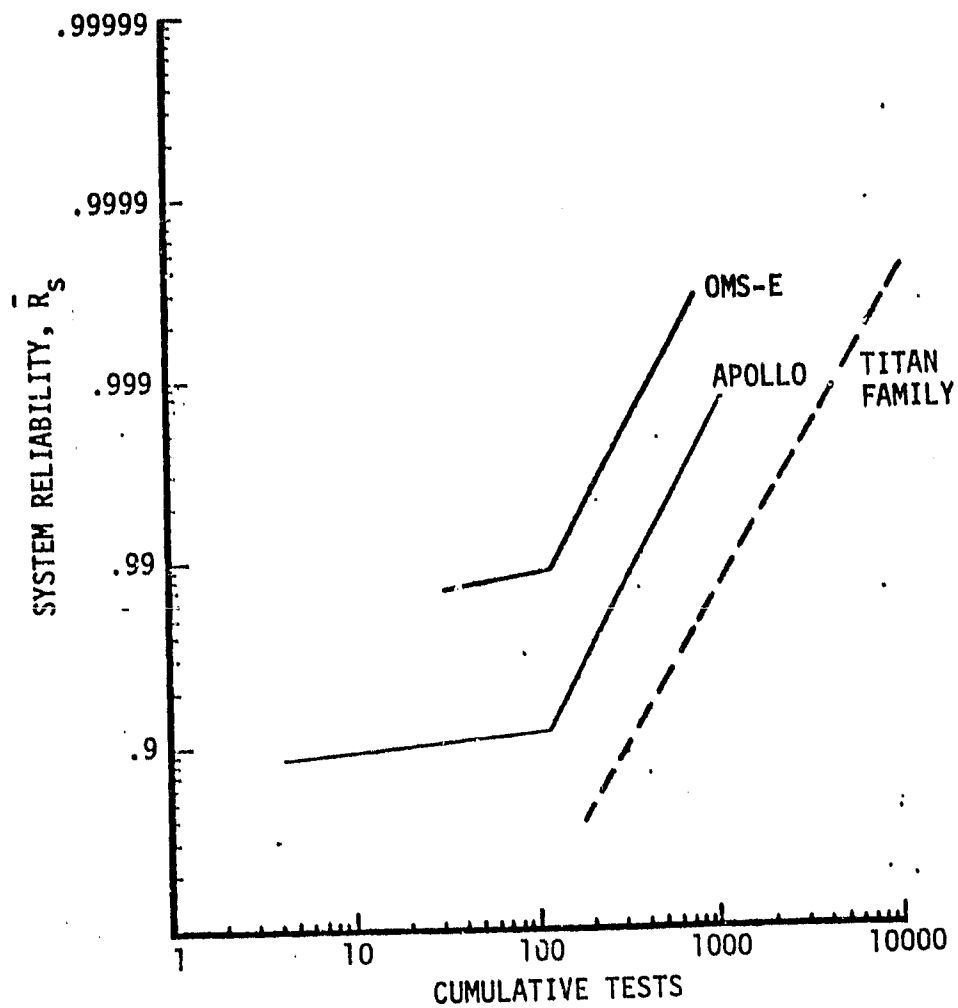


Figure 55. ALRC Engine Reliability History

TABLE XXVIII
FAILURE RATE DISTRIBUTION OF TWIN-ENGINE SYSTEM

Engine Failure Mode	% Failure Rate Distribution	Failure Rate Based on Man-Rating Requirements	Mission Phase Effect
Fails to Start	20%	140 ppm	LEO Departure (2 burns): 1st burn; loss of mission. Fail safe and burn; return to LEO on remaining engine. GEO Departure: complete mission on remaining engine.
Premature Shutdown	20%	140 ppm	LEO Departure: 1st burn; loss of mission, return to LEO. Fail safe 2nd burn; continue mission. GEO Departure: continue mission with remaining engine.
Low Performance	38%	226 ppm	LEO Departure: 1st burn; extend burn or abort mission. 2nd burn; extend burn GEO Departure: extend burn.
Catastrophic	5%	70 ppm	LEO Departure & GEO Departure Loss of mission Loss of vehicle Loss of crew
Fails to shut down	4%	28 ppm	LEO Departure: loss of mission, vehicle and crew stranded. GEO Departure: possible loss of mission and stranded crew.
Loss of Gimballing	4%	28 ppm	LEO Departure: shut down problem engine; use remaining to return to LEO or complete mission. GEO Departure: shut down problem engine; use remaining engine to return to LEO or complete mission.
High/Low Tank Pressure	1%	7 ppm	Within specified limits, the engine controller will compensate.
Fail Extension of Nozzle	4%	28 ppm	Deployment to LEO: Loss of mission; fail safe, EVA.
Fail Retraction of Nozzle	4%	28 ppm	Rendezvous and Capture: EVA required.

LEO Departure = Orbit Transfer Injection Burn and GEO Insertion Burn

GEO Departure = LEO Transfer Burn, Phasing Orbit Trim Burn and Shuttle Rendezvous Burn

III, F, Task VI - Engine Configuration Layout (cont.)

c. Propellant Leakage

Propellant leakage is usually divided into two categories: (1) "gross" leakage resulting from structural failures such as ruptures of bellows, lines, housings, manifolds, weld cracks, flange deformations, and fractured flange bolts and (2) "minor" leakage due to flange deflections, bolt torque relaxation, seal physical property degradation, seal installation damage, and damaged flange surfaces.

Because all propellant ducting components will be designed, stress-analyzed, and tested to withstand maximum expected engine operating pressures and loads with safety factors applied, it is reasonable to conclude that gross structural failures will not occur unless components are subjected to an overstress condition resulting from a failure of another part of the propulsion system.

Excluding leakage resulting from gross structural failures, the remaining task is to assess the effect of "minor" leakage at joints for the failure mechanisms denoted in the first paragraph. Considering the closed loop control afforded by the engine controller and the rigorous pre-flight leak checks conducted to detect any out-of-specification leakage, it is judged that engine performance will not be degraded below mission acceptable values by this degree of leakage. Similarly, the extent of damage to engine components caused by loss of coolant from external leakage is not considered sufficient to degrade engine performance for a specific mission though it may reduce component life.

The only other effect which must be considered is the possible safety hazard resulting from a fire and/or explosion hazard resulting from propellant external leakage. Our current conclusion is that elimination of fire and/or explosion hazards can be assured both on the ground and

III, F, Task VI - Engine Configuration Layout (cont.)

throughout the flight regime with design goal leakage rates. Based on the assumption that an inflight purge will not be required prior to or following engine operation because of the aspirating effect of space vacuum on the system, the only special precautions which should be taken are the following ones:

- ° Purge the engine system on the ground prior to engine test or prior to flight to remove any moisture or condensible gases.
- ° Purge the engine system of propellants following engine ground test or flight.
- ° Eliminate, if possible, ignition sources having energies equal to or greater than the minimum propellant ignition energies.

If it is determined later that an inflight purge is necessary, the ground purge valves, combined with some additional volume in the pneumatic supply system, could be used to satisfy the requirement.

Leakage into the Orbiter's payload bay is inhibited by the series-redundant main propellant shutoff valves. These valves, in conjunction with the vehicle pre-valves, satisfy the Space Transportation System (STS) environmental and safety criteria as stated in "The Safety Policy and Requirements for Payloads Using the Space Transportation System" (Ref. 24):

III, F, Task VI - Engine Configuration Layout (cont.)

"The premature firing of a liquid propellant propulsion system is a catastrophic hazard. Each propellant delivery system must contain three mechanically independent propellant flow control devices in series that remain closed during all ground and flight phases (except ground servicing) until the deployed payload has reached a safe distance from the Orbiter."

d. Engine Maintenance

The primary objective of the OTV engine maintenance concept is to maximize mission reliability and crew safety while minimizing the cost of meeting the OTV's operational requirements. To meet this objective, ALRC's maintenance concept emphasizes controlled preventive maintenance with short turnaround times and minimum life-cycle costs.

To implement such a program, it is necessary to provide adequate on-board information on engine performance and to follow specific guidelines. Correct engine operation must be confirmed by a performance monitor, and diagnostic data must be provided whenever either a malfunction or a discrepancy occurs.

In simple terms, a malfunction is defined as a hardware failure resulting in an actual mission loss; a discrepancy, on the other hand, is defined as a "specification" failure whose actual mission effect is unknown.

The diagnostic information supplied must be timely so that engine/component restoration can be safely accomplished within specified time constraints, yet it must not unbalance the OTV or flight and/or ground crews with superfluous weight or time-consuming activities. The engine

III, F, Task VI - Engine Configuration Layout (cont.)

on-board information system must utilize a logical process that will save weight, time and money without impairing the probability of mission success or crew survival.

According to an Aerospace Industries Association study, 20% of any vehicle subsystems will account for 80% of the total vehicle maintenance cost. Propulsion systems such as the OTV engine are in this 20% "high cost burner" bracket. In recognition of this fact, ALRC's approach to achieving optimum OTV engine reusability and a low operating cost has been to make maintenance a key parameter of engine system design.

ALRC recognizes that if short turnaround times are to be an OTV engine requirement, then maintenance and safety will require special accommodation in the basic engine design to allow for rapid assessment of engine condition in all respects and easy correction of deficiencies.

A logical way for implementing maintenance as a key parameter in engine design is to use component "failure rates", "failure indications," and "failure mode" data. By using these data, the expected maintenance action is identified specifically.

While the OTV engine design and maintenance concept is not fully developed at this time, it is apparent that some of the problems associated with the engine can be identified now. These basic problems are summarized as follows:

(1) Engine Durability

Since the OTV engine will be subjected to many cycles of high thermal and/or mechanical stresses during its service life, the question of fatigue and wear threat is a serious issue. The engine components

III, F, Task VI - Engine Configuration Layout (cont.)

have been designed to meet a service life between overhaul requirement of 300 start and shutdown cycles and 10 hours of accumulated run time. Design criteria are based upon available data. However, the limited service experience with reusable hydrogen/oxygen engines requires a heavy reliance on thorough inspection by nondestructive testing techniques. Engine and component designs must incorporate features of accessibility which make such inspections a relatively easy matter. Accessibility was considered in the preparation of the preliminary engine layout, and provisions for component inspections must be incorporated in the detailed design phases.

(2) Turbopump Bearings

The bearings of the propellant turbopumps and more particularly, those of the hydrogen pumps are vulnerable to failure within their extended service life. A major disassembly effort would be required to permit periodic visual inspection of these bearings. Therefore, it appears that a heavy reliance must be placed on acoustical methods for assessing bearing health.

Disassembly of the pumps can be awkward and time-consuming. Therefore, pump repair will probably entail removal and replacement of the entire engine in the early operational phases. When component data has been accumulated, consideration can then be given to making the pumps Line Replaceable Units (LRU). Replacement of the engine (or pumps) can be based upon the application of acoustic diagnostic techniques. It is then mandatory that the turbopumps be designed to accommodate acoustic pickups which can be attached to the pump housings adjacent to the bearings to assess actual bearing conditions resulting from cumulative mission operations.

III, F, Task VI - Engine Configuration Layout (cont.)

(3) Turbine Life

The expander cycle engine turbines operate in warm hydrogen gas which is a relatively benign environment. However, turbine life will be limited by blade life which, in turn, is limited by stress rupture through long-life mission application of tensile loads, and by low-cycle thermal fatigue.

Inspection of the turbine at frequent intervals should be practiced, particularly during the first few missions. For this reason, it is essential that a nondestructive testing technique providing an estimate of the remaining blade life be implemented. It is absolutely essential that this nondestructive testing technique be identified early in the next design phase of this program and that the pump be designed to accommodate the device to be used.

e. Conclusions and Recommendations

The following conclusions and recommendations are made on the basis of the safety and reliability analyses and a review of the engine and component designs.

(1) Maximum mission reliability and crew safety with minimum cost can be achieved by selected engine component redundancy combined with a twin-engine configuration.

(2) Man-rating requires a thorough hazard analysis followed by engine design changes to eliminate the hazards or provide protection, or escape in an emergency. In some cases, the presence of man may increase safety by providing for manual override, repair or corrective action. Extra-vehicular activity (EVA) may be a last resort, but it should still be factored into future design iterations.

III, F, Task VI - Engine Configuration Layout (cont.)

(3) A Component Failure Mode and Effects Analysis (FMEA) should be undertaken in the next design phase.

(4) The current purge subsystem concept uses check valves which are located at the interface between the purge system and the engine system. Replacement of the check valves with solenoid valves would improve redundancy verification. If a purge system is required for flight, solenoid valves would improve failure detection and engine controller corrective action in the event of a valve failure.

(5) The TPA "shrapnel barrier" is used to preclude a single TPA internal structural failure from causing a failure of both pumps and engines. Consideration should be given to designing the TPA housings so that they can withstand and contain the "Shrapnel Effects" of an internal structural failure. Materials able to absorb the explosive effects should be considered for the pump housings.

(6) The oxidizer pump impeller clearances must be sized to preclude rubbing during all modes of operation and to permit passage of contamination to minimize the probability of explosions due to rubbing.

(7) The effectiveness of using TPA shaft displacement sensors (for real-time engine controller action or for between-flight maintenance actions) to detect incipient oxidizer pump rubbing as the cause of a potential catastrophic failure should be evaluated.

III, F, Task VI - Engine Configuration Layout (cont.)

(8) The nozzle extension, deployment, and retraction mechanism is a critical mission subsystem even though its failure would not directly jeopardize the crew. While a hand crank is included in the design, a "jamming" mechanism of failure in the current design will negate the hand crank mechanical redundancy option. The nozzle then has to be removed in orbit. It is mandatory that this subsystem be designed by considering all possible mechanisms of failure and to provide sufficient redundancy to minimize single-failure points, recognize the constraints of EVA, and minimize crew risk by reducing the possibilities of EVA.

G. TASK VII - ENGINE DATA SUMMARY

The primary objective of this task was to prepare a document which summarized the engine performance, weight, envelope, and service life data and presented the engine and component layout drawings. This document was submitted as a Task VII, Engine Data Summary, report for this contract (Ref. 4).

The component and engine designs were presented in Sections III,C and III,F, respectively. The baseline engine data is presented in this section.

1. Engine Operating Characteristics

Based upon the results of design analyses, engine sensitivities, cycle optimization, and thrust chamber geometry optimization conducted in conjunction with both this Point Design Study and the OTV Phase A Engine Study, an engine with the characteristics summarized in Table XXIX was selected as a representative 1980 technology baseline. The data is presented for both nominal mixture ratio (6.0) and off-design mixture ratio (7.0) operation. The engine length with the extendible nozzle in the stowed

TABLE XXIX
ADVANCED EXPANDER CYCLE ENGINE OPERATING SPECIFICATION
SERIES TURBINE DRIVE CYCLE

Sheet 1 of 4

Rated Vacuum Thrust = 15,000 lb
Stowed Length = 60 in.

	<u>Engine Mixture Ratio</u>	
	<u>6.0</u>	<u>7.0</u>
<u>Engine</u>		
Vacuum Thrust, lb	15,000	15,000
Vacuum Specific Impulse, sec.	475.4	471.0
Total Flowrate, lb/sec	31.56	31.85
Mixture Ratio	6.0	7.0
Oxygen Flowrate, lb/sec	27.05	27.87
Hydrogen Flowrate, lb/sec	4.51	3.98
<u>Thrust Chamber</u>		
Vacuum Thrust, lb	15,000	15,000
Vacuum Specific Impulse, sec	475.4	471.0
Chamber Pressure, psia	1,200	1,162
Nozzle Area Ratio	435	435
Mixture Ratio	6.0	7.0
Throat Diameter, in.	2.79	2.79
Chamber Diameter, in.	5.34	5.34
Chamber Length, in.	18.0	18.0
Chamber Contraction Ratio	3.66	3.66
Nozzle Exit Diameter, in.	58.2	58.2
Percent Bell Nozzle Length	81.8	81.8
Nozzle Length, in.	84.4	84.4
Combustion Chamber Coolant Flowrate, lb/sec	3.834	3.383
Slotted Copper Chamber Area Ratio	10.6	10.6
Chamber Pressure Drop, psia	92	76
Coolant Inlet Temperature, °R	90	90
Chamber Coolant Temperature Rise, °R	411	431
Fixed Tube Bundle Nozzle Flowrate, lb/sec	0.677	0.597
Tube Bundle Nozzle Area Ratio	172	172
Tube Bundle Coolant Pressure Drop, psia	10	8
Tube Bundle Coolant Temperature Rise, °R	640	672

TABLE XXIX (cont.)

Sheet 2 of 4

	ENGINE MIXTURE RATIO		ENGINE MIXTURE RATIO	
	6.0		7.0	
	LOX	LH ₂	LOX	LH ₂
<u>Boost Pumps</u>				
Inlet Flow, GPM	171	456	175	401
Inlet Pressure, psia	16	18.5	16	18.5
Vapor Pressure, psia	15.2	18	15.2	18
Inlet Temperature, °R	167.2	37.8	162.7	37.8
NPSH, ft (not including TSH)	2	15	2	15
Discharge Pressure, psia	57	50	57	50
Head Rise, ft	82.3	1026	82.3	1026
Speed, RPM	7400	29650	7400	29650
Suction Specific Speed, (RPM)(GPM) ^{1/2} /ft ^{3/4}	25560	43080	25860	40400
Specific Speed, (RPM)(GPM) ^{1/2} /ft ^{3/4}	3540	3500	3580	3275
Efficiency, %	66	73	66	77
<u>Boost Pump hydraulic Turbines</u>				
Flow (GPM)	16.7	129	17.3	116
Efficiency, %	52	66	52	66
Horsepower	6.1	10.7	6.3	9.6

TABLE XXIX (cont.)

Sheet 3 of 4

	ENGINE MIXTURE RATIO		ENGINE MIXTURE RATIO	
	6.0		7.0	
	LOX	LH ₂	LOX	LH ₂
<u>Main Pumps</u>				
<u>Inducer</u>				
Flow, GPM	194	547	199	481
Head Rise, ft	460	5080	450	4645
Efficiency, %	75	82	75	81
Horsepower	34	64.2	34	49.4
Inlet Pressure, psia	48	49	48	49
NPSH, ft	66	997	66	997
Suction Specific Speed, (RPM)(GPM) ^{1/2} /ft ^{3/4}	20880	11860	21000	11100
Specific Speed, (RPM)(GPM) ^{1/2} /ft ^{3/4}	4870	3500	4980	3500
<u>Stage 1</u>				
Flow, GPM	223	572	229	503
Head Rise, ft	2450	26870	2410	24640
Efficiency, %	71	71	71	70
Horsepower	219	386	221	317
Specific Speed, (RPM)(GPM) ^{1/2} /ft ^{3/4}	1490	1025	1520	1024
<u>Stages 2 & 3</u>				
Flow, GPM	---	478	---	421
Head Rise, ft	---	23840	---	21940
Efficiency, %	---	71	---	70
Horsepower	---	286	---	236
Specific Speed, (RPM)(GPM) ^{1/2} /ft ^{3/4}	---	1025	---	1022

TABLE XXIX (cont.)

Sheet 4 of 4

	ENGINE MIXTURE RATIO		ENGINE MIXTURE RATIO	
	6.0		7.0	
	LOX	LH ₂	LOX	LH ₂
<u>Overall</u>				
Head Rise, ft	2910	79630	2860	73165
Efficiency, %	61.5	63.3	61.5	62.3
Horsepower	253	1030	255	838
Speed, RPM	34720	90000	34470	89800
<u>Main Pump Turbines</u>				
Inlet Pressure, psia	1512	2344	1469	2176
Inlet Temperature, °R	489	535	514.6	557
Flowrate lb/sec	4.22	4.22	3.71	3.71
Gas Properties				
Cp, Specific Heat at Constant				
Pressure, BTU/lb-°R	3.652	3.652	3.652	3.652
γ, Ratio of Specific Heats	1.395	1.395	1.395	1.395
Shaft Horsepower	253	1030	255	838
Pressure Ratio (Total to				
Static)	1.14	1.540	1.153	1.471
Static Exit Pressure, psia	1326	1522	1274	1479
Static Exit Temperature, R°	471.6	473.5	494.3	499.3
Efficiency, %	66.7	76.8	65.7	75.8
Turbine Bypass Flowrate lb/sec	0.27	0.27	0.24	0.24

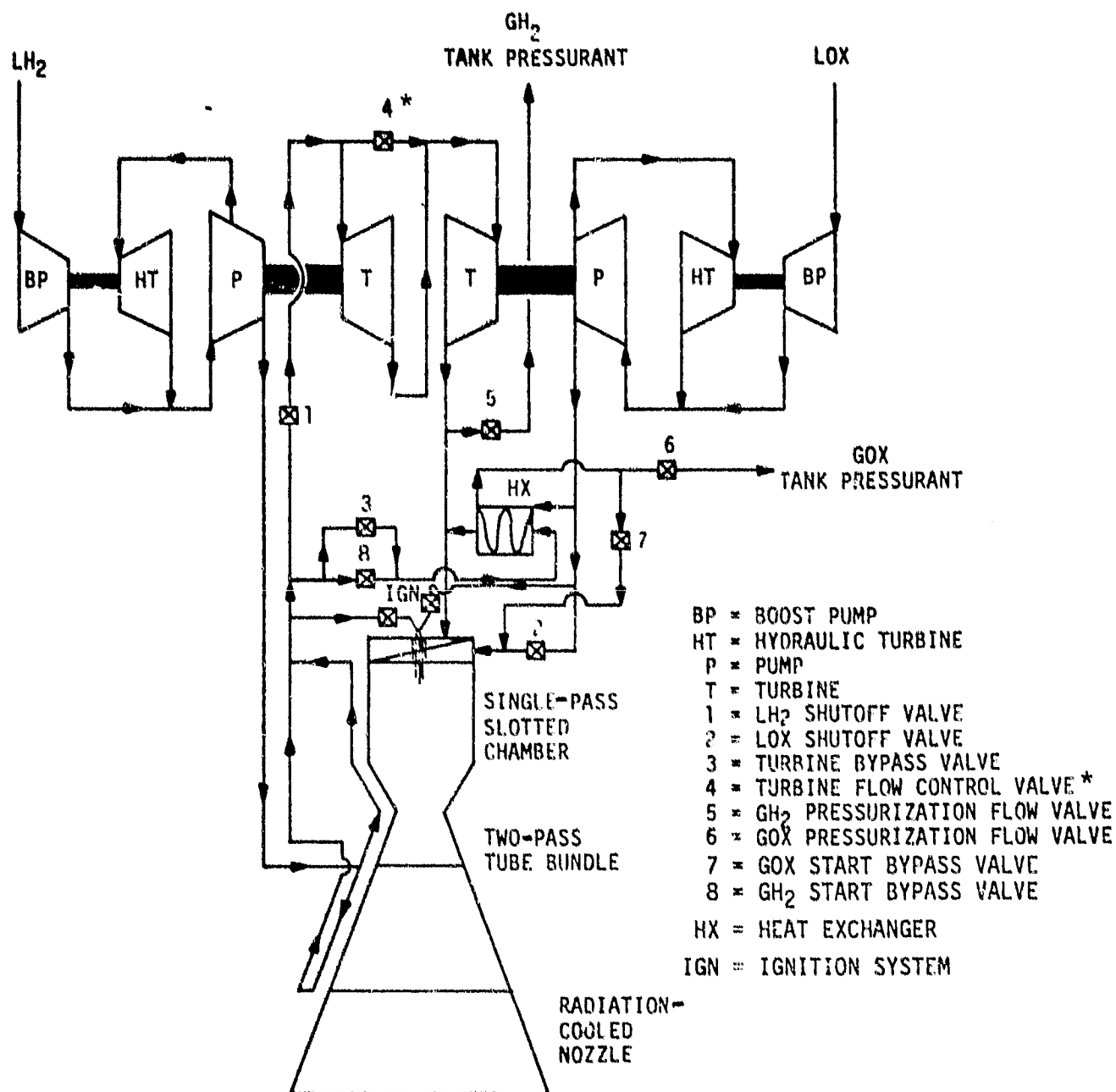
III, G, Task VII - Engine Data Summary (cont.)

position is 60 inches. With the extendible nozzle deployed, the engine length is 109.6 inches. The chamber pressure of 1200 psia was selected on the basis of cycle optimization and trade-off studies which evaluated specific impulse and weight changes with chamber pressure. Further optimization and tradeoffs are planned in future work, and some changes in operating chamber pressure and performance are anticipated.

The O_2/H_2 expander cycle engine uses a series turbine drive cycle which is shown on Figure 56. The engine uses hydraulically driven boost pumps, with the flow tapped off the main pump stages. Fuel flows from the pump discharge to the thrust chamber where 85% of the hydrogen flow is used to cool the slotted copper chamber in a single pass from an area ratio of 10.6:1 to the injector head end. Fifteen (15) percent of the hydrogen is used to cool the tube bundle nozzle in two passes from an area ratio of 10.6:1 to the end of the fixed nozzle ($r = 172:1$) and return. The coolant flows are merged, and 6% of the total engine hydrogen flow is used to bypass both turbines to provide cycle power balance margin and thrust control. The remaining hydrogen flow first drives the fuel pump turbine and then drives the oxidizer pump turbine. After driving the oxidizer pump turbine, a small amount of heated hydrogen is tapped off for hydrogen tank pressurization. The remaining hydrogen flow is then injected into the combustion chamber.

At rated thrust operation, oxidizer flows from the main pump discharge directly to the thrust chamber and is injected in a liquid state. A small amount of oxidizer is tapped off and heated by the hydrogen turbine bypass flowrate in a heat exchanger to provide LOX tank pressurization.

The engine is also capable of operating in a tank head idle mode and is adaptable to extended low-thrust operation at a thrust level of 1.5K lb.



*TO BE RELOCATED TO BYPASS THE OXYGEN PUMP TURBINE

Figure 56. Baseline Advanced Expander Cycle Engine Flow Schematic

III, G, Task VII - Engine Data Summary (cont.)

The purpose of the tank head idle mode is to thermally condition the engine without non-propulsive dumping of propellants. This is a pressure-fed mode of operation at a thrust level of approximately 50 lb and a vacuum specific impulse estimated to be 400 sec. During this mode of operation, the main fuel and oxygen valves (numbers 1 and 2 on the schematic) are closed. All of the fuel bypasses the turbines through valve number 8 so that the pumps are not rotating. The heat exchanger in the turbine bypass line gasifies the oxygen which then flows through valve number 7 to the chamber. Tank pressurization is not supplied during this operating mode, and valves 5 and 6 remain closed. The pressurization valves are opened as the engine is brought up to steady-state, full-thrust operation.

The OTV point design engine is adaptable to operation at 10% of rated thrust (i.e., 1.5K lbf) with minor modifications. This low-thrust operating point is a dedicated condition, and the engine is not required to operate at both the 15K and 1.5K thrust levels on the same mission. To operate at low thrust, the oxidizer injection elements must be changed to one of smaller size, and an orifice must be installed in the line downstream of the chamber coolant jacket.

The engine pressure schedule at rated thrust operation is shown on Table XXX for both the nominal and off-design mixture ratio conditions.

TABLE XXX
ADVANCED EXPANDER CYCLE ENGINE PRESSURE SCHEDULE
SERIES TURBINES DRIVE CYCLE
F = 15,000 lb

Pressure, psia (1)	ENGINE MIXTURE RATIO		ENGINE MIXTURE RATIO	
	6.0		7.0	
	LOX	LH ₂	LOX	LH ₂
Boost Pump Inlet	16	18.5	16	18.5
Boost Pump Discharge	56	50	56	50
Main Pump Inlet	48	49	48	49
Main Pump Discharge	1487	2531	1463	2328
ΔP Line	25	10	26	8
Main Shutoff Valve Inlet	1462	2521	1437	2320
ΔP Shutoff Valve	15	25	16	19
Shutoff Valve Outlet	1447	2496	1421	2301
ΔP Line	15	30	16	23
Coolant Jacket Inlet	---	2466	---	2278
ΔP Chamber Coolant Jacket	---	92	---	76
Coolant Jacket Outlet	---	2374	---	2202
ΔP Line	---	30	---	26
Fuel Turbine Inlet	---	2344	---	2176
Fuel Turbine Pressure Ratio (Total/Static)	---	1.540	---	1.471
Fuel Turbine Static Exit	---	1522	---	1479
Fuel Turbine Total Exit	---	1560	---	1516
ΔP Warm Gas Duct	---	48	---	47
OX Turbine Inlet	---	1512	---	1469
OX Turbine Pressure Ratio (Total/Static)	---	1.14	---	1.153
OX Turbine Static Exit	---	1326	---	1274
OX Turbine Total Exit	---	1360	---	1307
ΔP Warm Gas Duct	---	34	---	33
Injector Inlet	1434	1326	1405	1274
ΔP Injector	215	109	227	96
Injector Face	1217	1217	1178	1178
Chamber	1200	1200	1162	1162

(1) All pressures are total pressure except where noted.

III, G, Task VII - Engine Data Summary (cont.)

2. Engine Performance

Engine system delivered specific impulse for design and off-design operation is presented in Tables XXXI and XXXII, respectively. Table XXXII also shows the various performance efficiencies associated with design operation of the Advanced Expander Cycle Engine. These efficiencies have been calculated by using simplified techniques and were verified by the JANNAF rigorous performance prediction methodology (Ref. 10). In addition, the experimental RL-10 and ASE performance data were analyzed and correlated by using both the rigorous and simplified JANNAF performance methodologies. The rigorous method used both the Two-Dimensional Kinetic (TDK) with enthalpy addition and the BLIMP (Cebeci-Smith) boundary layer solution. The simplified model used ODK (One-Dimensional Kinetic) at propellant tank enthalpy with TBL-Chart/adiabatic wall conditions. While there were significant differences between the I_{spTDK} and the boundary layer performance losses (ΔI_{spBL}) between the two approaches, there was only 0.6 sec difference in the predicted specific impulse between the simplified and the TDK/BLIMP (Cebeci-Smith) results over a wide range of propellant mixture ratios, chamber pressures, area ratios, and wall temperature to total temperature ratios. Also, either approach predicted overall specific impulses which were within approximately 3.0% of the experimental value. A discussion of the performance and loss calculations follows.

As discussed in Section III,A, a modified simplified JANNAF performance procedure was used to calculate the performance of the engine at all of its operating points.

a. One-Dimensional Equilibrium (ODE) Performance

The first step is to determine the ODE performance at various operating conditions. This is accomplished by inputting the reactant

TABLE XXXI
ADVANCED EXPANDER CYCLE ENGINE BASELINE PERFORMANCE

1. Thrust (1bF)	15000.00
2. Chamber Pressure (psia)	1200.00
3. Mixture Ratio	6.00
4. Total Flowrate (lbm/sec)	31.56
5. LOX Flowrate (lbm/sec)	27.05
6. Fuel Flowrate (lbm/sec)	4.51
7. I_{sp} ODE (seconds)	486.11
8. Nozzle Efficiency	.9929
9. Energy Release Efficiency	1.0000
10. Kinetic Efficiency	.9957
11. Boundary Layer Loss (lb)	164.16
12. I_{sp} Delivered (seconds)	475.4

Note: Based upon Modified Simplified JANNAF procedures using Tank Propellant Conditions.

TABLE XXXII
 ADVANCED EXPANDER CYCLE ENGINE
 PERFORMANCE AT DESIGN AND
 OFF-DESIGN O/F
 RATED AND LOW-THRUST OPERATION

THRUST, LB	ENGINE MIXTURE RATIO	THRUST CHAMBER PRESSURE, PSIA	ENGINE DELIVERED VACUUM SPECIFIC IMPULSE, SEC.	FLOWRATES, LB/SEC	
				Fuel	O ₂
15000	6.0	1200	475.4	4.51	27.05
15000	6.5	1180	474.9	4.21	27.37
15000	7.0	1162	471.0	3.98	27.87
1500	6.0	125	459.7	.466	2.80
1500	7.0	121	451.7	.415	2.91

Note: Injector elements are modified for the low-thrust condition.

III, G, Task VII - Engine Data Summary (cont.)

propellant enthalpies and specifying the operating conditions of P_c , O/F , and nozzle expansion ratio. Two computer programs are currently available to determine ODE performance. They are described in References 25 and 26, respectively. Reference 26 (TRAN 72) was utilized because TRAN 72 also provides thermal transport properties which are used in the thermal analysis. These performance data are installed as tables in the engine model.

b. Kinetic Loss

The kinetic loss (KL) consists of the difference between the ODE and ODK I_{sp} 's. The ODK I_{sp} is calculated from Reference 25. Kinetic loss is a function of chamber pressure and nozzle expansion ratio for given engine thrust and engine mixture ratio. Kinetic loss progressively increases at higher nozzle expansion ratios, resulting in somewhat less gain in I_{spODK} with ϵ than predicted for I_{spODE} . Kinetic loss diminishes at higher P_c and more nearly approaches equilibrium performance. One-dimensional kinetic specific impulse data are also installed as tables in the engine model.

c. Nozzle Divergence Efficiencies

The nozzle divergence performance loss is closely approximated with the simplified technique, either by using the TDK-Ideal Gas option in Reference 25 or from such previously correlated graphical solutions as are available from Reference 27. Graphical techniques are sufficiently accurate and were used in the engine performance evaluations.

d. Nozzle Boundary Layer Loss

The boundary layer loss (BLL) is adequately approximated by using the TBL-Chart method described in Appendix B of CPIA No. 178 (Ref.

III, G, Task VII - Engine Data Summary (cont.)

27). This methodology has repeatedly proven its validity on engine development programs at ALRC. The BLL is affected most importantly by the operating chamber pressure and wall temperature, nozzle exit area ratio and contour, and combustion gas transport properties.

e. Injector Energy Release Efficiency (ERE)

The Energy Release Loss (ERL) accounts for injector-related performance inefficiencies due to incomplete propellant vaporization and/or non-uniform gas-phase mixing. Performance analysis conducted for the Phase A studies showed that a chamber length of approximately 11 in. would be adequate to achieve an ERE goal of 99.5%. Therefore an ERE closer to 100% can be expected with the 18 in. design chamber length.

f. Enthalpy Pumping Effects

Heat loss (or addition) efficiency accounts for the performance effect of heat that is either transferred to the combustion chamber/nozzle or injector upstream of the boundary layer attachment point or added from "free" outside sources of energy. It also accounts for heat being transferred from the boundary layer to the regenerative coolant and subsequently being added back into the combustion chamber in the form of higher propellant enthalpy. In regeneratively cooled engines, the gain in overall specific impulse due to higher propellant enthalpy resulting from heat addition to the regenerative coolant slightly exceeds the thermal BLL contribution due to heat extraction from the boundary layer. This leaves a small (< 1% Isp) net gain for a regeneratively cooled engine as opposed to an engine with an adiabatic wall. This increase is known as the "enthalpy pumping effect."

III, G, Task VII - Engine Data Summary (cont.)

Enthalpy pumping is more significant in low P_c (low ϵ) engines where the gas temperature increase due to higher propellant enthalpy has a noticeable effect upon combustion gas sonic velocity, resulting in higher exhaust velocity in regeneratively cooled engines than in an adiabatic system. For very large pressure ratios (high expansion ratio), this gain is diminished because the regenerative-to-adiabatic exhaust velocity ratio approaches unity. Sample calculations show that the enthalpy pumping gain in performance is reduced from +0.14% Isp to +0.03% Isp as nozzle area ratio is increased from $\epsilon = 10$ to $\epsilon = 1000$. When a large amount of heat is transferred, such that the combustion gas temperature is significantly changed (>5%), then a secondary impact resulting in higher kinetic losses due to increased thermal dissociation becomes important. This diminishes the enthalpy pumping gain even further.

Consequently, performance analysis of a regeneratively cooled engine is simplified by calculating the ODE and ODK Isp for propellants at tank enthalpy conditions (thus neglecting the heat transfer to the propellant in the regenerative circuit) and the boundary layer loss for an adiabatic wall (i.e., zero heat transfer) condition. In this manner, the same energy balance as in the regeneratively cooled case is achieved, but with the difference that the need to calculate the heat transfer and its corresponding effect on the boundary layer loss and ODE/ODK Isp is eliminated.

To further check this assertion, the experimental RL-10 and ASE performance data were analyzed and correlated by using both the rigorous and simplified JANNAF performance methodologies. The rigorous method used both the Two-Dimensional Kinetic (TDK) with enthalpy addition and the BLIMP (Cebeci-Smith) boundary layer solution. The simplified model used ODK at propellant tank enthalpy with TBL-Chart/adiabatic wall conditions.

III, G, Task VII - Engine Data Summary (cont.)

Table XXXIII presents a comparison of the simplified model results with those of both the standard rigorous procedure and the experimental data for an Advanced Space Engine (ASE) configuration as reported in References 28 and 29. It should be noted that while there are significant differences between the I_{spTDK} and the boundary layer performance losses (ΔI_{spBL}) between the two approaches there is only a 0.6 sec difference in the predicted specific impulse, with this difference probably being the result of a small performance loss due to heat transfer to the uncooled nozzle skirt ($c = 175$ to 400) which was included in the standard procedure but not in the tank/adiabatic procedure. Also, either procedure is within approximately 0.3% of the experimental value.

The calibrated ALRC simplified performance model using the shortcut tank/adiabatic method was also used to calculate the performance of both the ASE and RL-10 Derivative II baseline engine as a final check of its prediction capabilities. The results are shown in Table XXXIV. Also included in Table XXXIV is a similar prediction of the attainable specific impulse for the ALRC OTV Point Design Engine whose design characteristics in terms of propellants, thrust chamber pressure, and mixture ratio are bracketed by these existing engines. As shown, the simplified model provided calculated specific impulse values within 0.3% of the reported experimental values for both H_2/O_2 engine systems. The same model predicts an attainable specific impulse of approximately 477 sec for the ALRC OTV Point Design Engine at nominal operating conditions and an area ratio of 473:1.

TABLE XXXIII
COMPARISON OF THE STANDARD AND "SHORTCUT" PROCEDURE FOR
CALCULATING THE PERFORMANCE OF THE REGENERATIVELY COOLED ASE

Modeling Approach	Standard	Tank/Adiabatic
Configuration Area Ratio	400	400
Chamber Pressure (psia)	2287	2287
Mixture Ratio (O/F)	6.378	6.378
Equivalent Tank Enthalpy (Cal/Mole)		
O_2	-2948	-2948
H_2	-1977	-1977
Turbulent Model	Cebeci-Smith	Cebeci-Smith
ΣQ BLIMP (Btu/sec)	7580	0
Δh to H_2 (Cal/Mole)	1325	0
H_o for H_2 to TDK (Cal/Mole)	-652.3	-1977
I_{sp} TDK (sec)	488.5	481.4
ΔF_{BL} BLIMP (lbf)	574.2	202.5
$\Delta I_{sp_{BL}}$ (sec)	12.1	4.4
$I_{sp_{Predicted}}$ (sec)	476.4	477.0
$I_{sp_{Experimental}}$ (sec)	477.9	477.9
$[I_{sp_{Pred}} - I_{sp_{Exp}}]$ (sec)	-1.5	-0.9

TABLE XXXIV
COMPARISON OF SIMPLIFIED MODEL PREDICTIONS TO
EXPERIMENTAL SPECIFIC IMPULSE FOR H₂/O₂ ENGINE SYSTEMS

Engine System	ASE	RL-10	OTV
Thrust Level (lbF)	22K	15K	15K
Chamber Pressure (psia)	2287	400	1200
Mixture Ratio (O/F)	6.378	6.4	6.0
Area Ratio (A_E/A_T)	405	263	473
Chamber Enthalpy (Btu/lbm)	-382.7	-411.5	-411.5
$I_{sp_{ODE}}$	485.2	479.3	487.0
η_K	.9975	.990	.9955
η_{TD}	.9944	.988	.9946
η_{ERE}	1.000	.9941*	1.000
η_{HL}	1.000	1.000	1.000
ΔF_{BL}	215	262	165
$I_{sp_{Predicted}}$ (sec)	476.8	457.8	476.9
$I_{sp_{Experimental}}$ (sec)	477.9	459.2*	TBD

*Reported in "Design Study of RL-10 Derivatives," Final Report P&W FR-6011,
Contract NAS 8-28989, 15 December 1973.

III, G, Task VII - Engine Data Summary (cont.)

3. Engine Life

The engine has been designed for 1200 thermal cycles and 10 hours of accumulated run time. Therefore, all of the component designs (illustrated in Section III,C) are based on the minimum service life requirement (300 cycles or 10 hours) with a safety factor of 4 applied to lower-bound data. The structural analyses conducted in support of the life prediction shows a predicted chamber life of 350 cycles (see Section III,B,3).

This service life is not predicted to be reduced when the engine is operated at mixture ratios between 6.0 and 7.0. Similarly, low-thrust operation (i.e., 1500 lbf) at mixture ratios between 6.0 and 7.0 is not predicted to reduce this service life and may in fact, be better. Cooling the chamber and tube bundle nozzle was an area of concern, especially for low-thrust operation of the engine, but thermal analysis has shown that both of these components can be designed to meet the service life requirement at both thrust levels without compromising the basic engine.

4. Engine System and Component Weights

The Advanced Expander Cycle Engine weight breakdown is shown in Table XXXV. This table shows both "estimated" and "calculated" component weights. Estimated weights are based on known component weights from existing engines and estimated component weights from "study" engines, with appropriate weight scaling relationships applied to both sets of data. Calculated component weights are based upon the component weight as derived from the component layout preliminary design drawing. Thus, calculated component weights are considered more realistic. A calculated weight for the engine controller is unavailable because a preliminary design has not been completed. In this case, the estimated engine controller weight was used in determining the total engine system weight.

TABLE XXXV
ADVANCED EXPANDER CYCLE ENGINE WEIGHT DATA

<u>COMPONENT</u>	<u>INITIAL ESTIMATED WEIGHT, LB</u>	<u>CURRENT WEIGHT, LB</u>	<u>WEIGHT BASIS</u>
1. Gimbal	12.5	3.3	Calculated
2. Injector	16.2	30.6	Calculated
3. Chamber	48.1	47.3	Calculated
4. Copper Nozzle	20.5	27.0	Calculated
5. Tube Bundle Nozzle	46.7	38.4	Calculated
6. Radiation Nozzle	62.1	80.0	Calculated
7. Nozzle Deployment System	47.1	72.0	Calculated
8. Valves and Actuators	59.1	72.7	Calculated
9. LOX Boost Pump	8.8	5.6	Calculated
10. LH ₂ Boost Pump	3.2	8.5	Calculated
11. LOX TPA (HI SPD)	23.7	26.9	Calculated
12. LH ₂ TPA (HI SPEED)	33.4	26.3	Calculated
13. Misc. Valves & Pneumatic Pack	5.2	12.6	Estimated
14. Lines	28.6	37.0	Estimated
15. Ignition System	11.0	9.2	Calculated
16. Engine Controller	35.0	35.0	Estimated
17. Miscellaneous	36.1	37.0 ⁽¹⁾	Estimated
18. Heat Exchanger	4.8	5.0	Estimated
Total Engine Weight	502.1	574.4	

(1) Miscellaneous includes: Electrical harness, 12.5 lbs; service lines, 6.5 lbs; TPA protective bulkhead, 0.4 lbs; attachment hardware, 15.0 lbs; and instrumentation, 2.6 lbs.

III, G, Task VII - Engine Data Summary (cont.)

The present component designs will be reviewed and improved in subsequent studies. Other components, such as the engine controller, still need preliminary design definition. Both of these activities will result in refined component and total engine system weights as the expander cycle engine design matures.

5. Envelope Data

The engine envelope data are listed in Table XXXVI.

The gimbal and injector lengths are taken from the component drawings presented in Section III,C. The chamber length of 18 in. is an optimized value based on energy release efficiency, turbine inlet temperature, pressure drop, weight, and delivered engine performance. Finally, nozzle length (and exit diameter) result from the required engine stowed length (60 in.).

The nozzle area ratio is the highest value possible within the constraints of engine stowed length and the selected chamber pressure. The copper nozzle and tube bundle area ratios are primarily determined by heat transfer considerations. The primary thermal consideration is to limit the maximum temperatures and temperature gradients experienced by these two components to meet the design life.

The percent bell nozzle is the result of an optimization process in which specific impulse and nozzle weight have been traded off to maximize the performance and minimize the weight within the fixed available envelope of 60 in. with the extendible nozzle in the stowed position.

TABLE XXXVI
ADVANCED EXPANDER CYCLE ENGINE ENVELOPE DATA

1. Gimbal Length, in.	2.4
2. Injector Length, in.	4.8
3. Chamber Length, in.	18.0
4. Total Nozzle Length, in.	84.4
5. Radiation-Cooled Nozzle Length, in.	49.6
6. Engine Stowed Length, in.	60.0
7. Engine Deployed Length, in.	109.6
8. Exit Diameter, in.	58.2
9. Throat Radius, in.	1.395
10. Area Ratio	434.6
11. Cu. Area Ratio	10.6
12. Tube Bundle Area Ratio	172.
13. Percent Bell	81.8
14. Nozzle Length/Throat Radius	60.6
15. Percent Rao	108.2

III, Task Discussions (cont.)

H. TASK VIII - TECHNOLOGY REQUIREMENTS

The objective of this task was to identify any new technology required to perform the detailed design, construction, and testing of the Advanced Expander Cycle Engine.

A list of critical technology requirements for this engine was prepared as a result of this study, the Phase A Engine Study, and ALRC in-house efforts. We first recommended this point design study and a thrust chamber technology program in October 1978. Both of these recommendations have been pursued by NASA. We also submitted an Advanced Expander Cycle Engine Critical Component Technology and Experimental Engine Plan to NASA/MSFC in February 1980 (Ref. 7). The component technology information is presented in this section.

The three design drivers which the technology activities should address are as follows:

- ° Engine Turbopump Drive Power (P)
- ° Development and Operational Risk Reduction (R)
- ° Engine Performance, Impulse (I)

Power technology activities (P) are aimed at assuring or increasing the power available to the turbopump. The results of these programs are used to verify that the engine will operate at the selected design point chamber pressure, has the capability of operating at a higher pressure and performance level, or can accept greater component performance margins or tolerances. As a result, overall program economies are achieved by guaranteeing that the engine operating design point can be reached or exceeded (growth). This saves development dollars because large variations in costs result from parallel resolution of small instant problems.

III, H, Task VIII - Technology Requirements (cont.)

Risk reduction technologies (R) allow the solution of design deficiencies at the technology level prior to committing to a design specification and entering the engine development program. Making decisions at this point provides for design iterations and decisions to be made at the low expenditure level of the overall program. Risk reduction solutions provide for higher confidence in the engine operation, which is consistent with a man-rating design philosophy.

Performance technology programs (I) are geared to guarantee the performance level of the engine prior to a commitment to the specification. These programs provide a high confidence in the performance position so that payloads can be firmed up at reasonable levels prior to DDT&E. The level of performance growth is also determined by these programs.

Twenty-four technology programs were identified; these are summarized on Figure 57. These programs support the following key decision points and/or engine design and development logic which are also displayed on the figure.

- (1) Engine Power Balance
- (2) Throttling Power Balance
- (3) Cycle Optimization
- (4) Performance Optimization
- (5) Nozzle Extension Decision
- (6) Experimental Engine Design Decision
- (7) Experimental Engine Fabrication and Test

The twenty-four suggested programs, along with a priority designation, are also listed in Table XXXVII. The programs designated as priority "A" are those which have a major impact on the expander cycle engine design. As a minimum, the critical technology activity should address these items.

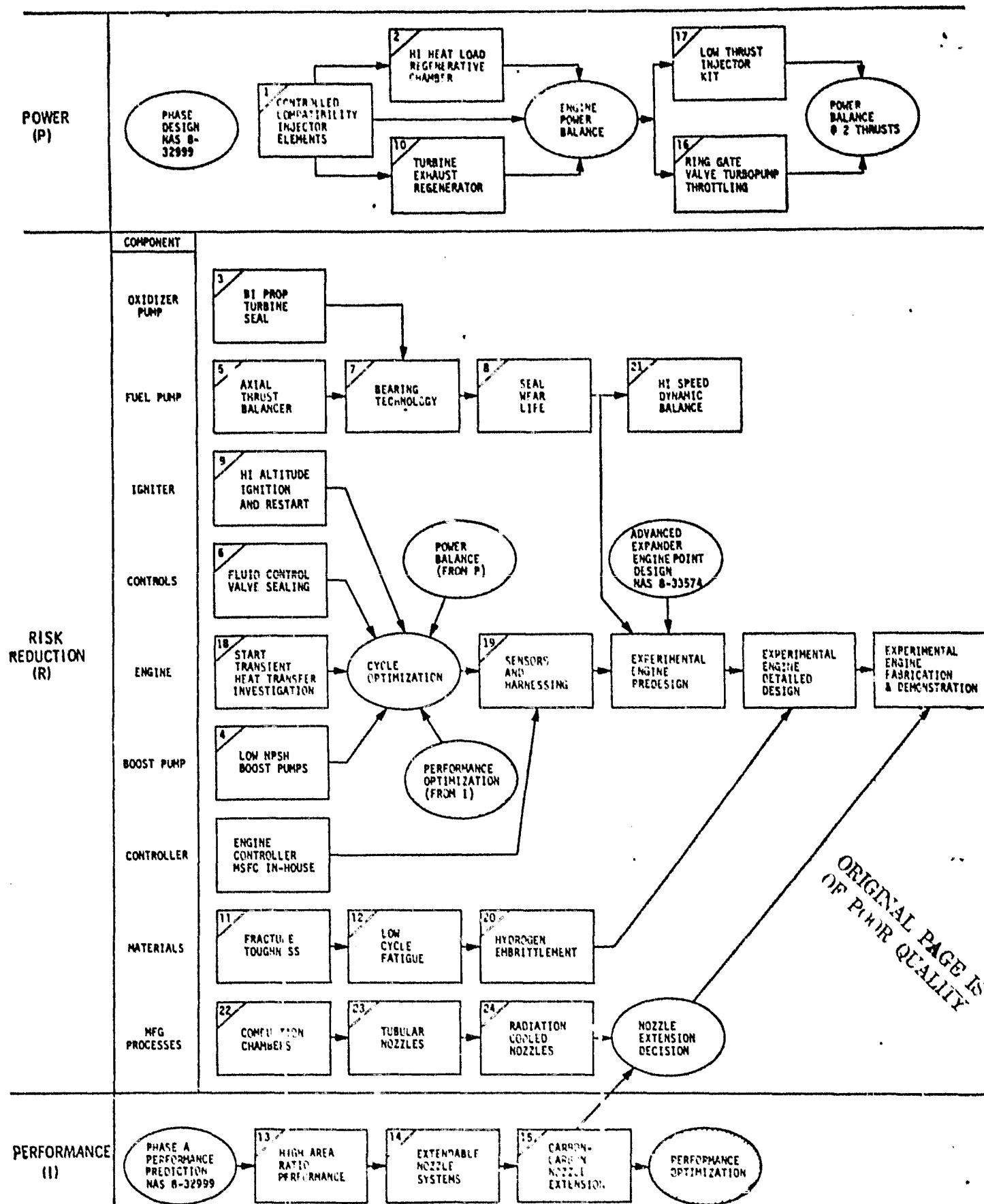


Figure 57. Critical Component Technology Program Logic

TABLE XXXVII
COMPONENT TECHNOLOGY PROGRAM PRIORITIES

PROGRAM	CATEGORY	PRIORITY
1. Controlled Compatibility Injector Elements	P	A
2. High Heat Load Regenerative Chamber	P	A
3. Oxidizer Turbopump Bipropellant Seal	R	A
4. Low NPSH Boost Pumps	R	A
5. Axial Thrust Balancer	R	A
6. Fluid Control Valve Sealing	R	A
7. Turbopump Bearing Technology	R	A
8. Turbopump Seal Technology	R	A
9. Igniter Development	R	B
10. Regenerator Development	P	B
11. Fracture Toughness Testing of Structural Alloys in Gaseous Hydrogen	R	B
12. Predictive Analysis of Low-Cycle Fatigue Life for OTV Alloys of Construction	R	B
13. High Area Ratio Nozzle Performance	I	B
14. Extendible Nozzle Systems	I	B
15. Carbon-Carbon Nozzle Extensions	I	C
16. Ring Gate Valve Turbopump Throttling	P	C
17. Low-Thrust Injector Kit	P	C
18. Start Transient Heat Transfer Coefficient Investigation	R	C
19. Sensors and Harnessing	R	C
20. Hydrogen Embrittlement Study of Columbian Alloys in OTV Radiation-Cooled Nozzle Environment	R	C
21. High-Speed Dynamic Balancing	R	C
22. Combustion Chamber Manufacturing Processes	R	C
23. Tubular Nozzle Manufacturing Process	R	C
24. Radiation-Cooled Nozzle Welding	R	C

III, H, Task VIII - Technology Requirements (cont.)

We recommended grouping programs 1, 2, and 9 into a single program. NASA/MSFC is currently evaluating proposals on an Expander Cycle Thrust Chamber Verification Program which has objectives similar to those of our suggested technologies (i.e., verify experimentally the analytically determined design and operating characteristics of an expander cycle thrust chamber). Program 10 could also be an added option to complete the evaluation of the expander cycle engine power balance.

Programs designated as priority "B" are those which have a definite bearing on the cost effectiveness of the OTV engine development program.

Priority "C" programs represent either expansion of the application of the expander cycle engine or activities which directly influence the production aspects of the engine program.

The various recommended component technology programs are discussed in the following paragraphs. The programs are grouped under the three major technology areas. The program numbers refer back to the figure and table listings.

1. Engine Turbopump Drive Power Technologies

a. Controlled Compatibility Injector Elements (Program 1)

(1) Objectives

The objectives of this program are to develop and verify an injector that would maximize the combustion chamber hydrogen coolant outlet temperature.

III, H, Task VIII - Technology Requirements (cont.)

(2) Justification

Expander cycle engines depend on high heat input to combustion chamber walls to achieve system power balance. Injector elements which can be designed to produce a high but predictable and controllable heat flux will allow engine optimization in terms of total heat input, chamber life, and coolant pressure drop.

b. High Heat Load Regenerative Chamber (Program 2)

(1) Objective

The objective of this program is to develop a regeneratively cooled combustion chamber that maximized the hydrogen coolant outlet temperature.

(2) Justification

High total flux, low ΔP , high ΔT , and good cycle life are essential for the expander cycle regenerative chamber. A demonstration program which considers fabricability along with the operational characteristics is required to establish a firm technology base for this critical component. This program will provide confidence in the thermal predictions and provide early data for the combustion chamber cycle life predictions.

c. Regenerator Development (Program 10)

(1) Objectives

The objectives of this program are to optimize, develop, and verify a regenerator for use in the expander cycle engine.

III, H, Task VIII - Technology Requirements (cont.)

(2) Justification

Increasing the combustion chamber coolant inlet temperature can increase the coolant outlet (turbine inlet) temperature with a small penalty in system pressure drops. To accomplish this, high-efficiency, lightweight, low ΔP regenerators are beneficial. An analytic and experimental comparison of tube-type and flat plate (platelet) concepts would identify the best approach to this component and also verify the performance capability and weight of this unit.

d. Ring-Gate Valve Turbopump Throttling (Program 16)

(1) Objectives

The objectives of this program are to design and demonstrate a throttling valve that is internal to the turbopump assembly.

(2) Justification

Studies which have been conducted for future engine systems have shown that deep thrust throttling of the main propulsion to achieve orbit adjustment and space rendezvous maneuvers can eliminate the need for auxiliary thrusters and the weight associated with these thrusters. In addition, operation of an OTV engine at low thrust may permit a single engine to perform both the MOTV and COTV missions.

The incorporation of a throttling valve, internal to the turbopump assembly and located at the discharge of the impeller, provides a throttling capability throughout the entire engine operating range without pump hydraulic instability. A pump with ring-gate valve concept has the capability of achieving stable HQ pump performance characteristics over a

III, H, Task VIII - Technology Requirements (cont.)

wide throttling range with either a radial vaned impeller or a backswept vaned impeller while maintaining high overall efficiency. Location of this throttling valve within the turbopump assembly offers an advantage in weight savings and eliminates an extra system valve which would be required if a portion of the discharge flow were recirculated to the pump inlet to maintain pump operation outside of the stall region during transient conditions.

e. Low-Thrust Injector Kit (Program 17)

(1) Objective

Develop and demonstrate combustor throttling capability and low-thrust "kit" capability.

(2) Justification

One possible means of reducing future liquid propulsion engine development costs is through utilization of the commonality of certain design components between the Manned (MOTV) and Cargo (COTV) Orbit Transfer Vehicle engines. Throttling of a MOTV engine designed for a thrust of 15K lb to the 1K to 2K thrust level required for COTV applications is desirable. One of the components which limits the low-thrust capability is the injector. A program to identify the injector modifications and to verify the stability and performance of the injector at low thrust is required.

III, H, Task VIII - Technology Requirements (cont.)

2. Development and Operational Risk Reduction Technologies

a. Oxidizer Turbopump Bipropellant Seal (Program 3)

(1) Objectives

The major objectives of this program are to identify and experimentally evaluate candidate approaches to the seal between the warm hydrogen turbine drive gas and the liquid oxygen bearing coolant for the LO₂ pump.

(2) Justification

The warm hydrogen turbine drive gas for the oxidizer pump turbine creates a bipropellant seal problem when the oxidizer pump bearings are cooled with oxygen and the turbine is on the same shaft as the pump (i.e., when there is no gearbox). This is the preferred configuration for a long-life, lightweight, minimum-maintenance reusable turbopump. The purpose of this activity is to address this obvious propellant incompatibility problem.

(3) Discussion

One approach to this problem is to develop a burn-off seal to replace the purge seal. The burn-off seal concept allows leakages from pump and turbine to mix. It is particularly attractive for the LOX pump of the OTV engine because the temperature of the hydrogen in the turbine is relatively low and no spontaneous reaction of the resulting potentially explosive O₂-H₂ mixture in the seal area of the turbopump is to be expected. The mixture will not burn or explode without being ignited.

III, H, Task VIII - Technology Requirements (cont.)

It seems feasible to transport the mixture collected in the seal cavity by means of a jet pump (eductor) to a catalyst bed where oxygen and hydrogen recombine to water (steam). By keeping the pressure in the interseal cavity low, the quantity and, therefore, the energy content of the mixture present in the turbopump that might be liberated in case of an accidental ignition (e.g., by metallic rub) is greatly reduced.

b. Low NPSH Boost Pumps (Program 4)

(1) Objective

The objectives of this program are to demonstrate the feasibility of both the fuel and oxidizer boost pumps and to provide the necessary cool-down and start transient operation as well full power NPSH for the main fuel and oxygen TPA's.

(2) Justification

Because of the low tank head associated with the OTV, the expander cycle engine start transient presents a potential technical risk area. It is expected to be slow and thus may be unpredictable. This program is required to establish minimum NPSH and chill-down requirements for these components. By demonstrating this capability early, the risks associated with the engine start transients in the engine demonstration program will be greatly reduced.

(3) Discussion

The program should also have an initial phase in which a detailed evaluation of various boost pump candidates for further engine optimization is conducted. If the OTV engine need date is such that advanced con-

III, H, Task VIII - Technology Requirements (cont.)

cepts can be considered, then concepts such as a fluid coupling, torque converter, or friction drive should be evaluated. These systems have a higher efficiency potential than the baseline design but are as yet unproven.

c. Axial Thrust Balancer (Program 5)

(1) Objectives

The major objectives of this program are to design and demonstrate a unique axial thrust balancer that is self-compensating.

(2) Justification

One of the components which limits the design of high-speed, high-pressure turbopumps is the axial thrust balancer. Present axial thrust balancers are limited in capacity and stability and require a large flowrate of high-pressure fluid.

Large forces are inherent in high-pressure turbopumps because of the high unit load imposed on the various rotating surfaces. Theoretically, these forces can be balanced by opposing pressurized surfaces so that the net rotor load is zero. In actual practice, asymmetry, tolerances, and off-design operation cause variations in the radial pressure gradients as well as differences in pressure level, with the result that the net axial force will vary over the operating range and from one assembly to another. Even though the percentage change may be small, the high pressure levels will create relatively large force variations which, in turn, require a thrust absorbing device outside the capability of mechanical bearings.

III, H, Task VIII - Technology Requirements (cont.)

The life and reliability of high-speed, high-head-rise turbopumps can be improved by using an articulated thrust balancer.

d. Fluid Control Valve Sealing (Program 6)

(1) Objectives

The objectives of this program are to select, design, and experimentally evaluate valve seals for operation in the OTV engine cryogenic environments.

(2) Justification

Most cryogenic engine valve experience has been with applications that did not require very low valve seal leak rates. Typical leak criteria were 10 scc/sec or 10 scc/sec/inch of seal. With the manned application and cargo bay location for the MOTV, leak rates in the range of 10 to several hundred scc/hr may be required. Another area of concern is that an effective low-pressure cryogenic seal may not be effective at high pressure and vice versa. A typical solution to many of the sealing problems is to use metal barrier seals such as bellows. However, for high-pressure, high cycle-life applications, bellows also have disadvantages with regard to size, weight, cost, maintainability, and design flexibility.

III, H, Task VIII - Technology Requirements (cont.)

e. Turbopump Bearing Technology (Program 7)

(1) Objectives

The objectives of this program are to establish propellant lubricated rolling contact bearing life/load characteristics and to evaluate the use of hydrostatic bearings in large high-speed, high-pressure turbomachinery.

(2) Justification

The design and life of high-speed, high-pressure turbopumps is limited by the conventional rolling contact bearings. The data base in the anticipated operating environments for these bearings is small. Life/load characteristics of these rolling contact bearings should be established to reduce development risk.

Another design approach is the use of unconventional hydrostatic bearings. The hydrostatic journal bearing presents a solution to the design deficiencies of the rolling element bearings. Hydrostatic fluid film bearings supplied from pump discharge pressure can provide very large radial load capacity consistent with design criteria for axial thrust balancers. By design, the radial stiffness would be very high and allow turbopump operation below critical speed ranges. Since these hydrostatic bearings are not speed- or diameter-limited (DN), they would allow design flexibility for stiffer shafts, higher speed, and inboard bearing locations, if desired. Higher speeds and shorter turbopumps result in lighter weights. A design data base for these bearings should be established.

III, H, Task VIII - Technology Requirements (cont.)

f. Turbopump Seal Technology (Program 8)

(1) Objectives

The objectives of this program are to establish turbopump seal wear and life data.

(2) Justification

Turbopump sealing is a basic design problem in all advanced engines. The data base for the life and load capability for TPA seals required in the OTV engine is very small and needs to be expanded to reduce the development risk and improve the life of these components.

Another design approach is the use of unconventional floating hydrostatic ring journal seals for application as interstage shaft seals and impeller wear ring seals. These seals can provide a considerable reduction in leakage flowrate and, due to their floating design, impose a low radial load on the rotating assembly.

g. Igniter Development (Program 9)

(1) Objective

The objective of this program is to conduct vacuum ignition tests to determine igniter tank head start and high altitude ignition restart capability.

III, H, Task VIII - Technology Requirements (cont.)

(2) Justification

The life capability of the ceramic coating on the igniter spark plug has been an area of continual concern. In addition, the ignition mixture ratio range needs to be defined for an ignition system having the OTV pressure/diameter requirements.

h. Fracture Toughness Testing of Structural Alloys in Gaseous Hydrogen (Program 7)

(1) Objective

To obtain (ΔK_0) threshold and low ΔK cycle crack growth data for various structural alloys in gaseous hydrogen.

(2) Justification

An extensive literature survey of hydrogen embrittlement references was unable to uncover any cyclic crack growth threshold findings for rocket engine applicable structural alloys in gaseous hydrogen. One reference reported an increase in crack growth rates of Inconel 718 below the steady stress crack growth threshold (K_{TH}) in hydrogen; however, the confirming data was not provided. Therefore, this critical design property must be established for use in high technology engines fueled by hydrogen, such as the OTV, COTV, and others.

Normally, cyclic crack growth threshold, ΔK_0 , testing is very difficult, expensive, and time-consuming, and testing in a high-pressure hydrogen environment further accentuates these difficulties. However, Aerojet has been using a new, simplified constant ΔK test technique through which this data can be rapidly and inexpensively obtained.

III, H, Task VIII - Technology Requirements (cont.)

This new technique, which obtains one crack growth rate for a selected ΔK level, does not depend on direct crack length measurements requiring a complex test apparatus. This allows the use of a simple three-point loading fatigue machine connected to a load cell, which has already been used for hydrogen environment fatigue testing.

By utilizing this new technique, the proposed test program would conveniently obtain ΔK_0 and low ΔK crack growth rate data for several structural alloys such as Inconel 718, A-286, EFNi, Ti5Al 2.5Sn, and Ti6Al4V in a high-pressure hydrogen environment. The A-286 and titanium alloys are generally judged to be free of hydrogen embrittlement below room temperature; however, this test program is designed to reveal any subtle effects of hydrogen on these alloys which could affect long-life data predictions.

i. Predictive Analysis of Low Cycle Fatigue Life for OTV Alloys of Construction (Program 12)

(1) Objective

To verify the applicability of the ductility-normalized strain-range partitioning low-cycle fatigue predictive technique to columbium and copper components.

(2) Justification

Existing cycle life prediction techniques and data needs to be updated if confidence in being able to meet the OTV engine life goals is to be established. To accomplish this, the program discussed in the following paragraphs should be conducted.

III, H, Task VIII - Technology Requirements (cont.)

The partition strain LCF life curves ($\Delta\epsilon_{pp}$, $\Delta\epsilon_{pc}$, $\Delta\epsilon_{cc}$ vs. cycle life) for FS-85 Cb and Zr-Cu will be estimated from creep ductility and plastic ductility data utilizing the ductility normalized strain range partitioning (DN-SRP) technique proposed by Manson, et al.

These curves will also be determined experimentally for comparison with the estimated curves. Using the DN-SRP technique to determine if better predictive accuracy is possible, the new ductility data obtained in these tests will then be used to reestimate the curves.

After establishing the partitioned LCF design curves, several complex thermal stress cycle hysteresis loops will be generated which will represent possible life cycles for radiation-cooled nozzles and regeneratively cooled combustion chambers. In addition, the hysteresis loop associated with the thermal stress cycle used in obtaining previous LCF data on FS-85 Cb will also be generated.

These hysteresis loops will be partitioned into their component strains, and LCF lives will be predicted on the basis of the established LCF design curves. Comparison of the predicted life of FS-85 undergoing the previous test program thermal cycle with the actual lives of the specimens tested in that program will give an indication of the total accuracy of the SRP technique. This, in turn, can be related to confidence in LCF lives based on other thermal stress cycles which would then be the basis of LCF design allowable curves.

III, H, Task VIII - Technology Requirements (cont.)

j. Start Transient Heat Transfer Coefficient Investigation (Program 18)

(1) Objectives

To conduct literature searches and testing to evaluate heat transfer characteristics in the critical pressure and temperature and two-phase flow regions.

(2) Justification

Heat transfer correlations for both the fuel and oxidizer in the critical pressure and temperature region are not well defined in the literature. Existing oxygen correlations are presented for temperatures and pressures in excess of 180°R and 730 psia. However, during the OTV engine start transient oxygen temperatures will be as low as 165°R and well into the lower pressure two-phase region. Heat transfer correlations suggested in the literature for two-phase flow are not supported with test results.

k. Sensors and Harnessing (Program 19)

(1) Objectives

The objectives of this program are to identify sensor and harness requirements and to select candidates for test evaluation.

(2) Justification

The MOTV engine, with several closed-loop controls, sensors, EMI shielding, and redundancy and maintainability requirements,

III, H, Task VIII - Technology Requirements (cont.)

represents a significant change from most prior engine experience. The size of more commonly used sensors, electrical interconnects, and harness bundles may not be amenable to packaging within the constraints of the MOTV application. Also, pressure sensors (both stabilized and ∇ gradients) are subject to inaccuracy as a function of temperature.

1. Hydrogen Embrittlement Study of Columbium Alloys in OTV Radiation-Cooled Nozzle Environment (Program 20)

(1) Objective

To determine the susceptibility of columbium alloys to hydrogen embrittlement in the OTV radiation-cooled nozzle environment.

(2) Justification

Previous investigations of hydrogen embrittlement of uncoated columbium alloys have indicated that, in pure hydrogen, embrittlement occurs under conditions of rapid heating, exposure at 3000°F, and rapid cooling. However, when tested in an inert gas or vacuum, the same exposure conditions do not result in embrittlement of columbium at temperatures above 1500°F. This possibly may be due to the presence of a protective oxide layer during heating and to the low solubility of hydrogen in columbium at temperatures above 1500°F. The latter exposure closely approximates the thermal cycle of a radiation-cooled nozzle. Considering the less severe exposure of the OTV nozzle (i.e., low partial pressure hydrogen coated columbium, and the satisfactory performance of radiation-cooled nozzles of storable engines with hydrogen potentials for shorter time and cycles), it is anticipated that the proposed OTV nozzle will perform satisfactorily. However, to definitely establish the adequacy of coated columbium for the longer OTV service life

III, H, Task VIII - Technology Requirements (cont.)

and cycles, it is proposed that uncoated and R5112E-coated FS-85 and C-103 columbium alloys be exposed to multiple cycles of rapid heating holding at elevated temperature to simulate OTV times and temperatures, and cooling in vacuum or inert gas.

m. High-Speed Dynamic Balancing (Program 21)

(1) Objectives

The objectives of this program are to research and evaluate dynamic balancing capabilities and requirements for the OTV engine turbomachinery.

(2) Justification

High-speed balancing of turbomachinery operating at speeds as high as 100,000 RPM is required for the OTV engine. Accurate balancing is required to avoid problems during the engine development phase, such as, for example, the subsynchronous whirl encountered on the SSME program.

n. Combustion Chamber Manufacturing Processes (Program 22)

(1) Objectives

The objectives of this program are to establish manufacturing processes, procedures, and techniques involved in fabricating a very small zirconium copper slotted chamber with an electroformed nickel closeout.

III, H, Task VIII - Technology Requirements (cont.)

(2) Justification

° Contour and Slot Machining

Although ALRC has extensive experience in machining slotted chambers, most of this experience has been in CRES alloys. Development experience is required with the change of materials from CRES to zirconium copper. Simple slotting experiments should be performed to determine cutter speeds, feeds, tool pressure, and resultant distortion to narrow lands, tolerances, etc.

° Electroforming

The electroform process is used to form a jacket around the slotted combustion chamber by electro-depositing a thin layer of copper followed by a heavier layer of nickel. This process has been successfully demonstrated on combustion chambers for the OMS engines and several other technology programs. Problems, have been experienced in adhesion, obtaining strength requirements, and porosity. If property requirements are not achieved, it is possible to remove the electroformed jacket by chemical stripping and have the jacket redeposited; however, this causes a time loss which adds to costs and puts schedules in jeopardy. Further development is required to review the problems and causes and to refine process parameters to assure repeatability.

° Welding to Electroformed Materials

It is advantageous to weld brackets, clips, manifolds, etc., to the electroformed jacket. In the past, there has been a difference between the electroformed materials supplied by two vendors, inasmuch as one type has been weldable while the other has been sensitive to

III, H, Task VIII - Technology Requirements (cont.)

weld cracking. Further development is required to establish parameters for weldable materials.

o. Tubular Nozzle Manufacturing Process (Program 23)

(1) Objectives

- ° To braze sample tube bundle sections under vacuum and vacuum partial pressure conditions using various material candidates.
- ° Inspect brazed parts for braze alloy wettability, flowability, diffusion, and undercutting.
- ° Establish heat profiles and atmospheric conditions.

(2) Justification

ALRC has been fabricating tubular chambers for years. These chambers have been brazed in a retort furnace using a hydrogen atmosphere. Over the years, the cost of rare gases for atmosphere use and the cost of maintaining this type of furnace have risen to where the process has ceased to be economical. In April of 1980, ALRC has installed a vacuum, partial pressure furnace to replace the hydrogen retort furnace. This furnace will have the flexibility of using vacuum or a combination of vacuum and partial pressure gases for atmosphere use, which has a major impact on reducing operating costs. Candidate materials for the OTV tubular chamber include A-286, Armco Nitronic 40, and CRES 347. For successful brazing, the atmosphere (vacuum, or vacuum partial pressure) must be capable of reducing metal oxides present on the surface of the base metal. These oxides vary with the different base materials.

III, H, Task VIII - Technology Requirements (cont.)

p. Radiation-Cooled Nozzle Welding (Program 24)

(1) Objectives

Develop weld-joint configurations and establish weld procedures for both TIG and EBW processes for both FS-85 and C-103 columbium alloys.

(2) Justification

Primary candidate materials are FS-85 and C-103 columbium alloys. Both of these materials have been used in the past to fabricate similar nozzles. Most fabrication problems have been related to welding. The FS-85 alloy appears to be more susceptible to weld cracking. However, when heated, both alloys are readily contaminated if proper atmospheres are not maintained.

3. Engine Performance Technologies

a. High Area Ratio Nozzle Performance (Program 13)

(1) Objective

The objective of this program is to verify that very high ($\epsilon = 400:1$ and greater) area ratio nozzles do provide the additional performance predicted by the theory.

(2) Justification

The OTV engines, as currently conceived, include two-position nozzles based on the improved performance predicted at area

III, H, Task VIII - Technology Requirements (cont.)

ratios of 400:1 and greater. The largest area ratio nozzle tested to date is 400:1, and the test data is very limited. The gain to be made by using very high area ratios should be verified by test before committing the OTV engine to the two-position nozzle.

b. Extendible Nozzle Systems (Program 14)

(1) Objectives

The objectives of this program are to design and demonstrate an extendible/retractable nozzle mechanism.

(2) Justification

High performance within a small overall engine length is required of the OTV engine. The use of extendible/retractable nozzles provide a means for meeting these requirements. The design problems associated with the extension, retraction, and sealing of the nozzle extension forward flange joint must be addressed.

c. Carbon-Carbon Nozzle Extensions (Program 15)

(1) Objective

The objective of this program is to evaluate the potential of carbon-carbon material for the nozzle extension.

(2) Justification

Nozzle weight and the handling of very thin-walled metallic nozzle extensions can pose problems for the OTV engine.

III, H, Task VIII - Technology Requirements (cont.)

Free-standing carbon-carbon nozzles may prove to be lighter in weight than metallic nozzles for high area ratio application. They may also prove to be less susceptible to handling damage as they are planned to be reused, offering a potential for reducing maintenance cost.

I. TASK IX - COMPUTER SOFTWARE/DOCUMENTATION

As part of this program, two engine computer models were delivered to NASA/MSFC. One of the programs is the Task I, Steady-State Computer Model (Ref. 5), and second is the Task IV, Engine Transient Simulation Computer Model (Ref. 6).

Documentation submitted for these computer models included:

- ° User's Manual
- ° FORTRAN Program Listing
- ° Program Flow Charts
- ° Sample Inputs and Outputs

At the request of the NASA/COR, a FORTRAN card deck was submitted for the steady-state model. The transient model was submitted on tape. Both programs are compatible with a Univac 1108 system.

IV. CONCLUSIONS AND RECOMMENDATIONS

A. CONCLUSIONS

The following conclusions were derived from this and related study efforts.

- ° A new engine is required to meet the OTV performance, man-rating, and life requirements.
- ° A 1980 state-of-the-art expander cycle engine can meet the OTV requirements.
- ° The advanced expander cycle engine is a high performance, low-risk, low-cost option.
- ° The benign turbine operating environment of an expander cycle reduces engine development risk and cost.
- ° Further design definition of the expander cycle engine and its components is required.
- ° The main fuel turbopump and the injector/chamber are the most critical expander cycle components.
- ° The performance of the expander cycle engine can be increased by removing the 1980 state-of-the-art requirement.
- ° Engine operation at 10% of rated thrust is feasible through engine "kitting."
- ° Experimental verification of low-thrust operation is required.

IV, Conclusions and Recommendations (cont.)

B. RECOMMENDATIONS

The recommendations for further study and advanced technology efforts that were identified during the course of this point design program are summarized herein.

- ° The point design studies should be continued to optimize the expander cycle engine and provide more design definition of its components. These studies should include the following criteria:

- (1) Technology advancements to increase component and engine performance.

- (2) Reevaluation of the boost pump/main pump designs to optimize the configurations and the system efficiency.

- (3) Incorporation of all recommended design modifications from the first iteration.

- (4) Conducting a component FMEA.

- (5) Updating of the structural analyses and materials selection.

- (6) Definition of the engine/vehicle interface and optimization of the engine configuration to maximize performance in a given engine stowed length.

- (7) Provision of further engine controller definition.

IV, B, Recommendations (cont.)

(8) Establishment of purge and relief system requirements and preliminary design definitions.

- ° Expander cycle engine component critical technology programs should be initiated to accomplish the following:
 - Reduce risk
 - Verify power balance
 - Verify performance
- ° Component technology should address both high- and low-thrust operation.
- ° Component technology programs should be followed by a detailed design of a breadboard expander cycle engine.
- ° Major breadboard engine components should be fabricated and tested.
- ° Breadboard engine components should be assembled into an engine configuration and tested.

REFERENCES

1. Mellish, J.A., Orbit Transfer Vehicle (OTV) Engine Phase A Study, Final Report, Contract NAS 8-32999, Report 32999F, ALRC, 29 June 1979.
2. Mellish, J.A., Advanced Expander Cycle Engine Optimization Task Report, Contract NAS 8-32999, OTV Engine Study Phase A Extension I, Report No. 32999E1-T1, ALRC, November 1979.
3. Mellish, J.A., Alternate Low-Thrust Capability Task Report, Contract NAS 8-32999, OTV Engine Study Phase A Extension I, Report No. 32999E1-T1, ALRC, April 1980.
4. Christensen, K.L., Orbit Transfer Vehicle (OTV) Advanced Expander Cycle Engine Point Design Study, Engine Data Summary, Contract NAS 8-33574, Report 33574-T7, ALRC, 1 October 1980.
5. Christensen, K.L., User's Manual: ALRC Advanced Expander Cycle Engine Steady-State Computer Model (OTVMODV7), Contract NAS 8-33574, Report No. 33574-UM1, ALRC, 28 July 1980.
6. Lawver, B.R., OTV Engine Simulation Computer Model Engineering and User's Manual, Contract NAS 8-33574, Report No. 33574-T1V, ALRC, 15 November 1980.
7. Advanced Expander Cycle Engine Critical Component Technology and Experimental Engine Plan, ALRC, 15 February 1980.
8. Orbit Transfer Systems with Emphasis on Shuttle Applications - 1986 - 1991, NASA Technical Memorandum TMX-73394, NASA/MSFC, April 1977.
9. Design Requirements Handbook, Contract NAS 8-33574, Advanced Expander Cycle Engine Point Design Study, ALRC, Revised 11 August 1980.
10. JANNAF Liquid Rocket Engine Performance Prediction and Evaluation Manual, CPIA Publication No. 246, April 1975.
11. Ainley, D.G. and Mathieson, C.R., A Method of Performance Estimation for Axial-Flow Turbines, R&M No. 2974, 1957.
12. Improvements to the Ainley-Mathieson Method of Turbine Performance Prediction, ASME Paper No. 70-GT-2, 1970.
13. Multistage Axial Flow Turbine Performance Analysis Program, Report No. 7740R-70-032, Aerojet General Corporation, Nuclear Rocket Operations, Sacramento, California, 16 January 1970.

REFERENCES (cont.)

14. Liquid Rocket Engine Centrifugal Flow Turbopump, NASA Space Vehicle Design Criteria, NASA SP-8109, December 1973.
15. Liquid Rocket Engine Turbopump Bearings, NASA Space Vehicle Design Criteria, NASA SP-8048, March 1971.
16. Liquid Rocket Engine Turbopump Shafts and Couplings, NASA Space Vehicle Design Criteria, NASA SP-8101, September 1972.
17. Csomar, A. and Sutton, R., Small, High-Pressure Liquid Oxygen Turbopump, Interim Report, Rockwell International Rocketdyne Division, NASA CR 135211, R76-178, Contract NAS 3-17800, July 1977.
18. Csomar, A. and Sutton, R., Small, High-Pressure Liquid Hydrogen Turbopump, Final Report, Rockwell International Rocketdyne Division, NASA CR-135186, R76-115, Contract NAS 3-17794, May 1977.
19. Luscher, W.P. and Mellish, J.A., Advanced High-Pressure Engine Study For Mixed-Mode Vehicle Applications, Aerojet Liquid Rocket Company, NASA CR-135141, Contract NAS 3-19727, January 1977.
20. Engine Design Definition Report, Volume IV Turbomachinery, AJ-550 Space Shuttle Main Engine, Contract NAS 8-26188, April 1971.
21. Buckmann, P.S., High-Speed Turbine Shaft Dynamics, Bearings and Seal for Rankine Cycle, ALRC Report No. 9725:0117, November 1973.
22. Winn, L.W., Small High-Speed Bearing Technology for Cryogenic Turbopumps, NASA CR-134675, July 1974.
23. Mellish, J.A., Orbit Transfer Vehicle Engine Study, Phase A, Extension 1, Contract NAS 3-32999, Bimonthly Status Report 32999E1-M4, ALRC, 15 March 1980.
24. Safety Policy and Requirements for Payloads Using the Space Transportation System, NASA/Headquarters NHB 1700.7, 16 June 1976.
25. Nickerson, G.R., Coates, D.E., and Bartz, J.L., Two-Dimensional Kinetics Reference Computer Program - TDK, Contract NAS 9-12652, December 1973.
26. Svehla, R.A. and McBride, B.J., Fortran IV Computer Program for Calculation of Thermodynamic and Transport Properties of Complex Chemical Systems, NASA TN D-7056, January 1973.

REFERENCES (cont.)

27. Pieper, J.L., ICRPG Liquid Propellant Thrust Chamber Performance Evaluation Manual, CPIA No. 178, September 1968.
28. Yost, M.C., Preburner of Staged Combustion Rocket Engine, Final Report, NASA-CR-135356, NAS 3-19713, Rocketdyne, February 1978.
29. Dennies, P.C., Marker, H.E., and Yost, M.C., Advanced Thrust Chamber Technology, Final Report, NASA-CR-135221, Contract NAS 3-17825, Rocketdyne, July 1977.